Structural variation
in π-conjugated DNA binders through click chemistry
synthesis and interaction studies

ISMAIL ALTHAGAFI

A thesis submitted for the Degree of Doctor of Philosophy

School of Chemistry

Cardiff University

August 2012

This thesis is sincerely dedicated to

My loving parents and to My wife

Acknowledgements

I would like to begin by extending my praise and thanks to Allah, for giving me the strength and ability to complete this work.

This work would not have been possible without the support and assistance of many people. My sincere apologies if I have forgotten to mention anyone. I would like to begin by expressing my profuse thanks to my supervisor, Dr. Niek Buurma, for his continual support throughout my Ph.D study and research. His encouragement, patience and extensive knowledge were absolutely invaluable to me. I sincerely appreciate his help in overcoming the challenges that I faced throughout my research, as well as through the writing of this thesis. It was a wonderful period of my life to work with him.

Special thanks also go to Dr Mihaela Dorin, for all of her help with starting the lab work involved in my PhD. I must thank my mentor, Prof. Barry Carpenter, for his invaluable consultations, as well as Dr. Eric Tippmann, for his comments and questions during my six-monthly *viva voce* examinations. My gratitude to prof. Allemann's group, for allowing me to use their CD machine for the CD-titrations, and the technical staff: Alun, Rob Jenkins, Robin, Sham, Gary and David.

My sincere thanks to the Ministry of Higher Education of Saudi Arabia, for the scholarship and funding my Ph.D study.

Thanks to my friends in Cardiff Dr. Ahmad Fikri, and all Saudi students in the School of Chemistry for their nice company. I would also like to thank my labmates and friends at the POC centre, especially Mazin, and Stefania. Additionally, my thanks to the undergraduate students, placement students from IUT Rennes, Erasmus students and

Nuffield bursary holders who worked with me in the synthesis lab: Luke, Thomas, Florian, Adam, Luke.R, Khadra and Merve.

Finally, I offer my deepest, heartfelt thanks to my family: to my loving parents and grandmother for their emotional support and prayers for me in the hard times; and to all of my beloved brothers, sisters and members of my wider family, for their encouragement throughout my Ph.D studies. Special thanks to my wife, for her unlimited love, help and support in all areas of my life. Lastly, but not least, a huge thank you to my wonderful daughters, Wasan and Shaden, for their patience and immeasurable love, which encouraged me to finish this thesis.

Summary

This thesis presents the design, synthesis and physical studies of new structurally-varied cationic oligoheteroaromatic DNA binders in six chapters.

Chapter 1 introduces DNA and its importance in modern science such as genetic and medicinal research. The interactions of DNA with small molecules are also discussed. A description is provided of click chemistry, a method for the synthesis and design of structurally-varied molecules, in this case designed to interact with DNA.

Chapter 2 presents the synthesis of alkyne-substituted oligoheteroaromatic compounds by means of bromination, iodination, and Suzuki, Stille and Sonogashira cross-coupling reactions. These alkyne-substituted oligoheteroaromatic compounds were designed to be used as building blocks for click reactions.

Chapter 3 describes the synthesis of azide-substituted oligoheteroaromatic compounds from amines by means of a safe method. The Pd-catalysed cross-coupling of azide-substituted building blocks to form oligoheteroaromatics is also described. The azide-substituted oligoheteroaromatic compounds were designed as building blocks complementary to the alkyne-substituted compounds described in Chapter 2.

Chapter 4 presents the synthesis and characterisation of new π-conjugated molecules utilising click chemistry between alkyne- and azide-substituted compounds leading to a series of structurally-varied di- and tricationic oligoheteroaromatic putative DNA binders.

Chapter 5 describes DNA-binding studies for the di- and tricationic oligoheteroaromatic compounds using a variety of biophysical techniques to quantify DNA binding and elucidate binding modes. Additionally, this chapter presents results from preliminary

exploration of the sequence selectivity of our cationic oligoheteroaromatics by comparing binding affinities and binding modes for two different sequences of DNA, viz. poly(dGdC)$_{40}$ and poly(dA)$_{80}$•poly(dT)$_{80}$.

Chapter 6 presents the preliminary synthetic and DNA-binding studies of selected extended cationic oligoheteroaromatic compounds.

 Finally, this chapter presents the overall conclusions of the study, including selected comments and suggestions about future studies and applications.

Contents

CHAPTER 6
EPILOGUE

Chapter 1

INTRODUCTION

Abstract

Because of its importance in the field of medicine, DNA has long been a highly tempting target for biosensors and drugs. For example, the ability to selective target DNA opens routes for the creation of antibiotic and antiviral compounds acting directly on the unique genome of pathogens. Chapter 1 offers a brief overview of the accumulated knowledge of DNA, and of the interactions of duplex DNA with small molecules, including electrostatic, intercalation and groove interactions. The most important target for synthetic duplex-DNA binders is the minor groove. Various examples of small-molecule DNA binders are discussed. Additionally, Chapter 1 describes click chemistry, and its role as a powerful method of organic synthesis. This chapter also suggests click chemistry as an efficient methodology for the creation of significant structural variation of ligands in the field of nucleic acid binding.

1.1 General introduction of thesis

DNA is a very significant target of modern genetic and medicinal research. The study of small molecules that target DNA is a promising field, and could lead to the discovery of means by which to control many genetic diseases. Routes leading to the synthesis of new antibiotic and antiviral compounds may also be opened. DNA possesses a rich structure which offers various modes of interaction between ligands and DNA, depending on the shape and size of the DNA-binding molecules. This thesis is focused on the synthesis and study of interactions of small molecules that target the minor groove (and not the major groove); this emphasis is due to the established promise of targeting the minor groove in medicine using small molecules, particularly in the fields of drug discovery and biosensors.[1]

The so-called "click chemistry" methodology has been used for the synthesis of a range of molecules, intrinsically designing in widely different shapes and sizes of compounds. The conjugated oligoheteroaromatic molecules developed here are of particular interest due to their marked variation in spectroscopic and electronic properties upon binding with DNA. The investigation of the strength and mode of the DNA binding of these compounds involved the use of many different techniques. The sequence selectivity of these molecules, which is fundamental to the discovery and development of drugs and biosensors, was also explored. These conjugated hetroaromatics compounds, in combination with DNA, could also form the building blocks of electronic nanostructures.

1.2 Deoxyribonucleic acid (DNA)

Deoxyribonucleic acid, more commonly known as DNA, was discovered by the Swiss biochemist Friedrich Miescher in the late 1800s. It was through the study of pus cell nuclei, found in discarded surgical material such as bandages, that Miescher was able to identify a phosphorous-based compound which he termed *Nuclein*.[2] Miescher went on to discover that Nuclein consisted of two sections, the first a basic protein and the second an acid-based fragment. We now know the first to be histones, which are responsible for the packing of DNA, and the acid fragment to be DNA itself. Some 40 years later, in 1919, Phoebus Levene identified the sugar, base and phosphate nucleotide units, which led him to suggest that DNA was a string of nucleotides joined by phosphate groupings. However, Levene hypothesised that the chain was actually short and the base units fixed in a repetitive order.[3]

1.3 Importance of DNA in Medicine

Without doubt, the elucidation of the structure of DNA was one of the most significant scientific discoveries of the 20th century. The impact of this discovery on medicine has been large; the identification of genes has led to an increased knowledge of diseases, and the development of the drugs that combat them. In genetic research and medicine, our understanding of the role of DNA as the carrier of genetic information has allowed for significant improvement in disease diagnosis, detection of genetic predispositions and gene therapy.[4] From the "central dogma of molecular biology", the information in DNA is transferred through RNA to proteins in the cell. Several important cellular processes surrounding the DNA can be happened such as replication, transcription and translation.

Furthermore, DNA-drug interactions are important. Specifically, DNA is replicated or transcribed to RNA following a signal to do so – this signal usually involves a particular protein binding to a specific site in the DNA framework. It is therefore clear that small molecule binding can emulate or block such binding, and cause or stop replication and/or transcription[5]; the small molecule may act as a drug either at activation or impedance of a given DNA response. Ideally, the future will bring compounds that can bind selectively to a specific genetic sequence, thus facilitating its use as a promotor or biosensor. Development of sequence-specific biosensors will produce a simple, rapid method with which to determine whether or not a given sequence is present in DNA.

In addition, our understanding of the interactions of DNA and their roles in biology is leading to the creation of "customised pharmaceuticals", which are based on information surrounding an individual's genetic profile. The pharmaceutical potential for such molecules is extraordinary; for example, designer molecules can have therapeutic potential as very selective anti-tumour agents, whereby the mutated sequences leading to the synthesis of misformed proteins are blocked. In addition to its impact on medicine, today's knowledge of DNA has resulted in numerous medical off-shoots crossing into society; examples include paternity testing[6] and criminalistics.[7]

1.4 DNA Structure

1937 saw William Astbury record the first X-ray diffraction pattern, indicating that DNA consisted of a regular structure.[8] However, just how important DNA was to living organisms became evident in 1953 as a result of the work of James Watson and Francis Crick.[9] These two researchers embarked upon the development of a structure representative of the wealth of chemical and structural evidence available at the time,

whilst remaining consistent with the structure of each unit involved in DNA, i.e. the shape, size, bond lengths and angles etc.

Through the utilisation of the X-ray diffraction data from the work of Franklin and Wilkins [10], and the building of many molecular models, Watson and Crick devised the double-helix structure. This structure enabled the interlocking of all of the groups, with no overlap, and allowed large stabilisation of the overall structure through hydrogen bonding. Research of Linus Pauling[11] had already shown such hydrogen bonds to be the strongest non-covalent bond and therefore the most important for the determination of protein structure, specifically N-H-N or N-H-O hydrogen bonds. The importance of the discovery of the structure of DNA is illustrated by the award of the Nobel Prize for medicine in 1962 to Watson, Crick and Wilkins, which sadly came after the death of Franklin.

To expand further, the helix structure of DNA is comprised of two long polymeric strands made from simple units that wind around each other to form a "twisted-ladder" shape (Figure 1.1). The two sides of the helix contain alternating sugars and phosphates linked via ester bonds. Each strand is made from similar repeat units (nucleotides), which are themselves made the aforementioned sugars and phosphates and nitrogen bases. The two sides (strands) are connected by the nitrogen-based species (nucleic acid bases) via hydrogen bonds (Figure 1.1).
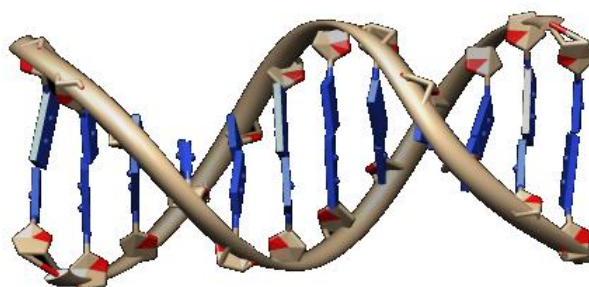
Figure 1.1 The DNA helix (NDB ID: BD0002).

The nucleotides are distinguished by the four nitrogen bases in natural DNA: the purines adenine (A) and guanine (G), and the pyrimidines cytosine (C) and thymine (T)[12] (Figure 1.2).
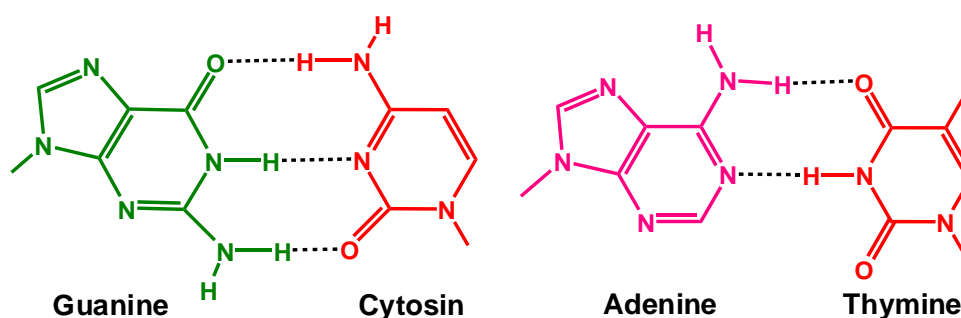
Figure 1.2 DNA base pairs.

The order of these bases determines the biological instructions contained within a strand of DNA (e.g. hair colour), with sets of three bases (codons) coding for an amino acid in an enzyme or protein. The chemical pairing of the nucleobases is very specific; base A always pairs with base T, and similarly base C always pairs with G - this process is called base pairing. Base pairing is especially evident in the most famous conformation of DNA, viz. B-DNA (Figure 1.3), which exhibits the characteristic right-handed double helix

structure; the right-handedness arises from the deoxyribose unit of the backbone which exists naturally as 2-deoxy-D-ribose.[13]
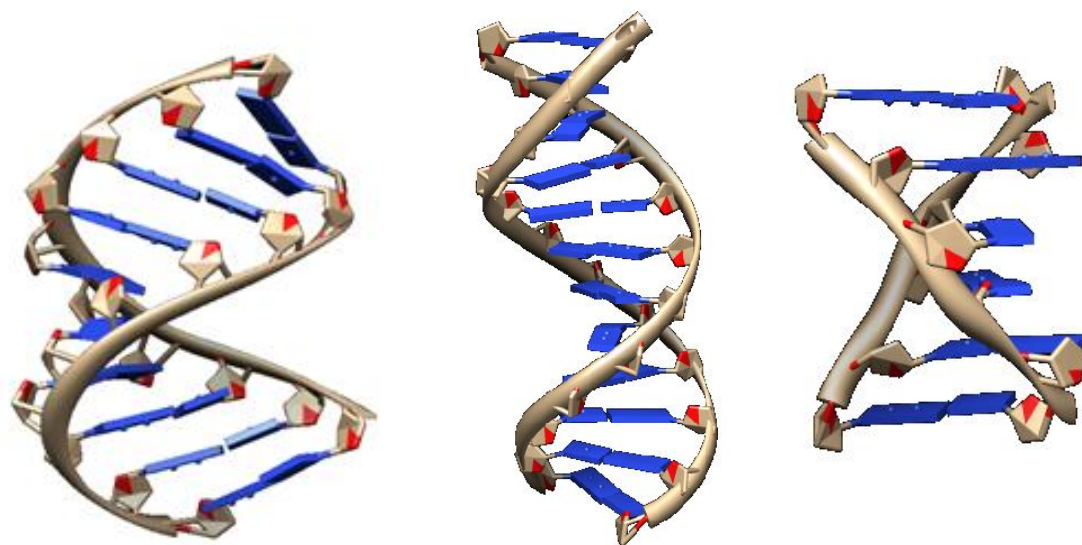
Figure 1.3 The conformations of DNA. (a) A-DNA (NDB ID: AD0046), (b) B-DNA (NDB ID: BD0003) and (c) Z-DNA (NDB ID: ZD0008).

As evidenced by the structures shown in Figures 1.2 and 1.3, hydrogen bonding is the key factor in the "rules" of base-pairing; the geometrical correspondence of hydrogen bond acceptors and donors only allow the G•C and A•T pairs to form stable interactions. G•C pairs form three hydrogen bonds while A•T pairs form two hydrogen bonds and it has been observed that DNA with a large concentration of G•C pairs is more stable than DNA with a lower G•C content. However, it has also been shown that this increased stability of G•C-rich DNA is not due to the additional hydrogen bonding interactions, but instead is due to stronger stacking interactions between the basepairs (i.e. along the helical stack).[14] Figures 1.2 and 1.3 show that purines are complementary to pyrimidines only, with pyrimidine-pyrimidine base pairing unfavourable energetically. This is because the spacing between the two molecules is too great to form a stable hydrogen bond; purine-

purine interactions are similarly unfavourable as the molecules are too close, therefore resulting in repulsion due to orbital overlap.

However, DNA does not exist solely in the B-DNA form; it is in equilibrium with other conformations, the most notable other conformations being A- and Z-DNA (Figure 1.3). DNA can adopt the Z form as a consequence of the repeated alternation of purine-pyrimidine nucleotides, for example in the $(dG-dC)_n$ polymer, giving rise to a staggered left-handed helix. Z-DNA is typically less stable than B-DNA, as the anionic backbones are pushed closer together.[15] Conversely, the bases of the A-DNA structure are positioned at a more highly inclined angle and pointing away from the backbone; this yields a much wider helix with more bases per turn and a greater difference between the two groove widths.

In addition to A-, B- and Z-DNA, there are more structural DNA conformations, such as G-quadruplex and triplex structures (Figure 1.4).
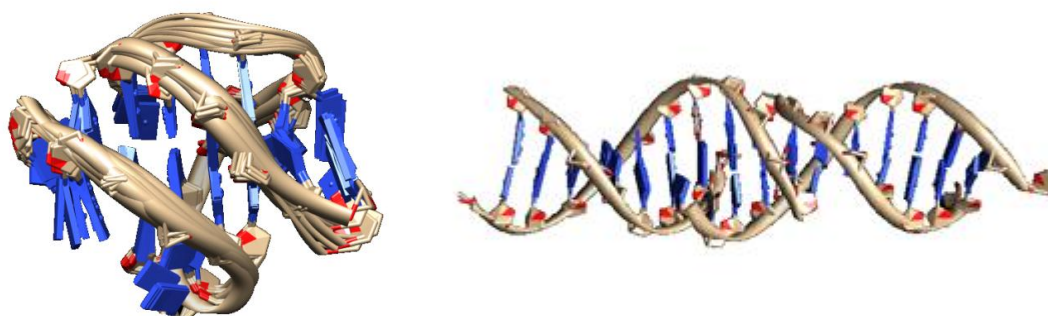
Figure 1.4 Other DNA conformations: G-quadruplex DNA (PDB: ID 2HY9) (left), triplex DNA (NDB ID: BD0017) (right).

1.5 DNA Grooves

As a result of the geometry of the base pairs and the double-helical structure of the two strands, the DNA structure is said to have two grooves that are not equal in size, viz. a "major" and a "minor" groove (Figure 1.5). The major-groove is (as the name suggests) larger than the minor. The major groove is *ca*. 12 Å wide while the minor groove is *ca*. 6 Å wide.[12,16]
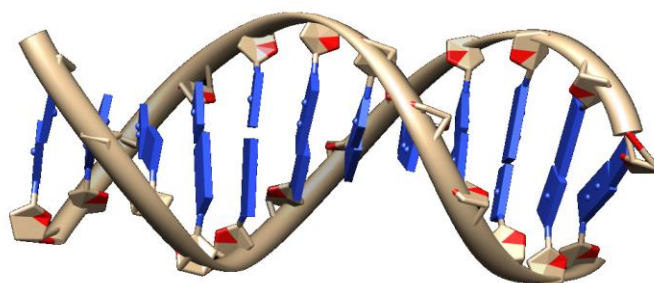
Figure 1.5 Major and minor grooves of DNA (NBD ID: BD003)

There are several differences between the major and minor grooves such as patterns of available hydrogen bond donors and acceptors, electrostatic potential and steric factors (Figure 1.6). The properties of the molecules in relation to the properties of the grooves control whether compounds bind either in the major or in the minor groove; providing ample opportunity for studies of sequence specific binding of small molecules to B-DNA.
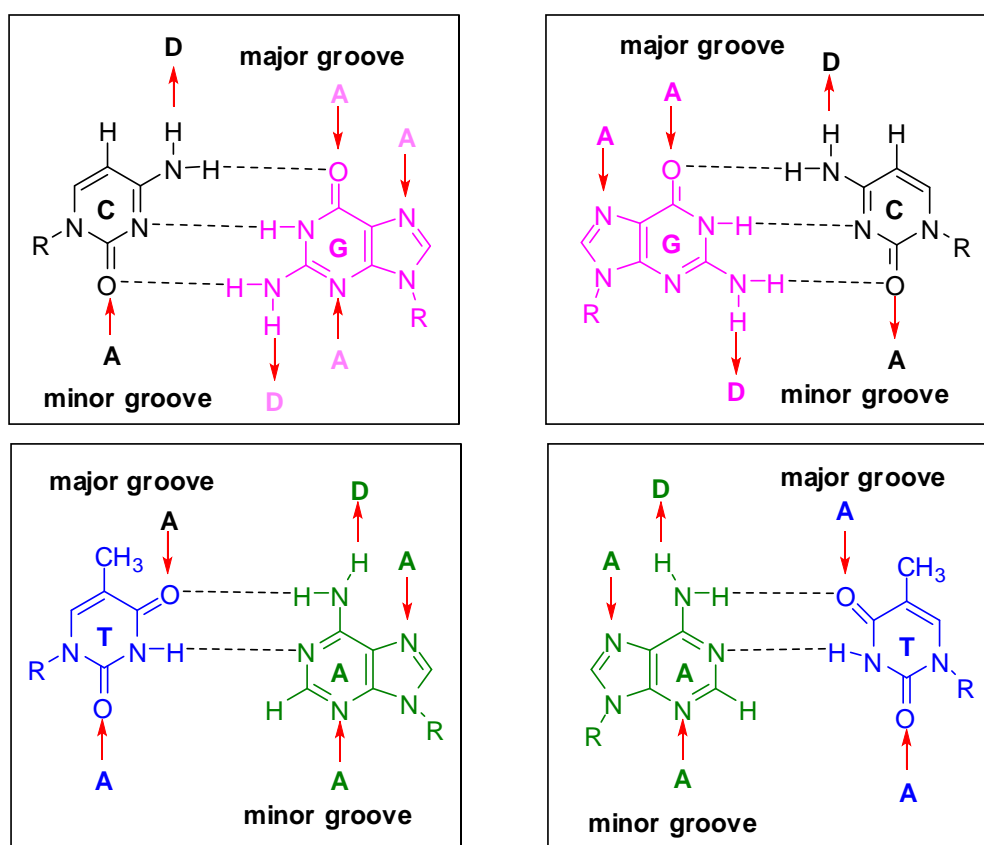
Figure 1.6 H-bond donor and acceptor sites for the base pairs in the minor and major groove of DNA.

Figure 1.6 shows that in the major groove, C•G base pairs offer a pattern of hydrogen bond donors and acceptors which is completely different from G•C. On other hand A•T and T•A base pairs offer the same pattern of hydrogen bonding donors and acceptors in the makor groove because of the symmetry of the pattern. This symmetry would make it difficult to distinguish between A•T and T•A, but the presence of the thymine methyl group causes asymmetry in the steric bulk in the major groove to break this symmetry (Table 1.1).

Table 1.1 The recognition pattern of the major and minor grooves.

Base pair	Major groove	Minor groove
AT	ADA(CH$_3$)	AA
TA	(CH$_3$)ADA	AA
GC	AAD	ADA
CG	DAA	ADA

In the case of the minor groove, the hydrogen bonding patterns of each base pair are symmetrical (Table 1.1). The differentiation between G•C and C•G is markedly more difficult, because there is no steric hindrance to aid distinction. For A•T and T•A pairs, the hydrogen between oxygen and nitrogen being bonded to the more electropositive carbon compared to an amine's nitrogen in all other cases. As a result, based on the hydrogen-bonding pattern alone, molecules binding in the minor groove can only distinguish AT/TA from GC/CG (Table 1.1).

In summary, interaction in the major groove provides more scope for specificity than interaction in the minor groove. It is therefore not surprising that most enzymes interact with DNA in the major groove. For synthetic ligands, the minor groove provides an interesting binding site, despite the lack of easily recognisable hydrogen bonding patterns because the "walls" of the minor groove are hydrophobic. The hydrophobic walls provide a readily available driving force for interactions which is absent in the major groove.

1.6 Interaction of small molecules with DNA

Understanding the interaction of molecules and proteins with DNA, and specifically the mode of interaction, is of great importance. This is firstly due to the quest to design DNA-sequence-specific drugs, which requires an understanding of the groove structure and the impact of structural modifications on medicines with specific DNA-binding properties. Secondly, an appreciation of the forces involved in binding is a fundamental prerequisite of molecular recognition and, therefore, of selective DNA binding.

Molecules can bind either reversibly or irreversibly to DNA. Irreversible binding typically involves non-specific covalent bonding to the phosphate or sugar parts of the DNA. This usually means that the DNA breaks and the cell housing the DNA dies. In addition, some sites on the DNA can be attacked; for example cisplatin can coordinate to the nitrogens in the basic sites in DNA (Figure 1.7).[17-19]
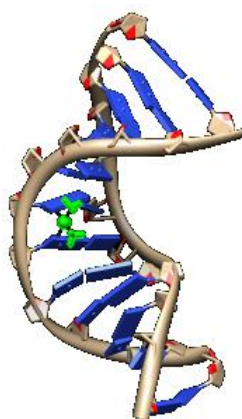
Figure 1.7 Cisplatin interaction with DNA (NDB ID: 1A84)

The ways in which molecules can bind reversibly to DNA are as follows: electrostatic interactions (a) intercalation (b) and groove binding (c). Electrostatic interactions occur on the outside of the helix, intercalation involves the separation of two DNA base pairs by a molecule, with the molecule sliding in between the bases and changing the DNA shape,

and (major and minor) groove binding is an interaction which occurs inside the curve of the DNA helix (Figure 1.8).[20]
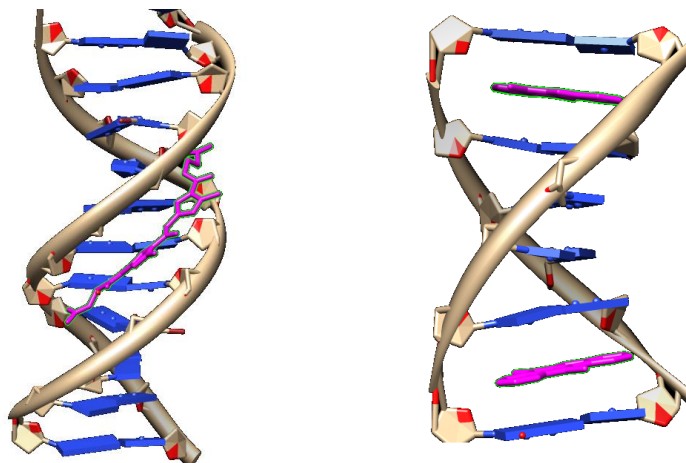
Figure 1.8 Examples of different reversible interactions between molecules and DNA (a) minor groove binding (NDB ID: GDLB05) (b) intercalation (NDB ID: DD0070).

The following three sub-sections describe these three types of interaction in more detail.

1.6.1 Electrostatic interactions

Electrostatic interactions are typically non-specific, and occur along the exterior surface of the double helix structure because DNA itself is highly anionic in nature, with the negative charge located on the phosphate groups.

The large density of charge localised on the phosphate groups can lead to electrostatic binding of cationic compounds to the phosphate backbone. This particular mode of binding is also known as external binding, with its strength potentially dictated by size of ligand, the charge on the ligand(s) and ligand hydrophobicity.[21-23] Non-specific interaction with, for example, Mg^{2+}, is referred to as counter ion condensation and assists in the stabilisation of DNA conformation through screening of the electrostatic repulsion between the phosphate groups. However, the release of these ions may be achieved

through the neutralisation of the phosphate backbone's charge as a result of interactions with organic cations; this release of ions causes a highly favourable entropy contribution to the binding free energy of cationic organic DNA binders.[24]

1.6.2 Intercalation and Intercalators

The idea of intercalation was introduced by Lerman in the 1960's [25, 26] and involves a form of binding whereby planar aromatic molecules can be accommodated between the base pairs of DNA. The complexes formed are believed to be stabilised by π-π stacking interactions and Van der Waals interactions between the (typically) aromatic DNA binder and the base pairs of DNA.[27, 28] In order to intercalate, intercalators must fit between adjacent base pairs [20].When accommodating intercalator molecules, the DNA helix lengthens and becomes partially "unwound"; this unwinding is a consequence of rotation around bonds in the sugar-phosphate-ester backbone.[29]

There are many examples of intercalators, such as ethidium bromide, acridine orange, actinomycin and daunomycin (Scheme1.1). All of these compounds have a flat aromatic intercalating motif in common.
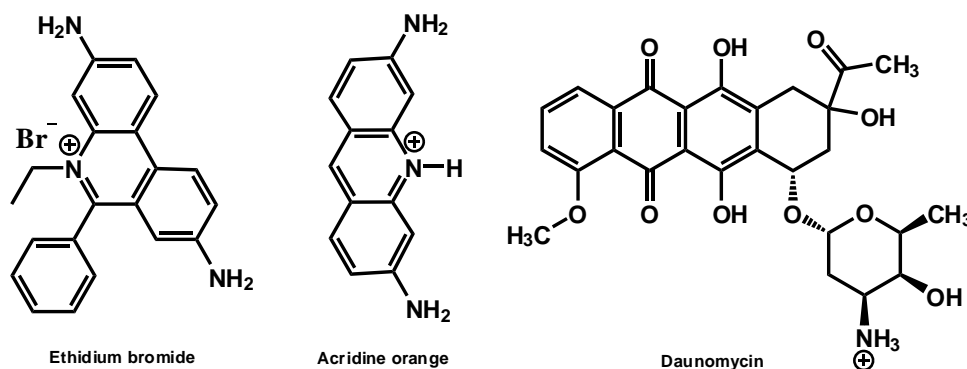
Scheme 1.1

Intercalating pharmaceuticals have been used for a number of years in the treatment of cancer. As mentioned above, Waring noted that intercalation has two effects: the DNA helix lengthens and slightly unwinds, and the phosphate backbone rotates around the torsional bonds within the DNA backbone.[29] This alteration to the DNA backbone, caused by the accommodation of the intercalating molecule, can block the DNA and consequently inhibit the synthesis of RNA and DNA replication; this results in cell death.

As mentioned previously, most intercalating species involve one or more planar aromatic rings. Anthracyclines, e.g. doxorubicin (Scheme 1.2) used for cancer chemotherapy, contain such planar structures and, as such, the inhibition of DNA replication through intercalation at the purine-pyrimidine interface is very effective.

Anthracyclines exhibit a preference for CG sequences.[30, 31] Upon interaction with the DNA, the tetrahydropryan function is placed within the minor groove and forms hydrogen bonds with base pairs below and above itself; in particular, the hydroxyl group in the C9 position hydrogen bonds to two nitrogens of the adjacent guanine. However, their lack of specificity for base pair sequences means that anthracyclines exhibit a very high level of toxicity resulting from interaction with DNA in non-targeted tissue.
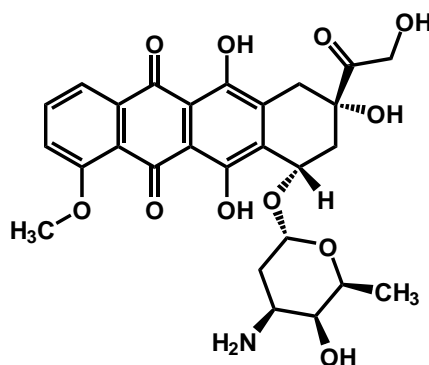
Scheme 1.2 Doxorubicin structure

A molecule that contains two planar aromatic systems connected through a flexible linker may actually intercalate twice to the DNA. Termed bis-intercalation, the double binding approximately doubles the extent of both the elongation and unwinding of the DNA helix.

An interesting example of intercalation is that provided by naphthalene diimine (Figure 1.9), which binds to DNA via a 'threading' mode of intercalation; this involves the insertion of the aromatic system between base pairs, with one of the ionic substituents binding in the minor groove and the other in the major groove.[32]
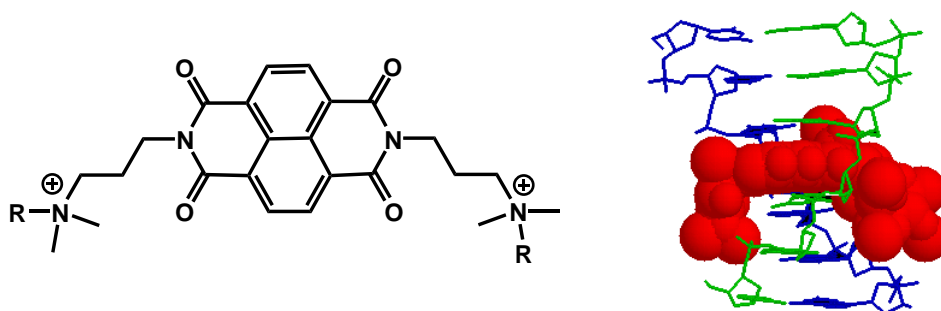
Figure 1.9 Naphthalene diimide structure (left) and binding mode (right).[33]

1.6.3   Minor Groove Binders

As described in Section 1.3, DNA has two types of groove; the major and the minor groove. The small molecules that typically interact with DNA in a non-covalent fashion either intercalate (see Section 1.4.2) or bind in the minor groove. Examples of groove binding are found for a diverse range of small molecules, including antibiotics and drugs. [34, 35]

DNA-binding polyamides are an important class of cell-permeable molecules capable of identifying predetermined and exact sequences within the DNA structure. Dervan *et al* in particular have contributed significantly to the sequence-selective targeting of DNA[36] (more on synthetic DNA-binding polyamides follows later). Dervan and Edelson reviewed

the development of the so-called hairpin polyamides[37] which started with the naturally found antibiotic distamycin (Figure 1.10), which is a good example of a minor-groove binder.[38]
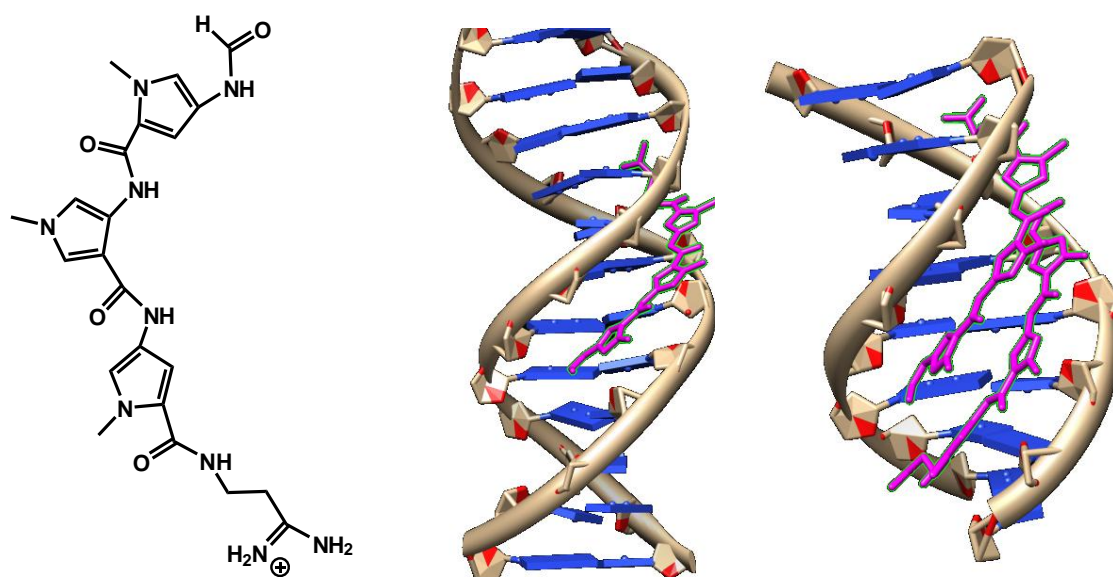
Figure 1.10 Structure of (a) Distamycin, the groove binding modes of distamycin with DNA duplexes, 1:1 binding of distamycin to DNA (NDB ID: GDL 003) (b); side-by-side binding of distamycin to DNA (NDB ID:GDH060) (c).

Figure 1.10 illustrates that Distamycin A has an oligopeptidic pyrrolecarbamoyl backbone, terminating in an amidino function. Distamycin A is found to reversibly bind to the minor groove by means of Van der Waals forces, hydrogen bonding and electrostatic contacts, especially with adenine-thymine (A●T) base pairs.[39] Changing the number of pyrrole units leads to greater availability of hydrogen bonding.[40]

Minor groove binders are typically formed from a chain of aromatic species (e.g. phenyl or pyrrole groups) and the bonds between the aromatic rings allow a large degree of torsional movement. This torsional freedom allows the contortion of the molecule to suitably fit the minor groove, and most minor groove binders are generally overall crescent-shaped.[41] An example of this crescent shape is provided by netropsin (Figure

1.11), an antibiotic active towards both gram-positive and gram-negative bacteria, which was isolated by Finlay *et al.*[42] Netropsin binds to AT-rich sequences of DNA.
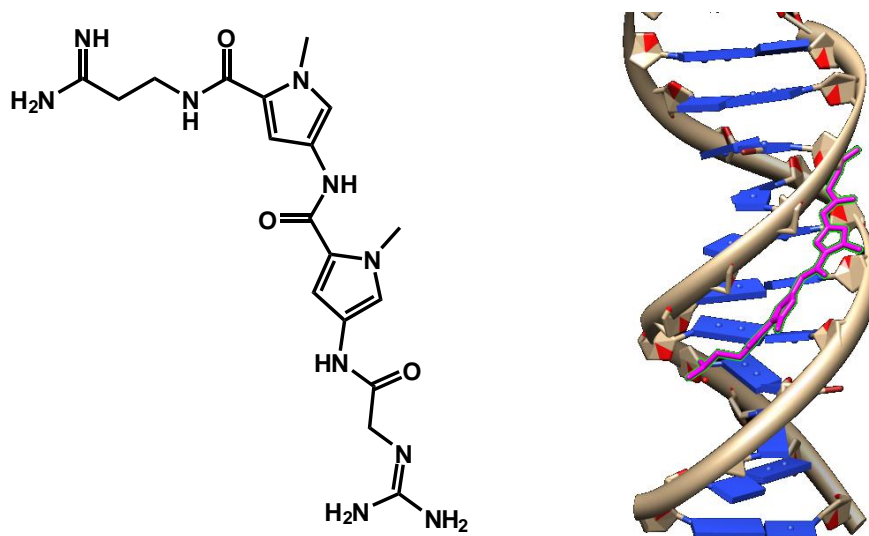
Figure 1.11 (a) Netrospin structure and (b) 1:1 binding of netropsin in the minor groove (based on NDB ID: GDL B05)

DNA-binding of netropsin is achieved through the displacement of water molecules that hydrate the minor groove of DNA. In doing this, the NH groups on netropsin form hydrogen bonds to the nitrogen in adenine and the oxygen of thymine on each adjacent base pair.[43]

Another class of minor groove binders are the DB-family of compounds developed by Boykin and Wilson. Boykin and Wilson have even identified examples of binders with sequence selectivity pertaining to sequences containing both A•T and G•C pairs. These binders are nediamidine compounds (Scheme 1.3) that bind to DNA with selectivity for ATGA and GCTCG.[44-47]
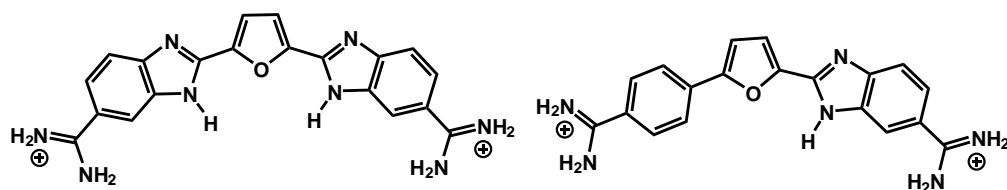
Scheme 1.3 DB270 (a) and DB293 (b).

Another example of a DNA binder, Hoechst 33258, has a π conjugated oligoheteroaromatic framework. Hoechst 33258 has a crescent shape, similar shape to netropsin, and the flexibility to fit into the minor groove (Figure 1.12).[48]
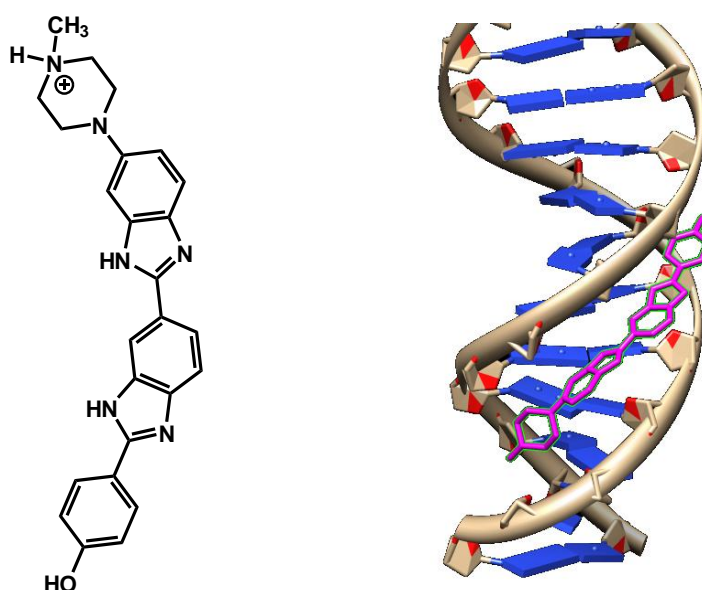
Figure 1.12 Structure of H33258 (left), binding of H33258 to the minor groove (NDB ID: GDL028) (right)

Hoechst 33258 binds to the minor groove specifically in A•T-rich sequences, with a stoichiometry (binding site size) between 4 and 5 base pairs. In addition, Hoechst 33258 binds to G•C-rich sequences in the minor groove with weak affinity.[49]

So far, the sequence selectivity of most minor groove binders is for tracts of A•T base pairs; this innate preference may be partially due to hydration effects in the minor groove resulting in more favourable thermodynamics for the binding process. In addition, the NH_2 group on guanines causes steric hindrance effects for ligands binding to sequences containing G•C pairs.

That binding of synthetic DNA-binders is not restricted to AT-rich DNA was shown by the development of sequence recognition of double-stranded DNA by Dervan's group, using synthetic hairpin polyamides, now commonly called Dervan's hairpin polyamides (DHP). DHPs bind to double stranded DNA in the minor groove in a "side-by-side" mode to form 1:1 complex (Figure 1.13). In addition, this class of compounds provides a 2:1 binding mode for 1-methylimidazole-2-carboxamide netropsin; this binds to TGAT base pairs.[37, 50, 51]

Compounds resulting from Dervan's work have been used against cancerous tumours[51], showing that clinically relevant DNA targeting may be achieved through the use of polyamides. The Dervan hairpin polyamides are probably the most successful concept for the development of DNA binders that are sequence selective.
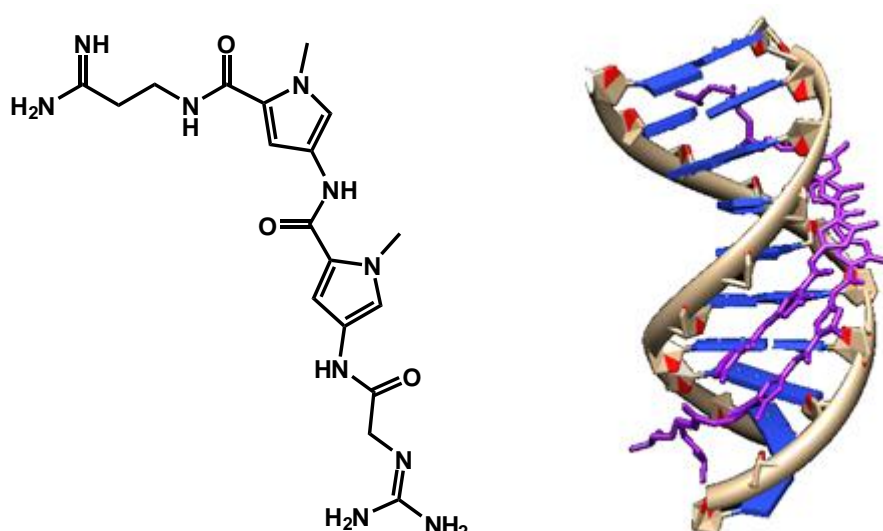
Figure 1.13 X-Ray structure of the "side by side" binding mode of Netropsin as an example of polyamide binders (NDB ID: BDD003).

Unfortunately, standard DHPs do not recognise sequences of more than five base pairs. The reason for this lies in the fact that the curvature of polyamide molecules does not exactly match with the minor groove curvature.[52] Drave's group developed a method with which to continue the polyamide through the creation of links between DHPs. The formation of polyamides that are candy cane shaped, and involve turn-to-tail or turn-to-turn connections maintains the recognition of DNA sequences whilst extending the selectivity to 10 base pairs (Figure 1.14).[53]
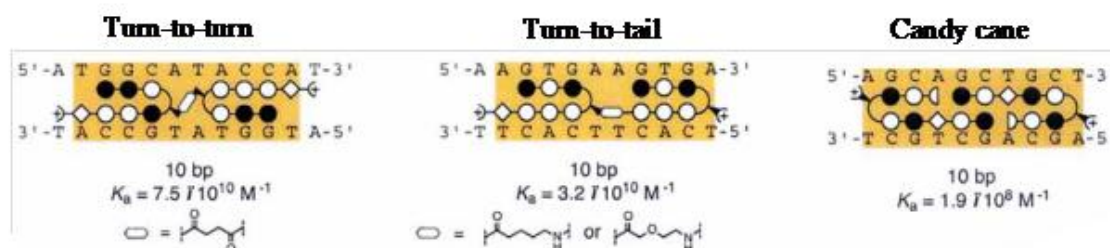
Figure 1.14 Polyamide models for binding to DNA sequences. Picture taken from reference 37.

1.6.4 Major groove binders

As discussed before, major and minor grooves have fundamental differences with regards to hydrogen bonding, the degree of hydration and geometry.[54] Consequently, the types of molecules able to bind to major and minor grooves are very different. Major-grooves in DNA are often optimal sites for the recognition and subsequent binding of larger molecules such as proteins.[55] Considering the structure and size of the major-grooves, it seems to be relatively clear that the recognition and binding properties arise from the possible interaction with a larger number of base-pairs; there is a possibility of increased functionality, and therefore a great increase in the number of sites primed for hydrogen bonding and Van der Waals' interactions.[56]

Due to the larger size of the molecules involved in major-groove binding, and without the increased rigidity of the minor grooves, considerable distortion of the DNA structure can occur.[56]

1.7 Conjugated Polymers

In essence, polymers are molecules constructed of a high but finite number of repeated monomer units, the polymerisation process covalently attaching the monomer units to form a long chained macromolecule. Polymers may be homopolymers (one type of repeat unit) or co-polymers (two or more types of monomer units).[57] Polymers can equally involve conjugated systems, leading to the creation of conjugated polymers. Unlike simple polymers, such as polyethylene, conjugated polymers can be regarded as organic semiconductors. This is due to the semiconducting properties arising from the π-molecular orbitals being delocalised along the polymer chain; specifically the π-bonding and π^*-

antibonding orbitals form both delocalised conduction and valence wave functions, which can act as charge carriers.[58]

Conjugated polymers have a wide range of applications, including applications such as fuel cells, bio-sensors and in drug release to name but three of an extensive list.[59] With respect to DNA, there are many conjugated oligomeric systems capable of binding to DNA. Typically, these conjugated DNA binders are either heteroaromatic species, with aromatic rings bonded to each other, or are extended using alkene units for further conjugation. Most of these systems carry cationic functional groups. The positive charge assists binding to the DNA due to favourable electrostatic interactions with the negatively charged phosphate ester backbone of DNA.[60] An example of this type of binders is provided by the aforementioned "DB"family of binders prepared by Boykin and Wilson (Scheme 1.4). The DNA affinity of this kind of molecules can be increased via alkylation. For example,the addition of cyclopentyl groups in DB244 allows these molecules to fit into the minor groove and hold the amidines in a more static position.[61, 62]
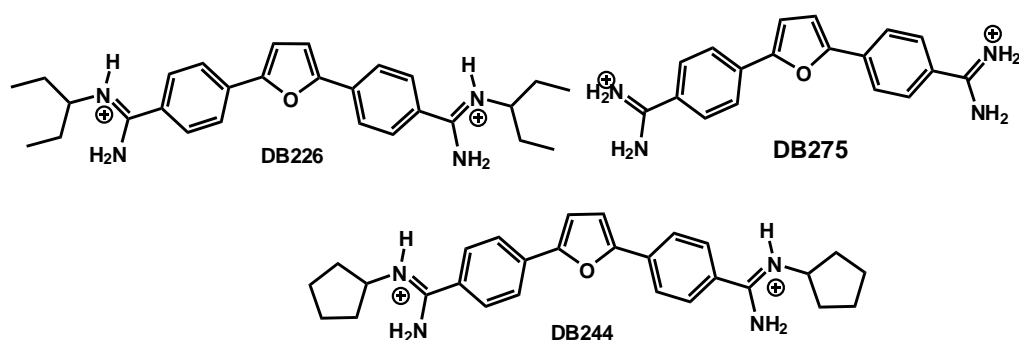
Scheme 1.4 DB226 (a), DB275 (b) and DB244 (c)

The substitution of conjugated polymers with specific functional groups opens routes to, for example, new sensing properties and control of solubility. Tang *et al* developed a conjugated polymer in which the DNA base thymine was covalently attached to a

polythiophene backbone. The thymine-polythiophene conjugate polymer (Scheme 1.5) was found to be a particularly effective sensor for mercury ions. In the absence of Hg(II) ions, the polythiophene strands are separated and give a strong fluorescence response. Upon addition of Hg(II) inter-polymer π-stacking is initiated through thymine-Hg-thymine interactions and this stacking results in quenching of the fluorescence.[63, 64]
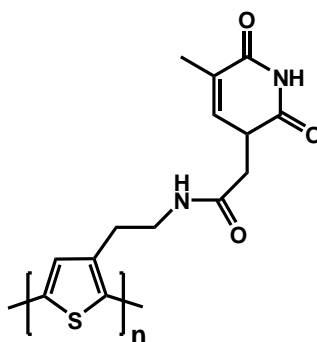
Scheme 1.5 Polythiophene carrying thymine functional groups.

Polythiophenes themselves are also of interest in sensing, for example of ions and nucleic acids in aqueous solution. Upon interaction with a target, the conjugated backbone may twist, leading to a change in effective conjugation and a concomitant change in the optoelectronic properties of the polymer. Examples of this use of polythiophenes are discussed in the next section.

1.8   Optical detection of DNA

As discussed before, DNA detection is of great significance to the biomedical field and for genetic analysis.[65, 66] The use of (cationic) polythiophenes to study DNA-hybridisation was introduced by Lecler and co-workers.[67] Some structures of oligo- and polythiophenes that have been used in the detection of DNA are illustrated in Scheme 1.5.
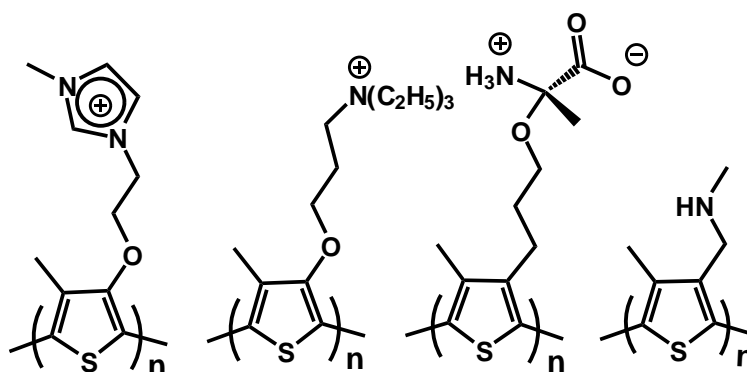
Scheme 1.5

The sequence-selective detection of single-stranded DNA employs the flexibility of the polythiophene backbone as follows. First, recording the UV-visible spectrum for a water-soluble cationic polythiophene in aqueous solution shows it to have a maximum absorption of around 397 nm. Second, adding a single strand of negatively charged DNA leads to the production of a strong red-shift, which has been attributed to "planarising" the polythiophene backbone. Third, if complementary single-stranded DNA was added, this resulted in the formation of the complex of double-stranded oligonucleotide with cationic polythiophene. A blue-shift was observed in the UV-visible spectrum relative to the single strand − polythiophene complex, but the final absorbance is still red-shifted when compared with the absorption of free cationic polythiophene. Practically, the colour of the optical change can be seen with the naked eye. The colour of the free cationic polythiophene changed from yellow to red after the addition of the single strand of DNA, and then back to yellow through the addition of the complementary single strand of DNA (Figure 1.15). An induced CD signal was observed throughout the interaction, suggesting a groove binding mode for cationic polythiophene.[68, 69]
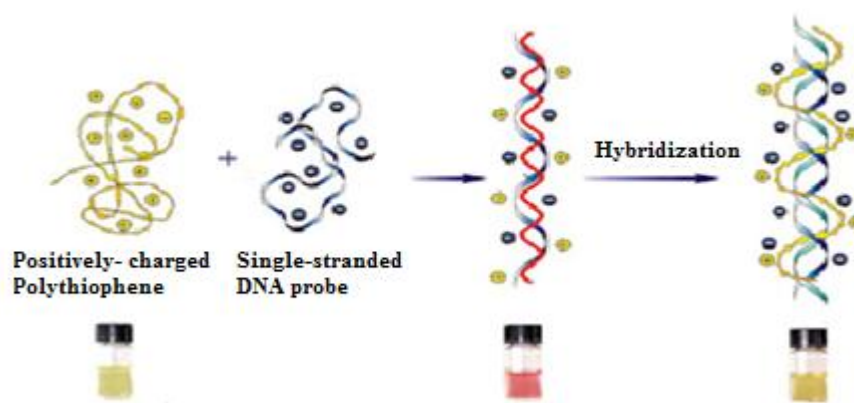
Figure 1.15 Optical detection of double-stranded DNA taken from reference 69.

1.9 Click chemistry

Click chemistry should be regarded as a philosophy of organic synthesis, and was first proposed by Sharpless *et al.* in 2001.[70]

Sharpless observed that, in conventional organic synthesis, a target molecule (typically a complex natural product) derives from a series of complicated steps comprising many intermediates. It was then proposed by Sharpless that the experimentalist should mimic the methodology of nature, specifically through the use of simple molecules to create novel products.[70] Sharpless states that the ideal reaction would be modular, provide high yields, and produce only harmless (i.e. green) by-products, which can be easily isolated. The process also needs to involve simple reaction conditions, available starting materials, ideally without solvent, with water utilised for the solvent, or another solvent that can be removed easily. In practical terms, this means that reactions should display a strong thermodynamic driving force of more than 20 $kcal\,mol^{-1}$ to fulfil click reaction characteristics.[70, 71]

These criteria are, of course, subjective, and although the philosophy is solid, it is highly unlikely that all the criteria are equally applicable to all possible click reactions.

Figure 1.16 shows possible reactions that could be considered to qualify as click chemistry.
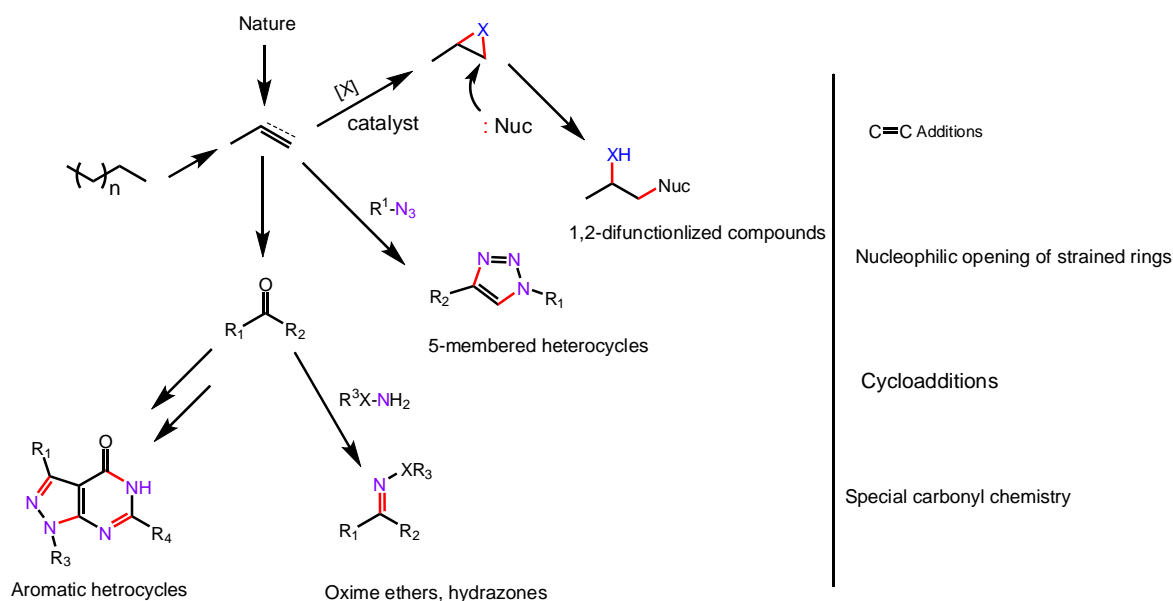
Figure 1.16 Possible click chemistry routes.[71]

When discussing click chemistry, the azide-alkyne Huisgen cycloaddition can perhaps be considered the 'classical' click reaction. This is the 1,3-dipolar cycloaddition of an alkyne with an internal or terminal azide function (Scheme 1.7).[72]
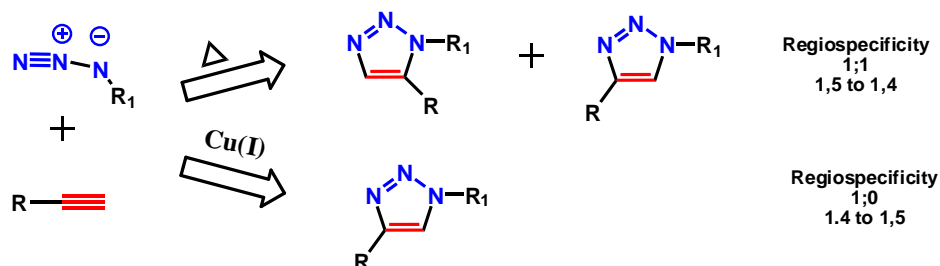
Scheme 1.7 The Huisgen cycloaddition reaction in the presence and absence of Cu(I).

The alkyne cleanly undergoes the reaction with the azide to form the 1,4 and 1,5 cycloadducts at 92 °C for 18 hrs; however, a high activation barrier is responsible for a very low rate constant, and hence rate of reaction.[73] A notable variation of this, wherein the reaction rates are increased by 10^6-fold, is the copper(I)-catalysed form of this reaction in which organic azides and terminal alkynes react, yielding 1,4-regioisomers of 1,2,3-triazoles as sole products (substitution at positions 1' and 4' as shown in Scheme 1.8). This catalysed reaction permits a much broader range of temperatures and pH, and products may be typically isolated using simple filtration, negating any chromatography.[74] The Cu(I) catalytic species may be introduced in several different ways. The first is perhaps the most widely used, especially due to the low cost of copper salts, and includes the use of a Cu(I) salt such as CuI or $[Cu(NCCH_3)_4][PF_6]$, although a nitrogen base (e.g. pyridine or triethylamine) is required, and the formation of diacetylenes and bis-triazoles are unwelcome side effects. A second method is to use a Cu(II)/Cu(0) cycling system, which is useful for systems sensitive to ascorbic acid, for example. The final method comprises the use of copper supported on carbon (Cu/C) in the presence of trimethylamine. This catalytic system is ideal for cases where simple and efficient removal of the catalyst is required; in this case, the catalyst is simply removed through filtration. Using ligands on the copper catalyst in the click reaction can also be used to increase the rate of the reaction, and for the protection of the Cu(I) from oxidation; this maintains the concentration of Cu(I).[75-77]
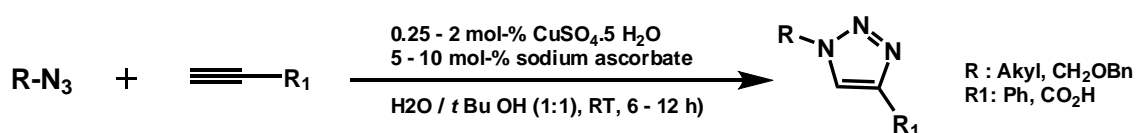
Scheme 1.8 The Cu-catalysed azide-alkyne cycloaddition (CuAAC)

Computational work using density functional theory (DFT)[74] has suggested a mechanism for the Cu-catalysed azide-alkyne cycloaddition (CuAAC - Scheme 1.9).
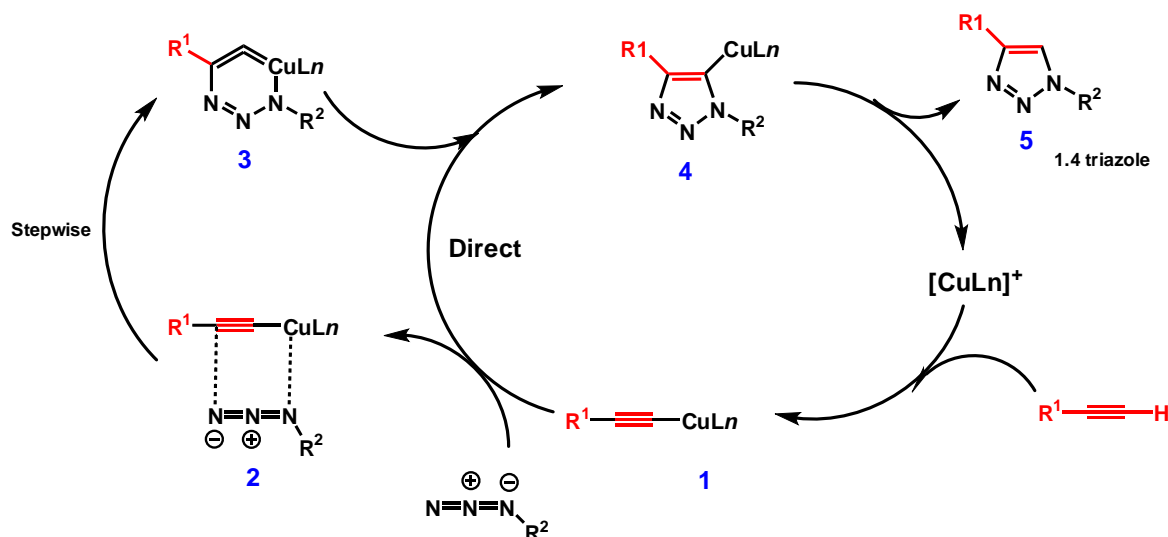
Scheme 1.9 Proposed mechanism for the CuAAC reaction.[73]

The mechanism involves two pathways. The first proposed pathway is a direct cycloaddition, with the second being a stepwise sequence (1→2→3). The DFT results yield strong evidence favouring the stepwise pathway, which is 50-62 kJ mol^{-1} more favourable than the direct pathway.[73]

The applicability of the click reaction is wide-spread; for example, in biological applications, click chemistry has been used to form and modify fluorescent oligonucleotides to improve study DNA sequencing[78] and biological inhibitors for enzymes such as HIV-1 protease.[79] Click chemistry is of great importance in drug discovery, aiding the development of discovery libraries and rapid optimisation of structures. The absence of by-products and high yields of click reactions also aids the screening, due to little or no purification requirements.[71]

An example of the biocompatibility of the click reaction is provided by the chemical derivatisation of the Copea mosaic virus (CPMV). Upon the discovery that the CuAAC could be performed with ease in water, Finn *et al.* used it to decorate CPMV with dyes. CPMV is a rigid ensemble of 60 identical copies of a 2-protein asymmetric unit surrounding the virus' RNA genome. The virus has lysine and cysteine residues at the exterior surface, which were decorated with alkynes and azides to allow the coupling of dyes *via* CuACC.[80-82]

This method was further developed in another study by Finn *et al* [83], who used a new water-soluble sulfonated bathophenanthroline ligand for the copper catalyst (1.10).
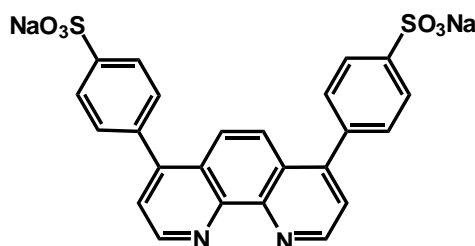
Scheme 1.10 Structure of sulfonated bathophenanthroline ligand.

Whilst the Cu-complex of this ligand displays high reaction rates with low concentrations of labelling substrates, the copper catalyst becomes more sensitive to oxidation, and so the reaction must be performed under an inert atmosphere.

With regards to carbohydrate chemistry, there are numerous examples in the literature that illustrate the linking of saccharides to a central structure or functionality, such as a peptide or pharmacologically active compound through CuAAC. For example, the synthesis of triazole-linked glycosaccharides has solved the problems associated with the sensitivity of glycoside links toward hydrolysis, which meant they were unsuitable lead compounds.[84, 85]

31

Danishefsky *et al.* used a series of triazole-forming click reactions to combine three carbohydrate tumour antigens on a polypeptide skeleton (Scheme 1.11).[86]
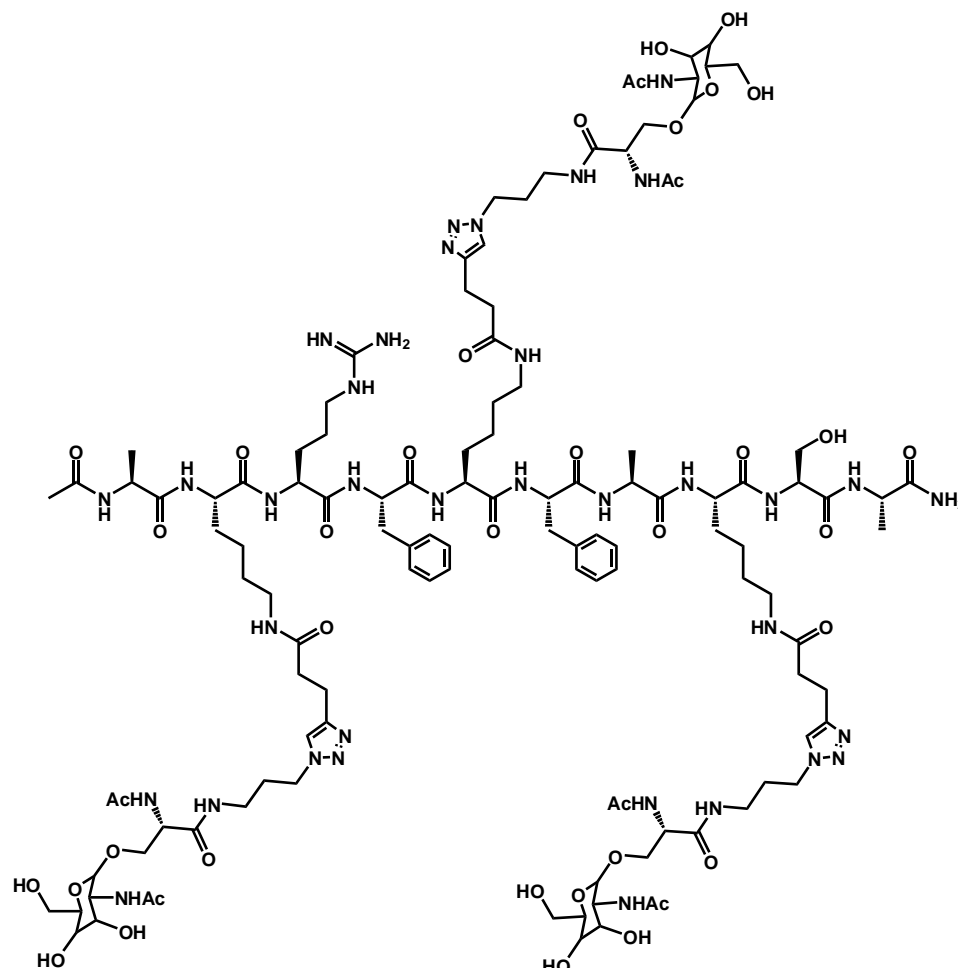
Scheme 1.11 Glycopeptide fragments joined *via* click chemistry. Taken from reference 86.

From the preceding, it is clear that click chemistry is an extremely useful synthetic route for bioconjugate production. The potential of click chemistry stretches further because it also lends itself to biomolecule labelling *in vivo*, especially for conjugation with saccharides, proteins, peptides and with DNA itself. Meldal *et al.*, for example, in their work on the triazole CuAAC, used it for peptides, demonstrating the reaction conditions to be wholly compatible with peptide synthesis.[76]

Uses of click chemistry in relation to DNA include the area of DNA sequencing, providing increased efficiency of the Sanger method under relatively mild conditions, and without by-product formation[87]. Carrell *et al.* used the CuAAC to decorate DNA, which had undergone alkyne modification, to a high-degree with azido-appended labels[88]. Complex biological species, including viruses, cells, enzymes, and proteins can be equally functionalised using azide-alkyne chemistry.[81, 89, 90]

The internal covalent cross-linking of complementary DNA strands has also been achieved through a click reaction between a number of azide- and alkyne-modified uracil monomers, yielding highly stable duplexes.[91] The synthesis of large, covalently closed DNA catenanes has been undertaken by Kumar *et al.,* who formulated an efficient methodology of oligonucleotide ligation through the use of CuAAC (Figure 1.17).[92]
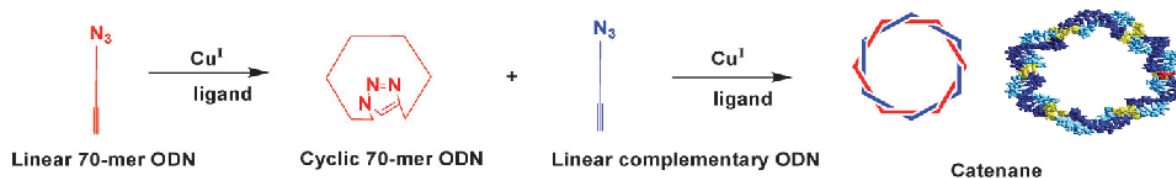
Figure 1.17 Preparation of a DNA catenane (double stranded) from the cyclic template.[92]

In this process, two strands, the first containing a 3'-azide and the second a 5'-alkyne, are joined through a template-controlled triazole cyclisation. The complementary DNA strand, which also possesses 3'-azide and 5'-alkyne terminal groups, was annealed to form the cyclic structure, before undergoing CuAAC to yield the double-stranded catenane with two stable triazole units. The method can equally be applied to the construction of smaller hexaethylene glycol bridge duplexes, which are highly stable.

The combination of DNA and click chemistry has also been efficiently used in the preparation of nano-and microscale assemblies, which can be used as nanoelectronic devices. The application of DNA metallization has been used to study the possibility of increasing the conductivity of DNA-based nano-and microstructures, thus enabling such DNA nanostructures to be used as molecular wires. The oligonucleotide metallisation process involves the chemical reduction of DNA-complexed metal. This metallisation process requires modified DNA which allows the metal complexation. The required DNA is conveniently generated using DNA polymerases which allow the incorporation of acetylene-appended nucleotides during the polymerase chain reaction (PCR). PCR is followed by a click reaction attaching aldehyde functional groups (precursors for metal-binding carboxylates) to the DNA. The click reaction can be carried out directly on a polyacrylamide gel (Figure 1.18). The advantage of inserting the alkyne group as a label biologically is that it facilities the preparation of DNA wires, and additionally provides the possibility of using the tools of molecular biology to create a conductive DNA nanodevice.[93]
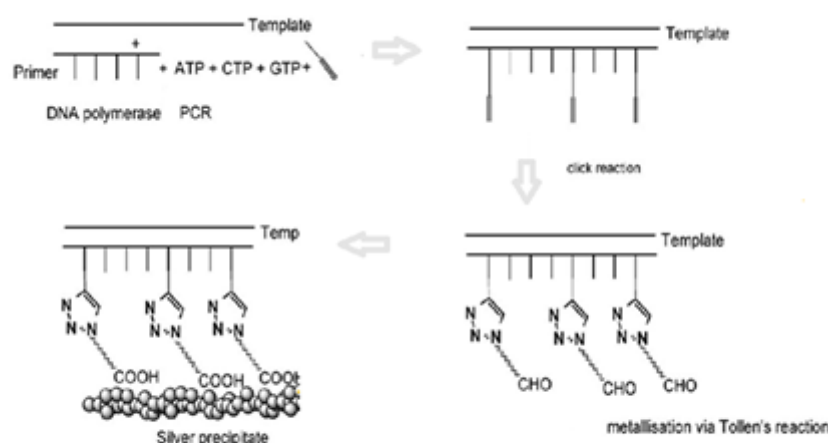
Figure 1.18 DNA metallisation *via* click chemistry.[93]

Oligonucleotide immobilisation is one of the most important applications of click chemistry, and various studies[94] indicate that click chemistry offers an efficient method for the immobilisation of DNA. Click chemistry was used to immobilise oligonucleotides by "microcontact printing". The alkyne functional groups on oligonucleotides were made to react with an azide-terminated glass slide, thus forming a triazole ring as a link between the surface and the oligonucleotides (Figure 1.19).[93, 94]
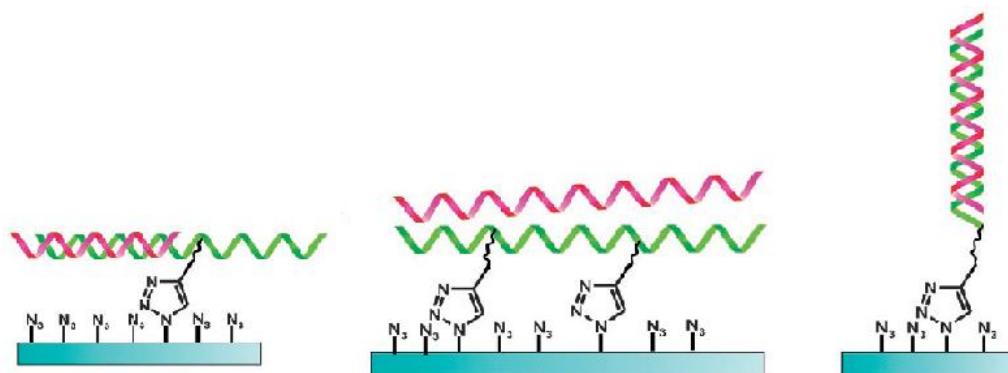
Figure 1.19 DNA immobilisation through click chemistry. Taken from reference 93.

1.10 Project Aims

The development of molecules that bind to specific DNA sequences is essential to the field of pharmaceuticals. Such species have therapeutic potential; for example, they can be employed as anti-tumor agents, blocking interaction of mutated sequences with proteins. Similarly, sequence-selective DNA binders undergoing significant changes in physical properties (absorbance spectra, redox properties) upon interaction with DNA can be used as components for genosensors (biosensors for DNA).

The project aims to prepare and develop new conjugated oligoheteroaromatic compounds with significant structural variation, which can be used as DNA binders. The targeted compounds have spectroscopic and electronic properties that may change upon interaction with DNA, potentially allowing various applications including in biosensors. The most significant goal of this thesis is the design and preparation of molecules that present selectivity for the minor groove in duplex DNA, ideally showing sequence selectivity as well. Click chemistry has been used as an important component of the synthetic strategy, creating various structures that offer the potential of providing affinities and specificities required for useful duplex DNA binding.

The overall design of our DNA binders is summarised in Scheme 1.12.
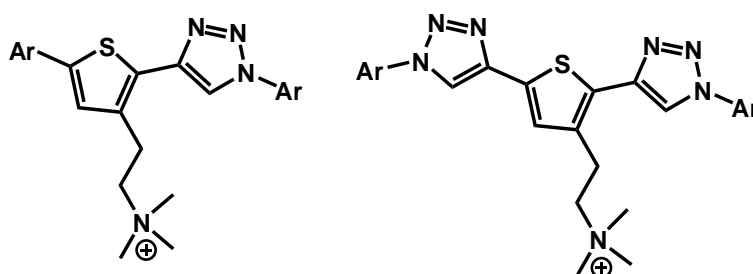
Scheme 1.12

All of these structures obviously include at least one triazole ring; the inclusion of a triazole ring could increase the affinity of these molecules for DNA by forming hydrogen bonds between the nitrogen atoms in the ligand and on the base pairs in DNA. We note that, whereas the triazole ring appears to extend the conjugated framework of these molecules rather nicely, it has been reported that the triazole ring is unfortunately similar to an amide functional group in terms of extending conjugation along conjugated polymers.

The cationic charges give the ligands the potential for electrostatic interaction with the negative charge backbone of duplex DNA, further increasing the binding affinity. The cationic charges further serve the purpose of making all of these molecules water soluble.

The anticipated effects of DNA binding on the electronic and spectroscopic properties of the compounds should result in the development of diagnostic applications. Moreover, the use of click chemistry and the associated synthesis of alkyne- and azide-appended oligoheteroaromatic intermediates generate the opportunity for the connection of these molecules to the surface of electrodes, which could form an important step in the development of these compounds as biosensors.

References

1.   Gottesfeld, J. M.; Neely, L.; Trauger, J. W.; Baird, E. E.; Dervan, P. B., *Nature* **1997,** *387* (6629), 202-205.

2.   Dahm, R., *Human Genetics* **2008,** *122* (6), 565-581.

3.   Levene, P. A., *Journal of Biological Chemistry* **1919,** *40* (2), 415-424.

4.   Urnov, F. D.; Rebar, E. J.; Holmes, M. C.; Zhang, H. S.; Gregory, P. D., *Nature Reviews Genetics* **2010,** *11* (9), 636-646.

5.   Sriram, M.; Vandermarel, G. A.; Roelen, H.; Vanboom, J. H.; Wang, A. H. J., *Embo Journal* **1992,** *11* (1), 225-232.

6.   Burton, P. R.; Clayton, D. G.; Cardon, L. R.; Craddock, N.; Deloukas, P.; Duncanson, A.; Kwiatkowski, D. P.; McCarthy, M. I.; Ouwehand, W. H.; Samani, N. J.; Todd, J. A.; Donnelly, P.; Barrett, J. C.; Davison, D.; Easton, D.; Evans, D.; Leung, H. T.; Marchini, J. L.; Morris, A. P.; Spencer, C. C. A.; Tobin, M. D.; Attwood, A. P.; Boorman, J. P.; Cant, B.; Everson, U.; Hussey, J. M.; Jolley, J. D.; Knight, A. S.; Koch, K.; Meech, E.; Nutland, S.; Prowse, C. V.; Stevens, H. E.; Taylor, N. C.; Walters, G. R.; Walker, N. M.; Watkins, N. A.; Winzer, T.; Jones, R. W.; McArdle, W. L.; Ring, S. M.; Strachan, D. P.; Pembrey, M.; Breen, G.; St Clair, D.; Caesar, S.; Gordon-Smith, K.; Jones, L.; Fraser, C.; Green, E. K.; Grozeva, D.; Hamshere, M. L.; Holmans, P. A.; Jones, I. R.; Kirov, G.; Moskvina, V.; Nikolov, I.; O'Donovan, M. C.; Owen, M. J.; Collier, D. A.; Elkin, A.; Farmer, A.; Williamson, R.; McGuffin, P.; Young, A. H.; Ferrier, I. N.; Ball, S. G.; Balmforth, A. J.; Barrett, J. H.; Bishop, D. T.; Iles, M. M.; Maqbool, A.; Yuldasheva, N.; Hall, A. S.; Braund, P. S.; Dixon, R. J.; Mangino, M.; Stevens, S.; Thompson, J. R.; Bredin, F.; Tremelling, M.; Parkes, M.; Drummond, H.; Lees, C. W.; Nimmo, E. R.; Satsangi, J.; Fisher, S. A.; Forbes, A.; Lewis, C. M.; Onnie, C. M.; Prescott, N. J.; Sanderson, J.; Mathew, C. G.; Barbour, J.; Mohiuddin, M. K.; Todhunter, C. E.; Mansfield, J. C.; Ahmad, T.; Cummings, F. R.; Jewell, D. P.; Webster, J.; Brown, M. J.; Lathrop, G. M.; Connell, J.; Dominiczak, A.; Marcano, C. A. B.; Burke, B.; Dobson, R.; Gungadoo, J.; Lee, K. L.; Munroe, P. B.; Newhouse, S. J.; Onipinla, A.; Wallace, C.; Xue, M. Z.; Caulfield, M.; Farrall, M.; Barton, A.; Bruce, I. N.; Donovan, H.; Eyre, S.; Gilbert, P. D.; Hider, S. L.; Hinks, A. M.; John, S. L.; Potter, C.; Silman, A. J.; Symmons, D. P. M.; Thomson, W.; Worthington, J.; Dunger, D. B.; Widmer, B.; Frayling, T. M.; Freathy, R. M.; Lango, H.; Perry, J. R. B.; Shields, B. M.; Weedon, M. N.; Hattersley, A. T.;

Hitman, G. A.; Walker, M.; Elliott, K. S.; Groves, C. J.; Lindgren, C. M.; Rayner, N. W.; Timpson, N. J.; Zeggini, E.; Newport, M.; Sirugo, G.; Lyons, E.; Vannberg, F.; Brown, M. A.; Franklyn, J. A.; Heward, J. M.; Simmonds, M. J.; Hill, A. V. S.; Bradbury, L. A.; Farrar, C.; Pointon, J. J.; Wordsmith, P.; Gough, S. C. L.; Seal, S.; Stratton, M. R.; Rahman, N.; Ban, M.; Goris, A.; Sawcer, S. J.; Compston, A.; Conway, D.; Jallow, M.; Bumpstead, S. J.; Chaney, A.; Downes, K.; Ghori, M. J. R.; Gwilliam, R.; Inouye, M.; Keniry, A.; King, E.; McGinnis, R.; Potter, S.; Ravindrarajah, R.; Whittaker, P.; Withers, D.; Pereira-Gale, J.; Hallgrimsdottir, I. B.; Howie, B. N.; Su, Z.; Teo, Y. Y.; Vukcevic, D.; Bentley, D.; Wellcome Trust Case Control, C.; Biol, R. A. G.; Genom Study, S.; Breast Canc Susceptib, C., *Nature* **2007,** *447* (7145), 661-678.

7.   Jeffreys, A. J.; Wilson, V.; Thein, S. L., *Nature* **1985,** *314* (6006), 67-73.

8.   Astbury, W. T., *Symposia of the Society for Experimental Biology* **1947,** (1), 66-76.

9.   Watson, J. D.; Crick, F. H. C., *Nature* **1953,** *171* (4356), 737-738.

10.   Wilkins, M. H. F.; Stokes, A. R.; Wilson, H. R., *Nature* **1953,** *171* (4356), 738-740.

11.   Pauling, L.; Corey, R. B., *Proceedings of the National Academy of Sciences of the United States of America* **1951,** *37* (5), 235-240.

12.   Jeremy M. Berg, J. L. T., Lubert Stryer, *Biochemistry,*. WH Freeman and Company: New York, 2006.

13.   Franklin, R. E.; Gosling, R. G., *Nature* **1953,** *172* (4369), 156-157.

14.   Yakovchuk, P.; Protozanova, E.; Frank-Kamenetskii, M. D., *Nucleic Acids Research* **2006,** *34* (2), 564-574.

15.   Rich, A.; Nordheim, A.; Wang, A. H. J., *Annual Review of Biochemistry* **1984,** *53*, 791-846.

16.   Wing, R.; Drew, H.; Takano, T.; Broka, C.; Tanaka, S.; Itakura, K.; Dickerson, R. E., *Nature* **1980,** *287* (5784), 755-758.

17.   Johnson, N. P.; Hoeschele, J. D.; Kuemmerle, N. B.; Masker, W. E.; Rahn, R. O., *Chemico-Biological Interactions* **1978,** *23* (2), 267-271.

18.   Sorenson, C. M.; Eastman, A., *Cancer Research* **1988,** *48* (16), 4484-4488.

19.   Sorenson, C. M.; Eastman, A., *Cancer Research* **1988,** *48* (23), 6703-6707.

20.   Richards, A. D.; Rodger, A., *Chemical Society Reviews* **2007,** *36* (3), 471-483.

21.   Osypov, A. A.; Krutinin, G. G.; Kamzolova, S. G., *Journal of Bioinformatics and Computational Biology* **2010,** *8* (3), 413-425.

22.   Polozov, R. V.; Dzhelyadin, T. R.; Sorokin, A. A.; Ivanova, N. N.; Sivozhelezov, V. S.; Kamzolova, S. G., *Journal of Biomolecular Structure & Dynamics* **1999,** *16* (6), 1135-+.

23.   West, S. M.; Rohs, R.; Mann, R. S.; Honig, B., *Journal of Biomolecular Structure & Dynamics* **2010,** *27* (6), 861-866.

24.   Blackburn GM, G., MJ, *Nucleic Acids in Chemistry and Biology*. OUP, Oxford: 1990.

25.   Lerman, L. S., *Journal of Molecular Biology* **1961,** *3* (1), 18-&.

26.   Luzzati, V.; Lerman, L. S.; Masson, F., *Journal of Molecular Biology* **1961,** *3* (5), 634-&.

27.   Boresch, S.; Karplus, M., *Journal of Molecular Biology* **1995,** *254* (5), 801-807.

28.   Strekowski, L.; Wilson, B., *Mutation Research-Fundamental and Molecular Mechanisms of Mutagenesis* **2007,** *623* (1-2), 3-13.

29.   Waring, M., *Journal of Molecular Biology* **1970,** *54* (2), 247-279.

30.   Temperini, C.; Messori, L.; Orioli, P.; Bugno, C. D.; Animati, F.; Ughetto, G., *Nucleic Acids Research* **2003,** *31* (5), 1464-1469.

31.   Wang, A. H. J. A., *Curr. Opin. Struct. Biol* **1992,** *2*, 361-368.

32.   Tanious, F. A.; Yen, S. F.; Wilson, W. D., *Biochemistry* **1991,** *30* (7), 1813-1819.

33.   V. Steullet, D. W. D., S. Takenaka, and W.D. Wilson Studies of Naphthalene Diimides

as DNA-binding Agents.

34.   Wemmer, D. E.; Dervan, P. B., *Current Opinion in Structural Biology* **1997,** *7* (3), 355-361.

35.   Neidle, S., *Biopolymers* **1997,** *44* (1), 105-121.

36.   Dickinson, L. A.; Burnett, R.; Melander, C.; Edelson, B. S.; Arora, P. S.; Dervan, P. B.; Gottesfeld, J. M., *Chemistry & Biology* **2004,** *11* (11), 1583-1594.

37.   Dervan, P. B.; Edelson, B. S., *Current Opinion in Structural Biology* **2003,** *13* (3), 284-299.

38.   Arcamone, F.; Nicolell.V; Penco, S.; Orezzi, P.; Pirelli, A., *Nature* **1964,** *203* (494), 1064-&.

39.   Pelton, J. G.; Wemmer, D. E., *Journal of the American Chemical Society* **1990,** *112* (4), 1393-1399.

40.   Marchini, S.; Broggini, M.; Sessa, C.; D'Incalci, M., *Expert Opinion on Investigational Drugs* **2001,** *10* (9), 1703-1714.

41.   Wang, L.; Kumar, A.; Boykin, D. W.; Bailly, C.; Wilson, W. D., *Journal of Molecular Biology* **2002,** *317* (3), 361-374.

42.   Finlay, A. C.; Hochstein, F. A.; Sobin, B. A.; Murphy, F. X., *Journal of the American Chemical Society* **1951,** *73* (1), 341-343.

43.   Kopka, M. L.; Yoon, C.; Goodsell, D.; Pjura, P.; Dickerson, R. E., *Proceedings of the National Academy of Sciences of the United States of America* **1985,** *82* (5), 1376-1380.

44.   Bailly, C.; Tardy, C.; Wang, L.; Armitage, B.; Hopkins, K.; Kumar, A.; Schuster, G. B.; Boykin, D. W.; Wilson, W. D., *Biochemistry* **2001,** *40* (33), 9770-9779.

45.   Munde, M.; Ismail, M. A.; Arafa, R.; Peixoto, P.; Collar, C. J.; Liu, Y.; Hu, L. X.; David-Cordonnier, M. H.; Lansiaux, A.; Bailly, C.; Boykin, D. W.; Wilson, W. D., *Journal of the American Chemical Society* **2007,** *129* (44), 13732-13743.

46.   Nguyen, B.; Hamelberg, D.; Bailly, C.; Colson, P.; Stanek, J.; Brun, R.; Neidle, S.; Wilson, W. D., *Biophys. J.* **2004,** *86* (2), 1028-1041.

47.   Wang, L.; Bailly, C.; Kumar, A.; Ding, D.; Bajic, M.; Boykin, D. W.; Wilson, W. D., *Proceedings of the National Academy of Sciences of the United States of America* **2000,** *97* (1), 12-16.

48.   Harshman, K. D.; Dervan, P. B., *Nucleic Acids Research* **1985,** *13* (13), 4825-4835.

49.   Moon, J. H.; Kim, S. K.; Sehlstedt, U.; Rodger, A.; Norden, B., *Biopolymers* **1996,** *38* (5), 593-606.

50.   Dervan, P. B., *Bioorg. Med. Chem.* **2001,** *9* (9), 2215-2235.

51.   Mrksich, M.; Wade, W. S.; Dwyer, T. J.; Geierstanger, B. H.; Wemmer, D. E.; Dervan, P. B., *Proceedings of the National Academy of Sciences of the United States of America* **1992,** *89* (16), 7586-7590.

52.   Kelly, J. J.; Baird, E. E.; Dervan, P. B., *Proceedings of the National Academy of Sciences of the United States of America* **1996,** *93* (14), 6981-6985.

53.   Hsu, C. F.; Phillips, J. W.; Trauger, J. W.; Farkas, M. E.; Belitsky, J. M.; Heckel, A.; Olenyuk, B. Z.; Puckett, J. W.; Wang, C. C. C.; Dervan, P. B., *Tetrahedron* **2007,** *63* (27), 6146-6151.

54.   Neidle, S., *DNA structure and recognition (in focus)*. Oxford University Press: 1994.

55.   Zimmer, C.; Wahnert, U., *Progress in Biophysics & Molecular Biology* **1986,** *47* (1), 31-112.

56.   Harrison, S. C.; Aggarwal, A. K., *Annual Review of Biochemistry* **1990,** *59*, 933-969.

57.   Painter, P. C. C., Michael M., *Fundamentals of Polymer Science: an introductory text. .* Technomic Pub. Co.: Lancaster, 1997.

58.   Burroughes, J. H.; Bradley, D. D. C.; Brown, A. R.; Marks, R. N.; Mackay, K.; Friend, R. H.; Burns, P. L.; Holmes, A. B., *Nature* **1990,** *347* (6293), 539-541.

59.   Reddinger, J. L.; Reynolds, J. R., *Radical Polymerisation Polyeletrolytes* **1999,** *145*, 57-122.

60.   Kenward, M.; Dorfman, K. D., *Journal of Chemical Physics* **2009,** *130* (9).

61.   Mazur, S.; Tanious, F. A.; Ding, D. Y.; Kumar, A.; Boykin, D. W.; Simpson, I. J.; Neidle, S.; Wilson, W. D., *Journal of Molecular Biology* **2000,** *300* (2), 321-337.

62.   Wilson, W. D.; Tanious, F. A.; Ding, D. Y.; Kumar, A.; Boykin, D. W.; Colson, P.; Houssier, C.; Bailly, C., *Journal of the American Chemical Society* **1998,** *120* (40), 10310-10321.

63.   Tang, Y. L.; He, F.; Yu, M. H.; Feng, F. D.; An, L. L.; Sun, H.; Wang, S.; Li, Y. L.; Zhu, D. B., *Macromolecular Rapid Communications* **2006,** *27* (6), 389-392.

64.   Chun Li, M. N., Masayuki Takeuchi, and; Shinka, S., *Angew. Chem. Int. Ed.* **2005,** *44*, 6371 –6374.

65.   McQuade, D. T.; Pullen, A. E.; Swager, T. M., *Chemical Reviews* **2000,** *100* (7), 2537-2574.

66.   Taton, T. A.; Mirkin, C. A.; Letsinger, R. L., *Science* **2000,** *289* (5485), 1757-1760.

67.   Ho, H. A.; Boissinot, M.; Bergeron, M. G.; Corbeil, G.; Dore, K.; Boudreau, D.; Leclerc, M., *Angewandte Chemie-International Edition* **2002,** *41* (9), 1548-1551.

68.   Aslund, A.; Nilsson, K. P. R.; Konradsson, P., *Journal of chemical biology* **2009,** *2* (4), 161-75.

69.   Hoang-Anh Ho, M. B.; Michel G. Bergeron, G. v. C., Kim Dore¬,; Denis Boudreau, a. M. L., *Angew. Chem. Int. Ed.* **2002,** *41*, 1548-1551.

70.   Kolb, H. C.; Finn, M. G.; Sharpless, K. B., *Angewandte Chemie-International Edition* **2001,** *40* (11), 2004-+.

71.   Kolb, H. C.; Sharpless, K. B., *Drug Discov. Today* **2003,** *8* (24), 1128-1137.

72.   Huisgen, R., *Proceedings of the Chemical Society of London* **1961,** (OCT), 357-&.

73.   Rostovtsev, V. V.; Green, L. G.; Fokin, V. V.; Sharpless, K. B., *Angewandte Chemie-International Edition* **2002,** *41* (14), 2596-+.

74.   Himo, F.; Lovell, T.; Hilgraf, R.; Rostovtsev, V. V.; Noodleman, L.; Sharpless, K. B.; Fokin, V. V., *Journal of the American Chemical Society* **2005,** *127* (1), 210-216.

75.   Meldal, M.; Tornoe, C. W., *Chemical Reviews* **2008,** *108* (8), 2952-3015.

76.   Tornoe, C. W.; Christensen, C.; Meldal, M., *Journal of Organic Chemistry* **2002,** *67* (9), 3057-3064.

77.   Lipshutz, B. H.; Taft, B. R., *Angewandte Chemie-International Edition* **2006,** *45* (48), 8235-8238.

78.   Seo, T. S.; Li, Z. M.; Ruparel, H.; Ju, J. Y., *Journal of Organic Chemistry* **2003,** *68* (2), 609-612.

79.   Brik, A.; Muldoon, J.; Lin, Y. C.; Elder, J. H.; Goodsell, D. S.; Olson, A. J.; Fokin, V. V.; Sharpless, K. B.; Wong, C. H., *Chembiochem* **2003,** *4* (11), 1246-1248.

80.   Wang, Q.; Chan, T. R.; Hilgraf, R.; Fokin, V. V.; Sharpless, K. B.; Finn, M. G., *Journal of the American Chemical Society* **2003,** *125* (11), 3192-3193.

81.   Speers, A. E.; Adam, G. C.; Cravatt, B. F., *Journal of the American Chemical Society* **2003,** *125* (16), 4686-4687.

82.   Speers, A. E.; Cravatt, B. F., *Chemistry & Biology* **2004,** *11* (4), 535-546.

83.   Sen Gupta, S.; Kuzelka, J.; Singh, P.; Lewis, W. G.; Manchester, M.; Finn, M. G., *Bioconjugate Chemistry* **2005,** *16* (6), 1572-1579.

84.   Baron, A.; Bleriot, Y.; Sollogoub, M.; Vauzeilles, B., *Organic & Biomolecular Chemistry* **2008,** *6* (11), 1898-1901.

85.   Gouin, S. G.; Bultel, L.; Falentin, C.; Kovensky, J., *Eur. J. Org. Chem.* **2007,** (7), 1160-1167.

86.   Wan, Q.; Chen, J. H.; Chen, G.; Danishefsky, S. J., *Journal of Organic Chemistry* **2006,** *71* (21), 8244-8249.

87.   Sanger, F.; Nicklen, S.; Coulson, A. R., *Proceedings of the National Academy of Sciences of the United States of America* **1977,** *74* (12), 5463-5467.

88.   Gierlich, J.; Burley, G. A.; Gramlich, P. M. E.; Hammond, D. M.; Carell, T., *Org. Lett.* **2006,** *8* (17), 3639-3642.

89.   Agard, N. J.; Prescher, J. A.; Bertozzi, C. R., *Journal of the American Chemical Society* **2004,** *126* (46), 15046-15047.

90.   Link, A. J.; Vink, M. K. S.; Tirrell, D. A., *Journal of the American Chemical Society* **2004,** *126* (34), 10598-10602.

91.   Kocalka, P.; El-Sagheer, A. H.; Brown, T., *Chembiochem* **2008,** *9* (8), 1280-1285.

92.   Kumar, R.; El-Sagheer, A.; Tumpane, J.; Lincoln, P.; Wilhelmsson, L. M.; Brown, T., *Journal of the American Chemical Society* **2007,** *129* (21), 6859-6864.

93.   El-Sagheer, A. H.; Brown, T., *Chemical Society Reviews* **2010,** *39* (4), 1388-1405.

94.   Rozkiewicz, D. I.; Gierlich, J.; Burley, G. A.; Gutsmiedl, K.; Carell, T.; Ravoo, B. J.; Reinhoudt, D. N., *Chembiochem* **2007,** *8* (16), 1997-2002.

Chapter 2

SYNTHESIS OF ALKYNE-SUBSTITUTED OLIGOHETEROAROMATIC

COMPOUNDS

Abstract

This chapter describes the synthesis of alkyne-substituted oligoheteroaromatic compounds by means of a range of reactions such as bromination, iodination, and Suzuki, Stille and Sonogashira cross-coupling reactions. The alkyne oligoheteroaromatic compounds, as building blocks for click reaction, were synthesised with good overall yield and purity.

2.1 Introduction

Palladium (Pd) catalysed reactions for C-C bond formation are some of the most widely used and useful reactions in synthesis[1] due to their wide functional group compatibility and the relatively mild reaction conditions.

Polythiophenes are without doubt amongst the most important classes of π-conjugated materials, as illustrated by their wide-scale use in organo-electronic devices and molecular electronics.[2] The frequent changes in either the electronic structure or other properties upon the formation of interactions makes polythiophenes particularly attractive materials for use as sensors with different electronic and optical responses.[3] This responsiveness has ultimately resulted in the synthesis and characterisation of a diverse range of functionalised oligo- and polythiophenes.

**Selected Literature on Pd Cross-Coupling reactions and Polythiophene Synthesis**

The work described within this thesis is principally based on two general reaction types; (a) cross-coupling reactions and (b) "click-chemistry". The latter topic, which was introduced in Chapter 1, is heavily reliant on the reaction between acetylene bonds and azide functions. In the following sections of this Chapter, Pd-catalysed coupling reactions are discussed in the introduction of acetylene groups and other functionalities.

These sections will provide an introduction to the underlying chemistry behind each class of Pd cross-coupling reaction, as well as provide some examples specific to coupling reactions involving thiophenes.

2.1.1 Sonogashira Reaction

The Sonogashira coupling reaction was first reported in 1975 as an extension of the Castro reaction.[4] This is the reaction of a terminal alkyne fragment with vinyl, or aryl halides in the presence of a palladium complex (typically tetrakis(triphenylphosphine)palladium(0), Pd(PPh$_3$)$_4$ or a Pd(II) complex which undergoes reduction in solution), in addition to a copper(I)halide salt, such as Cu(I)iodide.[5] The Sonogashira reaction is typically performed in a basic medium, such as an appropriate mixture of an alkylamine and DMF, enabling the neutralisation of the acidic hydrogen-halides that are formed as part of the coupling reaction, although alternative solvents may be used.[6, 7]

The mechanism of the Sonogashira reaction is summarised in scheme 2.1. The initial stage is the activation of a 1-alkyne by CuI to form a Cu-acetylide.[5] This then undergoes a transmetallation reaction to form an alkynylarylpalladium species, after which the product is formed by means of reductive elimination.

L=phosphene, base, solvent
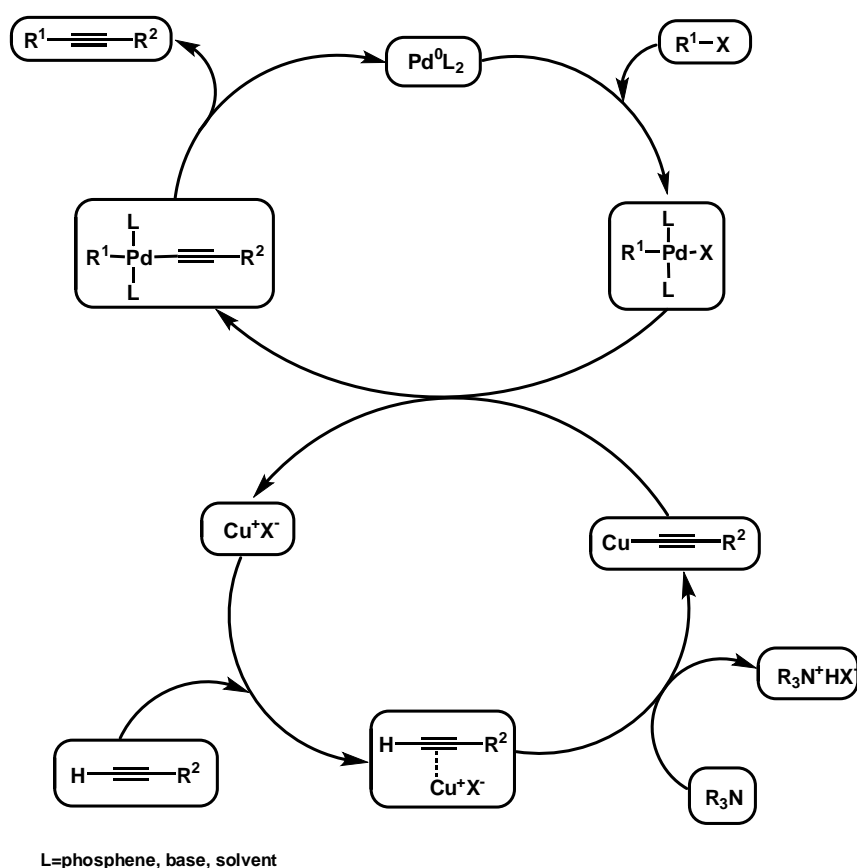
Scheme 2.1 General proposed mechanism for the Sonogashira coupling.[8]

The Sonogashira reaction is important in the connection of alkyne triple bond fragments to aromatic rings. A good review of the reaction can be found in Reference 8. With particular attention to the Sonogashira reaction in thiophene coupling reactions, in 2006 Pal *et al.* published the first successful Pd/C mediated Sonogashira coupling of an iodothiophene with terminal alkynes in aqueous media using Pd/C-CuI-PPh$_3$ (Scheme 2.2).[9]
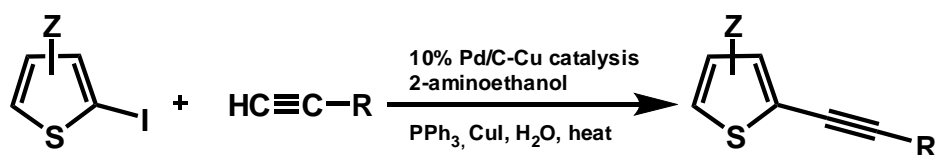
Scheme 2.2

Santelli *et al.* also studied the coupling of a variety of heteroaryl halides with a range of alkynes.[10] Despite the presence of S or N heteroatoms in the substrates, their work returned extremely good yields of alkynylated adducts (Scheme 2.3) regardless of the chain length of the alkyl functionality of the alkyne.


Halogeno thiphenes:
2-bromothiophene
2-iodothiophene
R = Ph, CH₂OH, (CH₂)₂OH
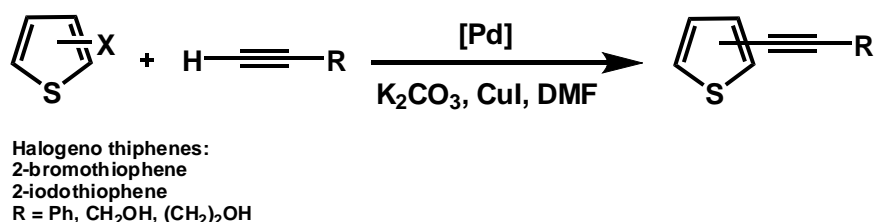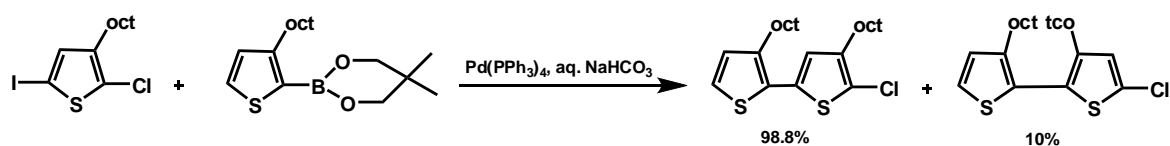
Scheme.2.3

2.1.2 Suzuki Coupling Reaction

The Suzuki (or Suzuki-Miyaura) reaction typically involves the reaction of an aryl or vinyl boronic acid with an aryl or vinyl halide; the reaction being catalysed by a Pd(0) complex – typically tetrakis(triphenylphosphine)palladium(0), $Pd(PPh_3)_4$, as also used in the Sonogashira coupling reaction.[11-13] The importance of this reaction is illustrated by Suzuki being jointly awarded the 2010 Nobel Prize in Chemistry.[14]

The mechanism of the Suzuki reaction is typically viewed from the perspective of the Pd catalyst (Scheme 2.4). In the first stage, the oxidative addition of Pd **1** to the halide **2** yields an organo-Pd complex **3**. The addition of base generates the intermediate **4**, which undergoes transmetalation with the boronic acid[15] to form the organo-Pd complex **8**. The original Pd centre **1** is then restored via the reductive elimination of the product (**9**).
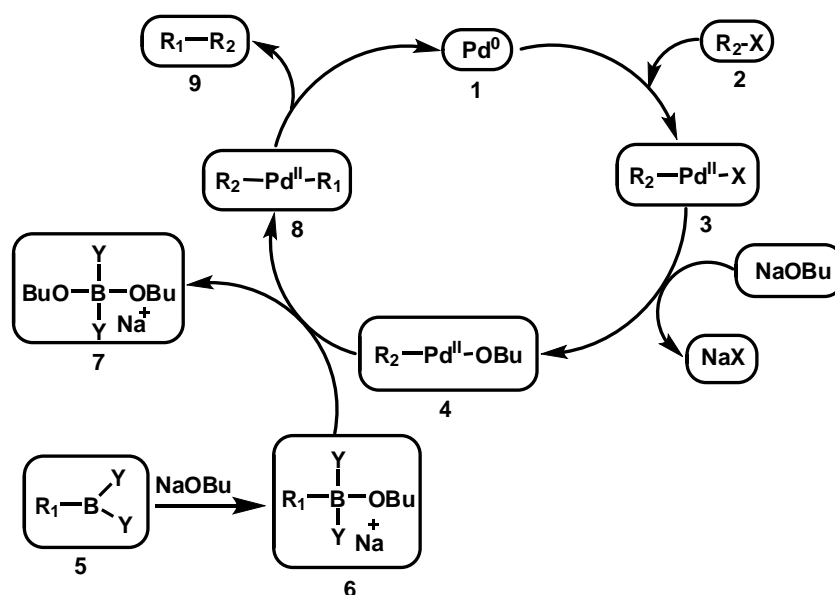
**Scheme 2.4** The general mechanism for the Pd-catalysed Suzuki cross coupling.[1]

In comparison with the Stille reaction (*vide infra*), the Suzuki coupling reaction tolerates a wider range of functional groups, making it broadly applicable to a wide number of syntheses. For example, Bidan *et al.*[16] formulated the synthesis of oligothiophenes, specifically oligo(3-octyltiophenes), through the continued use of the Suzuki cross-coupling reaction (Scheme 2.5).

Scheme2.5

In this reaction sequence, chain-growth was controlled through the incorporation of a non-reactive chloride function that blocked one of the reactive alpha positions. The product was subsequently reductively dehalogenated over Pd/C by H_2 in order to yield the unprotected molecule.

In a similar vein, a dihalogenated substituted thiophene was coupled with a boronic ester, which yielded a head-to-tail dihexylbiothiophene (Scheme 2.6).[17]
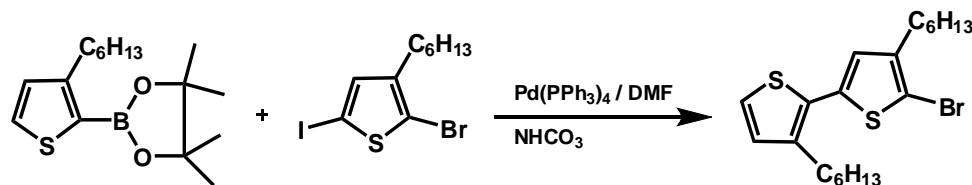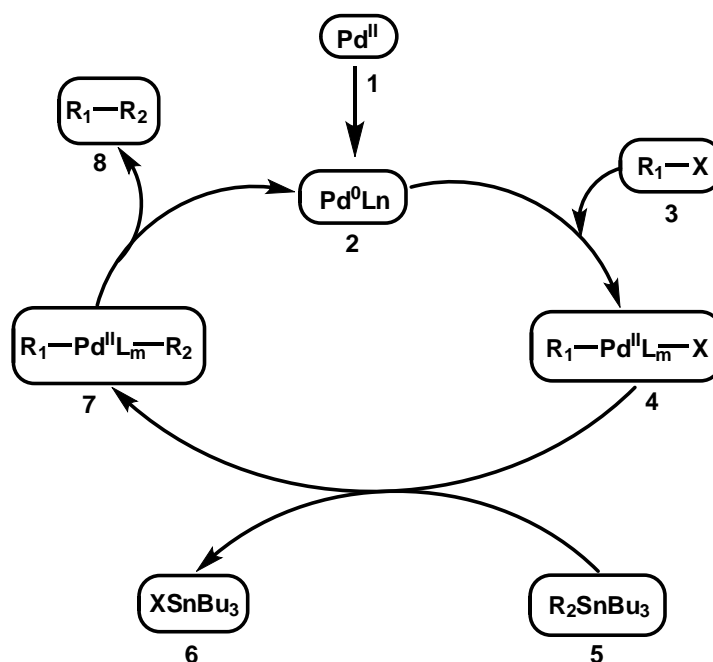

Scheme 2.6

In this synthesis, the bromide function is left untouched during the reaction because of the difference in the reactivity of aryl iodide and bromides for the Suzuki coupling reactions.

2.1.3 Stille Coupling Reaction

The Stille coupling reaction typically couples organotin compounds with an sp^2-hydridized organo-halide (or pseudo-halide, *e.g.* triflate), through the use of a Pd catalyst.[18-20] Unfortunately, the toxicity of the organotin reagents is potentially an issue, meaning that Suzuki coupling reactions (section 2.3.1) are generally preferred where possible as a greener alternative. Nevertheless, organotin compounds provide excellent scope in synthesis, due to the large number of organic electrophiles that may potentially be utilised, coupled with regioselectivity and relatively mild reaction conditions.[20]

The reaction mechanism for the Stille coupling is well established[21] and all stereochemical configurations of each reactant are retained.[22] As illustrated in scheme 2.7, the Pd catalyst (1) undergoes reduction from Pd(II) to Pd(0), generating the catalytic centre (2). The oxidative addition of an organo-halide then yields a *cis* intermediate (3), which under rapid kinetics isomerises to the *trans* from (4). Transmetallation via (5) yields the intermediate (7), which then expels the desired product through reductive-elimination (8) and regenerates the Pd(0) centre (2).

**Scheme 2.7** The general mechanism for the Stille coupling.[1]

Functionalised thiophenes derived through Stille cross-coupling reactions were first reported in 1994[23] and were later used in the regioselective synthesis of quater- and higher oligothiophenes (Scheme 2.8).[23]
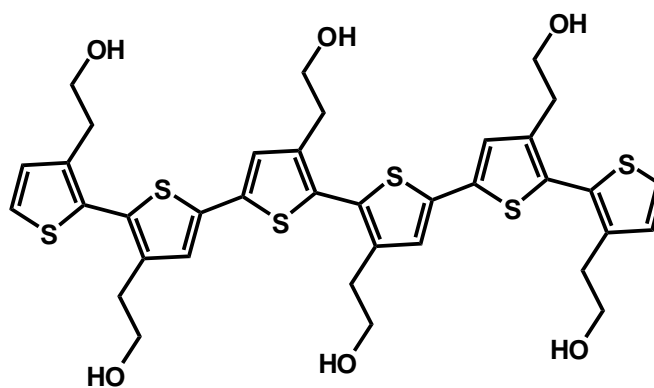
Scheme 2.8

Ewbank *et al.* published the synthesis of regioregular polythiophenes with an alkylamine side chain through a copper modified Stille reaction[24].

At the same time, Takahashi *et al.* used both Pd based Sonogashira C-H homocoupling as well as Ag based cross-coupling reactions in order to synthesise a series of well-defined oligothiophenes, as highlighted by the generalised (Scheme 2.9).[25]
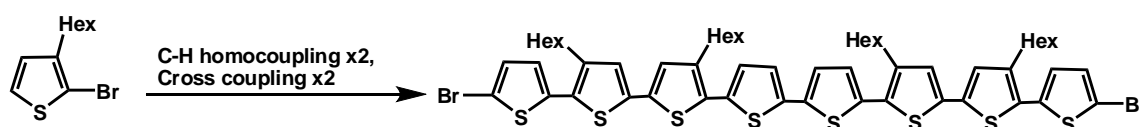
Scheme 2.9

2.2 Results and discussion

Several alkyne-substituted (hetero) aromatic building blocks for conjugated polymers are accessible starting from the commercially available 3-(2-hydroxyethyl)thiophene **2.1** (Scheme 2.10).
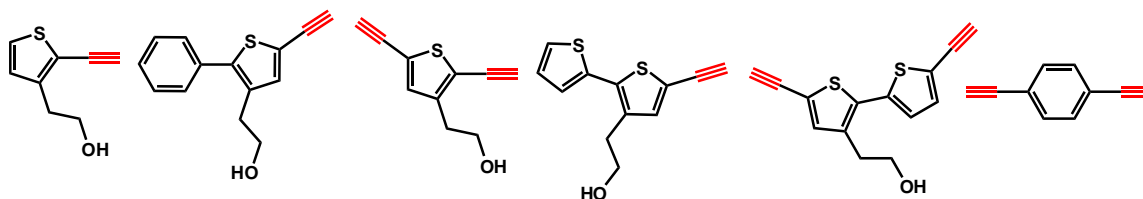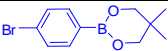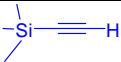

Scheme 2.10

Alkyne substituents can be introduced using the Sonogashira coupling reaction, while the (hetero)aromatic rings can be coupled using procedures such as Suzuki or Stille cross-coupling reactions.

These building blocks all carry hydroxyl functional groups, allowing for further functionalisation (following click reactions) to generate cationic products.

For the Sonogashira reactions, a number of approaches were tested in order to effectively achieve the reaction. It was found that using of bromides as the arylhalides under a variety

conditions typically gave poor yields. The range of conditions tested is summarised in Table **2.1**.

Table 2.1: Different conditions for Sonogashira reaction

| Reaction			Solvent	T	Time/h	Yield
1	0.0011 mol	2 eq	THF	RT	48	0%
2	0.0011 mol	2 eq	DMF	35°C	18	0%
3	0.0011 mol	5 eq	DMF	120°C (microwave)	0.5	Trace of product
4	0.0011 mol	5 eq	pyridine	75°C	18	30%

After this testing, the decision was made to use iodides as the arylhalides in the Sonogashira reactions, which gave excellent yields. This result suggests that the reactivity of iodine-substituted compounds in the Sonogashira reaction is better than bromine-substituted compound, as also reported by others[5, 26] (Scheme 2.11). The difference in reactivity between aryl bromides and aryl iodides also allowed the synthesis of 2-(2-Bromo-5-((trimethylsilyl)ethynyl)thiophen-3-yl)ethanol **2.14**.
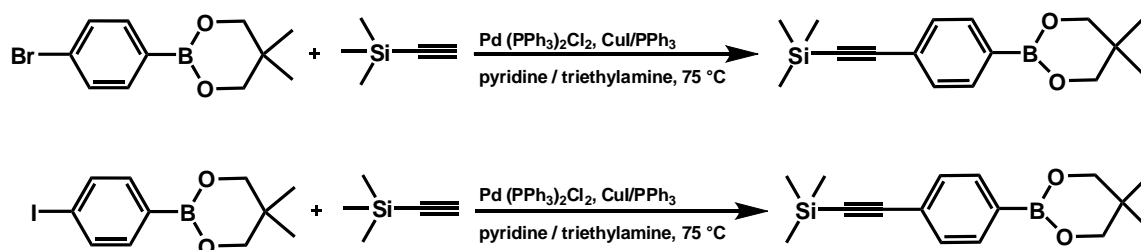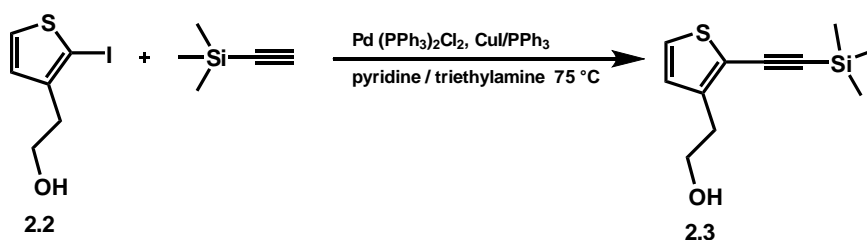

Scheme 2.11

2.2.1 Synthesis of 2-(2-ethynylthiophen-3-yl)ethanol 2.4

The iodination of 3-(2-hydroxyethyl)thiophene **2.1** using one equivalent of *N*-iodosuccinimide yielded 2-(2-iodothiophen-3-yl)ethanol **2.2** in 78% (Scheme 2.12) in addition to unreacted starting material **2.1** and the double iodination product 2-(2,5-diiodothiophen-3-yl)ethanol **2.10**. The reaction was monitored under a number of different conditions, first attempt 1 equivalent of *N*-iodosuccinimide (NIS) in DMF was added to **2.1** in chloroform and acetic acid (1:1) and the reaction heated to 40 ˚C for 24 hours, the second attempt 1 equivalent of *N*-iodosuccinimide (NIS) in DMF was added to **2.1** in DCM and acetic acid (5 ml) at 0 ^{O} C for 1 hour and the reaction stirring at the room temperature for 18 hours, but the same results were obtained. Column chromatography using 7:3 hexan:ethyl acetate as the eluent allowed the isolation of **2.2**.
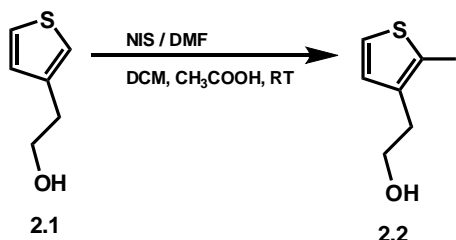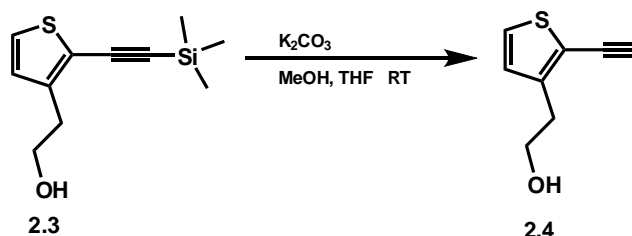

Scheme 2.12

2-(2-((Trimethylsilyl)ethynyl)thiophen-3-yl)ethanol **2.3** was prepared in 92% yield by means of a Sonogashira coupling reaction. 2-(2-Iodothiophen-3-yl)ethanol **2.2** was reacted with 1.2 equivalents of trimethylsilylacetylene with Pd(PPh$_3$)Cl$_2$ being used as a catalyst in the presence of copper iodide, triphenylphosphine and triethylamine (Scheme 2.13).

Scheme 2.13

Finally, 2-(2-ethynylthiophen-3-yl)ethanol **2.4** was obtained in 80% yield through the removal of the trimethylsilyl group by using potassium carbonate (2 M) as a base in a mixture of methanol and THF as solvent (Scheme 2.14).
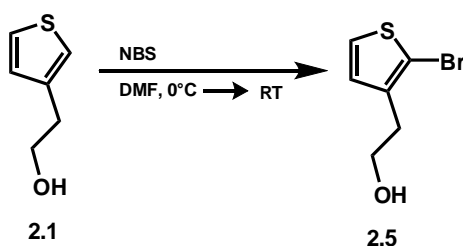

Scheme 2.14

In the deprotecting reaction to remove the trimethylsilyl group, first potassium hydroxide was used as a base, which returned a yield of 48%. After modifying the base to weak base potassium carbonate, the yield of the majority of reactions was improved to 78%.

2.2.2 Synthesis of 2-(5-ethynyl-2-phenylthiophen-3-yl)ethanol 2.9

The bromination of 3-(2-hydroxyethyl)thiophene **2.1** with one equivalent of *N*-bromosuccinimide resulted in 2-(2-bromothiophen-3-yl)ethanol **2.5** in 90% yield. Compound **2.5** is also a key intermediate in many of the reactions that follow. DMF has been found to be the best solvent for the bromination reaction, giving a high yield of the product in comparison with toluene or a mixture of acetic acid with chloroform (Scheme 2.15).
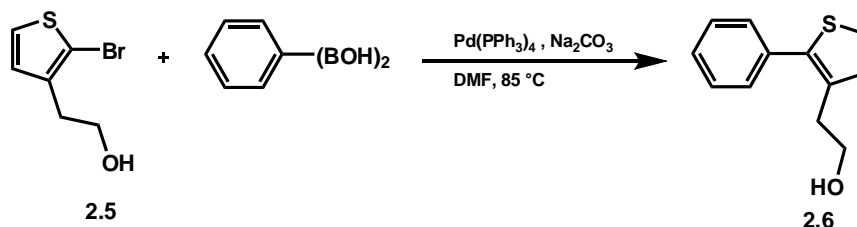
Scheme 2.15

In the bromination reaction it was discovered that the use of chloroform and acetic acid as a mixed solvent led to the formation of a mixture of thiophene ester **2.24** with a 34% yield and the desired product 66% (Scheme 2.16).
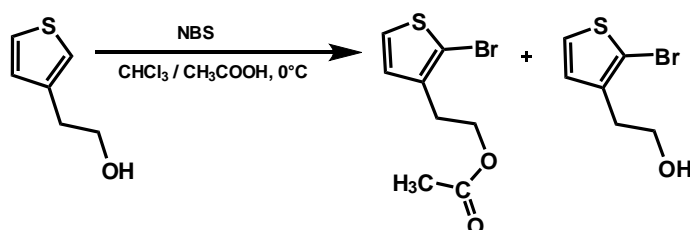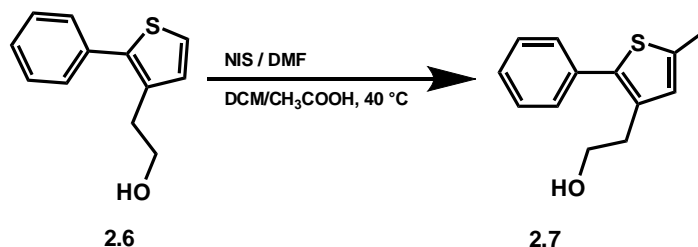

Scheme 2.16

2-Benzene-3-(2-hydroxyethyl)thiophene **2.6** was prepared through a Suzuki cross-coupling reaction. 2-Bromo-3-(2-hydroxyethyl)thiophene **2.5** was reacted with two equivalents of phenyl boronic acid using $Pd(PPh_3)_4$ as the catalyst, in the presence of Na_2CO_3 (1 M) as a base. The desired product was obtained in 75% yield (Scheme 2.17).

Scheme 2.17

The iodination of 2-phenyl-3-(2-hydroxyethyl) thiophene **2.6** using 2.5 equivalents of *N*-iodosuccinimide resulted in 2-benzene-5-iodo-3-(2-hydroxyethyl)thiophene **3.7** being produced in 75% yield (Scheme 2.18).

Scheme 2.18

2-Benzene-5-trimethylsilylethynyl-3-(2-hydroxyethyl)thiophene **2.8** was prepared through a Sonogashira cross-coupling reaction of 2.7 and trimethylsilylacetylene. The desired compound **2.8** was obtained in 80% yield (Scheme 2.19).
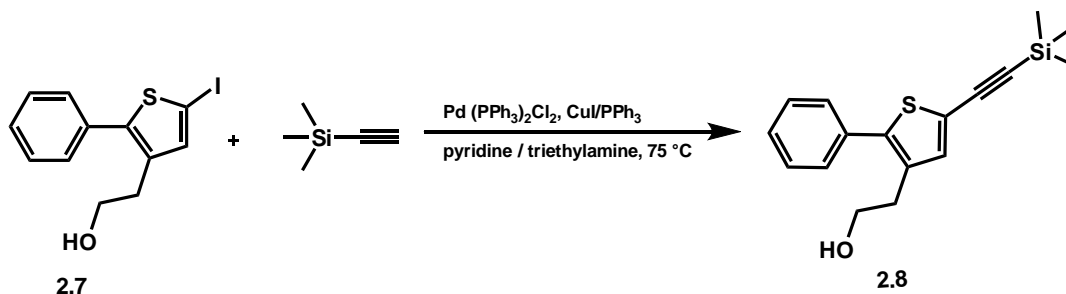
Scheme 2.19

2-Benzene-5-ethynyl-3-(2-hydroxyethyl)thiophene **2.9** was obtained by the removal of the trimethylsilyl group using potassium carbonate (2 M) in a mixture of methanol and THF 1:1 as solvent, yielding **2.9** in 78% (Scheme 2.20).
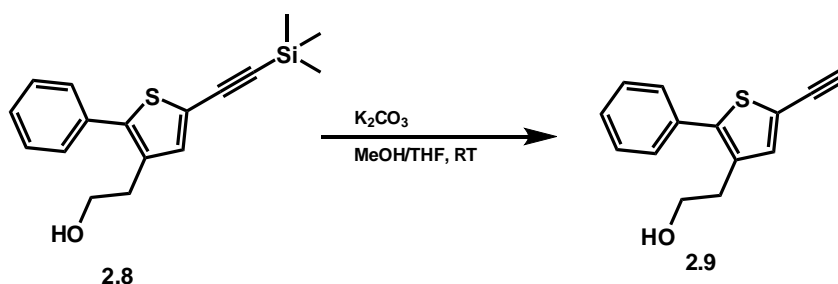
Scheme 2.20

2.2.3 Synthesis of 2-(2,5-diethynylthiophen-3-yl)ethanol 2.12

The iodination of 3-(2-hydroxyethyl)thiophene **2.1** using four equivalents of *N*-iodosuccinimide gave 2-(2,5-diiodothiophen-3-yl)ethanol **2.10** in 83% yield (Scheme 2.21).
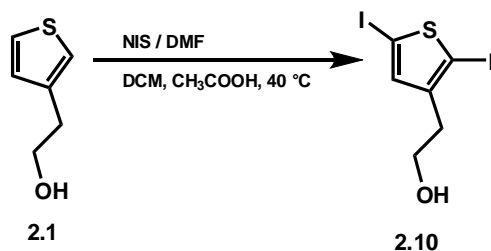
Scheme 2.21

2-(2,5-Bis((trimethylsilyl)ethynyl)thiophen-3-yl)ethanol **2.11** was prepared by means of a Sonogashira coupling reaction, producing **2.11** in a yield of 86% (Scheme 2.22).
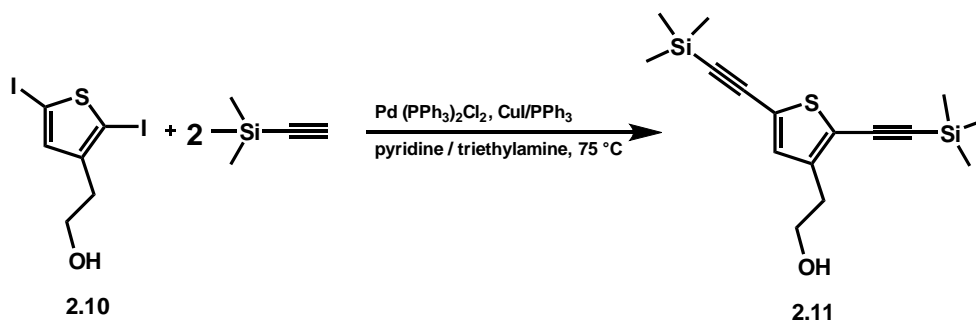
Scheme 2.22

The desired 2-(2,5-diethynylthiophen-3-yl)ethanol **2.12** was then obtained by the removal of the trimethylsilyl group using potassium carbonate (2 M) as a base in a mixture of methanol and THF 3:1 as solvent. The resulting yield of **2.12** was 80% (Scheme 2.23).
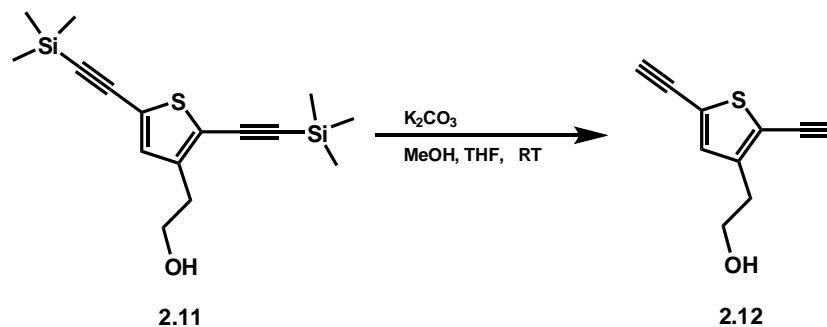
Scheme 2.23

2.2.4 Synthesis of 2-(5-ethynyl-2,2'-bithiophen-3-yl)ethanol 2.16

The bromination of 2-(2-iodothiophen-3-yl)ethanol **2.2**, using the same conditions as before, failed to produce **2.13** (Scheme 2.24). Because of this failure, the approach for the synthesis of 2-(2-bromo-5-iodothiophen-3-yl)ethanol **2.13** was modified, starting with bromination of 3-(2-hydroxyethyl)thiophene **2.1,** then iodination of 2-(2-bromothiophen-3-yl)ethanol **2.5**.

Scheme 2.24

The initial stage of the synthesis of 2-(5-ethynyl-2,2'-bithiophen-3-yl)ethanol **2.16** involved the bromination of 3-(2-hydroxyethyl)thiophene **2.1** as in scheme 2.5. The

subsequent iodination of 2-(2-bromothiophen-3-yl)ethanol **2.5** using 1.5 equivalents of *N*-iodosuccinimide yielded 2-(2-bromo-5-iodothiophen-3-yl)ethanol **2.13** in 75% (Scheme 2.25).
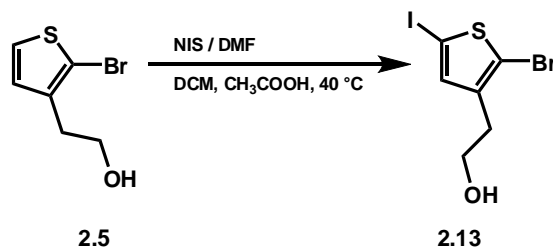
Scheme 2.25

2-(2-Bromo-5-((trimethylsilyl)ethynyl)thiophen-3-yl)ethanol **2.14** was then selectively prepared through a Sonogashira cross-coupling reaction of 2.13 with trimethylsilylacetylene, using toluene instead of pyridine as the solvent, at room temperature yielding **2.14** in 73% (Scheme 2.26).
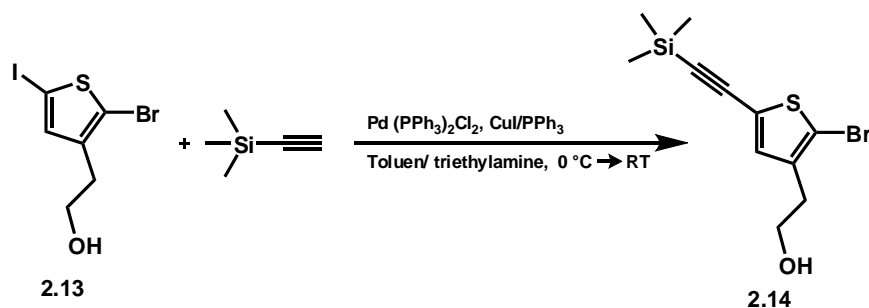
Scheme 2.26

2-(5-((Trimethylsilyl)ethynyl)-2,2'-bithiophen-3-yl)ethanol **2.15** was subsequently synthesised through the use of a Stille cross-coupling reaction in which 2-(2-bromo-5-((trimethylsilyl)ethynyl)thiophen-3-yl)ethanol **2.14** was reacted with 1.2 equivalents of 2-tributylstannylthiophene, using Pd(PPh$_3$)$_4$ as the catalyst in DMF at 105 °C. The desired product **2.15** was obtained in 81% yield (Scheme 2.27).
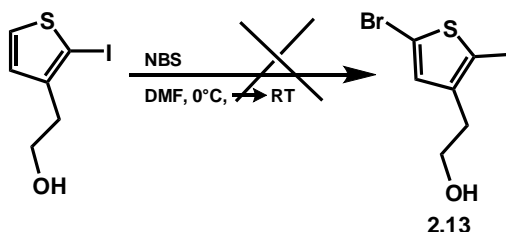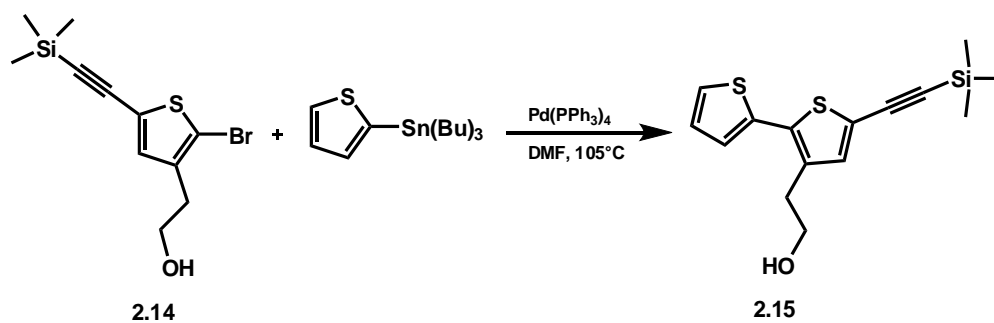
Scheme 2.27

2-(5-Ethynyl-2,2'-bithiophen-3-yl)ethanol **2.16** was synthesised by the removal of the trimethylsilyl group using potassium carbonate (2 M) as a base in a 3:1 mixture of methanol and THF as solvent, which produced **2.16** in 73% yield (Scheme 2.28).
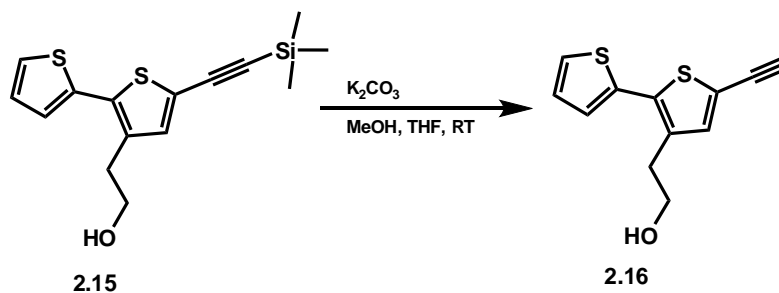
Scheme 2.28

2.2.5 Synthesis of 2-(5,5'-diethynyl-2,2'-bithiophen-3-yl)ethanol 2.20

2-(2,2'-Bithiophen-3-yl)ethanol **2.17** was prepared *via* a Stille cross-coupling reaction; 2-bromo-3-(2-hydroxyethyl)thiophene **2.5** was reacted with 1.2 equivalents of 2-tributylstannylthiophene using Pd(PPh$_3$)$_4$ as the catalyst in DMF at 105 °C. The desired product was obtained in 81% yield (Scheme 2.29).

Scheme 2.29

The iodination of (2,2'-bithiophen-3-yl)ethanol **2.17** using four equivalents of *N*-iodosuccinimide provided 2-(5,5'-diiodo-2,2'-bithiophen-3-yl)ethanol **2.18** in 67% yield (Scheme 2.30).
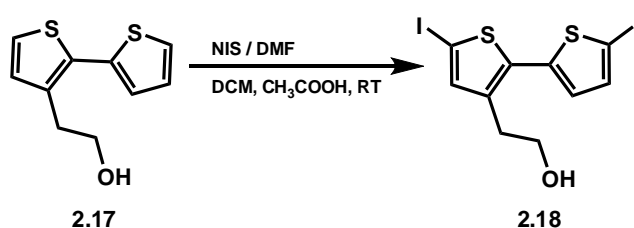
Scheme 2.30

2-(5,5'-Bis(trimethylsilyl)ethynyl)-2,2'-bithiophen-3-yl)ethanol **2.19** was prepared by means of a Sonogashira coupling reaction. In the presence of copper iodide, triphenylphosphine and triethylamine, 2-(5,5'-diiodo-2,2'-bithiophen-3-yl)ethanol **2.18** was reacted with 2.5 equivalents of trimethylsilylacetylene using $Pd(PPh_3)Cl_2$ as a catalyst. Compound **2.19** was obtained in 80% yield (Scheme 2.31).
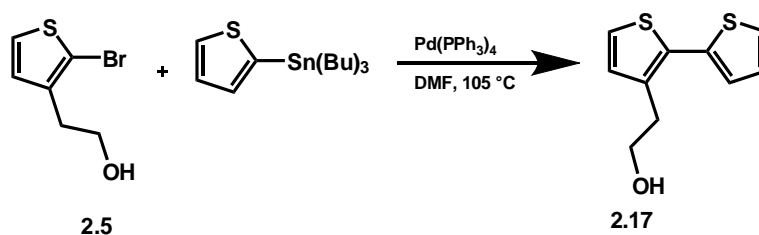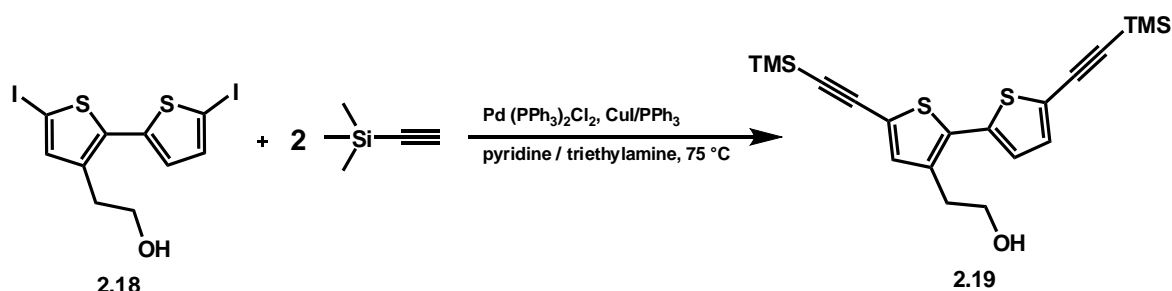
Scheme 2.31

2-(5,5'-Diethynyl-2,2'-bithiophen-3-yl)ethanol **2.20** was synthesised by the removal of the trimethylsilyl group, using potassium carbonate (2M) as a base in a mixture of methanol and THF (3:1) as the solvent, producing compound **2.20** in 75% yield (Scheme 2.32).
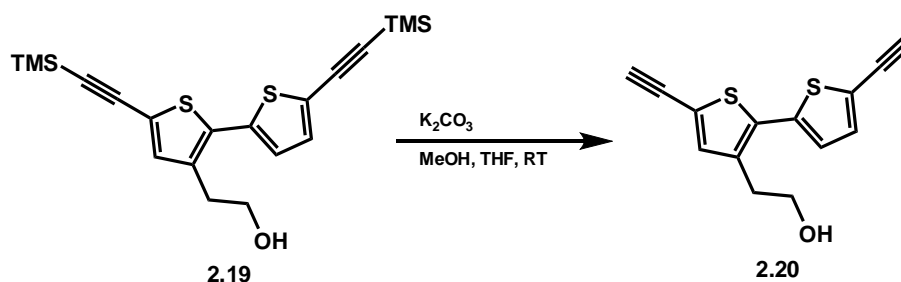
Scheme 2.32

2.2.6 Synthesis of 1,4-diethynylbenzene 2.23

1,4-Bis((trimethylsilyl)ethynyl)benzene **2.22** was prepared starting from 1,4-diiodobenzene **2.21**, which is commercially available, by a Sonogashira coupling reaction providing **2.22** in 93% yield (Scheme 2.33).
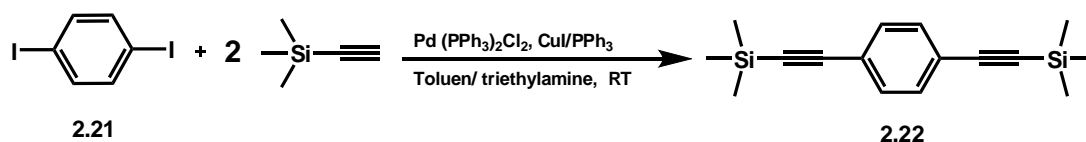
Scheme 2.33

1,4-Diethynylbenzene **2.23** was subsequently synthesised by removing the trimethylsilyl groups. This reaction was carried out using potassium carbonate (2 M) as a base in a mixture of methanol and THF (3:1) as solvent, yielding compound **2.23** in 75% yield (Scheme 2.34).

2.22   **2.23**
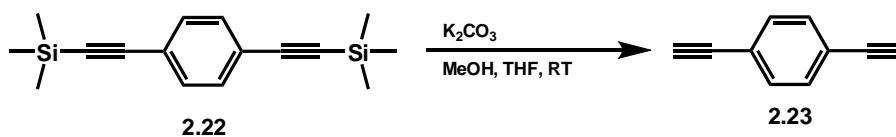
Scheme 2.34

2.3 Conclusion

A series of alkyne-substituted oligoheteroaromatic compounds has been successfully synthesised. The key step in the syntheses of these compounds was the Sonogashira cross coupling reaction that converts the iodine-substituted compound to the alkyne-substituted analogue. Additionally, different alkyne-substituted oligoheteroaromatics were prepared via Suzuki and Stille cross-coupling reactions.

2.4 Materials and methods

Commercially available reagents, starting materials and solvents were purchased from known commercial companies and used without further purification. A selection of the solvents, such as THF, DCM and DEE, were dried using an MBraun solvent purification system. ^{1}H-NMR, ^{13}C-NMR and 2D-NMR spectra were recorded at 400 MHz (for ^{1}H) on a Bruker B-ACS-6 or at 500 MHz (for ^{1}H) on a Bruker Avance 500 spectrometer. High resolution mass spectra were recorded utilising a Water Micromass LCT Premier, while low resolution mass spectra were recorded on a Perkin Elmer Turbo mass GC/MS. The Suzuki and Stille cross-coupling reactions were conducted under an N_2 atmosphere, with the solvent being degassed using the freeze-pump method. All purifications using column chromatography were performed with the use of silica gel.

2.5 Experimental procedures

Synthesis of 2-(2-iodothiophen-3-yl)ethanol **3.2**
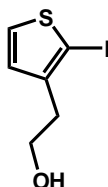
2.2 g (17.1 mmol) of 3-(2-hydroxyethyl)thiophene was dissolved in 60 ml of DCM, after which 3 ml of acetic acid was added to the solution. 3.86 g (17.1 mmol) of NIS in 10 ml of DMF was slowly added to the solution. The mixture was stirred at room temperature for 5 hours. Then, the reaction was quenched with water and washed with a saturated aqueous solution of Na_2CO_3. The aqueous layers were extracted with diethyl ether. All organic fractions (DCM and diethyl ether) were combined and dried over $MgSO_4$. The solvent was removed under reduced pressure and the crude product was purified with the use of silicagel chromatography with 300 ml of hexane first, then hexane / ethyl acetate (7:3) as eluent. 3.4 g of 2-(2-iodothiophen-3-yl)ethanol **3.2** was obtained as a pale red oil (78% yield). **^{1}H-NMR (CDCl$_3$, 400 MHz, ppm)**: 7.36 (d, *J*=1.2, 1H), 7.24 (d, *J*=1.2, 1H), 3.74 (t, *J*=5.2, 2H), 2.77 (t, *J*=5.4, 2H). **^{13}C-NMR (CDCl$_3$, 126 MHz, ppm)**: 143.04, 130.76, 128.27, 62.19, 35.24. **LRMS (EI)** *m/z* 222.8 (100%), 223.9.0 (12%), 253.9.0 (50%), 255.0 (5%). **HRMS (EI)** calcd for [C_6H_7OSI] 253.9262 found 253.9269.

Synthesis of 2-(2-((trimethylsilyl)ethynyl)thiophen-3-yl)ethanol **3.3**
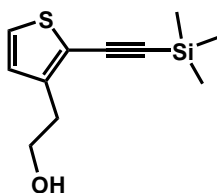
Initially, 2 g (7.87 mmol) of 2-(2-iodothiophen-3-yl)ethanol was added to a round-bottom tow necked flask equipped with magnetic stirrers and sealed with a rubber septum. 15 ml of pyridine and 10 ml of triethylamine were then added to the starting material under N_2. The mixture was then degassed several times. 0.055 g (0.078 mmol) of PdCl$_2$(PPh$_3$), 0.029 g (0.15 mmol) of CuI and 0.020 g (0.076 mmol) of PPh$_3$ were added to the mixture under N_2. After this, 1 ml (7.83 mmol) of trimethylsilylacetylene was added slowly to the mixture, which was then stirred at 75 °C for about 16 hours. The reaction was quenched with 10 ml of 2 M HCl and diluted with 30 ml of DCM. The organic layer was separated and washed with 60 ml of water, then dried over MgSO$_4$. The solvent was removed under reduced pressure. The crude product was purified by column chromatography, starting first with hexane, then continuing with hexane : ethyl acetate (8:2) as eluent. 1.62 g of 2-(2-((trimethylsilyl)ethynyl)thiophen-3-yl)ethanol **3.3** was obtained as a yellow oil (92% yield). **^{1}H-NMR (CDCl$_3$, 400 MHz, ppm)**: 7.19 (d, *J*=5.1, 1H), 6.92 (d, *J*=5.1, 1H), 3.90 (t, *J*=6.4, 2H) 2.99 (t, *J*=6.4, 2H), 0.26 (s, 9H). **^{13}C-NMR (CDCl$_3$, 101 MHz, ppm)**: 144.37, 128.49, 126.42, 119.94, 101.38, 97.10, 62.36, 32.98. **LRMS (EI)** *m/z* 75.0 (100%), 191.0 (30%), 223.9 (38%), 225.1 (5%). **HRMS (EI)** calcd for [C$_{11}$H$_{16}$OSSi] 224.0691 found 224.0687.

Synthesis of 2-(2-ethynylthiophen-3-yl)ethanol **3.4**
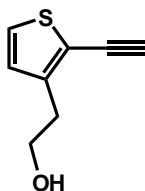
1 g (4.44 mmol) of 2-(2-((trimethylsilyl)ethynyl)thiophen-3-yl)ethanol **3.3** was dissolved in a mixture of methanol (20 ml) and THF (6 ml). An aqueous solution of potassium carbonate (2 M, 3 ml) was then added, and the mixture was stirred for 3 hours at room temperature. The reaction mixture was washed with 15 ml of water, the aqueous layer was extracted using diethyl ether several times and the combined organic phase was dried over $MgSO_4$. The solvent was removed under reduced pressure. 0.54 g of 2-(2-ethynylthiophen-3-yl)ethanol **3.4** was obtained as dark red oil (80% yield). **H-NMR (CDCl$_3$, 400 MHz, ppm)**: 7.13 (d, *J*=5.1, 1H), 6.85 (d, *J*=5.1, 1H), 3.79 (t, *J*=6.5, 2H) 3.38(s, 1H), 2.91 (t, *J*=6.5, 2H). **^{13}C-NMR (CDCl$_3$, 101 MHz, ppm)**: 145.09, 128.83, 127.13, 118.91, 84.17, 81.66, 62.92, 33.89. **LRMS (EI)** *m/z* 121.3 (100%), 122.3 (47%), 152.2 (45%). **HRMS (EI)** calcd for [C_8H_8OS] 152.0296 found 152.0295.

Synthesis of 2-(2-bromothiophen-3-yl)ethanol **3.5**
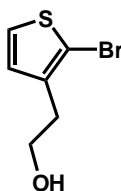
To a solution of 3.0 g (23.4 mmol) of 2-(3-thienyl)ethanol in 30 ml of DMF at 0 °C was slowly added 4.371 g (24.6 mmol) of NBS over a period of 30 minutes. The solution was stirred overnight, in the dark, and then quenched with water and washed with saturated aqueous Na_2CO_3, after which the combined aqueous fractions were extracted with ethyl

acetate. All organic fractions were combined and the solvent was removed under reduced pressure. The resultant product was purified by means of column chromatography using hexane : ethyl acetate (8:2) as eluent. 4.1 g of 2-Bromo-3-(2-hydroxyethyl)thiophene **3.5** was obtained as a pale yellow oil (85% yield). **^{1}H-NMR (CDCl$_3$, 400 MHz, ppm:)**: 7.18 (d, *J*=5.5, 1H), 6.80 (d, *J*=5.5, 1H), 3.79 (t, *J*=6.4, 2H), 2.87 (t, *J*=6.4, 2H) 1.53 (s,1H). **^{13}C-NMR (CDCl$_3$, 126 MHz, ppm)**: 138.41, 129.00, 126.13, 110.76, 62.95, 33.20.**LRMS (EI)** m/*z* 177 (100%), 206 (36%), 208 (37%). **HRMS (EI)** calcd for [C$_6$H$_7$OSBr] 205.9401 found 205.9400.

Synthesis of 2-phenyl-3-(2-hydroxyethyl) thiophene **3.6**
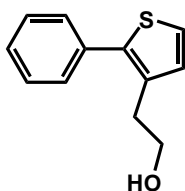
To a two-necked round-bottom flask equipped with a magnetic stirrer and a condenser was added 3.6 g (17.4 mmol) of 2-bromo-3-(2-hydroxyethyl)thiophene. Then 15 ml of DMF was added. The solution was degassed three times and brought under a nitrogen atmosphere. 2.54 g (20.87 mmol) of phenylboronic acid was then added, followed by the addition of 0.0255 g (mmol) of Pd(PPh$_3$)$_4$. The reaction was heated to 85 °C with the exclusion of oxygen and light for 24 hours. The reaction mixture was washed with distilled water (70 ml) and the aqueous fractions were extracted with DCM. The solvent was removed from the combined organic fractions under reduced pressure. Purification of the crude was conducted by column chromatography using hexane : ethyl acetate (8:2) as eluent. 2.88 g of 2-Phenyl-3-(2-hydroxyethyl) thiophene **3.6** was obtained as a yellow oil (82% yield). **^{1}H-NMR (CDCl$_3$, 400 MHz, ppm)**: 7.34-7.45 (m, 5H), 7.20 (d, *J*=5.1, 1H), 6.98 (d, *J*=5.1, 1H), 3.78 (t, *J*=6.5, 2H), 2.88 (t, *J*=6.6, 2H).. **^{13}C-NMR (CDCl$_3$, 101 MHz,**

ppm): 140.20, 135.75, 129.98, 1129.41, 126.23, 124.66, 122.09, 63.25, 31.41. **LRMS (EI)** m/z 129.4 (40%), 173.3 (100%), 204.3 (55%). **HRMS (EI)** calcd for [C$_{12}$H$_{12}$OS] 204.0609 found 204.0612.

Synthesis of 2-benzene-5-iodo-3-(2-hydroxyethyl)thiophene **3.7**
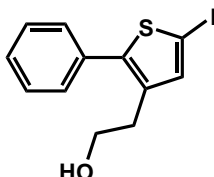
2-Phenyl-3-(2-hydroxyethyl)thiophene (0.5 g, 2.45 mmol) was dissolved in a mixture of chloroform (30 ml) and acetic acid (5 ml). 1.37 g (6.10 mmol) of NIS in DMF was then slowly added to the solution. The mixture was stirred at 40 °C for 16 h, in the dark. Once this stage was complete, the reaction was quenched with saturated Na$_2$CO$_3$ then washed with 70 ml of water and extracted with diethylether. The solvent was removed under reduced pressure and the crude product was purified by column chromatography, using first hexane then hexane : ethyl acetate (7:3) as eluent. 0.56 g of 2-Benzene-5-iodo-3-(2-hydroxyethyl)thiophene **3.7** was obtained a pale red oil (70% yield). **^{1}H-NMR (CDCl$_3$, 400 MHz, ppm**): 7.33-7.40 (m, 5 H), 7.11 (s, 1H), 3.75 (t, *J*=6.5, 2H), 2.82 (t, *J*=6.6, 2H). **^{13}C-NMR (CDCl$_3$, 101 MHz, ppm**): 144.90, 138.01, 135.22, 132.14, 128.31, 127.64, 127, 61.79, 30.34. **LRMS (EI)** m/z 172.0 (100%), 298.9 (15%), 330.0 (40%). **HRMS (EI)** calcd for [C$_{12}$H$_{11}$OSI] 329.9575 found 329.9576.

Synthesis of 2-benzene-5-trimethylsilylethynyl-3-(2-hydroxyethyl)thiophene **3.8**
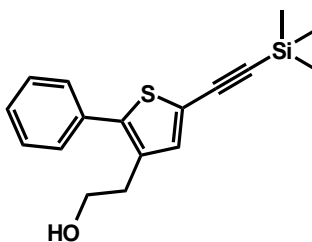
To a two-necked round-bottom flask equipped with a magnetic stirrer and sealed with a rubber septum was added 2.3 g (6.96 mmol) of 2-(2-iodothiophen-3-yl)ethanol. 20 ml of pyridine and 10 ml of triethylamine were then added to the starting material under N_2. The mixture was degassed several times. 0.048 g (0.069 mmol) of $PdCl_2(PPh_3)$, 0.026 g (0.139 mmol) of CuI and 0.018 g (0.069 mmol) of PPh_3 were then added to the mixture under N_2. After this, 1.9 ml (7.83 mmol) of trimethylsilylacetylene was slowly added to the mixture, and the liquid stirred at 75 °C for approximately 16 hours. The reaction was quenched with 10 ml of 2 M HCl and diluted with 30 ml of DCM. The organic layer was separated and washed with 80 ml of water, then dried over $MgSO_4$. The solvent was removed under reduced pressure. The crude product was purified by column chromatography, initially with hexane and then with hexane : ethyl acetate (7:3) as eluent. 1.79 g of 2-Benzene-5-trimethylsilylethynyl-3-(2-hydroxyethyl)thiophene **3.8** was obtained as a brown oil (86% yield). **^{1}H-NMR (CDCl$_3$, 400 MHz, ppm)**: 7.25-7.43 (m, 5 H), 7.20 (s, 1H), 3.84 (t, *J*=6.6, 2H), 2.89 (t, *J*=6.6, 2H), 0.26 (s, 9H). **^{13}C-NMR (CDCl$_3$, 101 MHz, ppm)**: 140.69, 133.89, 133.04, 132.34, 128.40, 127.66, 127.02, 120.58, 98.36, 96.44, 61.81, 30.62. **LRMS (EI)** m/*z* 269.3 (62%), 300.3 (100%). **HRMS (EI)** calcd for [C$_{17}$H$_{20}$OSSi] 300.1004 found 300.1001.

Synthesis of 2-benzene-5-ethynyl-3-(2-hydroxyethyl)thiophene **3.9**
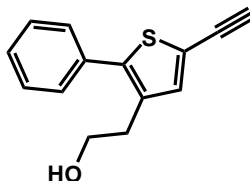
0.3 g (1 mmol) of 2-benzene-5-ethynyl-3-(2-hydroxyethyl)thiophene **3.9** was dissolved in a mixture of methanol (15 ml) and THF (4 ml). 3 ml of a 2 M aqueous solution of potassium carbonate was then added. The mixture was stirred for 3 hours at room temperature. The reaction mixture was washed with 15 ml of water, then the organic fractions were extracted from the aqueous layer by diethyl ether several times and the combined organic phase was dried over MgSO$_4$. The solvent was removed under reduced pressure. 0.18 g of 2-(2-Ethynylthiophen-3-yl)ethanol **3.4** was obtained as a brown oil (78% yield). **^{1}H-NMR (CDCl$_3$, 400 MHz, ppm)**: 7.30-7.40 (m, 5 H), 7.15 (s, 1H), 3.75 (t, *J*=6.6, 2H), 3.30 (s, 1H) 2.81 (t, *J*=6.6, 2H). **^{13}C-NMR (CDCl$_3$, 101 MHz, ppm)**: 140.93, 134.27, 133.23, 133.11, 128.24, 127.68, 127.11, 124.80, 119.38, 80.72, 61.78, 30.58. **LRMS (EI)** m/*z* 197.2 (100%), 228.2 (68%), 229.2 (17%). **HRMS (EI)** calcd for [C$_{14}$H$_{12}$OS] 228.0609 found 228.0611.

Synthesis of 2-(2,5-diiodothiophen-3-yl)ethanol **3.10**
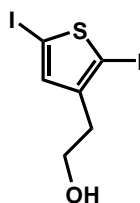
2 g (15.6 mmol) of 3-(2-hydroxyethyl)thiophene was dissolved in 60 ml of DCM. 3 ml of acetic acid was then added to the solution. 14.03 g (62.4 mmol) of NIS was slowly added to the solution, 10 ml of DMF was added to improve the solubility of NIS. The mixture

was stirred at 40 °C for 12 hours. After this, the reaction was quenched with water and washed with a saturated solution of Na_2CO_3, and the aqueous layers were extracted with diethyl ether. All organic fractions were combined and dried over $MgSO_4$. The solvent was removed under reduced pressure and the crude product was purified by column chromatography, first with 300 ml of hexane, then with hexane : ethyl acetate (7:3) as eluent. 4.92 g of 2-(2,5-Diiodothiophen-3-yl)ethanol **3.10** was obtained as a red oil (83% yield). **^{1}H-NMR (CDCl$_3$, 400 MHz, ppm)**: 6.89 (s, 1H), 3.66 (t, *J*=6.6, 2H), 2.69 (t, *J*=6.6, 2H). **^{13}C-NMR (CDCl$_3$, 101 MHz, ppm)**: 146.05, 138.64, 79.23, 77.11, 62.42, 35.53. **LRMS (EI)** *m/z* 222.9(35%), 348.8 (83%), 379.8 (55%). **HRMS (EI)** calcd for [$C_6H_6OSI_2$] 379.8229 found 379.8235.

Synthesis of 2-(2,5-bis((trimethylsilyl)ethynyl)thiophen-3-yl)ethanol **3.11**
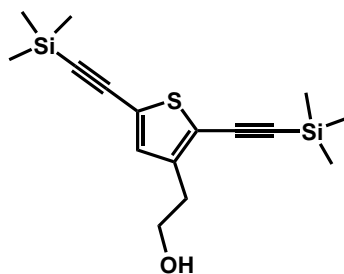
To a two-necked round-bottom flask equipped with a magnetic stirrer and sealed with a rubber septum was added 2 g (5.27 mmol) of 2-(2,5-diiodothiophen-3-yl)ethanol **3.10**. Pyridine (25 ml) and triethylamine (12 ml) were then added to the starting material under N_2. The mixture was degassed several times. 0.036 g (0.052 mmol) of PdCl$_2$(PPh$_3$), 0.019 g (0.105 mmol) of CuI and 0.013 g (0.052 mmol) of PPh$_3$ were added to the mixture under N_2. Afterward, 1.46 ml (10.54 mmol) of trimethylsilylacetylene was slowly added to the mixture. The mixture was stirred at 75 °C for about 16 hours. The reaction was quenched with 10 ml of 2 M HCl and diluted with 30 ml of DCM. The organic layer was then separated and washed with 60 ml of water, then dried over $MgSO_4$. The solvent was

removed under reduced pressure. The crude product was purified by column chromatography using hexane : ethyl acetate (8:2) as eluent. 1.45 g of 2-(2,5-Bis((trimethylsilyl)ethynyl)thiophen-3-yl)ethanol **3.11** was obtained as yellow oil (86% yield). **^{1}H-NMR (CDCl$_3$, 400 MHz, ppm)**: 7.05 (s, 1H), 3.86 (t, *J*=6.4, 2H), 2.91 (t, *J*=6.4, 2H), 0.26 (d, *J*=4.0, 9H). **^{13}C-NMR (CDCl$_3$, 101 MHz, ppm)**: 144.37, 134.12, 121.30, 123.50, 102.60, 100.40, 97.20, 96.80, 62.53, 33.20. **LRMS (EI)** m/z 289.1 (32%), 305.0 (40%), 320.1 (100%). **HRMS (EI)** calcd for [C$_{16}$H$_{24}$OSSi$_2$] 320.1086 found 320.1089.

Synthesis of 2-(2,5-diethynylthiophen-3-yl)ethanol **3.12**
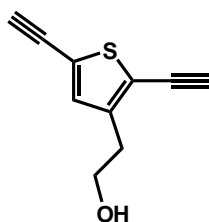
1.5 g (4.68 mmol) of 2-(2,5-bis((trimethylsilyl)ethynyl)thiophen-3-yl)ethanol **3.11** was dissolved in a mixture of methanol (20 ml) and THF (6 ml). 2 M aqueous solution of potassium carbonate (3 ml) was subsequently added to the mixture, which was then stirred for 3 hours at room temperature. The reaction mixture was washed with 15 ml of water, then the organic fractions were extracted from the aqueous layer by diethyl ether several times and the combined organic phase was dried over MgSO$_4$. The solvent was removed under reduced pressure. 0.66 g of 2-(2,5-Diethynylthiophen-3-yl)ethanol **3.12** was obtained as a brown oil (80% yield). **H-NMR (CDCl$_3$, 400 MHz, ppm)**: 7.02 (s 1H), 3.79 (t, *J*=6.4, 2H) 3.41(d, *J*=6.1, 1H), 3.28(s, 1H), 2.85 (t, *J*=6.4, 2H). **^{13}C-NMR (CDCl$_3$, 101 MHz, ppm)**: 143.36, 132.79, 121.50, 119.12, 83.48, 81.15, 61.26, 31.67. **LRMS (EI)** *m/z*

145.1 (100%), 146.1 (50%), 176.1 (52%). **HRMS (EI)** calcd for [$C_{10}H_8OS$] 176.0296 found 176.0291.

Synthesis of 2-(2-bromo-5-iodothiophen-3-yl)ethanol **3.13**
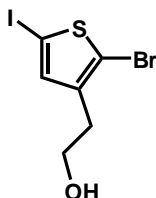
3 g (14.56 mmol) of 2-bromo-3-(2-hydroxyethyl)thiophene **3.5** was dissolved in 60 ml of $CHCl_3$. 5 ml of acetic acid was then added to the solution. 8.09 g (36.4 mmol) of NIS in 15 ml of DMF was slowly added to the solution. The mixture was stirred at 40 °C for 16 hours. The reaction was quenched with water and washed with a saturated solution of Na_2CO_3, after which the aqueous layers were extracted with diethyl ether. All organic fractions were combined and dried over $MgSO_4$. The solvent was removed under reduced pressure and the crude product was purified by column chromatography with of hexane : ethyl acetate 9:1 first, then with hexane : ethyl acetate (2:1) as eluent. 3.63 g of 2-(2-Bromo-5-iodothiophen-3-yl)ethanol **3.13** was obtained as a pale red oil (75% yield). **^{1}H-NMR (CDCl$_3$, 400 MHz, ppm)**: 6.97 (s, 1H), 3.69 (t, *J*=6.5, 2H), 2.72 (t, *J*=6.5, 2H). **^{13}C-NMR (CDCl$_3$, 101 MHz, ppm)**:139.32, 137.20, 112.12, 70.69, 60.73, 31.41. **LRMS (EI)** *m/z* 222.9 (40%), 302.8 (58%), 333.9 (40%). **HRMS (EI)** calcd for [C_6H_6OSBrI] 331.8367 found 331.8376.

Synthesis of 2-(2-bromo-5-((trimethylsilyl)ethynyl)thiophen-3-yl)ethanol **3.14**
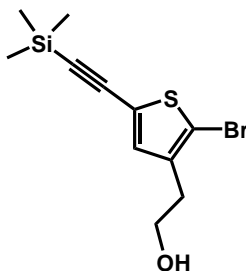
To a two-necked round-bottom flask equipped with a magnetic stirrer and sealed with a rubber septum was added 2 g (6 mmol) of 2-(2-bromo-5-iodothiophen-3-yl)ethanol **3.13**. 30 ml of toluene and 15 ml of triethylamine were then added to the starting material under N_2. The mixture was degassed several times. 0.042 g (0.06 mmol) of $PdCl_2(PPh_3)$, 0.022 g (0.12 mmol) of CuI and 0.015 g (0.06 mmol) of PPh_3 were added to the mixture under N_2. The mixture was cooled to 0 ° C using an ice bath. After this stage, 0.83 ml (6 mmol) of trimethylacetylene was slowly added to the mixture. The mixture was stirred at 0 ° C for about 15 minutes. Then, the ice bath was removed and the reaction was stirred at room temperature for 12 h. The reaction was quenched with 10 ml of 2 M HCl and diluted with 30 ml of DCM. The organic layer was separated and washed with 70 ml of water, then dried over $MgSO_4$. The solvent was removed under reduced pressure and purification of the crude product was conducted by means of column chromatography using hexane : ethyl acetate (2:1) as eluent. 1.33 g of 2-(2-Bromo-5-((trimethylsilyl)ethynyl)thiophen-3-yl)ethanol **3.14** was obtained as a yellow oil (73% yield). **^{1}H-NMR (CDCl_3, 400 MHz, ppm)**: 7.02 (s, 1H), 3.82 (t, *J*=6.5, 2H), 2.81 (t, *J*=6.5, 2H). **^{13}C-NMR (CDCl_3, 101 MHz, ppm)**: 138.60, 134.16, 123.90, 111.85, 100.65, 96.99, 62.25, 33.13. **LRMS (EI)** m/*z* 193.0 (50%), 286.9. (80%), 304.0 (40%). **HRMS (EI)** calcd for [$C_{11}H_{15}OSiSBr$] 303.9776 found 303.9785.

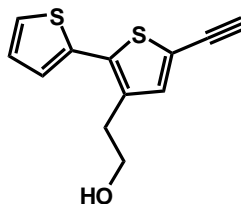Synthesis of 2-(5-((trimethylsilyl)ethynyl)-2,2'-bithiophen-3-yl)ethanol **3.15**
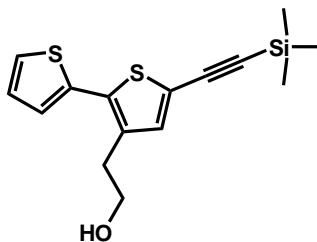
To a two-necked round-bottom flask equipped with a magnetic stirrer and sealed with a rubber septum was added 1.4 g (4.63 mmol**)** of 2-(2-bromo-5-((trimethylsilyl)ethynyl)thiophen-3-yl)ethanol **3.14**. 30 ml of DMF was then added. The solution was degassed three times and brought under a nitrogen atmosphere. 1.76 ml (5.56 mmol) of 2-tributylstannylthiophene was then added. 0.053 g of Pd(PPh$_3$)$_4$ was subsequently added. The reaction was heated to 105 °C for 24 hours, with the exclusion of oxygen and light. The reaction mixture was washed with water (100 ml) and the aqueous fractions were extracted with DCM. The solvent was removed from the combined organic fractions under reduced pressure and the crude product was purified using column chromatography using hexane : ethyl acetate (2:1) as eluent. 1.15 g of 2-(5-((Trimethylsilyl)ethynyl)-2,2'-bithiophen-3-yl)ethanol **3.15** was obtained as a brown oil (81% yield). **^{1}H-NMR (CDCl$_3$, 400 MHz, ppm**): 7.35 (d, *J*=5.1, 1H), 7.18 (d, *J*=3.5, 1H) 7.15 (s, 1H), 7.08 (d, *J*=3.8 1H) 3.88 (t, *J*=6.6 2H), 3.00 (t, *J*=6.6 2H), 0.27 (s, 9H). **^{13}C-NMR (CDCl$_3$, 101 MHz, ppm**): 135.84, 135.20, 134.50, 128.07, 127.30, 126.60, 121.90, 100.30, 97.30, 63.05, 32.64. **LRMS (EI)** *m/z* 275.1 (98%), 291.0 (40%), 306.0 (100%). **HRMS (EI)** calcd for [C$_{15}$H$_{18}$OS$_2$Si] 306.0568 found 306.0571.

Synthesis of 2-(5-ethynyl-2,2'-bithiophen-3-yl)ethanol **3.16**

0.5 g (1.63 mmol) of 2-(5-((trimethylsilyl)ethynyl)-2,2'-bithiophen-3-yl)ethanol **3.15** was dissolved in a mixture of methanol (20 ml) and THF (6 ml). A 2 M aqueous solution of potassium carbonate (3 ml) was then added. The mixture was stirred for 3 hours at room temperature, after which the reaction mixture was washed with 15 ml of water. The organic material was then extracted from the aqueous layer by diethyl ether several times and the combined organic phase was dried over $MgSO_4$. The solvent was removed under reduced pressure. The crude was purified by column chromatography using hexane : ethyl acetate (2:1) as eluent. 0.28 g of 2-(5-Ethynyl-2,2'-bithiophen-3-yl)ethanol **3.16** was obtained as a brown oil (73% yield). **H-NMR (CDCl$_3$, 400 MHz, ppm)**: 7.27 (q, *J*=5.1, 1H),), 7.10 (s, 1H) 7.00 (q, *J*=3.6, 2H), 3.80 (t, *J*=6.6, 2H), 3.31 (s, 1H) 2.92 (t, *J*=6.6, 2H). **^{13}C-NMR (CDCl$_3$, 101 MHz, ppm)**: **LRMS (EI)** *m/z* 171.2 (38%), 203.1 (100%), 234.1 (55%). **HRMS (EI)** calcd for [$C_{12}H_{10}OS_2$] 234.0173 found 234.0173.

Synthesis of 2-(2,2'-bithiophen-3-yl)ethanol **3.17**

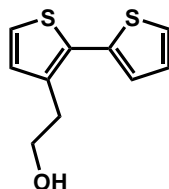
To a two-necked round-bottom flask equipped with a magnetic stirrer and sealed with a rubber septum was added 2 g (9.7 mmol) of 2-bromo-3-(2-hydroxyethyl)thiophene. 25 ml

of DMF was then added. The solution was degassed three times and brought under a nitrogen atmosphere. 4.35 g (38.8 mmol) of 2-(tributylstannyl)thiophene was then added, after which 0.0255 g (0.097 mmol) of Pd(PPh$_3$)$_4$ was added. The reaction was heated to 105 °C with the exclusion of oxygen and light for 24 hours. The reaction mixture was then washed with distilled water (70 ml) and the aqueous fractions were extracted with DCM. The solvent was removed from the combined organic fractions under reduced pressure and the crude purified by column chromatography using hexane : ethyl acetate (2:1) as eluent. 1.65 g of 2-(2,2'-Bithiophen-3-yl)ethanol was obtained as a yellow oil (81% yield). **^{1}H-NMR (CDCl$_3$, 400 MHz, ppm)**: 7.26 (q, *J*=1.1, 1 H), 7.16 (d, *J*=5.2, 1H), 7.08 (q, *J*=1.1, 1H) 7.00 (q, *J*=3.5, 1H), 6.94 (d, *J*=5.2, 1H) 3.83 (t, *J*=6.6, 2H), 2.97 (t, *J*=6.6, 2H). **^{13}C-NMR (CDCl$_3$, 126 MHz, ppm)**: 137.64, 137.52, 132.24, 130.10, 128.01, 127.89, 126.67, 125.76, 62.72, 32.56. **LRMS (EI)** *m/z* 179.1 (100%), 210.1 (67%), 211.1 (18%). HRMS (EI) calcd for [C$_{10}$H$_{10}$OS$_2$] 210.0173 found 210.0171.

Synthesis of 2-(5,5'-diiodo-2,2'-bithiophen-3-yl)ethanol **3.18**
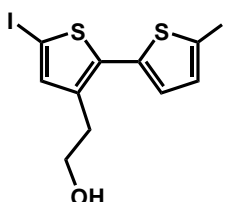
1.5 g (7.14 mmol) of 2-(2,2'-bithiophen-3-yl)ethanol was dissolved in DCM. 3 ml of acetic acid was then added. Subsequently, 6.42 g (28.5 mmol) of NIS in DMF was slowly added to the solution. The mixture was then stirred at room temperature for 7 hours. The reaction was quenched with water and washed with a saturated solution of Na$_2$CO$_3$ after which the combined aqueous layers were extracted with diethyl ether. All organic fractions were combined and the solvent was removed under reduced pressure. Finally, the product was purified by column chromatography using hexane : ethyl acetate (7:3) as eluent, producing

2.22 g of 2-(5,5'-diiodo-2,2'-bithiophen-3-yl)ethanol as a yellow powder (67% yield). **^{1}H-NMR (CDCl₃, 400 MHz, ppm)**: 7.13 (d, *J*=3.7, 1H), 7.08 (s, 1H), 6.72 (d, *J*=3.7, 1H), 3.75 (t, *J*=6.5, 2H) 2.88 (t, *J*=6.5, 2H). **^{13}C-NMR (CDCl₃, 126 MHz, ppm)**: 140.17, 139.66, 137.82, 137.43, 137.14, 128.45, 74.14, 73.06, 62.62, 31.92. **LRMS (EI)** *m/z* 303.9 (100%), 430.9 (10%), 462.0 (42%). **HRMS (EI)** calcd for [$C_{10}H_8OS_2I_2$] 461.8106 found 461.8117.

Synthesis of 2-(5,5'-bis(trimethylsilyl)ethynyl)-2,2'-bithiophen-3-yl)ethanol **3.19**
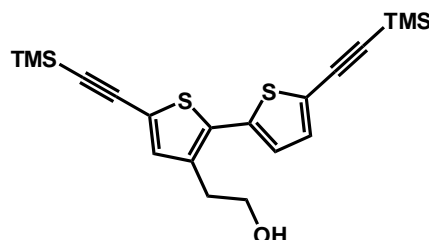
To a two-necked round-bottom flask equipped with a magnetic stirrer and sealed with a rubber septum was added 1.2 g (2.59 mmol) of 2-(5,5'-diiodo-2,2'-bithiophen-3-yl)ethanol. 25 ml of pyridine and 12 ml of triethylamine were then added to the starting material under N_2. The mixture was degassed several times. 0.018 g (0.025 mmol) of PdCl₂(PPh₃), 0.004 g (0.051 mmol) of CuI and 0.006 g (0.025 mmol) of PPh₃ were added to the mixture under N_2. After this, 0.70 ml (5.18 mmol) of trimethylsilyacetylene was added to the mixture. The mixture was stirred at 75 °C for approximately 16 hours. The mixture was then quenched with 10 ml of 2 M HCl and diluted with 30 ml of DCM. The organic layer was separated and washed with 60 ml of water, then dried over MgSO₄. The solvent was removed under reduced pressure and the crude was purified by column chromatography using first hexane and subsequently hexane : ethyl acetate (7:3) as eluent. 0.83 g of 2-(5,5'-bis(trimethylsilyl)ethynyl)-2,2'-bithiophen-3-yl)ethanol was obtained as yellow powder (80% yield). **^{1}H-NMR (CDCl₃, 400 MHz, ppm)**: 7.09 (d, *J*=3.8, 1H), 7.04 (s,

1H), 6.94 (d, *J*=3.8, 1H) 3.80 (t, *J*=6.6, 2H), 2.88 (t, *J*=6.6, 2H) 1.80 (d, *J*=3.2, 9H). [13]**C-NMR (CDCl$_3$, 126 MHz, ppm)**: 136.41, 135.79, 135.58, 133.47, 133.24, 126.49, 123.79, 122.15, 100.79, 100.69, 97.14, 97.12, 62.71, 32.53. **LRMS (EI)** *m/z* 371.1(36%), 402.2 (100%), 403.2 (38%). **HRMS (EI)** calcd for [C$_{20}$H$_{27}$OSi$_2$S$_2$] 403.1042 found 403.1038.

Synthesis of 2-(5,5'-diethynyl-2,2'-bithiophen-3-yl)ethanol **3.20**
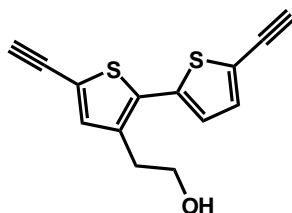
0.80 g (1.99 mmol) of 2-(5,5'-bis(trimethylsilyl)ethynyl)-2,2'-bithiophen-3-yl)ethanol was dissolved in a mixture of methanol (20 ml) and THF (6 ml). Once dissolved, 3 ml of a 2 M aqueous solution of potassium carbonate was added to the mixture, which was then stirred for 3 hours at room temperature. The reaction mixture was washed with water 15 ml, after which the organic fractions were extracted from the aqueous layer by diethyl ether several times and the combined organic phase was dried over magnesium sulfate. The solvent was subsequently removed under reduced pressure. 0.38 g of 2-(5,5'-Diethynyl-2,2'-bithiophen-3-yl)ethanol **3.20** was obtained in 75% yield as brown oil. **H-NMR (CDCl$_3$, 400 MHz, ppm)**: 7.09 (d, *J*=3.7, 1H), 7.04 (s, 1H), 6.94 (d, *J*=3.7, 1H) 3.80(t, *J*=6.5, 2H), 3.35 (d, *J*=10.5, 2H) 2.88 (t, *J*=6.5, 2H). [13]**C-NMR (CDCl$_3$, 126 MHz, ppm)**: 136.37, 135.98, 135.67, 133.56, 133.31, 126.54, 122.64, 121.02, 82.74, 82.59, 62.50, 32.29. **LRMS (EI)** *m/z* 221.0.0 (40%), 245.0 (42%), 258.0 (10%). **HRMS (EI)** calcd for [C$_{14}$H$_{10}$OS$_2$] 258.0173 found 258.0178.

Synthsis of 1,4-bis((trimethylsilyl)ethynyl)benzene **3.22**
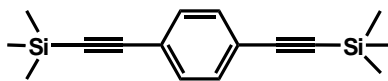
To a two-necked round-bottom flask equipped with a magnetic stirrer and sealed with a rubber septum was added 3 g (9 mmol) of 1,4-diiodobenzene **3.21**. 20 ml of pyridine and 10 ml of triethylamine were then added to the starting material under N_2. The mixture was degassed several times. 0.06 g (0.09 mmol) of PdCl$_2$(PPh$_3$), 0.03 g (0.18 mmol) of CuI and 0.02 g (0.09 mmol) of PPh$_3$ were added to the mixture under N_2. In the next stage, 2.5 ml (18 mmol) of trimethylsilylacetylene was added to the mixture. The mixture was stirred at 75 °C for approximately 16 hours. The mixture was quenched with 10 ml of 2 M HCl and diluted with 30 ml of DCM. The organic layer was separated and washed with 60 ml of water, then dried over MgSO$_4$. The solvent was removed under reduced pressure. The crude was purified by column chromatography using hexane : ethyl acetate (9:1) as eluent. 2.26 g of 1,4-Bis((trimethylsilyl)ethynyl)benzene **3.22** was obtained as a bright yellow solid (93% yield). **^{1}H-NMR (d6-DMSO, 400 MHz, ppm)**: 7.21 (s, 4H), 0.04 (s, 9H).**^{13}C-NMR (d6-DMSO, 101 MHz, ppm)**: 132.16, 123.52, 104.95, 96.71. **LRMS (EI)** *m/z* 255.2 (100%), 270.1 (30%). **HRMS (EI)** calcd for [C$_{16}$H$_{22}$OSi$_2$] 270.1268 found 270.1260.

Synthesis of 1,4-diethynylbenzene **3.23**
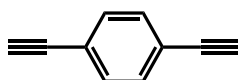
2.2 g (7.7 mmol) of 1,4-bis((trimethylsilyl)ethynyl)benzene **3.22** was dissolved in a mixture of methanol (25 ml) and THF (10 ml). 3 ml of a 2 M aqueous solution of potassium carbonate was then added, and the mixture was stirred for 3 hours at room

temperature. The reaction mixture was washed with 15 ml of water, after which the organic fractions were extracted from the aqueous layer by diethyl ether several times and the combined organic phase was dried over magnesium sulfate. The solvent was removed under reduced pressure. 0.73 g of 1,4-Diethynylbenzene **3.23** was obtained as a dark brown solid (75% yield). **H-NMR (CDCl$_3$, 400 MHz, ppm)**: 7.36 (s, 4H), 3.09 (s, 2H). **^{13}C-NMR (CDCl$_3$, 126 MHz, ppm)**: 130.99, 121.54, 82.01, 78.06. **LRMS (EI)** *m/z* 100.0 (5%), 126.2 (100%). **HRMS (EI)** calcd for [C$_{10}$H$_6$] 126.0470 found 126.0464.

References

1.   Tsuji, J., *Palladium Reagents and Catalysts: New Perspectives for the 21st Century2004*. Wiley: New York, 2004.

2.   Ortiz, R. P.; Casado, J.; Hernandez, V.; Navarrete, J. T. L.; Orti, E.; Viruela, P. M.; Milian, B.; Hotta, S.; Zotti, G.; Zecchin, S.; Vercelli, B., *Advanced Functional Materials* **2006,** *16* (4), 531-536.

3.   McQuade, D. T.; Pullen, A. E.; Swager, T. M., *Chemical Reviews* **2000,** *100* (7), 2537-2574.

4.   Stephens, R. D.; Castro, C. E., *Journal of Organic Chemistry* **1963,** *28* (12), 3313-&.

5.   Sonogashira, K.; Tohda, Y.; Hagihara, N., *Tetrahedron Letters* **1975,** (50), 4467-4470.

6.   Negishi, E.; Anastasia, L., *Chemical Reviews* **2003,** *103* (5), 1979-2017.

7.   Tsuji, J., *Palladium Reagents and Catalysts: Innovations in Organic Synthesis*. Wiley: New York, 1995.

8.   Chinchilla, R.; Najera, C., *Chemical Reviews* **2007,** *107* (3), 874-922.

9.   Raju, S.; Kumar, P. R.; Mukkanti, K.; Annamalai, P.; Pal, M., *Bioorg. Med. Chem. Lett.* **2006,** *16* (24), 6185-6189.

10.   Feuerstein, M.; Doucet, H.; Santelli, M., *J. Mol. Catal. A-Chem.* **2006,** *256* (1-2), 75-84.

11.   Miyaura, N.; Yamada, K.; Suzuki, A., *Tetrahedron Letters* **1979,** *20* (36), 3437-3440.

12.   Miyaura, N.; Suzuki, A., *J. Chem. Soc.-Chem. Commun.* **1979,** (19), 866-867.

13.   Miyaura, N.; Suzuki, A., *Chemical Reviews* **1995,** *95* (7), 2457-2483.

14.   chemistryworld/News

15.   Matos, K.; Soderquist, J. A., *Journal of Organic Chemistry* **1998,** *63* (3), 461-470.

16.   Bidan, G.; De Nicola, A.; Enee, V.; Guillerez, S., *Chemistry of Materials* **1998,** *10* (4), 1052-1058.

17.   Cremer, J.; Mena-Osteritz, E. M.; Pschierer, N. G.; Mullen, K.; Bauerle, P., *Organic & Biomolecular Chemistry* **2005,** *3* (6), 985-995.

18.   Milstein, D.; Stille, J. K., *Journal of the American Chemical Society* **1978,** *100* (11), 3636-3638.

19.   Stille, J. K., *Angew. Chem.-Int. Edit. Engl.* **1986,** *25* (6), 508-523.

20.   Kalinin, V. N., *Synthesis-Stuttgart* **1992,** (5), 413-432.

21.   Casado, A. L.; Espinet, P., *Organometallics* **1998,** *17* (5), 954-959.

22.   Leonardo S. Santos, G. B. R., Ronaldo A. Pilli, and Marcos N. Eberlin *J.Org. Chem* **2007,** *72* (15), 5809 -5812.

23.   Barbarella, G.; Zambianchi, M.; Bongini, A.; Antolini, L., *Journal of Organic Chemistry* **1996,** *61* (14), 4708-4715.

24.   Ewbank, P. C.; Nuding, G.; Suenaga, H.; McCullough, R. D.; Shinkai, S., *Tetrahedron Letters* **2001,** *42* (2), 155-157.

25.   Takahashi, M.; Masui, K.; Sekiguchi, H.; Kobayashi, N.; Mori, A.; Funahashi, M.; Tamaoki, N., *Journal of the American Chemical Society* **2006,** *128* (33), 10930-10933.

26.   Sonogashira, K., *Journal of Organometallic Chemistry* **2002,** *653* (1-2), 46-49.

Chapter 3

SYNTHESIS OF AZIDE-SUBSTITUTED OLIGOHETEROAROMATIC

COMPOUNDS

Abstract

This chapter describes the synthesis of azide-substituted oligoheteroaromatic compounds from the corresponding amines. The required amine-substituted oligoheteroaromatic compounds were synthesised using a range of reactions including bromination, lithiation and Suzuki cross coupling reactions. A second route to azide-substituted oligoheteroaromics involving Pd-catalysed cross coupling of azide-containing building blocks is also described.
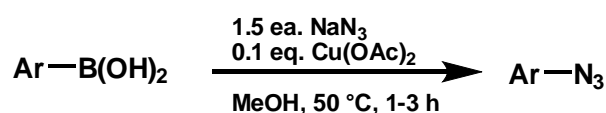
3.1 Introduction

Since the discovery of phenyl azide (PhN$_3$) nearly 150 years ago by Peter Grieß and the subsequent development of organic azides (RN$_3$) such as aryl, acyl, and alkyl azides, a great number of applications have been found for these compounds in a variety of organic reactions[1] with a particular increase since the 1940s.[2] In more modern times organic azides have been used widely in pharmaceuticals, for example the use of azidonucleotides for the treatment of acquired immune deficiency syndrome (AIDS).[3] The synthesis and properties of aliphatic and aryl azides are markedly different,[4, 5] and therefore this Chapter will limit itself to a consideration of the relevant aryl azides.

Synthesis of Organic Azides

The aryl azide compounds were synthesised using different routes, for example hydrazine reacting with diazonium salts, however these reactions were soon followed by the Cu(II) catalysed conversion of organoboron compounds to the corresponding azide (Scheme 3.1).[6, 7]

$$Ar-B(OH)_2 \xrightarrow[\text{MeOH, 50 °C, 1-3 h}]{\substack{\text{1.5 ea. NaN}_3 \\ \text{0.1 eq. Cu(OAc)}_2}} Ar-N_3$$

Scheme 3.1

The azides derived from heteroaryls play an increasingly important role in modern chemistry. Capitosti *et al.*[8] have demonstrated the introduction of an azide functional group in the formation of azido-thalidomide through the conversion of an intermediate diazonium salt into the respective aryl azide (Scheme 3.2).
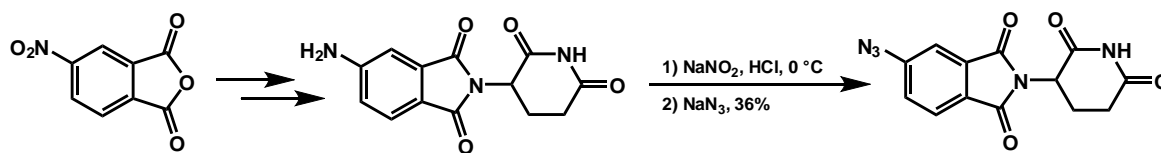
Scheme 3.2

Here, the heterocycle was prepared from nitrophtalic anhydride by means of classical organic chemistry, in which the amino function was formed through reduction of a nitro-substituted precursor. Subsequent diazotization and reaction with sodium azide (NaN$_3$) formed the azido-thalidomide, which has been shown to be more active than thalidomide in humans.[8] Activated aromatic systems suc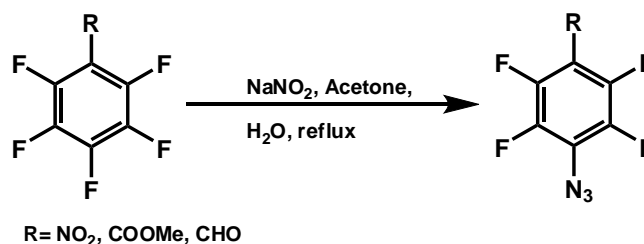h as halogenated arenes[9] (Scheme 3.3) and certain heteroaromatic systems[10] can also be subjected to nucleophilic attack by azide anions, and are typically electrophilic enough to produce high yields of the aryl azide.

Scheme 3.3

Over the last 15 years or so, a large number of papers have been published regarding the preparation of aryl azides using organometallic reagents with numbers obviously increasing following the introduction of the concept of "click chemistry".

In 2002, Tilley *et al*[11] published the reaction of lithium reagents (or Grignard reagents depending on the corresponding aryl halide) with tosyl azide, which can be used to form unique aryl azides (Scheme 3.4)
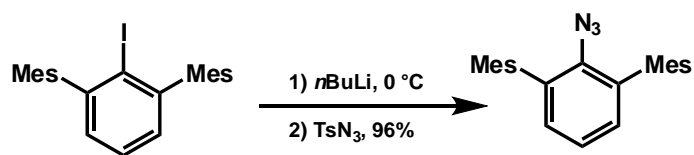
Scheme 3.4

(Mes = mesityl, Ts = para-toluenesulfonyl)

In this reaction, 2,6-dimesitylphenyl iodide was treated with *n*-butyllithium at 0 $^{\circ}$C, and the formed lithium salt was treated with *p*-toluenesulfonyl azide in order to produce the aryl azide in high (96%) yield. Similar-looking, but curiously different, chemistry was presented by Fisher in the 1960's who reacted of anilines with a strong base to form an aryl amide salt which was then reacted with tosyl azide to form the corresponding aryl azide and *p*-toluenesulfonamide (i.e. a nitrogen-nitrogen bond in the original tosyl azide is broken in the process).[12]

A widely used method for the formation of aryl azides (although is equally applicable to aliphatic, acyl and sulfonyl azides) is to react nitrosyl ions (or their precursors) with hydrazines. Nitrosyl salts[13], sodium nitrite[14] and even N_2O_4[15] or NO/O_2 gas mixtures[16] have all been shown to be particularly useful for these kinds of transformations (Scheme 3.5).
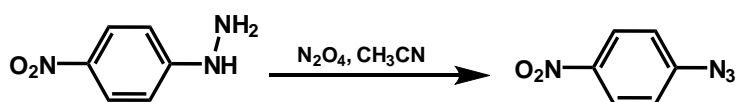
Scheme 3.5 The conversion of an aromatic hydrazine into an aryl azide.[15]

Preparation of aryl and heteroaryl azides can also be achieved through the reaction of an appropriate aniline with triflyl azide, as demonstrated by Liu and Tor[17] (see Scheme 3.6); as the reaction conditions are relatively mild and yet provide high product yields, this

synthetic route is widely used for the preparation of aromatic azides. A typical example of a reaction following Lin and Tor's method involves the reaction of 8-aminoquinoline with freshly prepared triflyl azide at room temperature in a methanol-dichloromethane solvent mixture, with triethylamine and copper sulphate present. The resulting 8-azidoquinoline is produced in an almost quantitative yield.
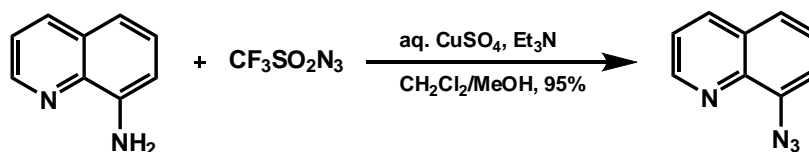
Scheme 3.6 Conversion of aromatic amines to the corresponding aryl azide.[17]

Of particular interest to our work is the report by Spinelli and Zanirato that the azide functional group is not stable when placed directly on a thiophene ring.[18] Azide functional groups in both position 2 and 3 on the thiophene ring generally result in ring opening (Scheme 3.7). For this reason, in our work the decision was made to synthesise compounds carrying the azide group on a benzene ring.
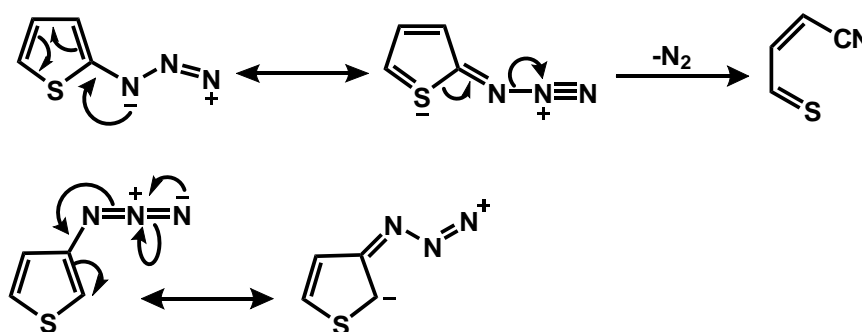
Scheme 3.7

In more complex applications, organic azides have been used as building blocks in the partial synthesis of complex natural products, and have been utilized in gene technology [19].

3.2 Result and discussion

A series of azide-substituted heteroaromatic compounds was targeted to complement our series of alkynes (Chapter 2). The targets (Scheme 3.8) were selected based on commercially available starting materials.
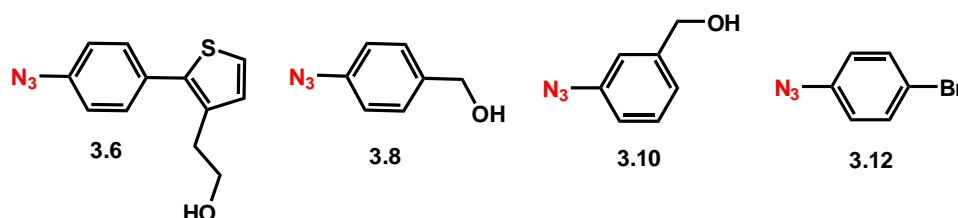
Scheme 3.8

Compound **3.6** can be traced back to commercially available 3-(2-hydroxyethyl)thiophene and bromoaniline; the order in which the azide group is introduced and the cross-coupling reaction is carried out can be varied. The precursor amines for **3.8**, **3.10** and **3.12** are all commercially available.

3.2.1 Synthesis of 2-(2-(4-azidophenyl)thiophen-3-yl)ethanol 3.6

The first step in the preparation of **3.6** is the protection of the hydroxyl group in 3-(2-hydroxyethyl)thiophene as a tetrahydropyran by means of reaction of the alcohol with 1,4-dihydropyran at room temperature (Scheme 3.9).
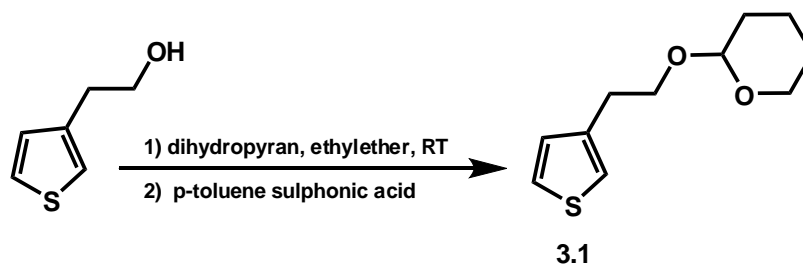
Scheme 3.9

This reaction produces 2-(2-(thiophen-3-yl)ethoxy)tetrahydro-2H-pyran **3.1** in 91%. 2-(2-(Thiophen-3-yl)ethoxy)tetrahydro-2H-pyran **3.1** was brominated using one equivalent of *N*-bromosuccinimide in DMF, which resulted in the production of 2-(2-(2-bromothiophen-3-yl)ethoxy)tetrahydro-2H-pyran **3.2** in 87% yield (Scheme 3.10).
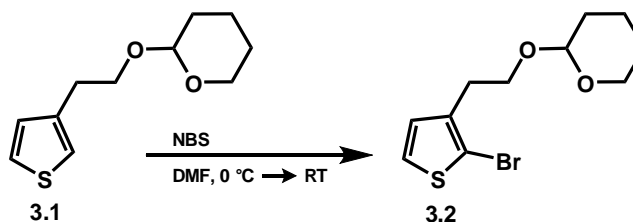
Scheme 3.10

The subsequent lithiation of 2-(2-(2-bromothiophen-3-yl)ethoxy)tetrahydro-2H-pyran **3.2** using n-BuLi readily took place at -78 °C, using THF as solvent. The lithiated species was quenched with borolane at -78 °C in order to obtain the desired boronic ester **3.3** in 78 % yield (Scheme 3.11).
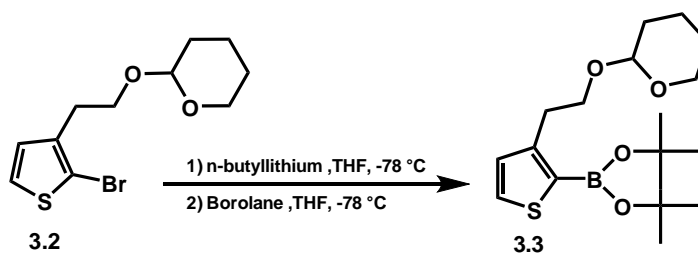
Scheme 3.11

Compound **3.3** was coupled with 4-bromoaniline by means of a Suzuki cross-coupling reaction. 2-Aniline-3-(2- tetrahydropyranyloxyethyl)thiophene **3.4** was obtained in 65% yield (Scheme 3.12).
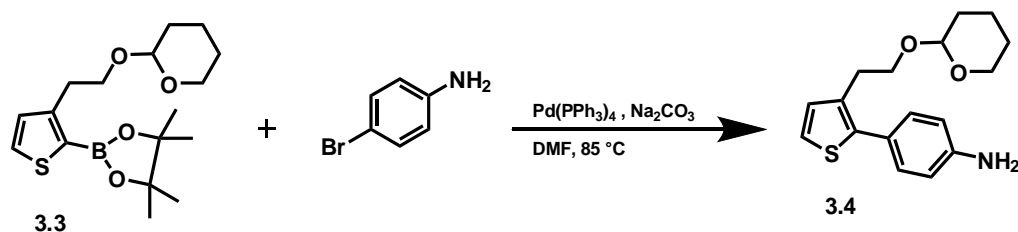
Scheme 3.12

The synthesis of 2-(2-(2-(4-azidophenyl)thiophen-3-yl)ethoxy)tetrahydro-2H-pyran **3.5** was achieved through the reaction of 2-aniline-3-(2- tetrahydropyranyloxyethyl)thiophene **3.4** with sodium nitrite at 0 °C to prepare the diazonium salt intermediate. The addition of sodium azide as nucleophile at 0 °C resulted in the formation of **3.5** in 78% yield (Scheme 3.13).
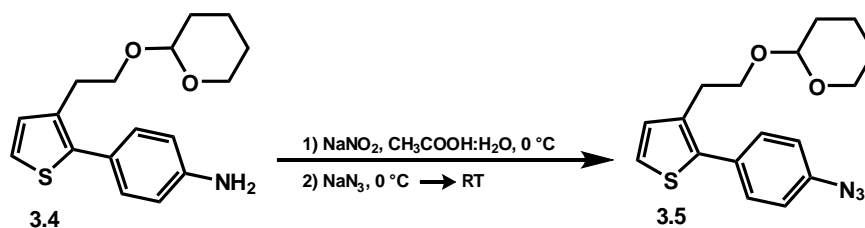
Scheme 3.13

Finally, the THP protecting group was removed using hydrochloric acid (2M) in THF as the solvent, providing 2-(2-(4-azidophenyl)thiophen-3-yl)ethanol **3.6** in 90% yield (Scheme 3.14).
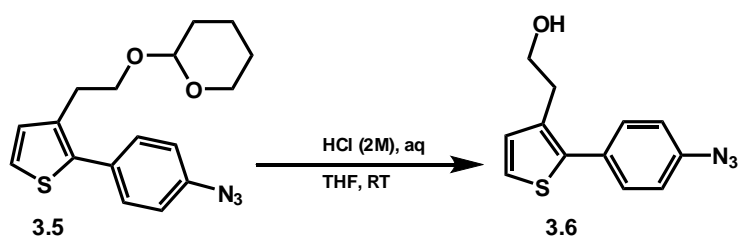
Scheme 3.14

3.2.2 Synthesis of (4-azidophenyl)methanol 3.8

(4-azidophenyl)methanol **3.8** was synthesised through the reaction of commercially available (4-aminophenyl)methanol **3.7** with sodium nitrite at 0 °C to produce the corresponding diazonium salt. The addition of sodium azide as a nucleophile at 0 °C yielded compound **3.8** in 82% yield (Scheme 3.15).
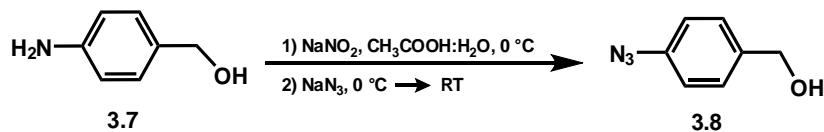
Scheme 3.15

3.2.3 Synthesis of (3-azidophenyl)methanol 3.10

Analogously, (3-azidophenyl)methanol **3.10** was synthesised by means of the reaction of commercially available (3-aminophenyl)methanol **3.9** with sodium nitrite at 0 °C in to synthesise the intermediate diazonium salt. The addition of sodium azide as a nucleophile to the intermediate diazonium salt at 0 °C produced compound **3.10** in 80% yield (Scheme 3.16).
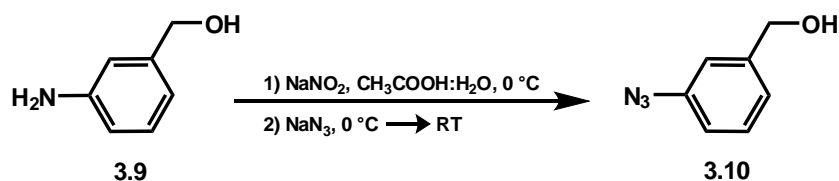
Scheme 3.16

3.2.4 Synthesis of 1-azido-4-bromobenzene 3.12

The preparation of 1-azido-4-bromobenzene **3.12** similarly involved the reaction of commercially available 4-bromoaniline **3.11** with sodium nitrite at 0 °C to synthesise the intermediate diazonium salt which was reacted without isolation with sodium azide as a nucleophile at 0 °C to yield **3.12** in 92% yield (Scheme 3.17).
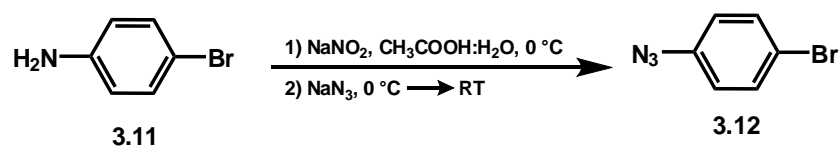
Scheme 3.17

3.2.5 Suzuki reactions in the presence of azide functional groups

A series of reactions has been carried out in order to test the feasibility of Suzuki reactions involving reactants carrying azide functionality, with a particular focus on the stability of azide and the yield (Scheme 3.18).
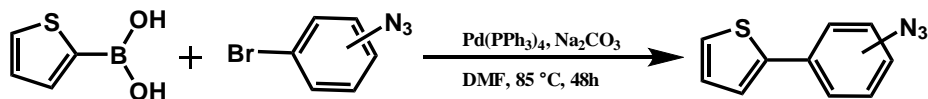
Scheme 3.18

Standard Suzuki conditions have been used for azide-substituted compounds (Scheme 3.11), which involved their reaction with a series of aryl boronic acids (phenyl boronic

acid, pyridine-3-boronic acid and thiophene-2-boronic acid). All 6 variations were successful in the coupling and the yields are summarised in Table 3.1.
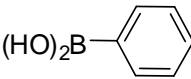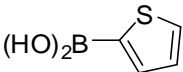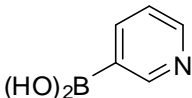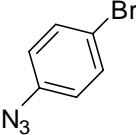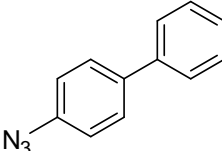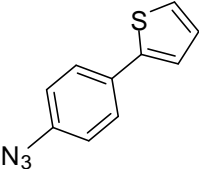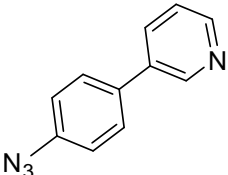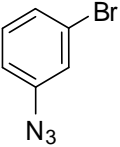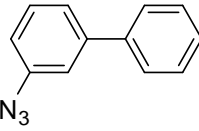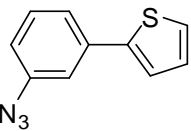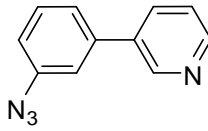
Table 3.1 yields for Suzuki cross-coupling reactions between azide-substituted compounds and different boronic acids.

Table 6.1 shows that all reactions suffered a loss in yield from near identical side reactions. Product analysis suggests that a principal source of reduced yield is the generation of amines, i.e. reduced versions of the final azides (with yields of ~15% respectively in all couplings). The reason for the formation of the amines could be a Staudinger reduction[20, 21] (Figure 3.1) with the required triphenylphosphine originating from the catalyst Pd(PPh$_3$)$_4$.
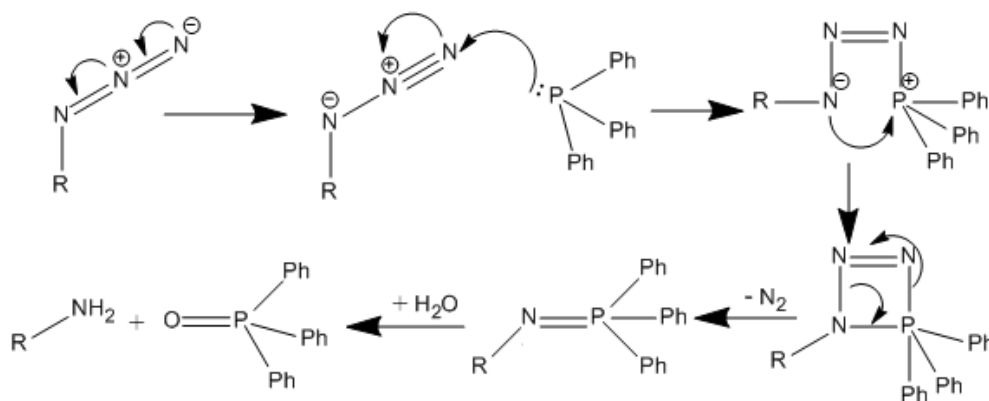
Figure 3.1 Staudinger reduction

The two synthetic strategies can now be compared. The strategy where the Suzuki reactions have been conducted first, using amine analogues (which are later converted to azides), tends to give yields of ~65%. The second strategy involves the synthesis of the azides from the amine groups, then coupling them by the Suzuki reaction. The Suzuki reaction in this case gives a lower yield (approximately 40% on average). As a result the preferable way to synthesise the azide building block is starting with the Suzuki coupling and then synthesising the azide.

3.3 Conclusion

A series of azide-substituted oligoheteroaromatic compounds have been synthesised through the conversion of amines to the azide group via the formation of the intermediate diazonium salt. All targeted azidoheteroaromatics were synthetically accessible without major problems. Tests have also been done for Suzuki cross coupling in the presence of azide functional groups. Our results indicate that the yield for such reactions is between 30% to 55%, the reason for the lower yield compared to ordinary Suzuki cross coupling reactions could be the Staudinger reduction of azide groups to the corresponding amines.

3.4 Materials and methods

Commercially available reagents, starting materials and solvents were purchased from commercial suppliers and used without further purification. Certain solvents, such as THF, were dried with the use of an MBraun solvent purification system. ^{1}H-NMR and ^{13}C-NMR spectra were recorded at 400 MHz and 100 MHz, respectively, on a Bruker B-ACS-6 or at 500MHz and 126 MHz, respectively, on a Bruker Avance 500 spectrometer. High resolution mass spectra (HRMS) were recorded by means of a Water Micromass LCT Premier; while low resolution mass spectra (LRMS) were recorded using a Perkin Elmer Turbo mass GC/MS. The Suzuki coupling reactions were conducted under an N_2 atmosphere and the solvent was degassed using the freeze-pump-thaw method. All column chromatography was performed using silica gel.

3.5 Experimental procedures

Synthesis of 2-(2-(thiophen-3-yl)ethoxy)tetrahydro-2H-pyran **3.1**
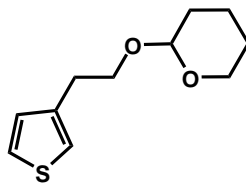
1 g (7.81 mmol) of 3-(2-hydroxyethyl)thiophene was added to a round-bottom flask equipped with a magnetic stirrer. To this, 25 ml of anhydrous diethyl ether was added. Subsequently, 0.98 g (11.7 mmol) of dihydropyran in 25 ml of anhydrous ether was added to the solution by syringe. 0.5 g (2.90 mmol) of p-toluenesulphonic acid was then added and the mixture was stirred at room temperature for approximately 12 h. After this time, the solution was washed with 10% Na_2CO_3. The aqueous layer was then extracted using ether and the combined organic layers were dried over $MgSO_4$. The solvent was removed under reduced pressure and the product was dried further under vacuum. The resulting product was purified through the use of column chromatography (hexane : diethyl ether 8:2). 1.48 g of the title compound was obtained as colourless oil (90% yield). **^{1}H-NMR (CDCl$_3$, 400 MHz, ppm)**: 7.25-7.33 (m, 1H), 7.02-7.13 (m, 2H), 4.54 (t, *J*=3.0, 1H), 3.76-3.83 (m, 4H), 2.87 (t, *J*=7.0, 2H), 1.6-1.67 (m, 6H). **^{13}C-NMR (CDCl$_3$, 126 MHz, ppm)**: 139.4, 128.6, 125.1, 121.1, 98.7, 67.6, 62.2, 30.8, 30.7, 25.5, 19.5. **LRMS (EI)** *m/z* 128.11 (30%), 212.11 (60%). **HRMS (EI)** calcd for [C$_{11}$H$_{15}$O$_2$S] 211.0793 found 211.0788.

Synthesis of 2-(2-(2-bromothiophen-3-yl)ethoxy)tetrahydro-2H-pyran **3.2**
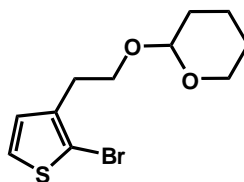
2.073 g (9.77 mmol) 3-[2-(Tetrahydropyranyloxy)ethyl]thiophene was added to a round-bottom flask equipped with a magnetic stirrer, which was subsequently placed in an ice bath. DMF (40 ml) was then added, after which 1.82 g (10 mmol) of *N*-bromosuccinimide was added to the solution, the ice bathe was removed after 1hour.The mixture was stirred at room temperature for approximately 12 h. Once this had been completed, the solution was washed using 10% Na_2CO_3. The aqueous layer was extracted with ethyl acetate and the organic layer was dried over $MgSO_4$. The solvent was then removed from the organic fractions under reduced pressure and the product dried under vacuum. The resulting crude product was purified utilising column chromatography with hexane : ethyl acetate (9:1) as eluent. 2.41 g of a pale yellow oil was obtained in 85% yield. **^{1}H-NMR (CDCl$_3$, 400 MHz, ppm)**: 7.42 (d, *J*=4.7, 1H), 7.02 (d, *J*=4.7, 1H), 4.50 (t, *J*=3.3, 1H), 3.83-3.90 (m,4H), 2.85 (t, *J*=7.1, 2H), 1.72-1.84 (m, 6H). **^{13}C-NMR (CDCl$_3$, 126 MHz, ppm)**: 138.94, 129.18, 125.63, 110.38, 99.00, 66.70, 62.50, 31.04, 30.41, 25.87, 19.83. **LRMS (EI)** *m/z* 190.0 (45%), 211.1 (16%) 291.9 (3%). **HRMS (EI)** calcd for [$C_{11}H_{15}O_2SBr_2$] 289.9976 found 289.9981.

Synthesis of 4,4,5,5-tetramethyl-3-**[**2-(tetrahydropyranyloxy)ethyl**]**thiophene-2-dioxaborolane **3.3**
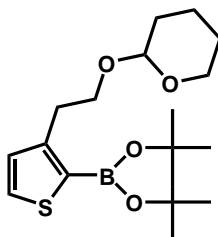
A solution of 3 g (10.3 mmol) 2-bromo-3-[2-(tetrahydropyranyloxy)ethyl]thiophene in 30 ml THF was cooled to -78 °C under nitrogen. A 6.22 ml (15.4 mmol) solution of n-butyl lithium in hexane (2.5 M) was then added by syringe under nitrogen. The mixture was allowed to reach room temperature, and stirred for 2 h. The mixture was then cooled again to -78 °C. At this temperature, 4.07 ml (20.6 mmol) 2-isopropoxy-4,4,5,5-tetramethyl dioxaborolane was added. The mixture was then allowed to return to room temperature and stirred for a further 15 h. The solution was washed with distilled water (3 times 20 ml) and the aqueous layer was extracted using diethyl ether. The combined organic layers were dried over $MgSO_4$ and the solvent was removed under reduced pressure. 2.72 g of yellow oil was obtained (78% yield). **^{1}H-NMR (CDCl$_3$, 400 MHz, ppm)**: 7.42 (d, *J*=4.6, 1H), 7.03 (d, *J*=4.7, 1H), 4.61 (t, *J*=3.1, 1H), 3.82-3.92 (m, 4H), 2.88 (t, *J*=6.7, 2H), 1.76-1.86 (m, 6H), 1.26 (s,16H). **^{13}C-NMR (CDCl$_3$,126 MHz, ppm)**: 150.42, 131.30, 130.89, 98.35, 83.62, 82.79, 67.93, 61.92, 30.70, 25.51, 24.79, 19.42, 13.87. **LRMS (EI)** *m/z* 337.3 (28%), 338.1 (100%). **HRMS (EI)** calcd for [C$_{17}$H$_{27}$O$_4$SB] 338.1723 found 338.1735.

Synthesis of 2-aniline-3-(2- tetrahydropyranyloxyethyl)thiophene **3.4**
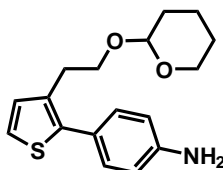
In a Schlenk tube with a condenser and a rubber septum under N_2 was placed 0.1 g (5.81 mmol) of 4-bromoaniline to which 10 ml of DMF was added. The solution was degassed three times under N_2, after which 2.95 g (11.62 mmol) of 4,4,5,5-tetramethyl-3-[2-(tetrahydropyranyloxy)ethyl]thiophene-1,3 2-dioxaborolane **3.3** was added. Once the addition had been completed, 0.06 g (0.058 mmol) of $Pd(PPh_3)_4$ was added. 3 ml of a (1 M) aqueous solution of Na_2CO_3 was injected into the reaction through a rubber septum. The reaction was heated to 85 °C under the exclusion of both oxygen and light for 24 hours. After this time, the reaction mixture was washed with distilled water (60 ml) and the combined organic fractions were extracted from the aqueous layer using DCM. The organic layer was dried over $MgSO_4$ and the solvent was removed under reduced pressure. The crude product was then purified by column chromatography using hexane : ethyl acetate (2:1) as eluent. 1.15 g of 2-Aniline-3-(2- tetrahydropyranyloxy)ethyl)thiophene **3.4** was obtained as a brown oil (65% yield). **^{1}H-NMR (CDCl$_3$, 400 MHz, ppm)**: 7.21 (d, *J*=8.3, 2H) 7.08 (d, *J*=5.3, 1H) 6.94 (d, *J*=5.2, 1H) 6.67 (d, *J*=8.3, 2H) 4.44 (t, *J*=3.5, 1H) 3.60-3.75 (m, 4H), 2.73 (t, *J*=6.9, 2H), 1.5-1.67 (m, 6H). **^{13}C-NMR (CDCl$_3$, 101MHz, ppm)**: 146.30, 140.11, 134.18, 130.93, 129.98, 124.95, 123.09, 115.38, 99.03, 68.09, 62.50, 31.05, 29.51, 25.88, 19.87. **LRMS (EI)** *m/z* 188.2 (88%), 219 (30%), 303 (18%) 304.2 (3%). **HRMS (EI)** calcd for [$C_{17}H_{21}NO_2S$] 303.1293 found 303.1292.

Synthesis of 2-(2-(2-(4-azidophenyl)thiophen-3-yl)ethoxy)tetrahydro-2H-pyran **3.5**
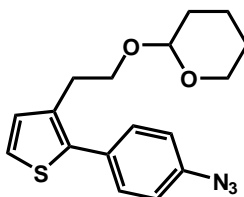
0.5 g (1.65 mmol) of 2-aniline-3-(2-tetrahydropyranyloxy)ethyl)thiophene **3.4** was dissolved in a 15 ml mixture of acetic acid and water (1:1). The solution was stirred at 0 °C for 15 minutes. Sodium nitrite (0.17 g, 2.47 mmol) was slowly added to the solution at 0 °C. The mixture was stirred for 1 h, after which 0.16 g (2.47 mmol) of sodium azide was slowly added, at a temperature of 0 °C. The reaction mixture was stirred for another 1 h, then quenched by adding 20 ml of water and diluted by 25 ml of DCM. After this, the mixture was washed with saturated of Na_2CO_3 and 60 ml water and the organic layer was washed with brine. Once this was completed, the combined organic fractions were dried over $MgSO_4$. The solvent was removed under reduced pressure and the crude was purified with column chromatography using hexane : ethyl acetate (9:1) as eluent. 0.38 g of **(**2-(4-Azidophenyl)thiophen-3-yl)ethoxy)tetrahydro-2H-pyran **3.5** was obtained as a pale red oil (71% yield). **^{1}H-NMR (CDCl$_3$, 400 MHz, ppm)**: 7.42 (d, *J*=8.4, 2H) 7.15 (d, *J*=5.3, 1H) 6.97 (d, *J*=8.4, 2H) 7.10 (d, *J*=5.1, 1H) 4.44 (t, *J*=3.5, 1H) 3.60-3.70 (m, 4H), 2.73 (t, *J*=6.9, 2H), 1.5-1.65 (m, 6H**). ^{13}C-NMR (CDCl$_3$, 126 MHz, ppm)**: 139.60, 138.63, 135.45, 131.66, 131.25, 130.18, 124.28, 119.54, 99.06, 67.91, 62.48, 31.00, 29.53, 25.84, 19.82. **LRMS (EI)** *m/z* 243.06 (18%), 303.13 (32%), 329.12 (5%). **HRMS (EI)** calcd for [C$_{17}$H$_{19}$N$_3$O$_2$S] 329.1198 found 329.1202. **IR** ν cm^{-1} 2126, 2091.

Synthesis of 2-(2-(4-azidophenyl)thiophen-3-yl)ethanol **3.6**
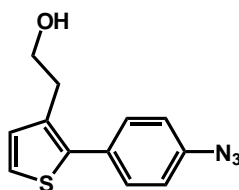
0.30 g (0.91 mmol) of **(**2-(4-azidophenyl)thiophen-3-yl)ethoxy)tetrahydro-2H-pyran **3.5** was dissolved in 20 ml THF. Subsequently, 10 ml of 2 M HCl was added to the solution, which was then stirred at room temperature for 5 h. After this, 10 ml aqueous solution of Na$_2$CO$_3$ was added. The organic fractions were extracted by DCM. The combined organic fractions were dried over MgSO$_4$ and the solvent was removed under reduced pressure. 0.20 g of (2-(4-Azidophenyl)thiophen-3-yl)ethanol was gathered as a yellow oil (90% yield) and did not require purification. **^{1}H-NMR (CDCl$_3$, 400 MHz, ppm)**: 7.32 (d, *J*=8.6, 2H), 7.20 (d, *J*=5.2, 1H), 6.99 (d, *J*=8.6, 2H), 6.94 (d, *J*=5.2, 1H) 3.79 (t, *J*=6.4, 2H) 2.86 (t, *J*=6.6, 2H). **^{13}C-NMR (CDCl$_3$, 126 MHz, ppm)**. 138.42, 137.89, 133.31, 130.01, 128.333, 124.56, 123.31, 118.19, 61.96, 30.79. **LRMS (EI)** *m/z* 200.05 (52%), 237.15 (23%), 246.06 (55%). **HRMS (EI)** calcd for [C$_{12}$H$_{12}$N$_3$OS] 246.0701 found 246.0696. **IR** ν cm^{-1} 2127, 2092.

Synthesis of (4-azidophenyl)methanol **3.8**
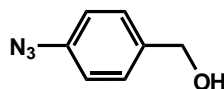
A procedure analogous to the procedure described above for the synthesis of **3.5** was used, using 1 g (8.10 mmol) of (4-aminophenyl)methanol **3.7**, 0.83 g (12.1 mmol) of sodium nitrite and 0.78 g (12.1 mmol) of sodium azide. 0.96 g of (4-azidophenyl)methanol **3.8** was obtained as a brown solid (80% yield). **^{1}H-NMR (CDCl$_3$, 400 MHz, ppm)**: 7.25 (d, *J*=8.3, 2H), 6.91 (d, *J*=4.8, 2H) 4.54 (s, 2H). **^{13}C-NMR (CDCl$_3$, 101 MHz, ppm)**: 139.72, 137.99, 128.93, 119.50, 64.99, 30.12. **LRMS (EI)** *m/z* 121.2 (90%), 123.1 (25%), 149.1 (20%). **HRMS (EI)** calcd for [C$_7$H$_7$N$_3$O] 149.0589 found 149.0586. **IR** ν cm^{-1} 2107.

Synthesis of (3-azidophenyl)methanol **3.10**
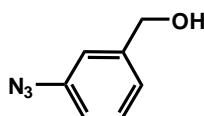
The procedure described for the synthesis of **3.5** was followed, using 1 g (8.11 mmol) of (3 aminophenyl)methanol **3.7**, 0.83 g (12.1 mmol) of sodium nitrite and 0.78 g (12.1 mmol) of sodium azide. 0.98 g of (3-Azidophenyl)methanol **3.10** was obtained as a dark brown solid (81% yield) **^{1}H-NMR (CDCl$_3$, 400 MHz, ppm)**: 7.29 (t, *J*=7.7, 2H), 7.06 (d, *J*=7.6, 2H) 6.99 (s, 1H), 6.91 (dd, *J*=2.1, 2H),) 4.6 (s, 2H). **^{13}C-NMR (CDCl$_3$, 126 MHz, ppm)**: 142.94, 140.33, 129.88, 123.23, 118.14, 117.30, 64.58. **LRMS (EI)** *m/z* 121.2 (90%), 123.1 (25%), 149.1 (20%). **HRMS (EI)** calcd for [C$_7$H$_7$N$_3$O] 149.0589 found 149.0588. **IR** ν cm^{-1} 2113.

Synthesis of 1-azido-4-bromobenzene **3.12**
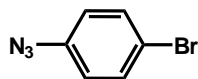
The procedure was analogous to the protocol described previously for the synthesis of **3.5**, using 0.1 g (0.58 mmol) of 4-bromoaniline **3.11**, 0.06 g (0.87 mmol) of sodium nitrite and 0.056 g (0.87 mmol) of sodium azide. 0.10 g of 1-Azido-4-bromobenzene **3.12** was obtained as brown oil (77% yield). **^{1}H-NMR (CDCl$_3$, 400 MHz, ppm)**: 7.39 (d, *J*=8.8, 2H), 6.83 (d, *J*=8.8, 2H). **^{13}C-NMR (CDCl$_3$, 101 MHz, ppm)**: 139.51, 133.20, 121.10, 118.19. **LRMS (EI)** *m/z* 170.3 (68%), 197.0 (92%). **HRMS (EI)** calcd for [C$_6$H$_4$N$_3$Br] 196.9589 found 196.9590. **IR** ν cm^{-1} 2128.

References

1.   Scriven, E. F. V.; Turnbull, K., *Chemical Reviews* **1988,** *88* (2), 297-368.

2.   Boyer, J. H.; Canter, F. C., *Chemical Reviews* **1954,** *54* (1), 1-57.

3.   Maag, H.; Rydzewski, R. M.; McRoberts, M. J.; Crawfordruth, D.; Verheyden, J. P. H.; Prisbe, E. J., *Journal of Medicinal Chemistry* **1992,** *35* (8), 1440-1451.

4.   Brase, S.; Gil, C.; Knepper, K.; Zimmermann, V., *Angewandte Chemie-International Edition* **2005,** *44* (33), 5188-5240.

5.   Hassner, A., *Accounts of Chemical Research* **1971,** *4* (1), 9-&.

6.   E. Noelting, O. M., Ber. Dtsch, *Chem. Ges* **1893,** *26*, 86 –87.

7.   Grimes, K. D.; Gupte, A.; Aldrich, C. C., *Synthesis-Stuttgart* **2010,** (9), 1441-1448.

8.   Capitosti, S. M.; Hansen, T. P.; Brown, M. L., *Org. Lett.* **2003,** *5* (16), 2865-2867.

9.   Chehade, K. A. H.; Spielmann, H. P., *Journal of Organic Chemistry* **2000,** *65* (16), 4949-4953.

10.   Miller, D. R.; Swenson, D. C.; Gillan, E. G., *Journal of the American Chemical Society* **2004,** *126* (17), 5372-5373.

11.   Gavenonis, J.; Tilley, T. D., *Organometallics* **2002,** *21* (25), 5549-5563.

12.   Fischer, W.; Anselme, J. P., *Journal of the American Chemical Society* **1967,** *89* (20), 5284-&.

13.   Pozsgay, V.; Jennings, H. J., *Tetrahedron Letters* **1987,** *28* (43), 5091-5092.

14.   Wamhoff, H.; Wambach, W., *Chemiker-Zeitung* **1989,** *113* (1), 11-15.

15.   Kim, Y. H.; Kim, K.; Shim, S. B., *Tetrahedron Letters* **1986,** *27* (39), 4749-4752.

16.   Matsuya, Y.; Itoh, T.; Nagata, K.; Ohsawa, A., *Tetrahedron* **1997,** *53* (46), 15701-15710.

17.   Liu, Q.; Tor, Y., *Org. Lett.* **2003,** *5* (14), 2571-2572.

18.   Domenico Spinelli, P. Z., *J. Chem. Soc. Perkin.Trans.* **1993,** *4* (1), 1129-1133.

19.   L. Wang, P. G. S., *Angew. Chem. Int. Ed.* **2005,** *44*, 34 – 6620.

20.   Fiona L. Lin, H. M. H., Herman van Halbeek, Robert G. Bergman,; Bertozzi, C. R., *J. Am. Chem. Soc.* **2005,** *127*, 2686-2695.

21.   Lin, F. L.; Hoyt, H. M.; van Halbeek, H.; Bergman, R. G.; Bertozzi, C. R., *Journal of the American Chemical Society* **2005,** *127* (8), 2686-2695.

Chapter 4

STRUCTURAL VARIATION OF OLIGOHETEROAROMATIC

COMPOUNDS USING CLICK CHEMISTRY

Abstract

This chapter describes the synthesis and characterisation of new π-conjugated molecules, utilising click chemistry between alkyne- and azide-substituted compounds to efficiently generate structural variety. A description is also provided of the synthesis of varied series of putative DNA binders, viz. di- and tricationic oligoheteroaromatic compounds based on the π-conjugated scaffolds created using click chemistry.

4.1 Introduction

As introduced and discussed in Chapter 1, Sharpless *et al.* developed the philosophy and concept of click chemistry as a method enabling the rapid tailoring and generation of a wide range of substances. The following chapters have introduced the development and subsequent synthesis of molecules designed to be the relatively small building blocks for larger DNA binders, "clicking" together like molecular LEGO. The "click" process has been used in this Chapter to construct synthetic intermediates and derived cationic structures, in relatively good yields.

4.2 Result and Discussion

4.2.1 Synthesis of di-cationically substituted oligoheteroaromatics

A series of conjugated dicationic oligoheteroaromatic compounds were synthesised, using the click reaction for the construction of the π-conjugated scaffolds, starting from the different building blocks (alkynes and azides) described in Chapters 2 and 3 (Scheme 4.1).
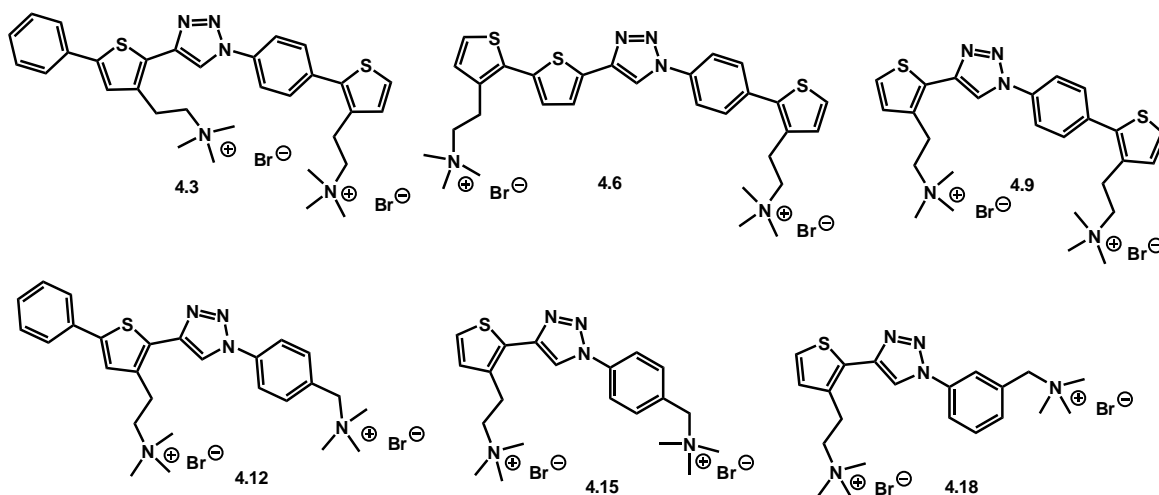
Scheme 4.1

The key synthetic step in the preparation of our conjugated oligoheteroaromatic compounds is the click reaction. The traditional click reaction involves the reaction of an alkyne and an azide compound in the presence of copper iodide as catalyst and triethylamine as a base, using H_2O as solvent with ethanol (EtOH) to improve the solubility of the stating materials at 60 °C.

We note that our experiments highlighted the need for the majority of products to undergo purification by column chromatography. It should also be mentioned that yields tended to be lower than many yields reported in the literature, which indicates that the click reaction does not always return a clean and high yield.

4.2.1a Synthesis of 4.3

Compound **4.3** was synthesised by reacting 1 equivalent of 2-benzene-5-ethynyl-3-(2-hydroxyethyl)thiophene **2.9** with 1 equivalent of 2-(2-(4-azidophenyl)thiophen-3-yl)ethanol **3.6,** in the presence of copper iodide as catalyst. Triethylamine was used as a base in the reaction and a mixture of EtOH: H_2O (1:1) was used as a solvent at 60 °C. The desired intermediate **4.1** was obtained in 77% yield. Intermediate **4.1** was subsequently converted into the corresponding dibromide **4.2** in an Appel reaction, usings an excess of carbon tetrabromide and triphenylphosphine at 0 °C under nitrogen atmosphere in extra dry DCM. To ensure a good yield in the Appel reaction, any traces of water were avoided. Dibromide **4.2** was obtained in 65 % yield. The final step in the synthesis of **4.3** is the conversion of dibromide **4.2** into the corresponding quaternary ammonium salt by a substitution reaction; the addition of trimethylamine in ethanol to **4.2** at room temperature for 5 days returned **4.3** in a 78% yield (Scheme 4.2).
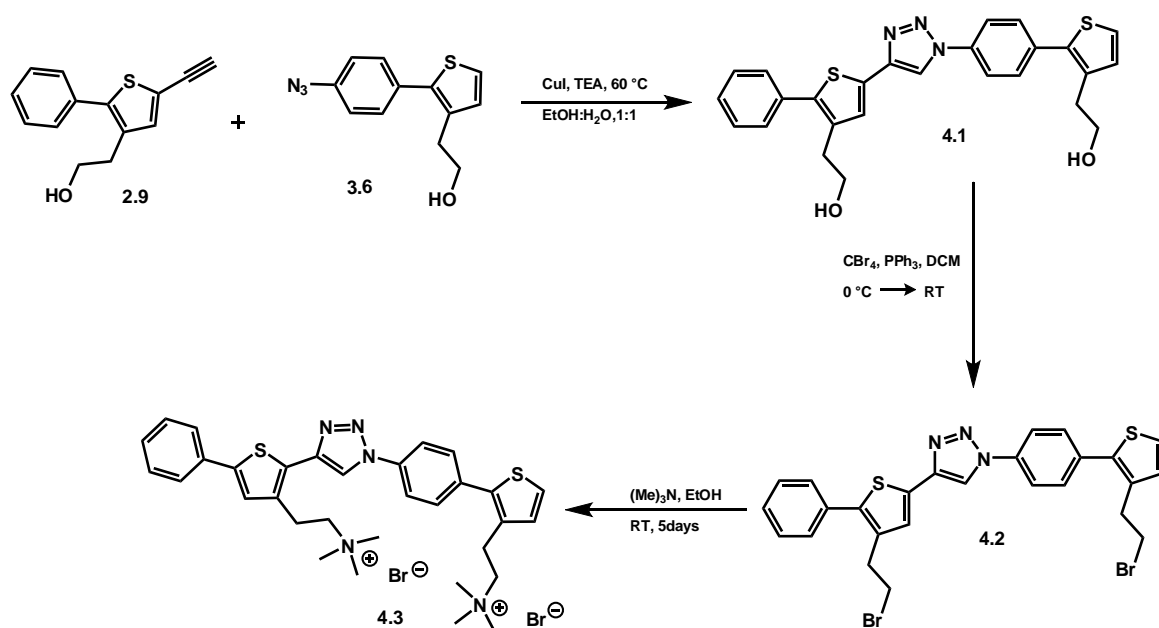
Scheme 4.2

4.2.1b Synthesis of 4.6

4.6 was prepared following the same synthetic strategy employed for **4.3**. Reacting 1.0equivalent of 2-(5-ethynyl-2,2'-bithiophen-3-yl)ethanol **2.16** with 1.0 equivalent of 2-(2-(4-azidophenyl)thiophen-3-yl)ethanol **3.6** yielded the desired intermediate **4.4** in 79% yield. A subsequent Appel reaction allowed conversion of the hydroxyl groups into the bromides, giving **4.5** in 62% yield. The final step involved converting dibromide **4.5** into the corresponding quaternary ammonium salt by means of a substitution reaction. The addition of trimethylamine in ethanol to **4.5** at room temperature for 5 days resulted in **4.6** in 60% yield (Scheme 4.3).
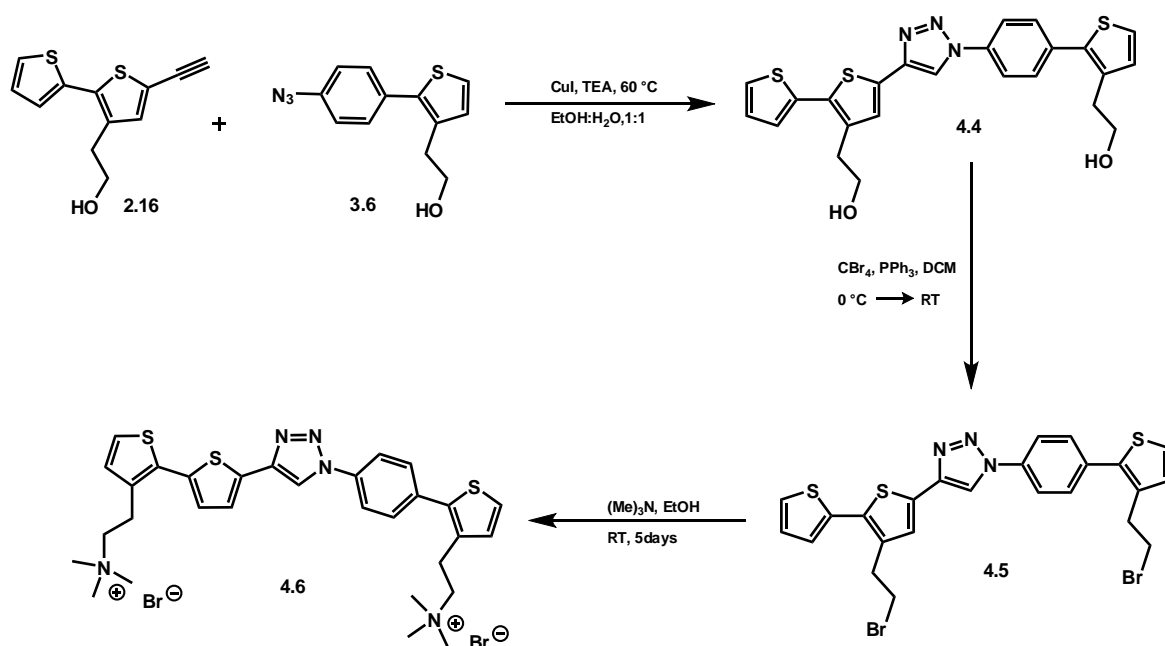
Scheme 4.3

4.2.1c Synthesis of 4.9

4.9 was synthesised following the same synthetic strategy used for the synthesis of **4.3**. This involved the reaction of 1 equivalent of 2-(2-ethynylthiophen-3-yl)ethanol **2.4** with 1 equivalent of 2-(2-(4-azidophenyl)thiophen-3-yl)ethanol **3.6** generating **4.7** in 73% yield. The hydroxyl groups were then converted to bromides using an Appel reaction, to produce a 67% yield of **4.8**. The final step involved the conversion of the dibromide **4.8** into the quaternary ammonium salt by a substitution reaction. The addition of trimethylamine in ethanol to **4.8** at room temperature for 5 days resulted in the production of **4.9** in 70% yield (Scheme 4.4).

Scheme 4.4

4.2.1d Synthesis of 4.12

4.12 was synthesised by the same synthetic strategy as used for **4.3**; reacting 1 equivalent of 2-benzene-5-ethynyl-3-(2-hydroxyethyl)thiophene **2.9** with 1 equivalent of (4-azidophenyl)methanol **3.8** led to the desired intermediate **4.10** being obtained in 80% yield. Using the Appel reaction, the hydroxyl groups were then converted to the corresponding bromides in providing **4.11** in 64% yield. The final step involved the conversion of the bromide **4.11** into the quaternary ammonium salt by a substitution reaction. The addition of trimethylamine in ethanol to **4.11** at room temperature for 5 days resulted in **4.12** in 66% yield (Scheme 4.5).

Scheme 4.5

4.2.1e Synthesis of 4.15

4.15 was synthesised following the same strategy used for **4.3**. By reacting 1 equivalent of 2-(2-ethynylthiophen-3-yl)ethanol **2.4** with 1 equivalent of (4-azidophenyl)methanol **3.8**, **4.13** was obtained in 72% yield. The hydroxyl groups were then converted to the bromides using an Appel reaction to give **4.14** in 49%. The addition of trimethylamine in ethanol to **4.14** at room temperature for 5 days yielded quaternary ammonium salt **4.15** in 62% yield (Scheme 4.6).
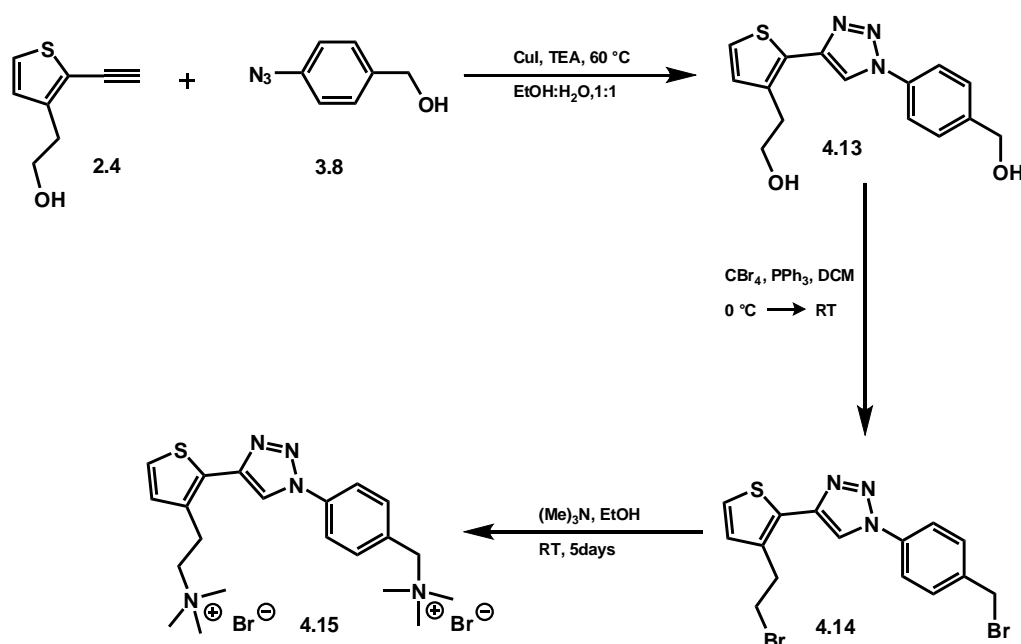
Scheme 4.6

4.2.1f Synthesis of compound 4.18

The synthesis of **4.18** again followed the same synthetic strategy used for **4.3**. The reaction of 1 equivalent of 2-(2-ethynylthiophen-3-yl)ethanol **2.4** with 1 equivalent of (3-azidophenyl)methanol **3.10** generated the desired compound **4.16** in 65% yield. The hydroxyl groups were then converted to the corresponding bromides in an Appel reaction, producing an excellent yield in comparison with the other Appel reactions reported in this Chapter, namely providing **4.17** in 82% yield. The final step involved the conversion of the bromide **4.17** into the quaternary ammonium salt which was achieved through the addition of trimethylamine in ethanol to **4.17** at room temperature for 5 days, yielding **4.18** in 68% yield (Scheme 4.7).
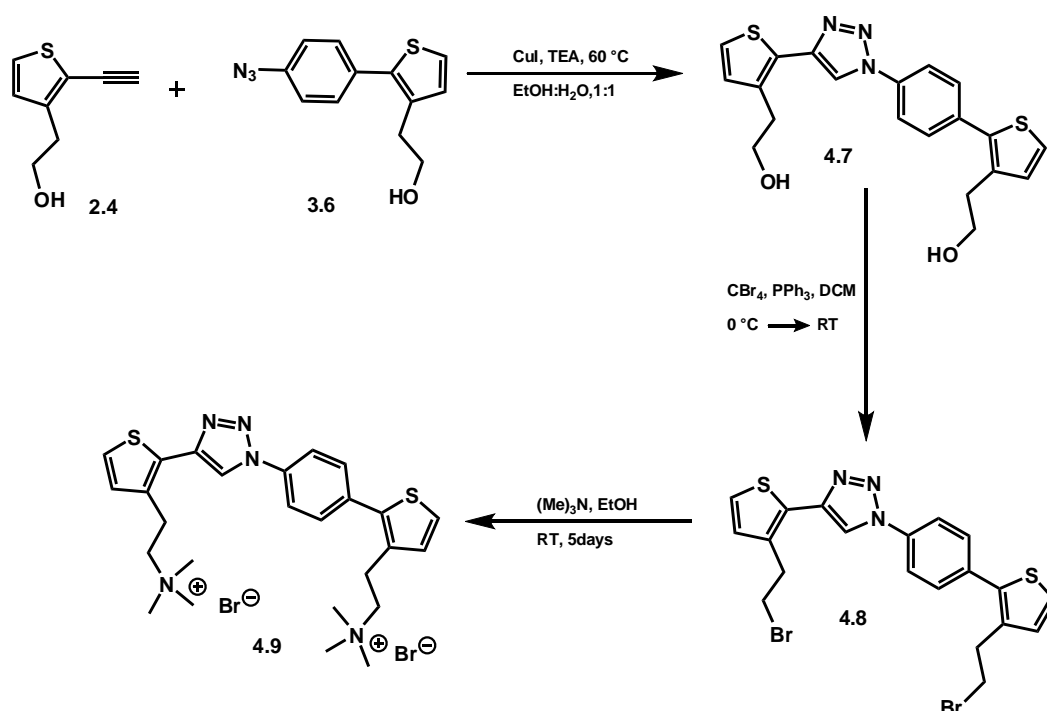
Scheme 4.7

4.2.2 Synthesis of tri-cationically substituted oligoheteroamatics

A series of conjugated tricationic oligoheteroaromatic compounds was synthesised using the click reaction for the construction of the π-conjugated scaffold (Scheme 4.8).
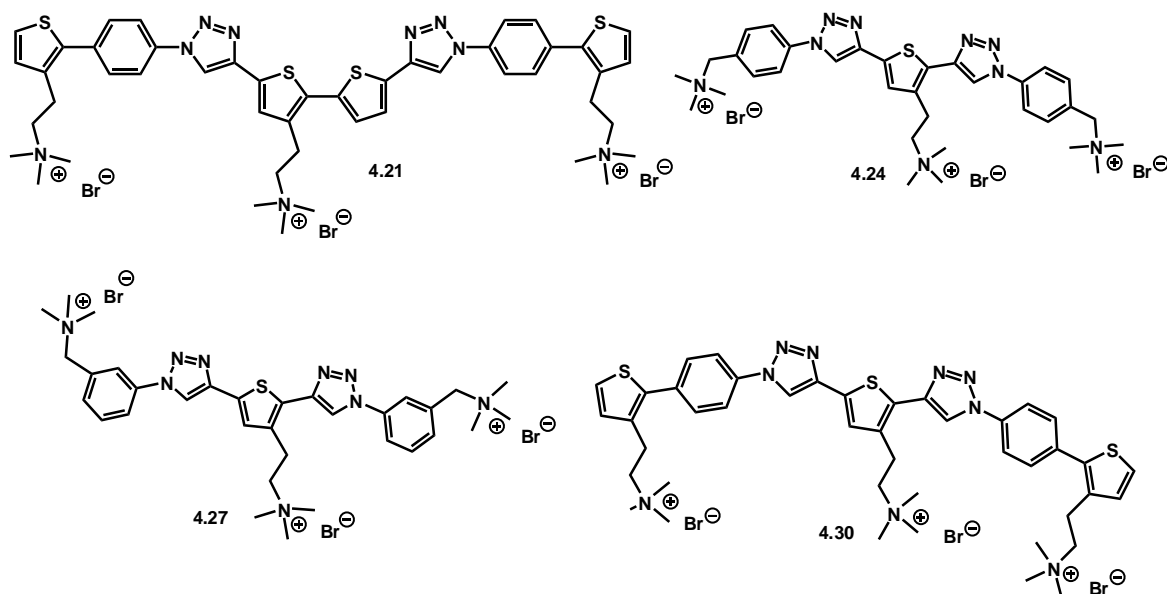
Scheme 4.8

4.2.2a Synthesis of 4.21

Tricationic **4.21** was synthesised by first reacting 1 equivalent of 2-(5,5'-diethynyl-2,2'-bithiophen-3-yl)ethanol **2.20** with 2 equivalents of 2-(2-(4-azidophenyl)thiophen-3-yl)ethanol **3.6** in the presence of copper iodide as catalyst. Triethylamine was used as a base in the reaction, a mixture of EtOH and H_2O (1:1) as the solvent and the reaction was carried out at 60 °C. Compound **4.19** was obtained in 70% yield. The subsequent Appel reaction to prepare the tribrominated conjugated oligoheteroaromatic **4.20** converted the hydroxyl groups into the corresponding bromides; **4.19** was reacted with an excess of carbon tetrabromide and triphenylphosphine at 0 °C under a nitrogen atmosphere in extra dry DCM, resulting in **4.20** being obtained in 60 % yield. Putative DNA binder **4.21** was then synthesised through the conversion of **4.20** into the corresponding quaternary ammonium salt by adding trimethylamine in ethanol to **4.20** at room temperature for 5 days, producing **4.21** in 55% yield (Scheme 4.9).
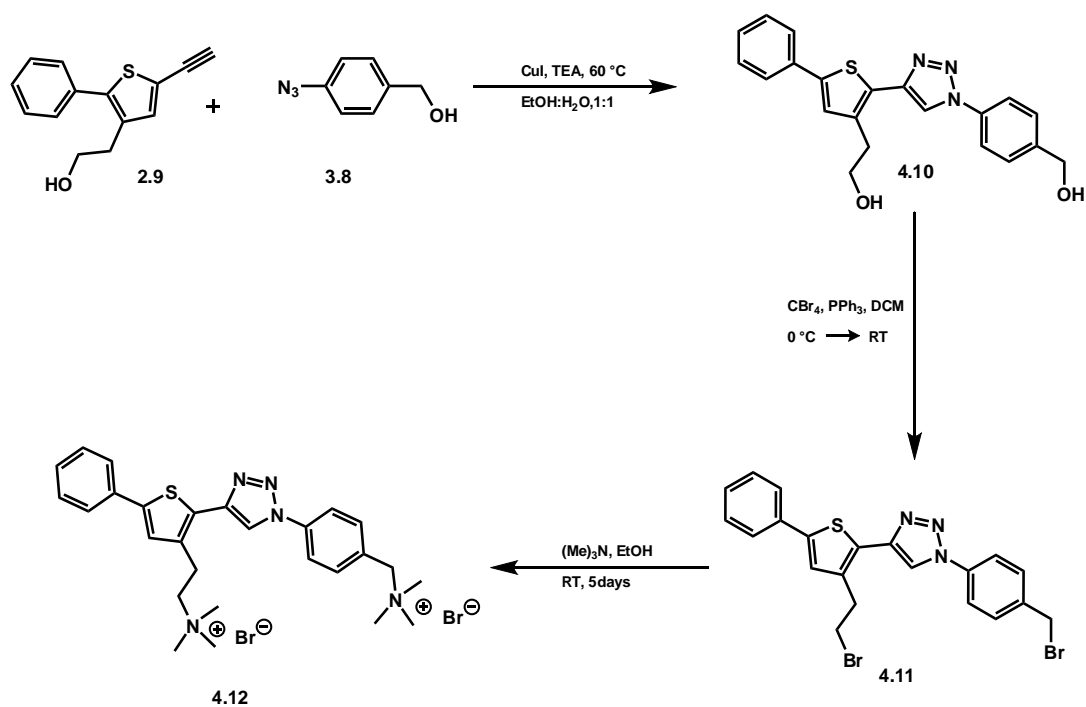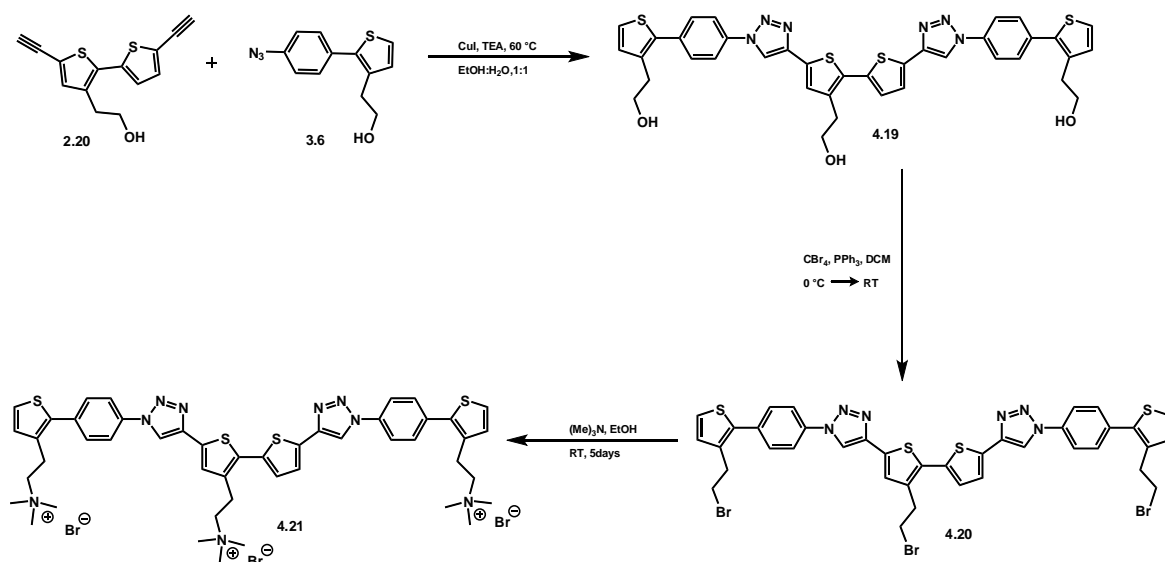

Scheme 4.9

4.2.2b Synthesis of 4.24

Compound **4.24** was synthesised using the same synthetic strategy as used for **4.21**. Reaction of 1 equivalent of 2-(2,5-diethynylthiophen-3-yl)ethanol **2.12** with 2 equivalents of (4-azidophenyl)methanol **3.8**, resulted in compound **4.22** in 70% yield. An Appel reaction then converted the hydroxyl groups to the bromides, giving **4.23** in 65% yield. The final step involved the conversion of the bromide **4.23** into the quaternary ammonium salt by addition of trimethylamine in ethanol to **4.23** at room temperature for 5 days, yielding **4.24** in 72% yield (Scheme 4.10).
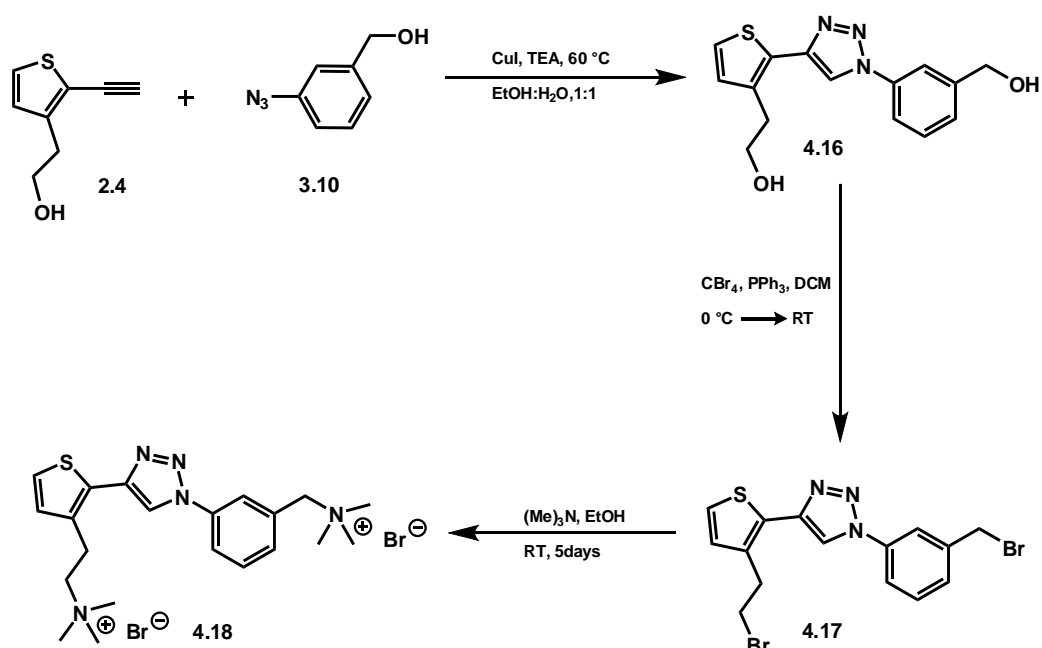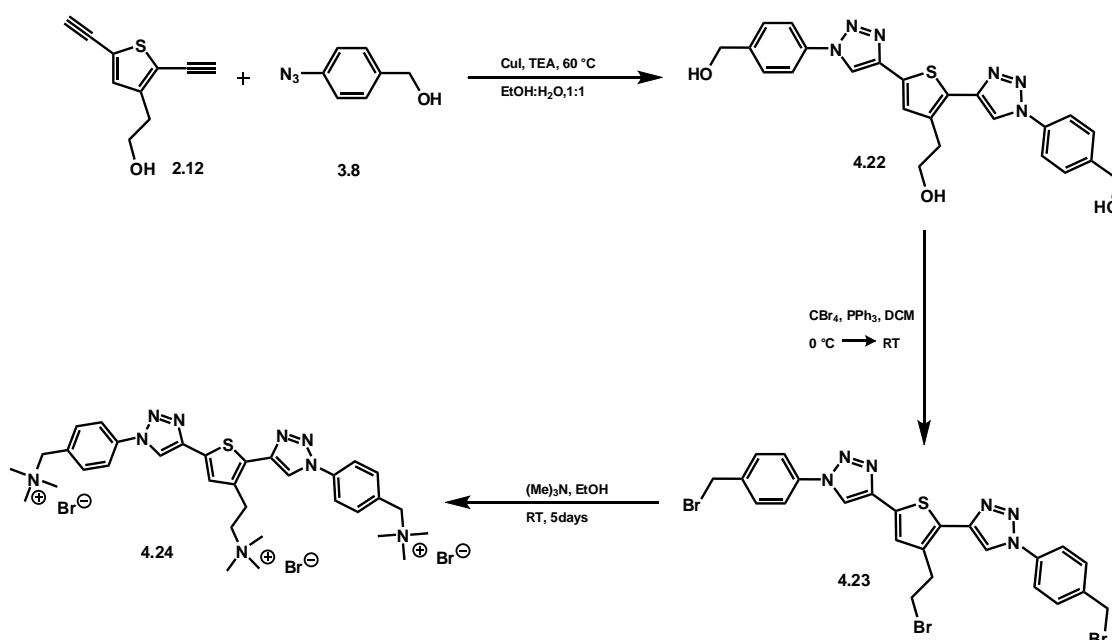

Scheme 4.10

4.2.2c Synthesis of 4.27

Analogously, **4.27** was synthesised by reacting 1 equivalent of 2-(2,5-diethynylthiophen-3-yl)ethanol **2.12** with 2 equivalents of (3-azidophenyl)methanol **3.10**. The desired compound **4.25** was obtained in 65% yield. The hydroxyl groups were then converted to the bromides using an Appel reaction to give **4.26** in 67% yield. The final step involved the conversion of the bromide **4.26** into the quaternary ammonium salt by a substitution

reaction; addition of trimethylamine in ethanol to **4.26** at room temperature and reaction

for 5 days yielded **4.27** in 61% yield (Scheme 4.11).
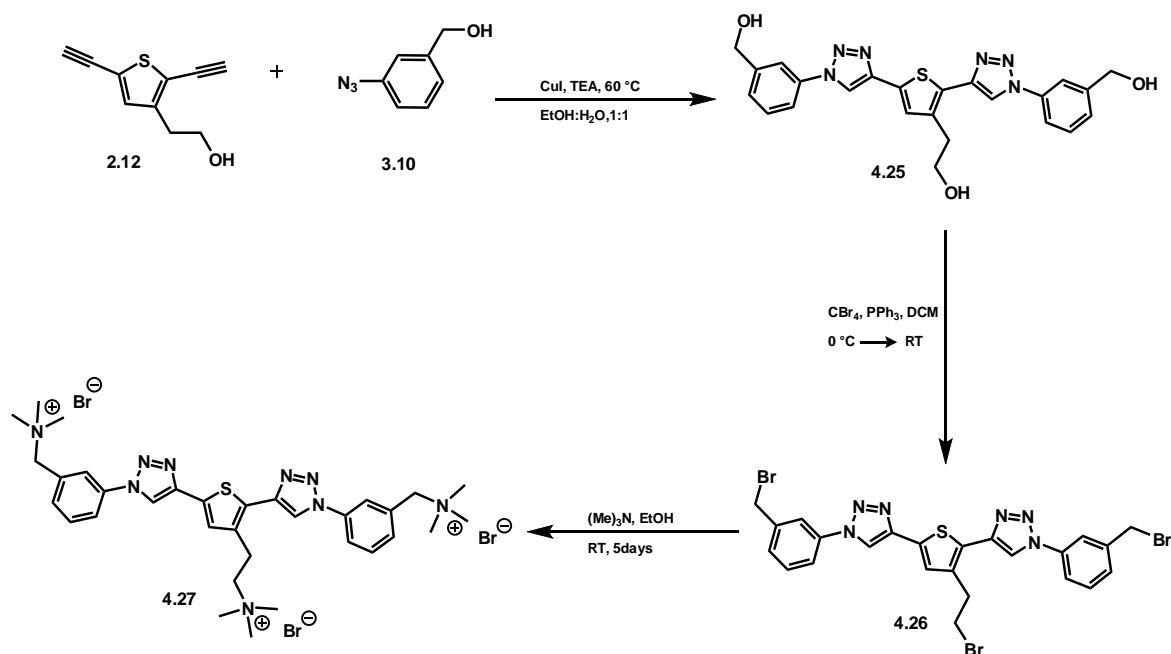
Scheme 4.11

4.2.2d Synthesis of 4.30

As before, synthesis of **4.30** followed the same strategy employed for the production of

4.21. By reacting 1 equivalent of 2-(2,5-diethynylthiophen-3-yl)ethanol **2.12** with 2

equivalents of 2-(2-(4-azidophenyl)thiophen-3-yl)ethanol **3.6** the desired intermediate **4.28**

was obtained in 72% yield. The hydroxyl groups were subsequently converted to the

bromides in an Appel reaction giving **4.29** in 59% yield. Substitution of the bromide **4.29**

with trimethylamine generated the quaternary ammonium salt **4.30** (reaction in ethanol at

room temperature for 5 days) yielded in 62% yield (Scheme 4.12).
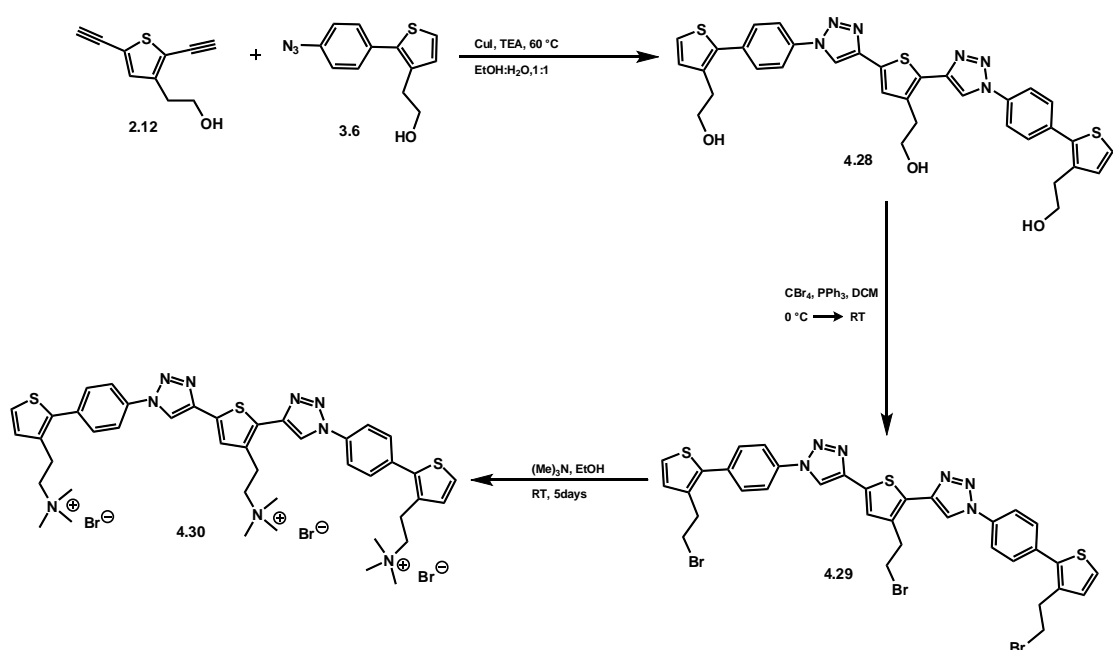
Scheme 4.12

4.3 Conclusions

We successfully synthesised a range of conjugated oligoheteroaromatic compounds. These experiments demonstrated that click chemistry is a viable and useful method in the design and subsequent synthesis of a variety of structurally different oligoheteroaromatic compounds. Several of di- and tricationic oligoheteroaromatic putative DNA binders were derived from the oligoheteroaromatics constructed using click chemistry.

4.4 Materials and methods

Commercially available reagents, starting materials and solvents were purchased from known commercial companies and used without purification. Certain solvents, such as THF, were dried using an MBraun solvent purification system. ^{1}H-NMR and ^{13}C-NMR spectra were recorded at 400 MHz on a Bruker B-ACS-6 and at 500 MHz on a Bruker Avance 500 spectrometer (i.e. 100 MHz and 126 MHz for ^{13}C). High resolution mass spectra were recorded using a Water Micromass LCT Premier and low resolution mass spectra were recorded on a Perkin Elmer Turbo Mass GC/MS. All column chromatography purifications were performed with the use of silica gel.

4.5 Experimental procedures

Synthesis of **4.1**
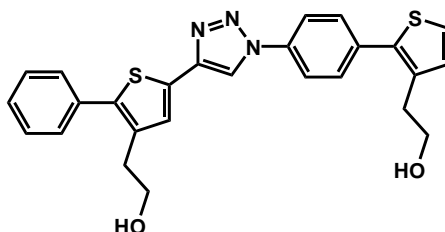
2-Benzene-5-ethynyl-3-(2-hydroxyethyl)thiophene **2.9** (0.05 g, 0.219 mmol) was dissolved in 10 ml of a mixture of ethanol and H_2O (1:1). Copper iodide (0.004 g) and

0.002 g of triethylamine were then added to the solution. The mixture was stirred for 20 minutes at room temperature. After this, 0.053 g (0.219 mmol) of 2-(2-(4-azidophenyl)thiophen-3-yl)ethanol **3.6** was slowly added to the mixture. The resulting mixture was heated to 60 °C and stirred at this temperature for 18 h. 60 ml of water was added to the reaction mixture and the organic fractions were extracted with diethyl ether. The combined organic fractions were dried over $MgSO_4$. Following drying, the solvent was removed under reduced pressure. The crude product was then purified by column chromatography using DCM : ethyl acetate : methanol (9:0.5:0.5) as eluent, and 0.083 g of compound **4.1** was obtained as a yellow powder (83% yield). **^{1}H-NMR (CDCl$_3$, 400 MHz, ppm)**: 8.04 (s, 1H) 7.72 (d, *J*=8.5, 2H) 7.55 (d, *J*=8.6, 2H) 7.44 (d, *J*=8.4, 2H), 7.32-7.38 (m, 4H), 7.30 (d, *J*=5.1, 1H), 6.99 (d, *J*=5.2, 1H), 3.80 (q, *J*=7.1 , 4H), 2.85-2.91 (m, 4H). **^{13}C-NMR (CDCl$_3$, 126 MHz, ppm)**: 142.39, 138.89, 137.01, 134.82, 134.16, 132.77, 129.71, 129.18, 128.59, 128.37, 127.95, 127.68, 126.83, 124.67, 123.96, 119.53, 119.44, 115.81, 62.08, 61.87, 30.94, 30.86. **HRMS (ES)** calcd for $[C_{26}H_{24}N_3O_2S_2^+]$ (M$^+$+H) 474.1310 found 474.1327.

Synthesis of **4.2**
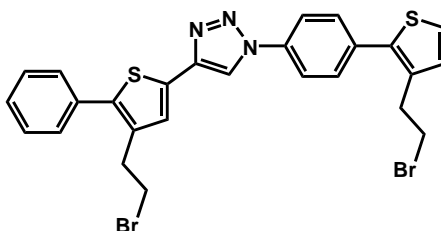
Compound **4.1** (0.1 g, 0.232 mmol) was dissolved in 25 ml of dry DCM, after which the solution was stirred at 0 °C for 15 minutes. 0.30 g (0.928 mmol) of carbon tetrabromide was added to the solution under nitrogen, after which 0.24 g (0.928 mmol) of triphenylphosphine was added and the mixture was stirred at 0 °C for 1h. The mixture was then allowed to reach room temperature and was stirred overnight. The solvent was

removed under reduced pressure and the crude product was purified by column chromatography, first using hexane 200 ml, then DCM : diethyl ether (9:1) as eluent. 0.085 g of compound **4.2** was obtained as a white solid (65% yield). **^{1}H-NMR (CDCl$_3$, 400 MHz, ppm)**: 8.08 (s, 1H) 7.72 (d, *J*=8.5 , 2H) 7.55 (d, *J*=8.6, 2H) 7.44 (d, *J*=8.4, 2H), 7.33-7.40 (m, 4H), 7.30 (d, *J*=5.1, 1H), 6.99 (d, *J*=5.2, 1H), 3.42-3.50 (m, 4H), 3.12-3.19 (m, 4H). **^{13}C-NMR (CDCl$_3$, 126 MHz, ppm)**: 142.42, 141.90, 139.42, 138.53, 137.35, 135.65, 134.01, 133.10, 132.39, 130.67, 130.31, 129.50, 128.90, 128.01, 126.63, 125.40, 120.39, 118.91, 33.13, 32.30, 31.61, 30.76. **LRMS (ES)** *m/z* 519.98(50%), 597.90 (48%), 599.90 (100%).

Synthesis of **4.3**
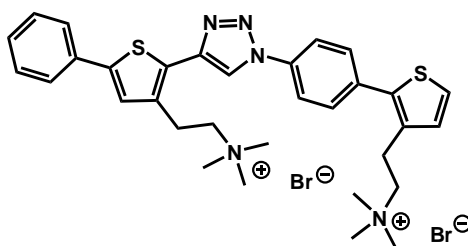
Compound **4.2** (0.05 g, 0.232 mmol) was added to a round-bottom flask, 25 ml of trimethylamine in ethanol was added and the resulting mixture was stirred at room temperature for 5 days. The solvent was removed under reduced pressure, and the product was washed with acetone and centrifuged three times for 7 minutes three times. The solid was re-dissolved in a small amount of ethanol and precipitated with ether at 0 °C. After this, the mixture was centrifuged again for 7 minutes. The product was dried under high vacuum, with ammonium salt **4.3** being obtained as a white solid (0.10 g, 78% yield). **^{1}H-NMR (D$_2$O, 400 MHz, ppm)**: 8.21 (s, 1H) 7.38 (d, *J*=8.4, 2H) 7.20 (d, *J*=1.9, 2H) 7.14 (d, *J*=8.2, 2H), 7.09 (t, *J*=3.8, 4H), 7.05 (s, 1H), 6.93 (d, *J*=5.2, 1H), 2.18-3.23 (m, 4H),

2.87-2.94 (m, 22H). ^{13}**C-NMR (CDCl$_3$, 126 MHz, ppm)**: 142.26, 139.03, 137.87, 135.77, 133.65, 132.63, 132.27, 131.02, 130.43, 129.85, 129.18, 128.87, 128.35, 127.25, 126.19, 120.52, 119.20, 118.95, 64.44, 52.16, 22.25, 22.12. **HRMS (ES)** calcd for [C$_{32}$H$_{39}$N$_5$O$_2$S$_2$Br] (M$^+$+Br) 636.1830 found 636.1802.

Synthesis of **4.4**
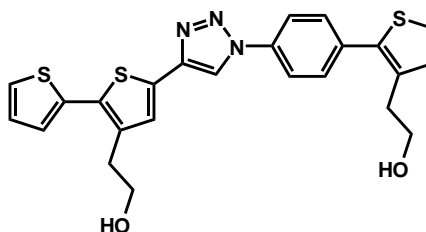
The procedure selected for this reaction was as described for **4.1**. 0.25 g (1 mmol) of 2-(5-ethynyl-2,2'-bithiophen-3-yl)ethanol **2.16** was reacted with 0.026 g (1 mmol) of 2-(2-(4-azidophenyl)thiophen-3-yl)ethanol **3.6**. Purification of the crude product involved column chromatography using DCM : ethyl acetate : methanol (9:0.5:0.5) as eluent. 0.38 g of compound **4.4** was obtained as a yellow powder (79% yield). ^{1}**H-NMR (d6-DMSO, 400 MHz, ppm)**: 9.32 (s, 1H), 8.05 (d, *J*=8.5, 2H) 7.80 (d, *J*=8.4, 2H), 7.70 (d, *J*=5.1, 1H), 7.60 (d, *J*=5.1, 1H) 7.52 (s, 1H) 7.30 (d, *J*=5.1, 1H), 7.19-7.22 (m, 2H) 4.90 (t, *J*=5.1, 1H), 4.87 (t, *J*=5.1, 1H), 3.64-3.70 (m, 4H), 2.96 (t, *J*=6.8, 2H), 2.89 (t, *J*=6.9, 2H). ^{13}**C-NMR (CDCl$_3$, 126 MHz, ppm)**: 142.32, 136.91, 136.46, 136.34, 135.43, 134.77, 134.54, 130.39, 130.29, 129.94, 128.10, 127.93, 126.41, 125.03, 120.52, 120.31, 118.84, 61.22, 60.84, 32.49, 31.91. **HRMS (EI)** calcd for [C$_{24}$H$_{21}$N$_3$O$_2$S$_3$] 479.0796 found 479.0786.

Synthesis of **4.5**
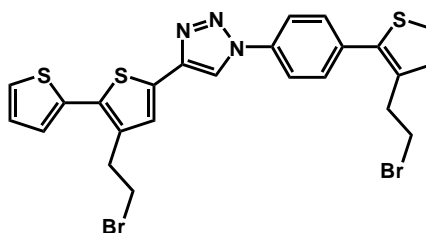
The experimental procedure chosen for this reaction was as described for **4.2**. 0.35 g (0.73 mmol) of **4.4** was reacted with 0.969 g (2.92 mmol) of carbon tetrabromide and 0.765 g (2.92 mmol) of triphenylphosphine. The crude product was purified by column chromatography using DCM : diethyl ether (9:1) as eluent and 0.27 g of compound **4.5** was obtained as a yellow powder (62% yield). **¹H-NMR (CDCl₃, 400 MHz, ppm)**: 8.17 (s, 1H), 7.70 (d, *J*=8.5, 2H) 7.45 (d, *J*=8.5, 2H), 7.227.27 (m, 3H), 7.05 (d, *J*=3.5, 1H) 6.87-6.93 (m, 2H), 3.39-3.45(m, 4H), 3.20 (t, *J*=7.6, 2H), 3.11 (t, *J*=7.5, 2H). **¹³C-NMR (CDCl₃, 126 MHz, ppm)**: 143.39, 138.55, 136.34, 136.30, 135.80, 135.17, 133.02, 131.04, 129.48, 128.25, 127.36, 127.16, 127.05, 126.62, 125.62, 125.27, 120.96, 117.48, 33.10, 32.75, 32.38, 32.01. **HRMS (EI)** calcd for [$C_{24}H_{19}N_3S_3Br_2$] 604.9087 found 604.9084.

Synthesis of **4.6**
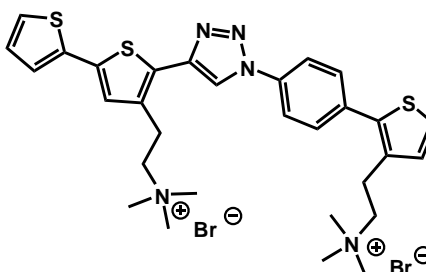
The experimental procedure used for this reaction was as described for **4.3**. 0.15 g (0.294 mmol) of **4.5** was reacted with trimethylamine in ethanol. The product was obtained as a

yellow powder (0.096 g, 60% yield). **^{1}H-NMR (d6-DMSO, 400 MHz, ppm)**: 9.35 (s, 1H), 8.08 (d, *J*=8.3, 2H) 7.75 (m, 4H), 7.63 (s, 1H), 7.41 (d, *J*=3.1, 1H) 6.89-6.93 (m, 2H), 3.60 (t, *J*=8.8, 4H) 3.23 (t, *J*=8.5, 4H), 3.18 (s, 9H), 3.12 (s, 9H). **^{13}C-NMR (d6-DMSO, 126 MHz, ppm)**: 141.99, 137.90, 135.68, 133.71, 133.57, 132.68, 132.13, 131.81, 130.77, 130.39, 129.84, 128.52, 127.59, 127.28, 127.05, 126.17, 120.63, 119.03, 64.59, 64.36, 52.37, 52.22, 22.57, 22.05. **HRMS (ES)** calcd for [$C_{30}H_{37}N_5O_2S_3Br$] (M$^+$+Br) 642.1394 found 642.1388.

Synthesis of **4.7**
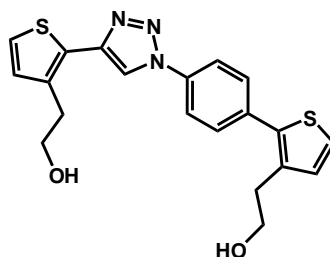
The experimental procedure used was as analogous to that for **4.1**. 0.3 g (1.97 mmol) of 2-(2-ethynylthiophen-3-yl)ethanol **2.4** was reacted with 0.484 g (1.97 mmol) of 2-(2-(4-azidophenyl)thiophen-3-yl)ethanol **3.6**. Purification of the crude product involved the use of column chromatography using DCM : ethyl acetate: methanol (9:0.5:0.5) as eluent. Product **4.7** was obtained as a white powder (0.57 g, 73% yield). **^{1}H-NMR (CDCl$_3$, 400 MHz, ppm)**: 8.10 (s, 1H) 7.53 (d, *J*=8.5, 2H), 7.45 (d, *J*=8.5, 2H), 7.15 (t, *J*=5.2 , 2H), 6.88-6.95 (dd, *J$_1$*=5.1, *J$_2$*=5.0, 2H), 3.76 (t, *J*=6.4, 2H), 3.71 (t, *J*=6.8, 2H), 2.92 (t, *J*=6.4, 2H), 2.79 (t, *J*=6.7, 2H). **^{13}C-NMR (CDCl$_3$, 101 MHz, ppm)**: 143.04, 138.10, 137.55, 135.88, 135.76, 135.51, 130.91, 130.56, 130.19, 127.60, 126.63, 125.56, 120.99, 119.04, 63.07, 62.91, 32.92, 32.35. **HRMS (ES)** calcd for [$C_{20}H_{20}N_3O_2S_2^+$] (M$^+$+H) 398.0997 found 398.1010.

Synthesis of **4.8**
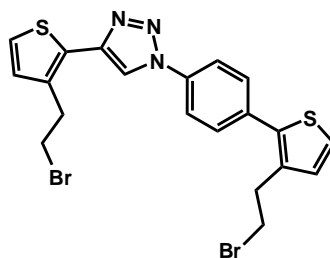
The experimental procedure was as described for **4.2**. 0.40 g (1 mmol) of **4.7** was reacted with 1.32 g (4 mmol) of carbon tetrabromide and 1.04 g (4 mmol) of triphenylphosphine. The resulting product was purified utilising column chromatography using first hexane, then DCM : diethyl ether (9:1) as eluent. 0.35 g of compound **4.8** was obtained as a white powder (67% yield). **^{1}H-NMR (CDCl$_3$, 400 MHz, ppm)**: 8.10 (s, 1H) 7.79 (d, *J*=8.6, 2H), 7.50 (d, *J*=8.6, 2H), 7.27 (t, *J*=5.1, 2H), 3.86-6.90 (dd, *J$_1$*=5.1, *J$_2$*=5.0, 2H), 3.60 (t, *J*=7.3, 2H), 3.41-3.45 (m, 4H), 3.18 (t, *J*=7.6, 2H). **^{13}C-NMR (CDCl$_3$, 101 MHz, ppm)**: 142.74, 138.18, 137.04, 136.63, 135.45, 131.02, 129.98, 129.22, 127.73, 126.99, 125.17, 121.60, 120.67, 118.20, 34.69, 32.89, 32.11, 31.73. **HRMS (EI)** calcd for [C$_{20}$H$_{18}$N$_3$S$_2$Br$_2$] 521.9309 found 521.9302.

Synthesis of **4.9**
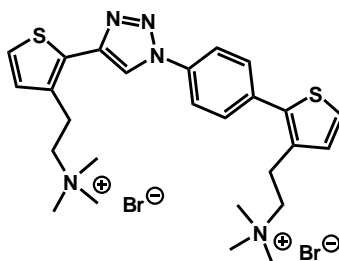
The experimental procedure was as described for **4.3**. 0.1 g (0.191 mmol) of **4.8** was reacted with trimethylamine in ethanol. The product was obtained as a white powder (0.064 g, 70% yield). **^{1}H-NMR (D$_2$O, 400 MHz, ppm)**: 8.64 (s, 1H), 7.82 (d, *J*=8.5, 2H), 7.61 (d, *J*=8.5, 2H), 7.48 (q, *J*=5.2, 2H), 7.09 (q, *J*=5.1, 2H), 3.55 (t, *J*=6.2, 2H), 3.41-3.45

(m, 4H), 3.18 (t, *J*=8.0.1, 2H), 3.12 (s, 9H), 3.02 (s, 9H). **^{13}C-NMR (d6-DMSO, 126 MHz, ppm)**: 141.47, 137.90, 135.80, 133.64, 132.25, 130.77, 129.92, 127.88, 126.17, 121.91, 120.85, 120.09, 64.45, 52.36, 52.17, 22.67, 22.14. **HRMS (ES)** calcd for [$C_{26}H_{35}N_5S_2Br$] (M$^+$+Br) 560.1517 found 560.1494.

Synthesis of **4.10**
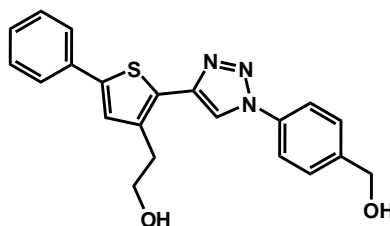
An analogous procedure to that used for the synthesis of **4.1** was used. 2-Benzene-5-ethynyl-3-(2-hydroxyethyl)thiophene **2.9** (0.61 g, 2.6 mmol) was reacted with 0.40 g (2.6 mmol) of (4-azidophenyl)methanol **3.8**. The resulting product was purified by column chromatography, first using hexane, then DCM : ethyl acetate: methanol (9:0.5:0.5) as eluent. 0.79 g of compound **4.10** was obtained as a white solid (80% yield). **^{1}H-NMR (d6-DMSO, 400 MHz, ppm)**: 9.22 (s, 1H), 7.90, (d, *J*=8.4, 2H), 7.56, (d, *J*=8.5, 4H), 7.51 (s, 1H), 7.48 (d, *J*=7.7, 2H), 3.36-7.40 (m, 1H), 5.93, (t, *J*=5.7, 1H), 4.83 (t, *J*=5.1, 1H), 4.59 (d, *J*=5.5, 2H), 3.69 (t, *J*=6.6, 2H), 2.81 (t, *J*=6.9, 2H). **^{13}C-NMR (d6-DMSO, 101 MHz, ppm)**: 149.05, 148.21, 141.87, 140.67, 139.17, 136.00, 135.34, 134.14, 133.74, 132.51, 126.20, 125.24, 124.52, 123.26.67.90, 66.84, 36.40. **HRMS (EI)** calcd for [$C_{21}H_{19}N_3O_2S$] 377.1198 found 377.1206.

Synthesis of **4.11**
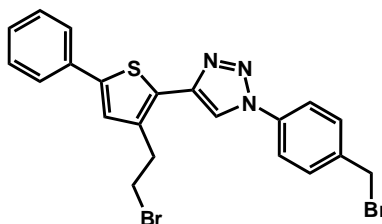
The experimental procedure used was analogous to that described for **4.2**. 0.45 g (1.19 mmol) of **4.10** was reacted with 1.58 g (4.76 mmol) of carbon tetrabromide and 1.28 g (4.76 mmol) of triphenylphosphine. The crude product was purified by column chromatography using first hexane, then DCM : diethyl ether (9:1) as eluent. 0.38 g of compound **4.11** was obtained as a white solid (64% yield). **^{1}H-NMR (d6-DMSO, 400 MHz, ppm)**: 9.23 (s, 1H), 7.95, (d, *J*=8.5, 2H), 7.70, (d, *J*=8.6, 4H), 7.60 (s, 1H), 7.51 (d, *J*=6.9, 2H), 7.41-7.45 (m, 1H), 4.80 (d, *J*=3.5, 2H), 3.78 (t, *J*=7.1, 2H), 3.22 (t, *J*=7.1, 2H). **^{13}C-NMR (d6-DMSO, 101 MHz, ppm)**: 143.55, 142.38, 138.76, 136.04, 135.04, 133.42, 132.48, 130.76, 129.16, 127.64, 125.42, 120.31, 119.80, 118.84, 33.27, 32.28, 31.61.

Synthesis of **4.12**
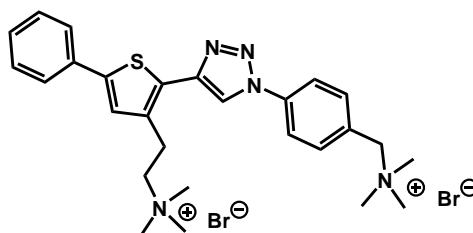
The experimental procedure was as described for **4.3**. 0.13 g (0.258 mmol) of **4.11** was reacted with trimethylamine in ethanol. The product was obtained as a white powder (0.073 g, 66% yield). **^{1}H-NMR (d6-DMSO, 400 MHz, ppm)**: 9.39 (s, 1H), 8.16 (d, *J*=8.5, 2H), 7.83 (d, *J*=8.5, 4H), 7.70 (s, 1H), 7.51-7.55, (m, 3H), 7.70 (s, 1H), 3.74 (t, *J*=6.8, 2H), 3.22 (t, *J*=6.5, 2H), 3.16 (s, 9H), 3.11 (s, 9H). **^{13}C-NMR (d6-DMSO, 101 MHz,**

ppm): 142.73, 139.47, 137.88, 134.93, 135.43, 132.97, 131.27, 129.62, 129.27, 128.80, 127.71, 124.76, 120.48, 119.37, 67.03, 52.46, 52.18, 22.63. **HRMS (ES)** calcd for [$C_{27}H_{35}N_5SBr$] (M^++Br) 540.1797 found 540.1812.

Synthesis of **4.13**
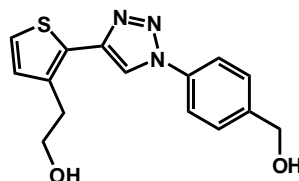
The experimental procedure used was as described for **4.1**. 0.5 g (3.28 mmol) of 2-(2-ethynylthiophen-3-yl)ethanol **2.4** was reacted with 0.48 g (3.28 mmol) of (4-azidophenyl)methanol **3.8**. The crude product was purified with the use of column chromatography using first with DCM : ethyl acetate 2:1, then DCM : ethyl acetate : methanol (8:1:1) as eluent. 0.72 g of compound **4.13** was obtained as a white solid (72% yield). **^{1}H-NMR (CDCl$_3$, 400 MHz, ppm)**: 8.07 (s, 1H), 7.67, (d, *J*=8.4, 2H), 7.46 (d, *J*=8.2, 2H), 7.25 (d, *J*=5.1, 1H), 6.98, (d, *J*=5.1, 1H), 4.70 (s, 2H), 3.92 (t, *J*=6.0, 2H), 3.07 (t, *J*=6.0, 2H). **^{13}C-NMR (CDCl$_3$, 101 MHz, ppm)**: 142.64, 142.25, 137.34, 135.81, 130.17, 128.00, 127.35, 125.05, 120.44, 118.70, 64.15, 63.06, 32.44. **HRMS (EI)** calcd for [$C_{15}H_{16}N_3O_2S$] (M^++H) 302.0963 found 302.0976.

Synthesis of **4.14**
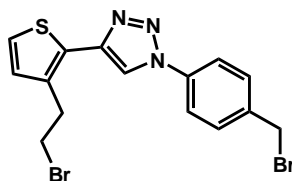
Dibromide 4.14 was synthesised analogously to **4.2**. 0.37 g (1.20 mmol) **4.13** was reacted with 1.62 g (4.8 mmol) of carbon tetrabromide and 1.28 g (4.8 mmol) of

triphenylphosphine. The resulting product was purified by column chromatography using first hexane, then DCM : diethyl ether (9:1) as eluent. 0.25 g of compound **4.14** was obtained as a white solid (49% yield). **^{1}H-NMR (CDCl$_3$, 400 MHz, ppm)**: 8.02 (s, 1H), 7.67, (d, *J*=8.4, 2H), 7.46 (d, *J*=8.3, 2H), 7.19 (d, *J*=5.1, 1H), 6.93 (d, *J*=5.1, 1H), 4.44 (s, 2H), 3.59 (t, *J*=7.3, 2H), 3.38 (t, *J*=7.3, 2H). **^{13}C-NMR (CDCl$_3$, 101 MHz, ppm)**: 141.68, 137.32, 135.48, 129.94, 128.94, 126.64, 123.89, 120.61, 119.68, 117.21, 31.84, 30.33, 29.98. **HRMS (EI)** calcd for [C$_{15}$H$_{14}$N$_3$SBr$_2$] 425.9275 found 425.9257.

Synthesis of **4.15**
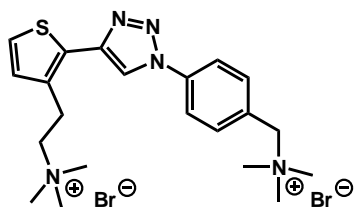
The experimental procedure used for the synthesis of 4.15 was analogous to that used for **4.3**. 0.25 g (0.586 mmol) of **4.14** was reacted with trimethylamine in ethanol. The product was obtained as a brown powder (0.137 g, 62% yield). **^{1}H-NMR (d6-DMSO, 400 MHz, ppm)**: 8.59 (s, 1H), 7.81 (d, *J*= 7.6, 2H), 7.64 (d, *J*= 7.4, 2H), 7.40 (d, *J*= 4.5, 1H), 7.00 (d, *J*= 4.7, 1H), 4.46 (s, 2H), 3.69 (t, *J*= 6.6, 2H), 3.45 (t, *J*= 6.5, 2H) 3.23 (s, 9H), 3.10 (s, 9H). **^{13}C-NMR (D$_2$O, 126 MHz, ppm)**: 142.05, 137.59, 134.98, 133.50, 131.98, 129.97, 128.48, 127.06, 121.95, 120.90, 68.60, 68.40, 58.79, 23.36. **HRMS (ES)** calcd for [C$_{22}$H$_{31}$N$_5$SBr] (M$^+$+Br) 464.1484 found 464.1494.

Synthesis of **4.16**
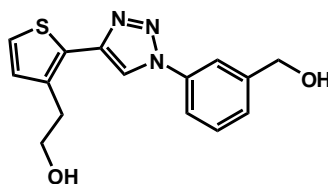
The synthesis of **4.16** was analogous to the synthesis of **4.1**. 0.5 g (3.28 mmol) of 2-(2-ethynylthiophen-3-yl)ethanol **2.4** was reacted with 0.49 g (3.28 mmol) of (3-azidophenyl)methanol **3.10**. The purification of the resulting product was conducted by column chromatography, first with DCM : ethyl acetate 2:1, then DCM : ethyl acetate : methanol (8:1:1) as eluent. Product **4.16** was obtained as a white solid (0.64 g, 65% yield). **^{1}H-NMR (CDCl$_3$, 400 MHz, ppm)**: 8.09 (s, 1H), 7.70 (s,1H), 7.59 (d, *J*=7.9, 1H), 7.80 (t, *J*=7.8, 1H), 7.34 (d, *J*=7.6, 1H), 7.23 (d, *J*=5.1, 1H), 6.94 (d, *J*=5.1, 1H), 4.72 (s, 2H), 3.90 (t, *J*=6.1, 2H), 3.05 (t, *J*=6.1, 2H). **^{13}C-NMR (CDCl$_3$, 126 MHz, ppm)**: 143.24, 142.72, 137.38, 137.00, 130.18, 127.41, 127.09, 125.10, 119.56, 118.80. **HRMS (EI)** calcd for [C$_{15}$H$_{15}$N$_3$O$_2$S] 301.0885 found 301.0892.

Synthesis of **4.17**
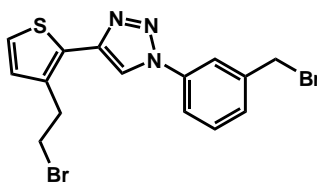
The experimental procedure was as described for the synthesis of **4.2**. 0.62 g (2.05 mmol) **4.16** of was reacted with 2.72 g (8.20 mmol) of carbon tetrabromide and 2.09 g (8.20 mmol) of triphenylphosphine. The product was purified by column chromatography, first using hexane and then DCM : diethyl ether (9:1) as eluent. 0.71 g of compound **4.17** was obtained as a yellow solid (82% yield). **^{1}H-NMR (CDCl$_3$, 126 MHz, ppm)**: 8.04 (s, 1H),

7.79 (s,1H), 7.65 (d, *J*=7.8, 1H), 7.45 (m, 2H), 7.24 (d, *J*=5.1, 1H), 6.97 (d, *J*=5.1, 1H), 4.49 (s, 2H), 3.63 (t, *J*=7.3, 2H), 3.42 (t, *J*=7.4, 2H). **^{13}C-NMR (CDCl$_3$, 126 MHz, ppm)**: 142.73, 139.98, 137.12, 130.33, 129.38, 127.63, 124.89, 121.02, 120.29, 118.30, 33.94, 32.41, 30.99. **HRMS (EI)** calcd for [C$_{15}$H$_{13}$N$_3$SBr$_2$] 424.9197 found 424.9195.

Synthesis of **4.18**
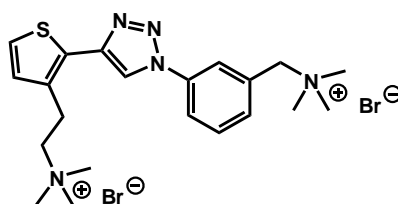
The experimental procedure used for the synthesis of **4.18** was analogous to that described for **4.3**. 0.70 g (1.64 mmol) of **4.17** was reacted with trimethylamine in ethanol. The product was obtained as a white powder (0.43 g, 68% yield). **^{1}H-NMR (D$_2$O, 400 MHz, ppm)**: 9.30 (s, 1H), 8.36 (s, 1H), 8.21 (t, *J*=7.7, 1H), 7.80 (t, 1H), 7.69 (q, *J*=6.1, 2H), 7.19 (d, *J*=5.1, 1H), 4.74 (s, 1H), 3.66 (t, *J*=6.1, 2H), 3.45 (t, *J*=6.2, 2H), 3.23 (s, 9H), 3.12 (s, 9H). **^{13}C-NMR (d6-DMSO, 126 MHz, ppm)**: 141.12, 137.81, 132.74, 130.49, 130.19, 129.95, 129.65, 125.93, 124.44, 124.12, 121.58, 119.98, 67.81, 67.42, 53.35, 52.06, 22.42. **HRMS (ES)** calcd for [C$_{21}$H$_{31}$N$_5$SBr] (M$^+$+Br) 464.1484 found 464.1468.

Synthesis of **4.19**
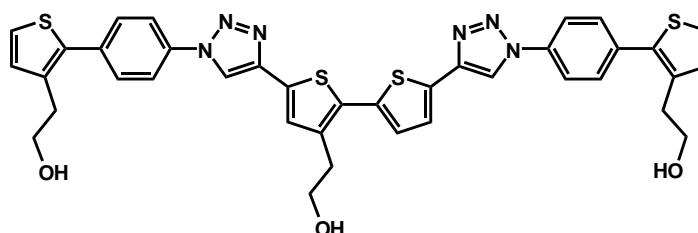
Compound **4.19** was synthesised analogously to **4.1** 2-(5,5'-Diethynyl-2,2'-bithiophen-3-yl)ethanol **2.20** (0.1 g, 0.387 mmol) was reacted with 0.18 g (0.774 mmol) of 2-(2-(4-

azidophenyl)thiophen-3-yl)ethanol **3.6**. The desired product was obtained without further purification as a yellow solid (0.40 g, 70% yield). **^{1}H-NMR (d6-DMSO, 250 MHz, ppm)**: 9.3 (s, 1H), 9.2 (s, 1H), 8.04 (d, *J*=8.2, 4H) 7.78 (d, *J*=8.3 , 4H), 7.58 (q, *J*=4.1, 4H), 7.42 (d, *J*=3.7, 1H), 7.17 (d, *J*=5.1 ,2H), 4.9 (t, *J*= 4.8, 1H), 4.80 (t, *J*=4.8, 2H), 3.80 (q, *J*= 5.5, 2H) 3.70 (q, *J*=6.1, 4H), 3.05 (t, *J*=6.1, 2H), 2.85 (t, *J*=6.4, 4H). **^{13}C-NMR (CDCl$_3$, 126 MHz, ppm)**: 142.75, 137.84, 136.96, 136.88, 136.59, 135.91, 135.00, 132.75, 130.77, 130.57, 128.60, 127.50, 125.87, 125.52, 120.84, 120.79, 119.54, 119.41, 61.72, 61.31, 33.16, 32.42. **HRMS (ES)** calcd for [C$_{38}$H$_{32}$N$_6$O$_3$S$_4$] (M$^+$+H) 749.1497 found 749.1517.

Synthesis of **4.20**
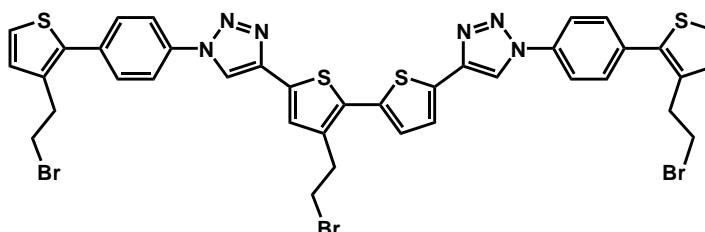
The experimental procedure used was as described for **4.2**. 0.088 g (0.117 mmol) of **4.19** was reacted with 0.233 g (0.705 mmol) of carbon tetrabromide and 0.183 g (0.705 mmol) of triphenylphosphine. 15 ml of DMF was then added to the mixture in order to solubilise all of the starting material. The crude product was purified by column chromatography, first using hexane, and then DCM : diethyl ether (9:1) as eluent. The title compound was obtained as a yellow solid (0.06 g, 60% yield). **^{1}H-NMR (d6-DMSO, 400 MHz, ppm)**: 9.39 (s, 1H), 9.34 (s, 1H), 8.06 (d, *J*=8.4, 4H) 8.74 (d, *J*=8.4, 4H), 7.61 (q, *J*=4.2, 3H), 7.41 (d, *J*=3.6, 2H), 7.25 (d, *J*= 5.1, 2H), 3.87 (t, *J*=7.4, 2H), 3.78 (t, *J*=7.5, 4H), 3.40 (t, *J*=7.4, 2H), 3.25 (t, *J*=7.4, 4H). **HRMS (ES)** calcd for [C$_{38}$H$_{30}$N$_6$S$_4$Br$_3$] 940.8904 found 940.8924.

Synthesis of **4.21**
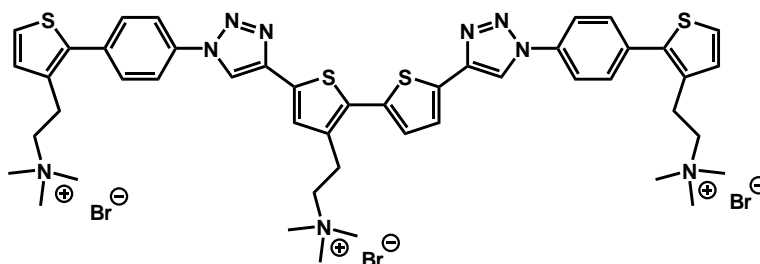
Tricationic 4.21 was synthesised analogously to **4.3**, reacting 0.05 g (0.053 mmol) of **4.20** with trimethylamine in ethanol but with the addition of 7 ml of THF. The product was obtained as a yellow powder (0.025 g, 55% yield). **^{1}H-NMR (d6-DMSO, 400 MHz, ppm)**: 9.32 (s, 1H), 9.21 (s, 1H), 8.0 (d, *J*=8.1, 4H) 7.69-7.73 (m, 8H), 7.50 (s, 1H), 7.23 (d, *J*=4.7, 2H), 3.25 (t, *J*=6.5, 6H), 3.23 (s, 9H), 3.14 (s, 18H). **^{13}C-NMR (CDCl$_3$, 126 MHz, ppm)**: 142.30, 137.86, 136.43, 135.78, 134.35, 133.73, 133.29, 132.29, 131.90, 131.23, 130.42, 129.81, 127.82, 126.27, 125.86, 120.56, 119.32, 119.21, 64.49, 52.35, 52.18, 22.72, 22.10. **HRMS (ES)** calcd for [C$_{47}$H$_{56}$N$_9$S$_4$Br$_2$] (M$^+$+Br) 1032.1908 found 1032.1875.

Synthesis of **4.22**
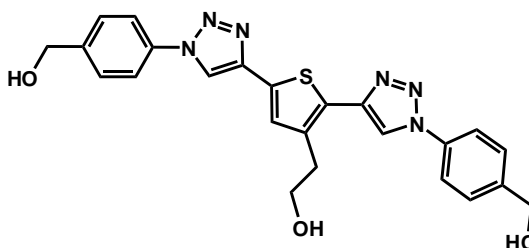
The experimental procedure used for the synthesis of **4.22** was as described for **4.1**. 2-(2,5-Diethynylthiophen-3-yl)ethanol **2.12** (0.78 g, 4.40 mmol) was reacted with 1.32 g (8.81 mmol) of (4-azidophenyl)methanol **3.8**. The desired product was obtained after filtration as a brown solid (1.3 g, 65% yield). **^{1}H-NMR (d6-DMSO, 400 MHz, ppm)**: 9.23 (s, 1H),

9.07 (s, 1H), 7.93 (dd, J_1=8.3, J_2=8.4, 4H), 7.57 (d, J=6.8, 4H), 7.52 (s, 1H) 5.38 (t, J=3.3, 2H), 4.81 (t, J=5.2, 1H), 4.60 (s, 4H), 3.75 (t, J=6.3, 2H), 3.03 (t, J=6.6, 2H). **^{13}C-NMR (d6-DMSO, 126 MHz, ppm)**: 143.47, 142.40, 137.87, 135.08, 130.70, 127.64, 126.56, 120.11, 119.83, 118.89, 62.22, 60.76, 32.61. **HRMS (EI)** calcd for [$C_{24}H_{22}N_6O_3S$] 474.1474 found 474.1482.

Synthesis of **4.23**
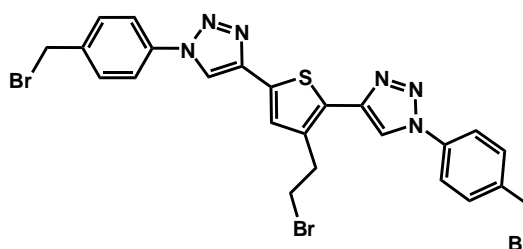
The experimental procedure used for **4.23** was as described for **4.2**. 1.1 g (2.3 mmol) of **4.22** was reacted with 4.61 g (13.8 mmol) of carbon tetrabromide and 3.65 g (13.8 mmol) of triphenylphosphine. DMF (10 ml) was added to solubilise the starting material. The crude product was purified by column chromatography using first hexane, then DCM : diethyl ether (9:1) as eluent. 1.01 g of compound **4.22** was obtained as a yellow solid (67% yield). **^{1}H-NMR (d6-DMSO, 400 MHz, ppm)**: 9.30 (s, 1H), 9.15 (s, 1H), 8.04 (dd, J_1=8.5, J_2=8.5, 4H), 7.72 (d, J=6.3, 4H), 7.59 (s, 1H) 4.83 (s, 4H), 3.87 (d, J=6.8, 2H), 3.50 (t, J=6.9, 2H). **^{13}C-NMR (d6-DMSO, 126 MHz, ppm)**: 143.78, 139.98, 137.43, 133.35, 127.96, 127.65, 124.76, 121.50, 120.98, 120.06, 33.94, 32.41, 32.06.

Synthesis of **4.24**
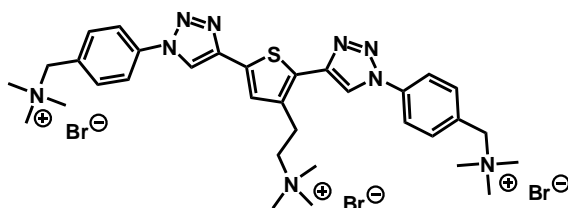
The experimental procedure was as described for **4.3**. 0.25 g (0.377 mmol) of **4.23** was reacted with trimethylamine in ethanol, but 7 ml of THF was added. The product was obtained as a brown powder (0.16 g, 72% yield). **^{1}H-NMR (d6-DMSO, 400 MHz, ppm)**: 9.48 (s, 1H), 9.41 (s, 1H), 8.23 (dd, J_1=8.5, J_2=8.4, 4H), 7.84 (q, J=4.7, 4H), 7.67 (s, 1H) 4.68 (d, J=5.4, 4H), 3.74 (t, J=6.2, 2H), 3.62 (t, J=6.3, 2H), 3.24 (s, 9H), 3.10 (s, 18H) . **^{13}C-NMR (d6-DMS, 126 MHz, ppm)**: 142.23, 137.55, 134.98, 134.53, 131.41, 128.96, 127.50, 121.68, 120.41, 119.26, 66.77, 52.42, 51.91, 22.89. **HRMS (ES)** calcd for [$C_{33}H_{46}N_9SBr_2$] (M^++Br) 758.1964 found 758.1946.

Synthesis of **4.25**
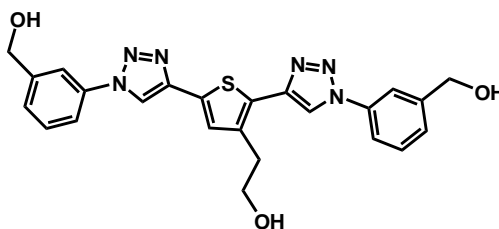
The syntheticprocedure was analogous to the procedure described for **4.**1. 2-(2,5-Diethynylthiophen-3-yl)ethanol **2.12** (0.5 g, 2.8 mmol) was reacted with 0.85 g (5.6 mmol) of (3-azidophenyl)methanol **3.10**. After filtration the product was obtained as a brown solid (0.92 g, 70% yield). **^{1}H-NMR (d6-DMSO , 400 MHz, ppm)**: 9.07 (s, 1H), 9.29 (s, 1H), 7.94 (dd, J_1=9.1, J_2=16.1, 4H), 7.56 (d, J= 7.8, 2H), 7.46 (s, 2H), 5.46 (s, 2H), 4.83 (s, 1H), 4.64 (s, 4H), 3.75 (t, J=6.2. 2H), 3.04 (t, J=6.3. 2H). **^{13}C-NMR (d6-**

DMSO, 126 MHz, ppm): 144.80, 142.46, 137.88, 136.38, 129.65, 127.66, 126.58, 119.52, 118.90, 118.64, 118.13, 117.77, 62.31, 60.74, 32.60. **HRMS (ES)** calcd for [$C_{24}H_{23}N_6O_3S$] (M^++H) 475.1552 found 475.1532.

Synthesis of **4.26**
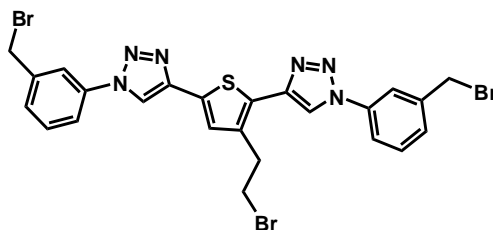
Compound 4.26 was synthesised following the same procedure as used for **4.2**. 1.2 g (2.5 mmol) of **4.25** was reacted with 5 g (15.1 mmol) of carbon tetrabromide and 3.96 g (15.1 mmol) of triphenylphosphine. 10 ml of DMF was then added to the mixture in order dissolve the starting material. The product was purified by column chromatography using first hexane, then DCM : diethyl ether (9:1) as eluent. 1.08 g of compound **4.26** was obtained as a yellow solid (65% yield). **^{1}H-NMR (d6-DMSO, 400 MHz, ppm**): 9.35 (s, 1H), 9.22 (s, 1H), 8.17 (d, *J*=17.6, 2H), 7.99 (dd, *J₁*= 7.5, *J₂*= 7.5, 2H), 7.66-7.70 (m, 4H), 7.67 (s, 1H), 4.90 (s, 4H), 3.93 (t, *J*=6.9. 2H), 3.56 (t, *J*=6.9, 2H). **^{13}C-NMR (d6-DMSO**, **126 MHz, ppm**): 142.30, 141.40, 140.08, 137.10, 130.85, 130.29, 129.57, 128.98, 127.15, 120.91, 119.90, 119.09, 33.16, 32.28, 32.03.

Synthesis of **4.27**
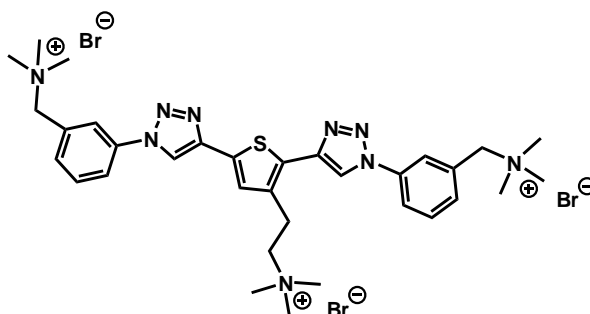
The experimental procedure used for **4.27** was as described for **4.3**. 0.39 g (0.588 mmol) of **4.26** was reacted with trimethylamine in ethanol with the addition of 10 ml of THF. The product was obtained as a yellow powder (0.21 g, 61% yield). **^{1}H-NMR (d6-DMSO, 400 MHz, ppm)**: 9.45 (s, 1H), 9.41 (s, 1H), 7.67 (s, 2H), 8.25 (d, J=9.2, 2H), 8.14 (d, J= 7.7, 2H), 7.75-7.80 (m, 4H), 7.70 (s, 1H), 7.75 (d, J=8.7, 4H), 3.78 (t, J=6.7, 2H), 3.44 (t, J=6.9, 2H), 3.26 (s, 9H), 3.15 (s, 18H). **^{13}C-NMR (d6-DMSO, 126 MHz, ppm)**: 142.10, 141.94, 139.99, 136.54, 133.12, 130.57, 130.20, 127.10, 124.41, 120.51, 119.47, 119.35, 66.85, 52.35, 52.02, 22.63. **HRMS (ES)** calcd for [$C_{33}H_{46}N_9SBr_2$] (M[+]+Br) 758.1964 found 758.1929.

Synthesis of **4.28**
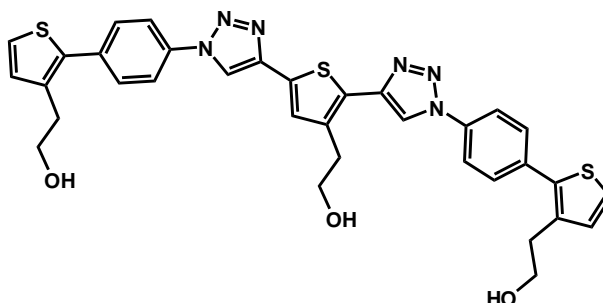
The experimental procedure used for **4.29** was as described for **4.1**. 0.1 g (0.56 mmol) of 2-(2,5-diethynylthiophen-3-yl)ethanol **2.12** was reacted with 0.77 g (0.11 mmol) of 2-(2-

(4-azidophenyl)thiophen-3-yl)ethanol **3.6**. The resulting product was purified by column chromatography using DCM : ethyl acetate : methanol (9:0.5:0.5) as eluent. 0.27 g of compound **4.28** was obtained as a yellow powder (73% yield). **^{1}H-NMR (d6-DMSO, 400 MHz, ppm)**: 9.30 (s, 1H), 8.11(s, 1H), 8.14 (dd, J_1=8.7 J_2=8.6, 4H), 7.78(dd, J_1=8.5, , J_2=8.6, 4H), 7.50-7.56 (m, , 2H), 7.46 (s, 1H), 7.10-7.15 (m, 2H), 7.77-4.80 (m 3H) 3.66 (t, J=6.6, 6H), 2.84 (t, J=6.6, 6H). **^{13}C-NMR (d6-DMSO, 126 MHz, ppm)**: 142.52, 141.72, 137.99, 136.46, 135.47, 134.54, 130.63, 130.23, 127.80, 126.56, 125.03, 120.70, 119.56.118.92, 61.23, 60.72, 32.62, 31.89. **HRMS (ES)** calcd for [$C_{34}H_{31}N_6O_3S_3$] (M$^+$+H) 667.1620 found 667.1589.

Synthesis of **4.29**
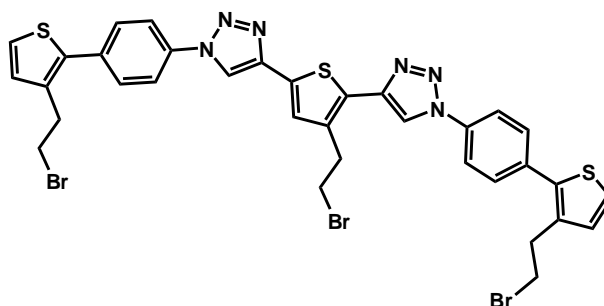
The bromination procedure used for the synthesis of **4.29** was as described for **4.2**. **4.28** (0.5 g, 0.750 mmol) was reacted with 1.49 g (4.5 mmol) of carbon tetrabromide and 1.18 g (4.5 mmol) of triphenylphosphine. 10 ml of DMF was added to the mixture in order to solubilise the starting material. The purification of the product was conducted by column chromatography using first hexane, then DCM : diethyl ether (9:1) as eluent compound. Title compound **4.29** was obtained as a yellow solid (0.38 g, 59% yield). **^{1}H-NMR (CDCl₃, 400 MHz, ppm)**: 9.14 (s, 1H), 8.08 (s, 1H), 7.81 (dd, J_1=8.5, J_2=8.6, 4H), 7.50-7.54 (m, 4H), 7.39 (s, 1H), 7.28 (d, J=5.2, 2H), 7.0 (d, J=5.1, 2H) 3.71 (t, J=6.8, 2H), 3.47-3.50 (m, 6H), 3.20 (t, J=6.6, 4H). **^{13}C-NMR (d6-DMSO , 126 MHz, ppm)**: 142.61,

141.28, 139.84, 138.16, 136.06, 135.48, 135.02, 130.75, 128.99, 127.37, 126.21, 125.17, 123.11, 120.71, 33.03, 32.54, 32.11, 32.03, 31.62, 30.90.

Synthesis of **4.30**
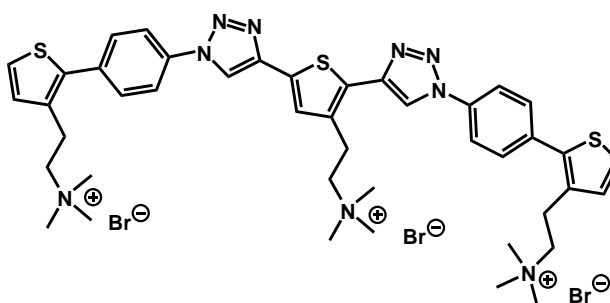
The synthesis of **4.30** again followed the procedure described previously for **4.3**. 0.1 g (0.117 mmol) of **4.29** was reacted with trimethylamine in ethanol with the addition of 7 ml of THF. The product was obtained as a yellow powder (0.056 g, 62% yield). **^{1}H-NMR (d6-DMSO, 400 MHz, ppm)**: 9.39 (s, 1H), 9.36 (s, 1H), 8.16 (dd, J_1=8.5, J_2=8.4, 4H), 8.078.11 (m, 4H), 7.71 (d, *J*= 6.4, 2H), 7.62, (s, 1H), 7.21, (d, *J*=5.0, 2H), 3.67, (t, *J*=6.5, 6H), 3.45 (t, *J*=6.4, 6H), 3.19, (s, 9H), 3.13 (s, 18H). **^{13}C-NMR (d6-DMSO, 126 MHz, ppm)**: 142.20, 141.15, 138.52, 137.89, 136.47, 134.90, 133.72, 132.26, 130.43, 129.86, 126.45, 126.20, 120.96, 120.58, 64.48, 52.17, 22.11.   **HRMS (ES)** calcd for [$C_{43}H_{54}N_9S_3Br_2$] (M$^+$+Br) 950.2031 found 950.2078.

DNA BINDING STUDIES

Abstract

This chapter describes the binding studies of di and tricationic oligoheteroaromatics, the synthesis of which was described in Chapter 4, with double-stranded calf thymus DNA using UV-visible and circular dichroism spectroscopy, calorimetry and viscosimetry. The selectivity of our cationic oligoheteroaromatics for selected sequences of DNA, viz. poly(dGdC)$_{40}$ and poly(dA)$_{80}\bullet$poly(dT)$_{80}$ *was also determined. All synthesised cationic oligoheteroaromatics bind to double-stranded calf thymus DNA with high affinity and in the minor groove. All compounds display selectivity for* poly(dA)$_{80}\bullet$poly(dT)$_{80}$ *sequence over poly(dGdC)$_{40}$.*

5.1 Introduction

DNA-binding can be studied through a range of techniques, including UV-visible and circular dichroism spectroscopy, viscosimetry. A brief description and discussion of these methods is provided below.

5.1.1 UV-Visible Spectroscopy (UV-Vis)

As its name implies, UV-visible (hereafter UV-vis) spectroscopy is an absorption spectroscopic method that operates in the ultraviolet-visible region of the electromagnetic spectrum. UV-vis spectroscopy is widely used for a wide range of quantitative analyses, including the analysis of highly conjugated organic compounds, biological macromolecules (DNA) and transition metal ions.

The conjugation in our DNA binders enables these organic compounds to absorb light in the UV and visible regions, making UV-vis spectroscopy a particularly appropriate tool for DNA binding studies with these compounds. Spectra are typically either recorded in water (for water soluble materials) or in acetonitrile or ethanol (for organic soluble materials). Care must be taken with other organic solvents as these can also absorb in the UV-vis region.

The interaction of a chromophore with DNA can result in an alteration of the spectroscopic response, typically as a consequence of the environmental change experienced by the chromophore or a structural change. An example of this is a change from aqueous solution to a more hydrophobic environment, such as that provided by a DNA-based binding site. Alternatively, DNA binding may cause a change in (average) conformation of a binder. The possible absorption changes involve either an increase (hyperchromicity) or decrease (hypochromicity) in the extinction coefficient, as well as

shifts to a higher (red shift) or lower (blue shift) wavelength. Plotting several spectra in one graph may reveal an isosbestic point (*i.e.* the point where two species have the same molar absorptivity) which is typically interpreted as indicating the presence of two species in equilibrium.[1, 2]

Analysis of spectroscopic data for a binding process may provide the binding constant (K_{bind}), and the stoichiometry of the interaction, which for interactions with DNA is typically expressed in terms of a binding site size (measured in base pairs). We define the formation of a complex (C) by the coupling of a ligand (L) with the binding site (bs) and the concentrations of each are related through K_{bind}, (equation 5.1). Each binding site will cover a ligand-specific number of bases, the binding site size (N), and so the concentration of binding sites can be defined as the concentration of DNA base pairs divided by N (Equation 5.2).

K_{bind} is defined based on the equilibrium between the free ligand, free DNA and the ligand bound (complex) (5.1). Because the concentration of free ligand [L]f and the complex concentration [C] are related through the total ligand concentration [L]tot, it is possible to establish an overall equation describing the equilibrium (5.5), which may be re-arranged to provide the quadratic representation of the complex concentration (5.7).

$$[C] = K_{bind}.[bs]_f.[L]_f \tag{5.1}$$

$$[bs] = [DNA] / N \tag{5.2}$$

$$[L]_{tot} = [C] + [L]_f \qquad \longleftrightarrow \qquad [L]_f = [L]_{tot} - [C] \tag{5.3}$$

$$[bs]_{tot} = [C] + [\,bs]_f \qquad \longleftrightarrow \qquad [bs]_f = [bs]_{tot} - [C] \tag{5.4}$$

$$[C] = K_{bind}.([bs]_{tot} - [C]).([L]_{tot} - [C]) \tag{5.5}$$

$$[C] = K_{bind}\,[bs]_{tot}.[L]_{tot} - K_{bind}.[C].[bs]_{tot} - K_{bind}.[C].[L]_{tot} - K_{bind}.[C]^2 \tag{5.6}$$

By the Rearrangement of equation 5.6 give a quadratic equation:

$$K_{bind}\,[C]^2 - (1 + K_{bind}.[bs]_t + K_{bind}.[L]_{tot}).[C] + K_{bind}.[bs]_{tot}.[L]_{tot} = 0 \qquad (5.7)$$

The quadratic equation can be solved using the classic equation: $[C] = \frac{-b \pm \sqrt{b^2 - 4ac}}{2a}$ to

provide an expression for the concentration of complex [C] as a function of total ligand

and DNA concentrations.

$$[C] = \frac{1 + k[bs]_{tot}\,k[L]_{tot} \pm \sqrt{(1 + k[bs]_{tot} + k[L]_{tot})^2 - 4K^2[bs]_{tot}[L]_{tot}}}{2k}$$

Equation 5.8

By inserting the Beer-Lambert Law (A = ε·l·[C]), modified for background absorbance,

into equation 5.8 the absorbance is given by Equation 5.9. This equation can be fit to a

plot of absorption against total DNA concentration in order to find the best

approximations for K_{bind} and the binding site size.

$$\text{signal}_{obsd} = \text{background} + \text{signal}_{free.m}.[L]_{tot} + \Delta_{binding}\,\text{signal}_m \frac{1 + K_{bind}.\frac{[DNA]}{N} + K_{bind}.[L]_{tot} - \sqrt{(1 + K_{bind}.\frac{[DNA]}{N} + K_{bind}.[L]_{tot})^2 - 4.K_{bind}{}^2.\frac{[DNA]}{N}.[L]_{tot}}}{2K_{bind}}$$

Equation 5.9

The terms in the equation are detailed below:

signal_{obs} = observed absorbance.   Background = buffer absorbance.

$\text{signal}_{free,}$ = the product of the cuvette path length and the extinction coefficient

$\Delta_{binding}\text{signal}_m$ = product of the cuvette path length and the change in extinction coefficient upon binding.

K = binding constant   [DNA] = DNA concentration in base pairs.

N = binding site size in base pairs $[L]_{tot}$ = total ligand concentration.

5.1.2 Circular Dichroism Spectroscopy (CDS)

Circular dichroism spectroscopy (CDS) is a useful technique for studying DNA binding. Circular dichroism measures the difference in absorption between left- and right-handed circularly polarised light for chiral molecules, or for non-chiral molecules in a chiral environment. Such absorbance differences are very small, typically in the range of 1×10^{-4} absorbance units. The difference in absorbance of the two forms of polarised light for enantiomers of a chiral compound arises as a consequence of the structural asymmetry in enantiomers. Induced circular dichroism signals on the other hand are a result of the coupling that occurs between electric transition moments and a chiral environment, for example betweena ligand and DNA.[3, 4]

Induced circular dichroism signals have great value in exploring the binding mode of DNA binders. The reason for this is that for molecules interacting with DNA, the interaction between the transition dipole moment of the ligand and the nucleotide bases significantly affects the induced CD signal of the binder. Typically, the binding of the ligand in the minor groove results in a transition moment that is orientated along the groove of B-form DNA and is at an angle of 45° with the DNA bases, resulting in an induced CD signal that is strongly positive. In the case of major groove binding there are numerous ligand orientations that are accessible within the groove, which results in a negative ICD signal.

The induced CD signal for an intercalator is largely dependent on the displacement experienced with respect to the double helix and the nature of the base-pairs on either side of the site of intercalation. For the type of the intercalators that have transition moments oriented along the main axis of the DNA, a negative ICD signal is introduced.[4]

5.1.3 Viscosimetry

Viscosimetry is an effective technique for the investigation of interactions of a binder with DNA in aqueous solution.[5, 6]

Intercalation of a species between the base pairs of DNA results in the separation of these bases, which results in an overall increase in the length of the DNA helix and therefore an increased viscosity of the DNA solution. The interaction of a minor groove binder, on the other hand, results in negligible perturbation of the DNA length, the net result of which is a negligible change or no change in the viscosity of the DNA solution.

The relative viscosity (η) of a solution as determined using a glass capillary viscometer is given by equation 5.10.

$$\eta = \frac{t - t_0}{t_0} \qquad\qquad \text{Equation 5.10}$$

Where t is the observed time of flow of the DNA solution in the viscometer and t_0 is the buffer flow time. From the work of Cohen and Eisenberg[7], the calculation of the contour length change between free and bound DNA (L/L_0) is conducted through equation 5.11.

$$\frac{L}{L_0} = \left[\frac{\eta}{\eta_0} \times \frac{f(p)_0}{f(p)} \right]^{1/3} \approx 1 + r \qquad\qquad \text{Equation 5.11}$$

Where L is the contour length the rod-like macromolecules, p the axial ratio of said rods, r the ratio of bound complex to DNA and η the relative viscosity of the DNA solution at given binding ratios, r. The subscripts "o" refer to the absence of binder. Therefore a plot of the viscosity data as relative viscosity $(\eta/\eta_0)^{1/3}$ against the binding ratio r would

indicates an increase or no increase in the viscosity of the DNA solution depending on the particular DNA binding mode.

5.1.4 Isothermal Titration Calorimetry (ITC)

Isothermal titration calorimetry (ITC) is a very powerful physical technique for the study of biomolecule-ligand interactions in aqueous media. ITC measures the heat released (or absorbed) upon a binding process. The measurement and analysis of the heat effects enables the effective determination of binding site size(s), binding affinities and enthalpies (ΔH). Knowing the binding affinity allows the determination of the Gibbs free energy (ΔG) which together with the enthalpy changes ΔH also provides the entropy changes (ΔS) for the binding process. A potential drawback of ITC is the requirement for high concentrations of ligand and biomolecule (in our case DNA), meaning that due consideration must be given to the potential for self-aggregation of the molecules.[8, 9]

The ITC instrumentation (Figure 5.1) consists of two identical cells. One (the reference cell) normally contains water or buffer, whereas the other contains a solution of the host molecule *e.g.* DNA. A syringe containing a concentrated solution of the ligand is injected in pre-programmed amounts and at pre-selected intervals.[10]
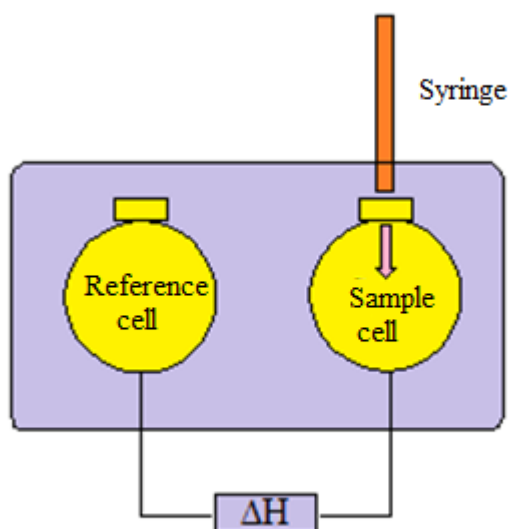
Figure 5.1 Schematic representation of the ITC equipment

As a consequence of the binding event under study in the sample cell, a difference in temperature (ΔT) between reference and sample cells is created. In order to accurately determine this, the cells are situated within isothermal jackets and allowed to equilibrate to a constant temperature before the experiment and after every injection. The equilibration after an injection corresponds to the relative addition or removal of heat (i.e. a differential heat flow). The relative energy flow necessary for maintaining both cells at a constant temperature is measured and integrated with respect to time. This then provides the total uptake/release of heat q for the interactions of making/breaking bonds. The process of injecting the ligand into the DNA solution is then repeated until a full titration profile is obtained. Because the experiment is carried out under isobaric conditions, the heat effects for the injections i, q_i, correspond to the interaction enthalpies.

Isothermal Titration Calorimetry data analysis by IC-ITC

In the ITC experiment, the use of high concentrations of ligand in the titration syringe in many cases results in self aggregation of the ligand. This self aggregation affects the calorimetric studies and, as a result, self aggregation of the ligand should be taken in account during the data analysis, in conjunction with the consideration of DNA binding processes. The addition of the self aggregation terms to the equations involving DNA binding is relatively complex and these equations cannot be solved analytically. As a consequence specific data analysis software for this purpose, IC-ITC, has been developed in-house.[10, 11] IC-ITC can be used to perform the analysis of calorimetric data in the case of simultaneous ligand self aggregation and DNA binding in order to determine the thermodynamic parameters for the various equilibria (Scheme 5.1). IC-ITC uses simulated annealing for the parameter optimisation with the equilibrium concentrations determined numerically using the Newton-Raphson algorithm.[12]
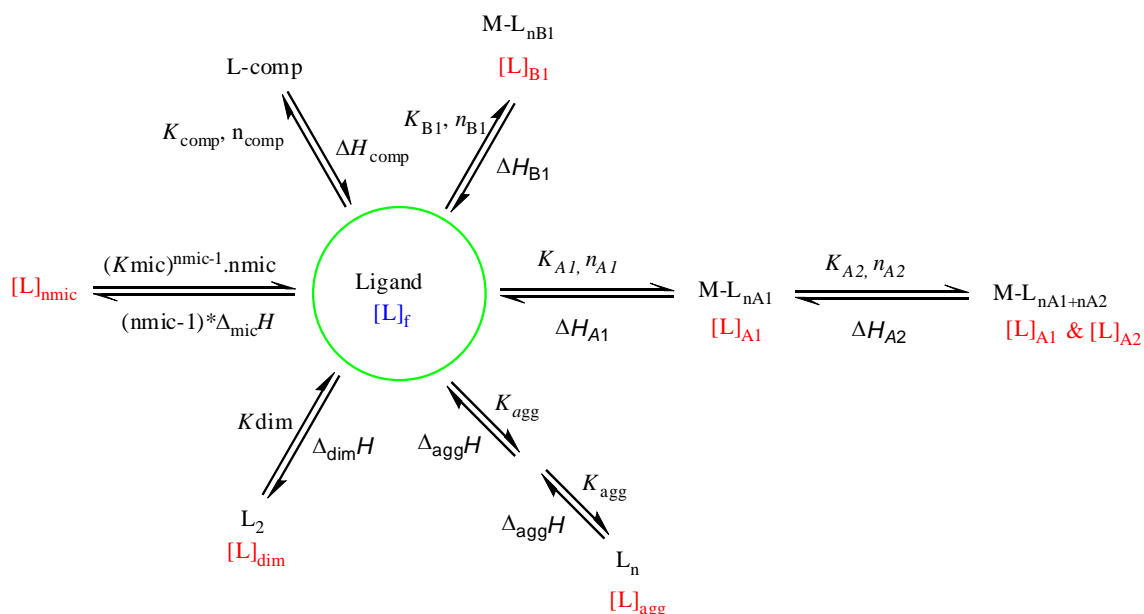
Scheme 5.1

The calculation of all relevant total concentrations (*e.g.* macromolecule, ligand) in the sample cell after each addition of ligand is the first important step in the analysis of binding by IC-ITC.[10] This is followed by solving the mass balance equation in order to determine the free ligand concentration $[L]_f$.

$$-[L]_{ot} + \sum_X [L]_X = 0$$

Equation 5.12

Here, $[L]_{tot}$ is the total ligand concentration, and $[L]_x$ are the concentrations of ligand in all possible ligand states X, e.g. free, DNA-bound, aggregated, etc.

Equation 5.3 illustrates the formal link between the concentrations of ligand taken up in the complexes and in the aggregates, $[L]_X$, the free ligand concentration, total macromolecule concentrations $[M]_{tot}$ and interaction parameters $\mathbf{a}_X$ for the complexation events, *i.e.* equilibrium constants and stoichiometries.

$$[L]_X = f([L]_f, [M]_{ot}, \mathbf{a}_X)$$

Equation 5.13

During the optimisation, IC-ITC determines the optimal parameter values, as identified by the lowest sum over square deviations, and allows the determination of the error margins and covariances for different variables through analysis of the parameters goodness of fit hyperspace.

5.2 Aims

Techniques such UV-visible spectroscopy, circular dichroism spectroscopy (CD), viscosimetry and isothermal titration calorimetry (ITC) were used to determine the binding affinity, binding site size, and mode of interaction of cationic oligoheteroaromatics **5.1-5.6** (Scheme 5.2) with double-stranded DNA.
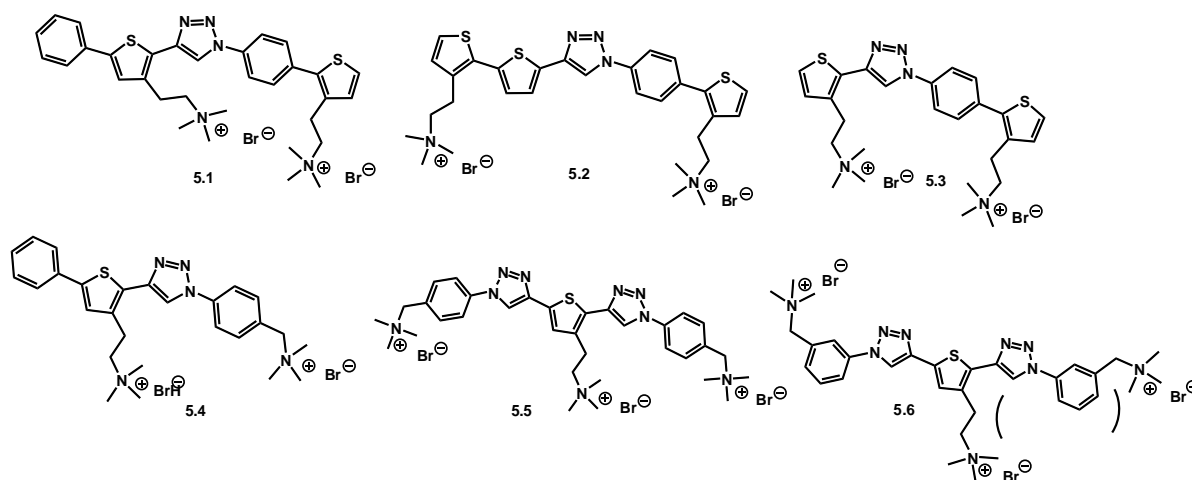
Scheme 5.2

5.3 Results and discussion

The results of the interaction studies for compounds **5.1-5.6** with DNA will be presented

and discussed for each individual compound.

5.3.1 Dicationic oligoheteroaromatic 5.1 binding to DNA

UV-visible spectroscopy

The binding of dicationic oligoheteroaromatic **5.1** to calf thymus DNA was studied using

UV-visible spectroscopy; the changes in absorption of **5.1** upon addition of calf thymus

DNA were measured in buffer (25 mM MOPS, 50 mM NaCl and 1 mM EDTA) at 25 °C
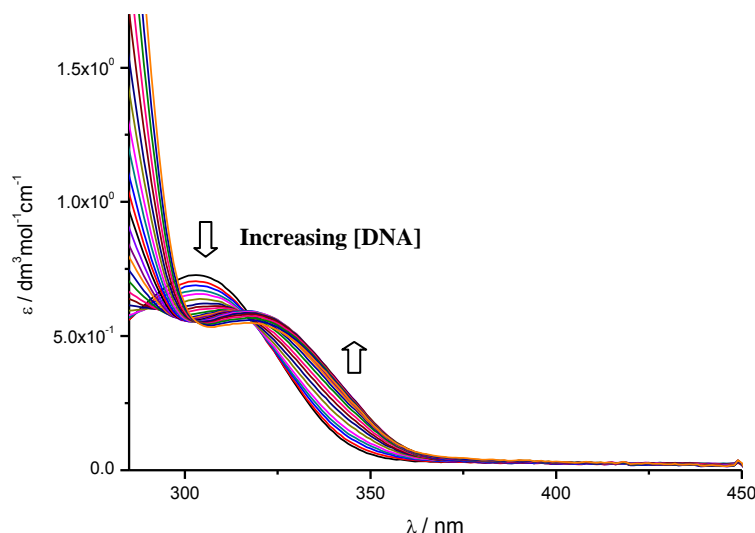
(Figure 5.2).

Figure 5.2 UV-visible spectra for 1.35×10^{-2} mM dicationic oligoheteroaromatic **5.1** upon addition of aliquots of a 3 mM solution of calf thymus DNA in 25 mM MOPS, 50 mM NaCl and 1 mM EDTA, pH 7.0, at 25 °C.

Figure 5.2 shows that the absorption of the free ligand (with a maximum at 303 nm)

decreases while the absorption around 330 nm, attributed to the DNA-ligand complex,

increases. DNA-binding of **5.1** is therefore accompanied by a bathochromic shift. This

bathochromic shift is attributed to an increasing effective conjugation length; upon

binding to DNA the freely rotating rings in the ligand become fixed.

159

Titration data for selected wavelengths was extracted from the UV-visible data in Figure

5.2 and from a second titration to generate binding isotherms for **5.1** interacting with DNA

(Figure 5.3).
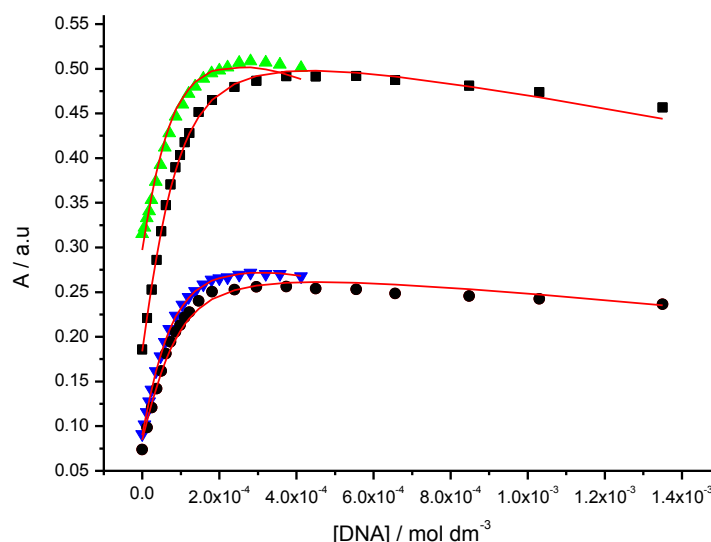
Figure 5.3 Absorbance at (■) 340 nm, (●) 350 nm, (▲) 330 nm and (▼) 345 nm plotted against DNA concentration. Solid lines represent a global fit to a multiple independent sites model for **5.1** (2.35×10^{-2} mM and 2.96×10^{-2} mM), in 25 mM MOPS, 50 mM NaCl and 1 mM EDTA, pH 7.0, at 25 °C.

The data in the titration curve of Figure 5.3 was analysed globally using the multiple

independent binding site model. The binding constant (K) for **5.1** binding to DNA is $(7.7 \pm$

$1.5) \times 10^4$ M^{-1} and the stoichiometry (n) is 2.8 ± 0.2, i.e. 2.8 base pairs of DNA are needed

for the ligand to bind. This binding site is rather short in comparison with the length of

5.1, suggesting that **5.1** may be binding in a side-by-side manner, or that other

complexities are playing a role.

Circular dichroism

In order to study the binding mode for the interaction of **5.1** with calf thymus DNA we used circular dichroism spectroscopy. Induced circular dichroism spectra for **5.1** in the presence of varying concentrations of calf thymus DNA in 25 mM MOPS, 50 mM NaCl and 1 mM EDTA, pH 7 at 25 ^{O}C were recorded (Figure 5.4).
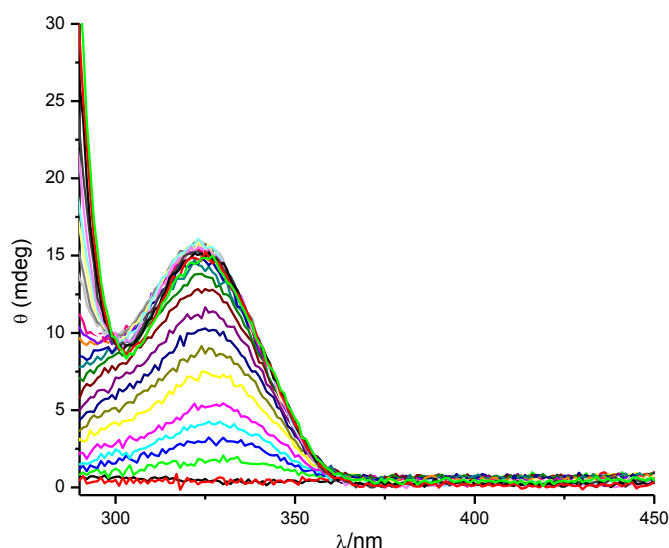
Figure 5.4 Induced circular dichroism spectra for 1.35×10^{-2} mM **5.1** upon addition of aliquots of a 3 mM calf thymus DNA solution (in 25 mM MOPS, 50 mM NaCl and 1 mM EDTA, pH 7 at 25 °C).

A positive induced signal around 325 nm is observed and this signal increases upon addition of DNA during the titration. This positive signal suggests that **5.1** is a minor groove binder.[3]

A titration curve (Figure 5.5) was extracted from the ICD titration data.
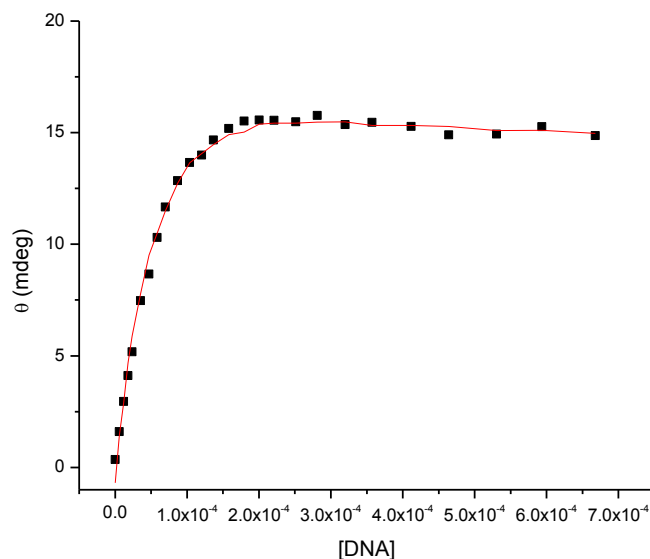
Figure 5.5 Ellipticity at (■) 325 nm against DNA concentration, the solid line represents a global fit to a multiple independent sites model for **5.1** (1.35×10^{-2} mM), in 25 mM MOPS, 50 mM NaCl and 1 mM EDTA, pH 7.0, at 25 °C.

The data in Figure 5.5 was analysed using the multiple independent binding site model. The binding constant (K) for **5.1** binding to DNA is $(3.4 \pm 0.3)\times10^{4}$ M^{-1} and the stoichiometry (n) is 1.5 with error margin 0 (restricted). The stoichiometry was restricted because the fit does not give reasonable parameters with variable stoichiometry.

Viscosity

The mode of binding for **5.1** interacting with double-stranded DNA was further studied by viscosimetry to confirm the conclusion from circular dichroism spectroscopy that **5.1** is a groove binder. The relative viscosity of DNA solutions after the addition of **5.1** was compared with the viscosity of equivalent DNA solutions in the presence of a known DNA binder which interacts as an intercalator (ethidium bromide). Figure 5.6 shows the relative viscosities for a 0.5 mM calf thymus DNA solution in the presence of varying

concentrations of dicationic oligoheteroaromatic **5.1** and in the presence of ethidium bromide in 25 mM MOPS, 50 mM NaCl and 1 mM EDTA, pH 7.0, at 25 °C.
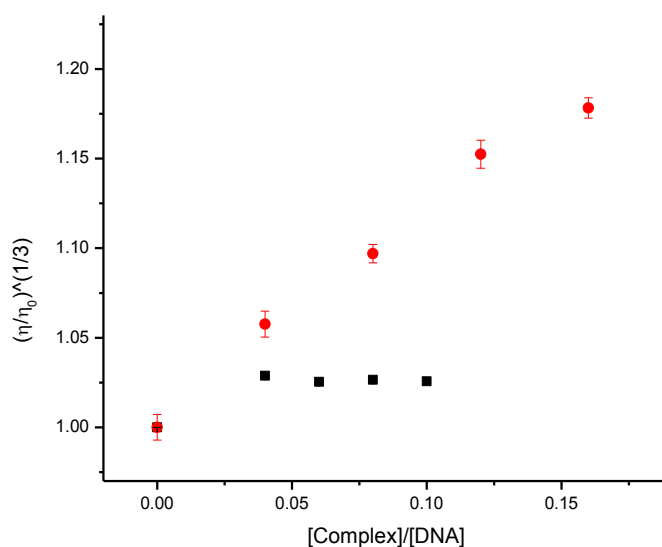
Figure 5.6 Relative viscosities of 0.5 mM CT DNA solutions upon addition of **5.1** (■) and ethidium bromide (●) at 25 °C in 25 mM MOPS, 50 mM NaCl, 1mM EDTA, pH 7.0.

Figure 5.6 shows a small increase in viscosity upon the first addition of **5.1** followed by no further increase, suggesting a dominant minor groove binding mode, confirming the minor groove binding mode for **5.1**.

Isothermal titration calorimetry (ITC)

To further explore the binding of dicationic oligoheteroaromatic **5.1** with DNA, we used isothermal titration calorimetry (ITC). The differential heat flow and derived integrated heat effects for titration of a 4.86 mM solution of **5.1** into a 0.5 mM calf thymus DNA solution were measured in 25 mM MOPS, 50 mM NaCl and 1 mM EDTA, pH 7.0, at 25 °C (Figure 5.7).
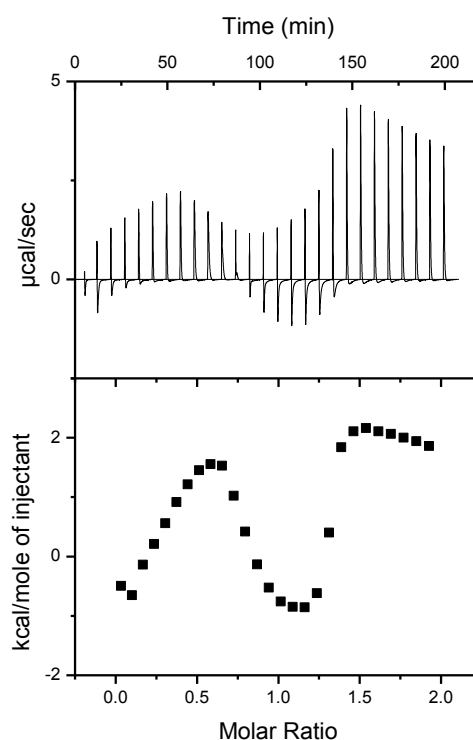
Figure 5.7 Titration of a 4.86 mM solution of **5.1** into a 0.5 mM solution of CT-DNA in 25 mM MOPS, 50 mM NaCl and 1 mM EDTA, pH 7, at 25 °C.

The enthalpogram for binding of **5.1** to CTDNA in Figure 5.7 suggests three different binding events. We decided against attempting to analyse this data by our ITC data analysis software IC ITC because the complexity of the data requires a complex data analysis model. It would be difficult to validate the correctness of such a model based on the currently available data for this system. The highest affinity DNA binding of **5.1** appears to be weakly exothermic (leading to an overall negligible heat effect for the early injections). Weakly exothermic binding is in line with a groove binding mode.[13]

Sequence selectivity

The selectivity of **5.1** for selected specific sequences of DNA, viz. poly(dGdC)$_{40}$ and poly(dA)$_{80}$•poly(dT)$_{80}$, was studied using UV-visible and circular dichroism spectroscopy.

UV-visible spectroscopy for 5.1 with poly(dGdC)$_{40}$ The binding of oligoheteroaromatic **5.1** to poly(dGdC)$_{40}$ was studied using UV-visible spectroscopy. The titration of **5.1** with poly(dGdC)$_{40}$ was carried out in buffer (25 mM MOPS, 50 mM NaCl and 1 mM EDTA) at 25 °C. Figure 5.8 shows the changes in absorbance of **5.1** with increasing poly(dGdC)$_{40}$ concentration.

Figure 5.8 UV-visible spectra for $1.50{\times}10^{-2}$ mM dicationic oligoheteroaromatic **5.1** upon addition of 2.85 mM poly(dGdC)$_{40}$ in 25 mM MOPS, 50 mM NaCl and 1 mM EDTA, pH 7.0, at 25 °C.

Figure 5.8 shows that the absorption maximum of the free ligand decreases while the absorption maximum of the complex increases with an isosbestic point at 320 nm suggesting the presence of only two ligand species in solution (free and bound ligand). DNA-binding of **5.1** is accompanied by a bathochromic shift, which is attributed to the

ligand adopting a more planar conformation when bound to DNA, increasing the effective conjugation length.

The titration in Figure 5.9 was extracted from the UV-visible data to quantify the binding of **5.1** to poly(dGdC)$_{40}$.
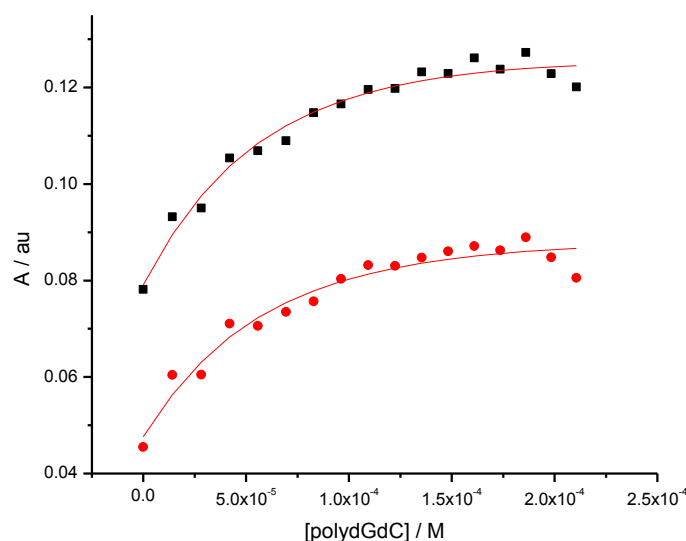
Figure 5.9 Absorbance at (■) 336 nm and (●) 346 nm plotted against poly(dGdC)$_{40}$ concentration, solid lines represent a global fit to a multiple independent sites model for **5.1** (1.50×10^{-2} mM), in 25 mM MOPS, 50 mM NaCl and 1 mM EDTA, pH 7.0, at 25 °C.

The data in Figure 5.9 were analysed using the same model as used for the data in Figure 5.2. The binding constant (K) for **5.1** binding to poly(dGdC)$_{40}$ is $(4.1 \pm 0.8) \times 10^4$ M^{-1} for a stoichiometry (n) or binding site size restricted to 2 base pairs. The stoichiometry was restricted because the fit does not give reasonable parameters with variable stoichiometry. The observed increase in absorbance is rather small, suggesting that the interaction between **5.1** and poly(dGdC)$_{40}$ is not particularly intimate (*Cf.* the lack of induced circular dichroism – *vide infra*).

166

Circular dichroism for 5.1 interacting with poly(dGdC)$_{40}$

In order to study the binding mode of **5.1** with poly(dGdC)$_{40}$, circular dichroism spectra were recorded (Figure 5.10).
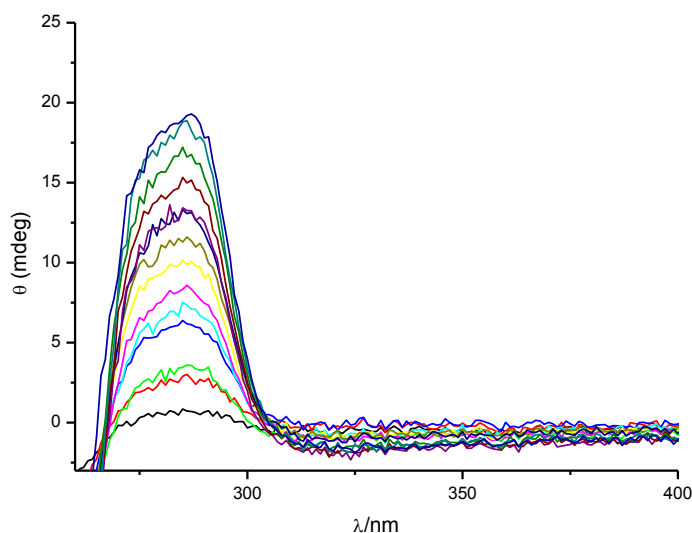
Figure 5.10 Circular dichroism spectra for 1.50×10^{-2} mM **5.1** in the presence of varying concentrations of poly(dGdC)$_{40}$ (added as aliquots of a 2.85 mM solution of poly(dGdC)$_{40}$ in buffer 25 mM MOPS, 50 mM NaCl and 1 mM EDTA, pH 7 at 25 °C.

Figure 5.10 shows the circular dichroism spectra for a solution of **5.1** in the presence of varying concentrations of poly(dGdC)$_{40}$, in 25 mM MOPS, 50 mM NaCl and 1 mM EDTA, pH 7 at 25 °C. No ICD spectrum is observed for wavelengths above 300 nm upon addition of poly(dGdC)$_{40}$ up to concentrations of poly(dGdC)$_{40}$ of 2.1×10^{-1} mM. This result suggests that **5.1** does not bind particularly intimately to poly(dGdC)$_{40}$ and most likely not through groove binding or intercalation. The binding of **5.1** could be due to electrostatic interactions and may involve the ligand stacking outside the helix. Such a binding mode is unlikely to be specific.

UV-visible spectroscopy for 5.1 interacting with poly(dA)$_{80}$•poly(dT)$_{80}$

The binding of oligoheteroaromatic **5.1** to poly(dA)$_{80}$•poly(dT)$_{80}$was studied using UV-visible spectroscopy. The titration of **5.1** with poly(dA)$_{80}$•poly(dT)$_{80}$was carried out in buffer (25 mM MOPS, 50 mM NaCl and 1 mM EDTA) at 25 °C. Figure 5.11 shows the changes in absorbance with increasing poly(dA)$_{80}$•poly(dT)$_{80}$concentration.
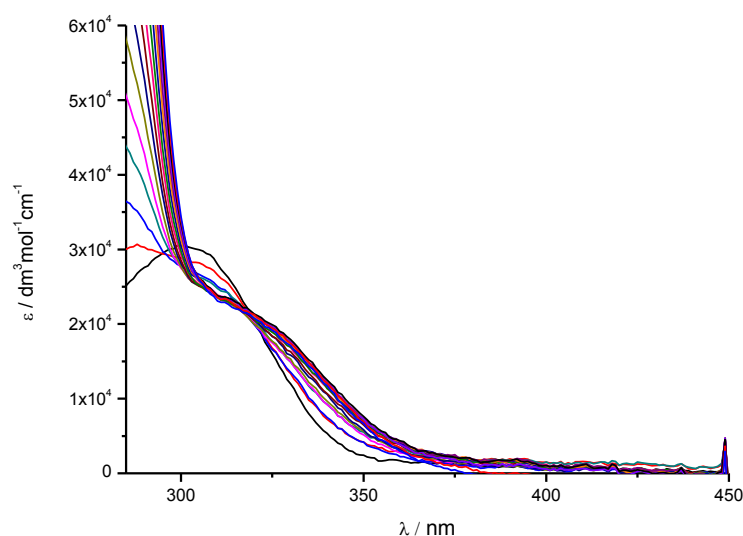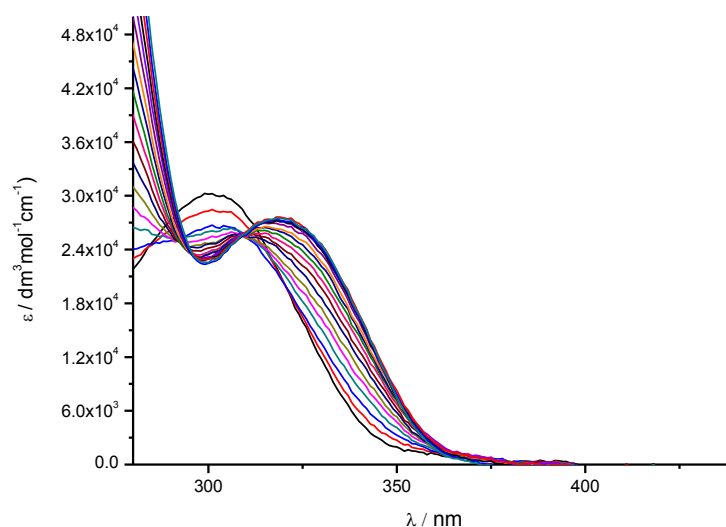

Figure 5.11 UV-visible spectra for 2.01×10^{-2} mM dicationic oligoheteroaromatic **5.1** upon addition of aliquots of a 1.83 mM solution of poly(dA)$_{80}$•poly(dT)$_{80}$in 25 mM MOPS, 50 mM NaCl and 1 mM EDTA, pH 7.0, at 25 °C.

The absorption maximum of the free ligand decreases while the absorption maximum of the complex increases and DNA-binding of **5.1** is accompanied by a bathochromic shift. As before, we attribute the bathochromic shift to formation of a complex in which the bound ligand is forced to adopt a more planar conformation, increasing effective conjugation length.

A binding isotherm (Figure 5.12) was extracted from the UV-visible data to quantify the binding of **5.1** to poly(dA)$_{80}$•poly(dT)$_{80}$.
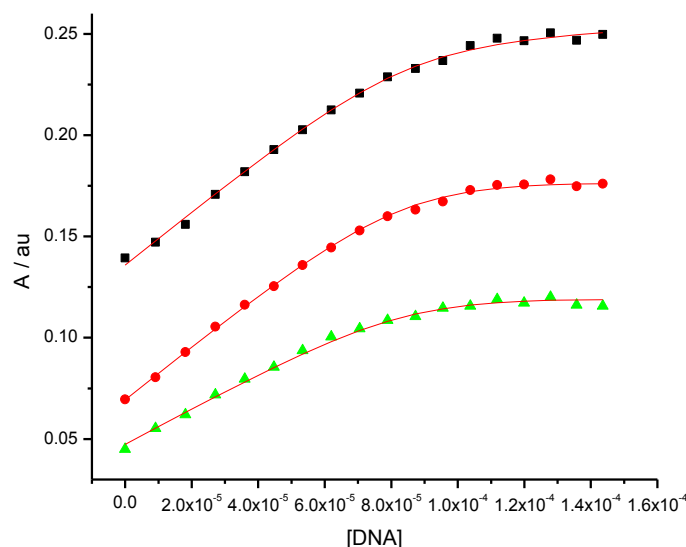
Figure 5.12 Absorbance at (■) 330 nm, (●) 340 nm and (▲) 347 nm plotted against poly(dA)$_{80}$•poly(dT)$_{80}$concentration, solid lines represent a global fit to a multiple independent sites model for **5.1** (2.01×10^{-2} mM) interacting with poly(dA)$_{80}$•poly(dT)$_{80}$, in 25 mM MOPS, 50 mM NaCl and 1 mM EDTA, pH 7.0, at 25 °C.

The binding isotherm in Figure 5.12 was analysed using the same model as was used for

the data in Figure 5.2. The binding constant (K) for **5.1** binding to poly(dA)$_{80}$•poly(dT)$_{80}$is

$(1.2 \pm 0.3) \times 10^{6}$ M^{-1} and the binding site size (n) is 4.49 ± 0.09 base pairs. The affinity of

5.1 for poly(dA)$_{80}$•poly(dT)$_{80}$is high compared with its affinity for poly(dGdC)$_{40}$. This is

in agreement with the general observation that minor groove binders typically prefer A•T-

rich sequences over G•C rich sequences.

Circular dichroism for 5.1 interacting with poly(dA)$_{80}$•poly(dT)$_{80}$

In order to study the binding mode, circular dichroism spectra were recorded for **5.1** in the

presence of varying concentrations of poly(dA)$_{80}$•poly(dT)$_{80}$ (Figure 5.13).
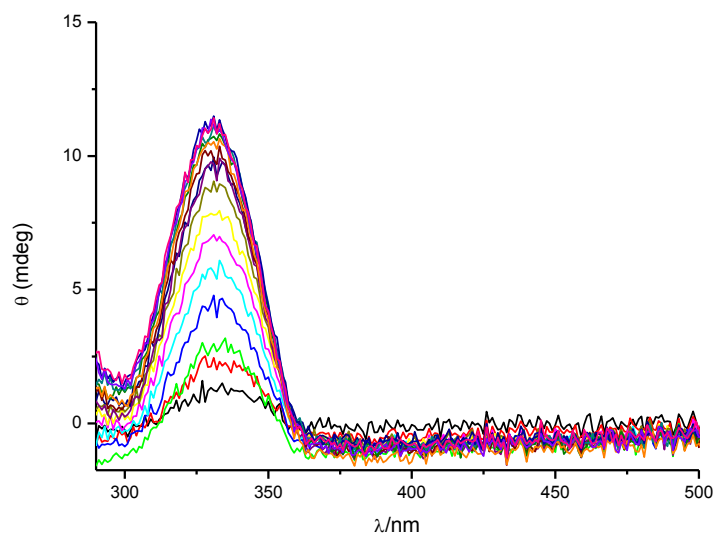
Figure 5.13 Induced circular dichroism spectra for 2.01×10^{-2} mM of **5.1** in the presence of varying concentrations of poly(dA)$_{80}$•poly(dT)$_{80}$ (added as aliquots of a 1.83 mM of poly(dA)$_{80}$•poly(dT)$_{80}$) in buffer (25 mM MOPS, 50 mM NaCl and 1 mM EDTA, pH 7) at 25 °C.

Figure 5.13 shows positive induced circular dichroism at wavelengths above 300 nm for the interaction of **5.1** with poly(dA)$_{80}$•poly(dT)$_{80}$, in 25 mM MOPS, 50 mM NaCl and 1 mM EDTA, pH 7 at 25 °C. This result suggests a minor groove binding mode for **5.1** binding to poly(dA)$_{80}$•poly(dT)$_{80}$.

A binding isotherm (Figure 5.14) was extracted from the ICD titration data.
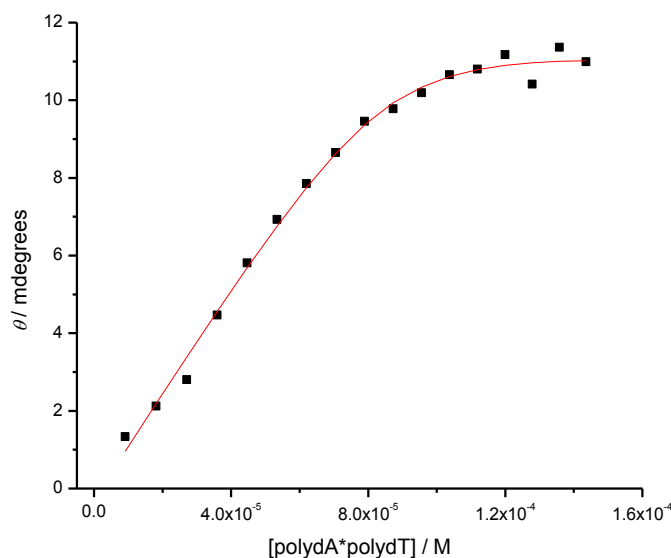
Figure 5.14 Ellipticity at (■) 330 nm plotted against poly(dA)$_{80}$•poly(dT)$_{80}$concentration, solid lines represent a global fit to a multiple independent sites model for **5.1** (2.01×10^{-2} mM) interacting with poly(dA)$_{80}$•poly(dT)$_{80}$, in 25 mM MOPS, 50 mM NaCl and 1 mM EDTA, pH 7.0, at 25 °C.

The data in the titration curve (Figure 5.14) were analysed using the same multiple independent binding sites model as before. The binding constant (*K*) for **5.1** binding to poly(dA)$_{80}$•poly(dT)$_{80}$is (1.4 ± 1.0) $\times 10^6$ M^{-1} and the stoichiometry (*n*) of 4.47 ± 0.22 is in agreement with the UV-visible data. These results again indicate sequence selectivity of **5.1** for poly(dA)$_{80}$•poly(dT)$_{80}$.

Summary

Dicationic oligoheteroaromatic **5.1** binds to calf thymus DNA binds with a binding constant of (7.7 ± 1.5)$\times 10^4$ M^{-1} and a binding site size of 2.8 ± 0.2 base pairs. The interaction of dicationic **5.1** with CT-DNA results in a positive ICD signal, suggesting binding of **5.1** in the minor groove. The small binding site size may indicate that this involves a "side-by-side" groove binding mode. Following a small increase in the viscosity for the first addition of **5.1**, there is no further increase in the viscosity of a DNA

solution for dicationic oligoheteroaromatic **5.1** interacting with CT-DNA, suggesting dominant minor groove binding. The complex binding mode is supported by ITC, which shows at three binding events for **5.1** interacting with DNA. Dicationic oligoheteroaromatic **5.1** weakly bound to poly(dGdC)$_{40}$, but no indications of a specific binding mode were observed. On the other hand, **5.1** strongly bound to poly(dA)$_{80}$•poly(dT)$_{80}$in the minor groove.

The driving forces for binding of **5.1** to DNA are a combination of hydrophobic interactions of the π-conjugated system with the hydrophobic walls of the minor groove and electrostatic interactions between the positive charges on the ammonium groups and the negative charges on the DNA. Formation of hydrogen bonds between the base pairs and the triazole ring of the ligand may be acting as an additional driving force.

5.3.2 Dicationic oligoheteroaromatic 5.2 binding to DNA

UV-visible spectroscopy

The binding of dicationic oligoheteroaromatic **5.2** to calf thymus DNA was studied using UV-visible spectroscopy; the changes in absorption of **5.2** upon addition of calf thymus DNA were measured in buffer (25 mM MOPS, 50 mM NaCl and 1 mM EDTA) at 25 °C (Figure 5.15).
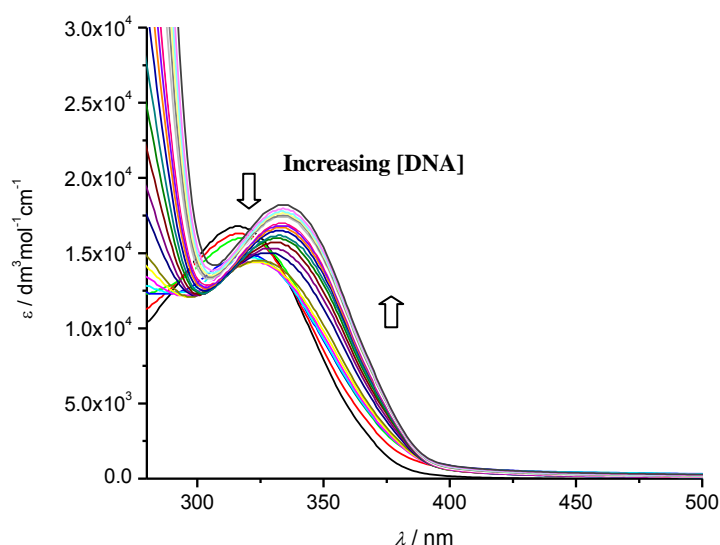
Figure 5.15 UV-visible spectra for 6.85×10^{-2} mM dicationic oligoheteroaromatic **5.2** upon addition of aliquots of a 5.2 mM solution of calf thymus DNA in 25 mM MOPS, 50 mM NaCl and 1 mM EDTA, pH 7.0, at 25 °C.

Figure 5.15 shows that the absorption of the free ligand decreases while the absorption of the complex increases. DNA-binding of **5.2** is accompanied by a bathochromic shift. This bathochromic shift is attributed to an increasing effective conjugation length; upon binding to DNA the freely rotating rings in the ligand become fixed in coplanar orientations.

Titration data for selected wavelengths was extracted from the UV-visible data in Figure 5.15 and from a second titration to generate binding isotherms for **5.2** interacting with DNA (Figure 5.16).
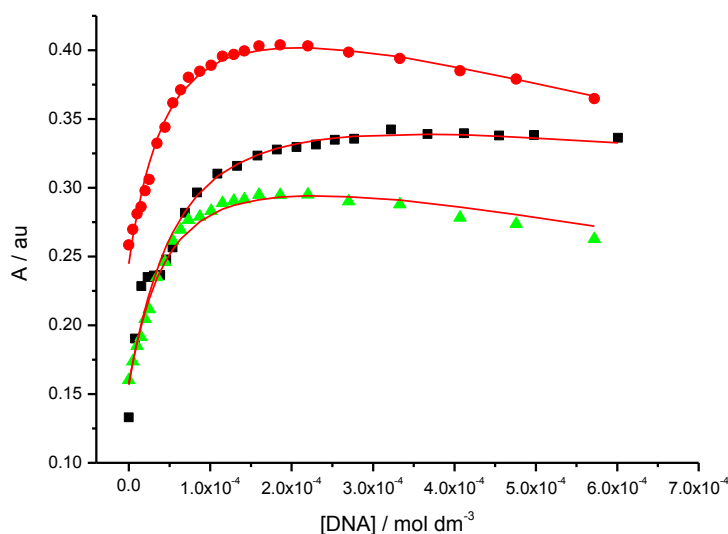
Figure 5.16 Absorbance at (■) 376 nm, (●) 350 nm and (▲) 360 nm plotted against DNA concentration. Solid lines represent a global fit to a multiple independent sites model of **5.2** (6.85×10^{-2} mM and 3.07×10^{-2} mM) in 25 mM MOPS, 50 mM NaCl and 1 mM EDTA, pH 7.0, at 25 °C.

The titration curves in Figure 5.16 were analysed globally using the multiple independent binding site model. The binding constant (*K*) for **5.2** binding to DNA was found to be (1.1 ± 0.6) $\times 10^{4}$ M^{-1} and the stoichiometry (*n*) is 1.4 ± 0.18, i.e. 1.4 base pairs of DNA are needed for the ligand to bind. This binding site is rather short in comparison with the length of **5.2**, suggesting that **5.2** may be binding in a side-by-side manner, or that other complexities are playing a role.

Circular dichroism

In order to study the interaction mode for **5.2** with calf thymus DNA we used circular dichroism spectroscopy. Induced circular dichroism spectra for **5.2** in the presence of varying concentrations of calf thymus DNA in 25 mM MOPS, 50 mM NaCl and 1 mM EDTA, pH 7 at 25 °C were recorded (Figure 5.17).
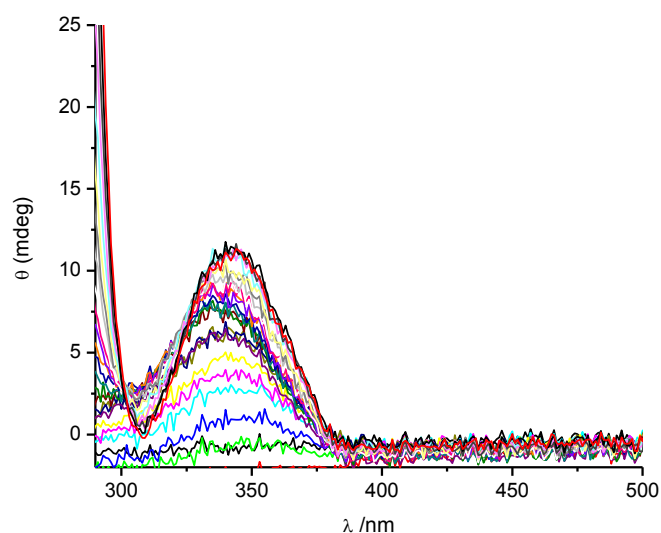
Figure 5.17 Induced circular dichroism spectra for 3.07×10^{-2} mM **5.2** upon addition of aliquots of a 2.6 mM calf thymus DNA solution (in 25 mM MOPS, 50 mM NaCl and 1 mM EDTA, pH 7 at 25 °C).

A positive induced signal around 341 nm is observed and this signal increases upon addition of DNA during the titration. This positive signal suggests that **5.2** is a minor groove binder.[3]

A titration curve (Figure 5.18) was extracted from the ICD titration data.
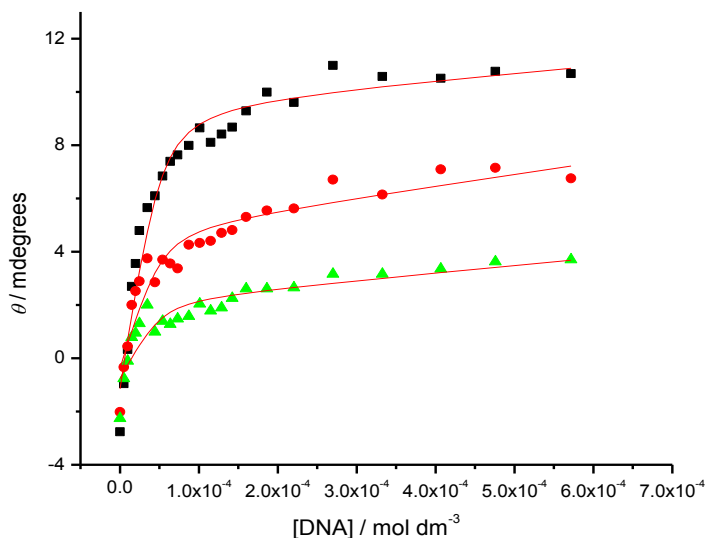
Figure 5.18 Ellipticity at (■) 339 nm, (●) 360 nm and (▲) 370 nm plotted against calf thymus DNA concentration for 3.07×10^{-2} mM **5.2**. The solid lines represent a global fit to a multiple independent sites model , in 25 mM MOPS, 50 mM NaCl and 1 mM EDTA, pH 7.0, at 25 °C.

The titration curve (Figure 5.18) was analysed using the multiple independent binding sites model. The binding constant (*K*) for **5.2** binding to DNA is $(2.8 \pm 0.9)\times10^{5}$ M^{-1} and the stoichiometry (*n*) is 1.7 (restricted). The stoichiometry was restricted because the fit does not give reasonable parameters with variable stoichiometry.

Viscosity

The mode of binding for **5.2** interacting with double-stranded DNA was further studied by viscosimetry to confirm the conclusion from circular dichroism spectroscopy that **5.2** is a groove binder (Figure 5.19).
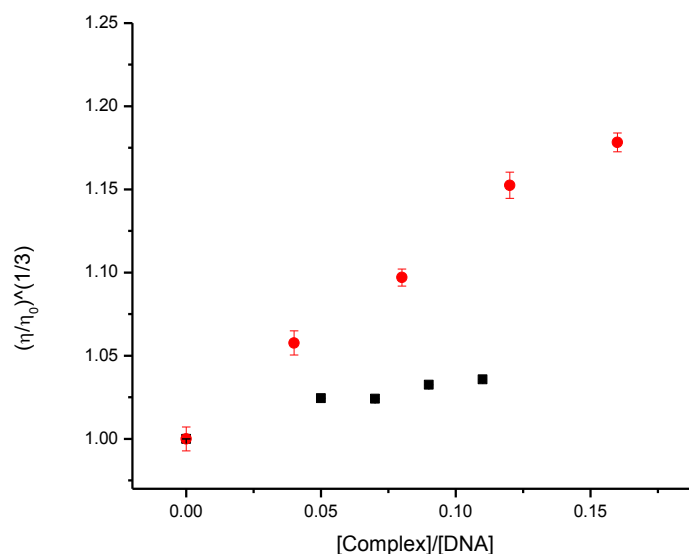
Figure 5.19 Relative viscosities of 0.5 mM CT-DNA solutions upon addition of **5.2** (■) and ethidium bromide (●) at 25 °C in 25 mM MOPS, 50 mM NaCl, 1mM EDTA, pH 7.0.

Figure 5.19 shows a small increase in viscosity upon the first addition of **5.2** followed by no further increase, suggesting a dominant minor groove binding mode, confirming the conclusion from the circular dichroism experiments.

Isothermal titration calorimetry (ITC)

To investigate further the binding of dicationic oligoheteroaromatic **5.2** with DNA, we used isothermal titration calorimetry (ITC). The differential heat flow and derived integrated heat effects for titration of a 3.95 mM solution of **5.2** into a 0.5 mM calf thymus DNA solution were measured in 25 mM MOPS, 50 mM NaCl and 1 mM EDTA, pH 7.0, at 25 °C (Figure 5.20).
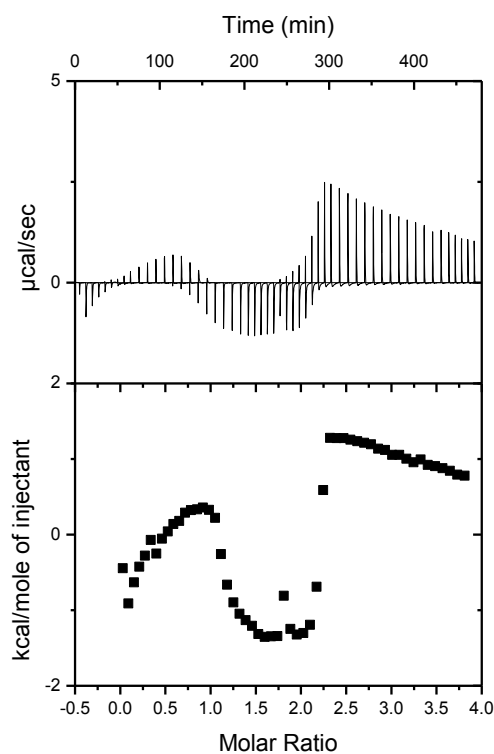
Figure 5.20 Titration of a 3.95 mM solution of **5.2** into a 0.5 mM solution of CT DNA in 25 mM MOPS, 50 mM NaCl and 1 mM EDTA, pH 7, at 25 °C.

The enthalpogram for binding of **5.2** to CT-DNA in Figure 5.19 suggests three different binding events. This result is in agreement with the result for dicationic oligoheteroaromatic **5.1** (vide supra).

Sequence selectivity

The selectivity of **5.2** for selected specific sequences of DNA, viz. poly(dGdC)$_{40}$ and poly(dA)$_{80}$•poly(dT)$_{80}$, was studied using UV-visible and circular dichroism spectroscopy.

UV-visible spectroscopy for dicationic oligoheteroaromatic 5.2 interacting with poly(dGdC)$_{40}$

The binding of oligoheteroaromatic **5.2** to poly(dGdC)$_{40}$ was studied using UV-visible spectroscopy. The titration of **5.2** with poly(dGdC)$_{40}$ was carried out in buffer (25 mM MOPS, 50 mM NaCl and 1 mM EDTA) at 25 °C. Figure 5.21 shows the changes in absorbance of **5.2** with increasing poly(dGdC)$_{40}$ concentration.

Figure 5.21 UV-visible spectra for 3.25×10^{-2} mM dicationic oligoheteroaromatic **5.2** upon addition of 2.85 mM poly(dGdC)$_{40}$ in 25 mM MOPS, 50 mM NaCl and 1 mM EDTA, pH 7.0, at 25 °C.

Figure 5.21 shows that the absorption maximum of the free ligand decreases while the absorption maximum of the complex increases with an isosbestic point at 338 nm suggesting the presence of only two ligand species in solution (free and bound ligand). DNA-binding of **5.2** is accompanied by a bathochromic shift, which is attributed to the

179

ligand adopting a more planar conformation when bound to DNA, increasing the effective conjugation length.

The titration curve in Figure 5.22 was extracted from the UV-visible data to quantify the binding of **5.2** to poly(dGdC)$_{40}$.
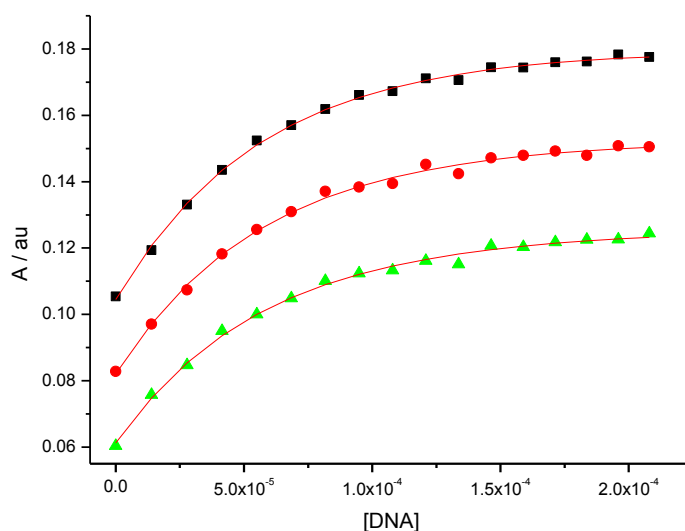
Figure 5.22 Absorbance at (■) 359 nm, (●) 365 nm and (▲) 372 nm plotted against poly(dGdC)$_{40}$ concentration for 3.25×10^{-2} mM **5.2**, solid lines represent a global fit to a multiple independent sites model , in 25 mM MOPS, 50 mM NaCl and 1 mM EDTA, pH 7.0, at 25 °C.

The data in Figure 5.22 were analysed using the same model as used for the data in Figure 5.2. The binding constant (K) for **5.2** binding to poly(dGdC)$_{40}$ is $(2.2 \pm 0.9) \times 10^{4}$ M^{-1} and the binding site size (n) is 1.02 ± 0.3. The interaction between **5.2** and poly(dGdC)$_{40}$ does not appear to be particularly intimate as also found for **5.1**.

Circular dichroism for 5.2 interacting with poly(dGdC)$_{40}$ In order to study the binding mode, circular dichroism spectra were recorded (Figure 5.23).
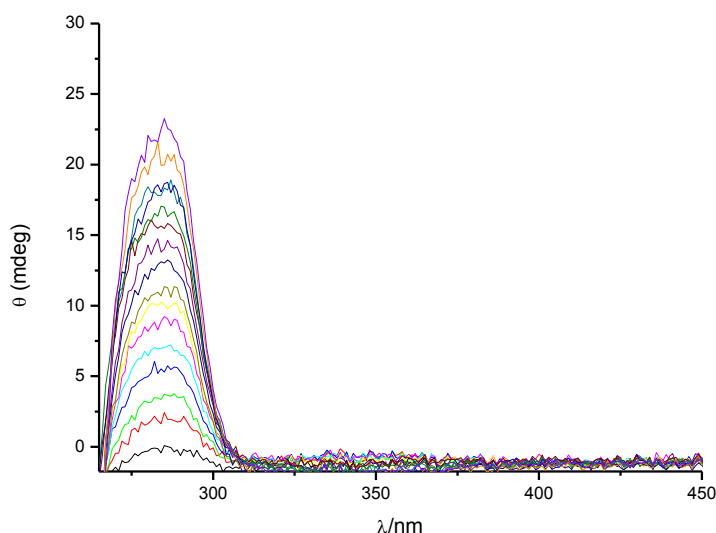
Figure 5.23 Circular dichroism spectra for 3.25×10^{-2} mM **5.2** in the presence of varying concentrations of poly(dGdC)$_{40}$ (added as aliquots of a 2.85 mM solution of poly(dGdC)$_{40}$) in buffer 25 mM MOPS, 50 mM NaCl and 1 mM EDTA, pH 7 at 25 °C.

Figure 5.23 illustrates the circular dichroism spectra for a solution of **5.2** in the presence of varying concentrations of poly(dGdC)$_{40}$, in 25 mM MOPS, 50 mM NaCl and 1 mM EDTA, pH 7 at 25 °C. No ICD spectrum is observed for wavelengths above 300 nm upon addition of poly(dGdC)$_{40}$ up to concentrations of poly(dGdC)$_{40}$ of 2.1×10^{-1} mM. This result suggests that **5.2** does not bind particularly intimately to poly(dGdC)$_{40}$ and most likely not through groove binding or intercalation, as also found for **5.1**.

UV-visible spectroscopy for 5.1 interacting with poly(dA)$_{80}$•poly(dT)$_{80}$

The binding of oligoheteroaromatic **5.2** to poly(dA)$_{80}$•poly(dT)$_{80}$was studied using UV-visible spectroscopy. The titration of **5.2** with poly(dA)$_{80}$•poly(dT)$_{80}$ was carried out in buffer (25 mM MOPS, 50 mM NaCl and 1 mM EDTA) at 25 °C. Figure 5.24 shows the changes in absorbance with increasing poly(dA)$_{80}$•poly(dT)$_{80}$concentration.
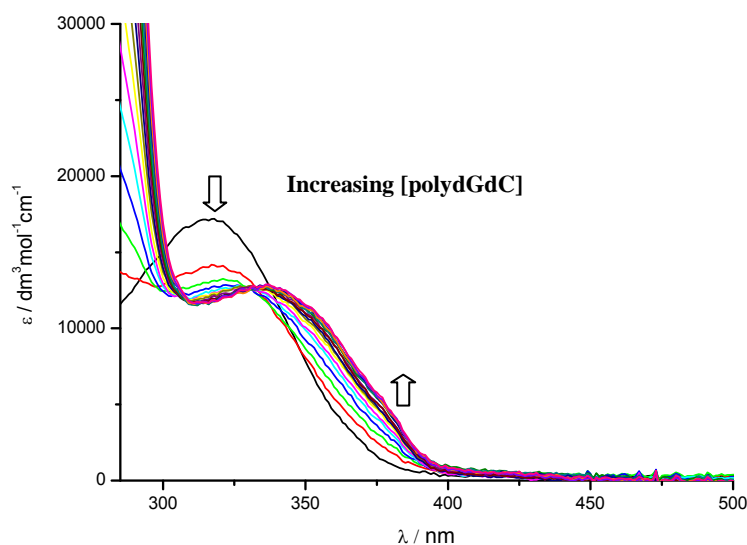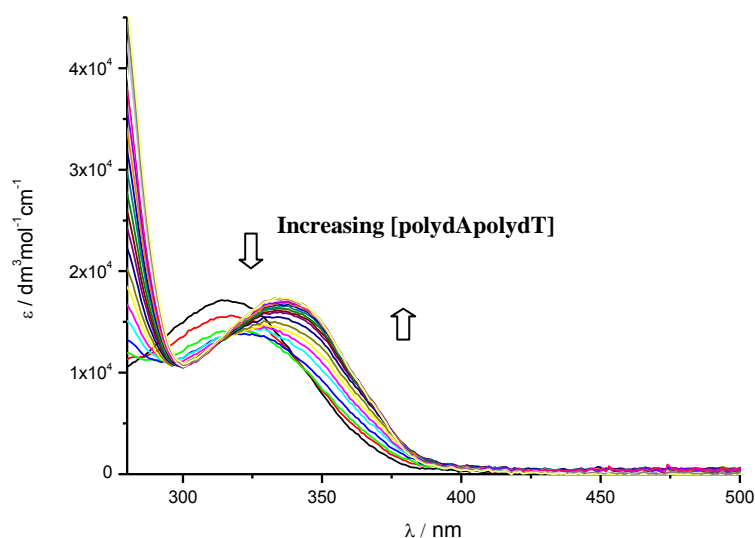

Figure 5.24 UV-visible spectra for 3.15×10^{-2} mM dicationic oligoheteroaromatic **5.2** upon addition of aliquots of a 1.83 mM solution of poly(dA)$_{80}$•poly(dT)$_{80}$in 25 mM MOPS, 50 mM NaCl and 1 mM EDTA, pH 7.0, at 25 °C.

The absorption maximum of the free ligand decreases while the absorption maximum of the complex increases and DNA-binding of **5.2** is accompanied by a bathochromic shift. As before, we attribute this to formation of a complex in which the bound ligand is forced to adopt a more planar conformation, increasing effective conjugation length.

Binding isotherms (Figure 5.25) were extracted from the UV-visible data to quantify the binding of **5.2** to poly(dA)$_{80}$•poly(dT)$_{80}$.
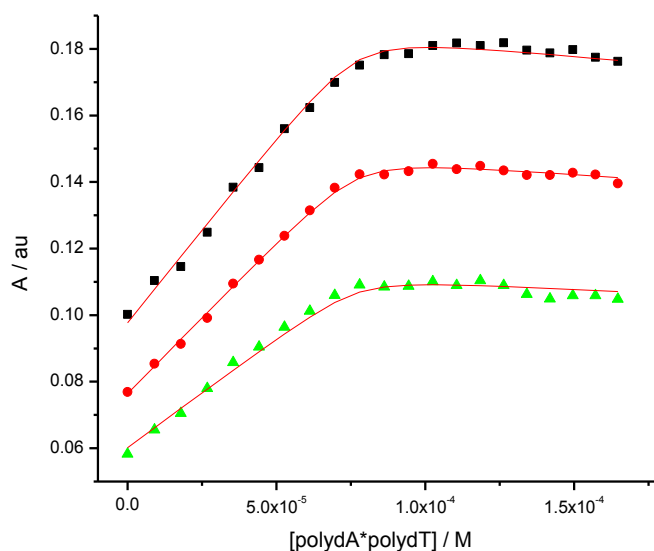
Figure 5.25 Absorbance at (■) 360 nm, (●) 366 nm and (▲) 372 nm plotted against poly(dA)$_{80}$•poly(dT)$_{80}$concentration for 3.15×10^{-2} mM **5.2**, solid lines represent a global fit to a multiple independent sites model , in 25 mM MOPS, 50 mM NaCl and 1 mM EDTA, pH 7.0, at 25 °C.

The binding isotherms in Figure 5.25 were analysed using the same model as was used for the data in Figure 5.2. The binding constant (*K*) for **5.2** binding to poly(dA)$_{80}$•poly(dT)$_{80}$is $(3.5 \pm 1.2) \times10^{6}\,M^{-1}$ and the binding site size (*n*) is 2.6 ± 0.04 basepairs. The affinity of **5.2** for poly(dA)$_{80}$•poly(dT)$_{80}$is high compared with its affinity for poly(dGdC)$_{40}$. This observation is in agreement with the general observation that minor groove binders typically prefer A●T-rich sequences over G●C rich sequences.

Circular dichroism for 5.2 interacting with poly(dA)₈₀•poly(dT)₈₀

In order to study the binding mode, circular dichroism spectra were recorded for **5.2** in the presence of varying concentrations of poly(dA)$_{80}$•poly(dT)$_{80}$ (Figure 5.26).
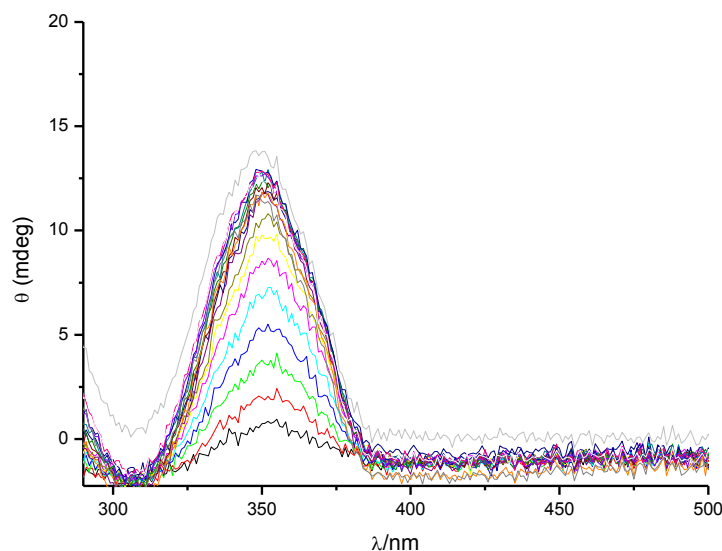
Figure 5.26 Induced circular dichroism spectra for $3.15{\times}10^{-2}$ mM of **5.2** in the presence of varying concentrations of poly(dA)$_{80}$•poly(dT)$_{80}$ in buffer (25 mM MOPS, 50 mM NaCl and 1 mM EDTA, pH 7 at 25 °C).

Figure 5.26 shows positive induced circular dichroism at wavelengths above 300 nm for the interaction of **5.2** with poly(dA)$_{80}$•poly(dT)$_{80}$, in 25 mM MOPS, 50 mM NaCl and 1 mM EDTA, pH 7 at 25 °C. This result suggests a minor groove binding mode for **5.2** binding to poly(dA)$_{80}$•poly(dT)$_{80}$.

A binding isotherm (Figure 5.27) was extracted from the ICD titration data.
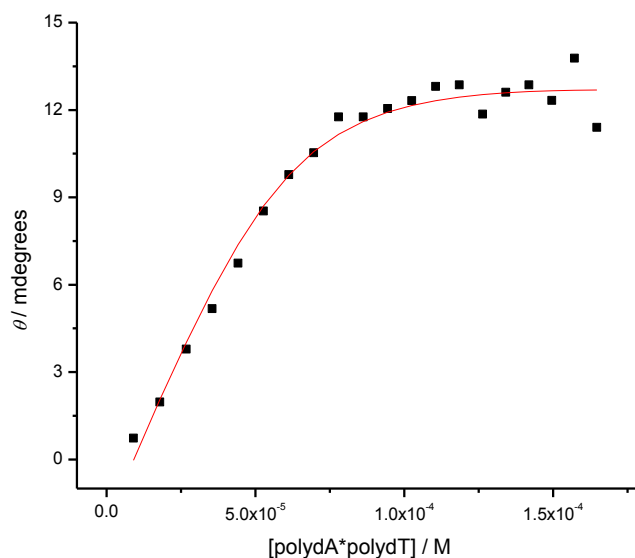
Figure 5.27 Ellipticity at (■) 350 nm plotted against poly(dA)$_{80}$•poly(dT)$_{80}$concentration, solid lines represent a global fit to a multiple independent sites model, for **5.2** (3.15×10^{-2} mM) interacting with poly(dA)$_{80}$•poly(dT)$_{80}$, in 25 mM MOPS, 50 mM NaCl and 1 mM EDTA, pH 7.0, at 25 °C.

The data in the titration curve in Figure 5.27 were analysed using the same multiple independent binding sites model as before. The binding constant (*K*) for **5.2** binding to poly(dA)$_{80}$•poly(dT)$_{80}$is $(2.9 \pm 0.1) \times 10^5$ M^{-1} and the stoichiometry (*n*) of 2 (restricted). The stoichiometry was restricted because the fit does not give reasonable parameters with variable stoichiometry. This result is in good agreement with the UV-visible data. These results again indicate strong binding of **5.2** to poly(dA)$_{80}$•poly(dT)$_{80}$.

Summary

Dicationic oligoheteroaromatic **5.2** binds to calf thymus DNA with a binding constant of $(1.1 \pm 0.6) \times 10^4$ M^{-1} and a binding site size of 1.4 ± 0.18, i.e, 1.4 base pairs. The interaction of dicationic **5.2** with CT-DNA results in a positive ICD signal, suggesting binding of **5.2** in the minor groove. Apart from a small initial increase, no further increase in the viscosity of a DNA solution was observed for increasing amounts of dicationic

oligoheteroaromatic **5.2** interacting with CT-DNA, suggesting a minor groove binding. ITC suggests a complex combination of three binding events for **5.2** interacting with calf thymus DNA. Dicationic oligoheteroaromatic **5.2** weakly bound to poly(dGdC)$_{40}$ without specific binding mode. On the other hand, **5.2** strongly bound to poly(dA)$_{80}$•poly(dT)$_{80}$following the minor groove binding mode.

The driving forces for binding of **5.2** to DNA are assumed as described for **5.1**.

5.3.3 Dicationic oligoheteroaromatic 5.3 binding to DNA

The binding of dicationic oligoheteroaromatic **5.3** to calf thymus DNA was studied using UV-visible spectroscopy; the changes in absorption of **5.3** upon addition of calf thymus DNA were measured in buffer (25 mM MOPS, 50 mM NaCl and 1 mM EDTA) at 25 °C (Figure 5.28).
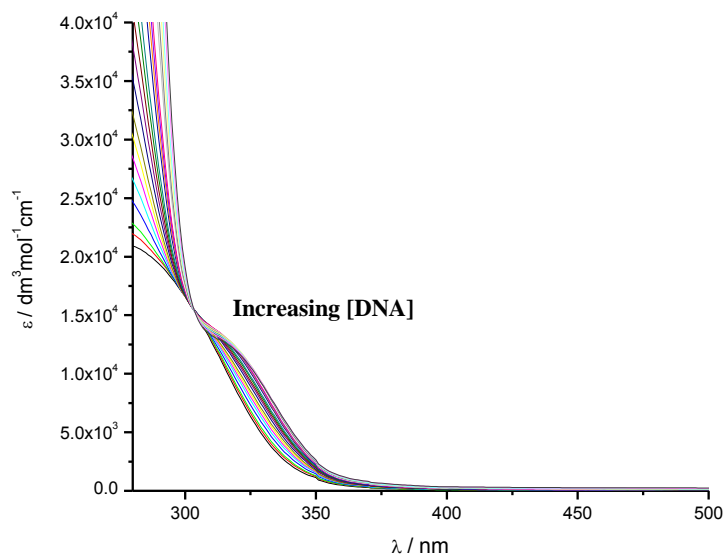
Figure 5.28 UV-visible spectra for 3.44×10^{-2} mM dicationic oligoheteroaromatic **5.3** upon addition of aliquots of a 5.2 mM solution of calf thymus DNA in 25 mM MOPS, 50 mM NaCl and 1 mM EDTA, pH 7.0, at 25 °C

Figure 5.28 shows that the absorption corresponding to the free ligand decreases while the absorption attributed to the complex increases. DNA-binding of **5.3** is accompanied by a bathochromic shift. This bathochromic shift is attributed to an increasing effective conjugation length; upon binding to DNA the freely rotating rings in the ligand become fixed in more planar relative orientations.

Titration data for selected wavelengths was extracted from the UV-visible data in Figure 5.28, and from a second titration, to generate binding isotherms for **5.3** interacting with DNA (Figure 5.29).
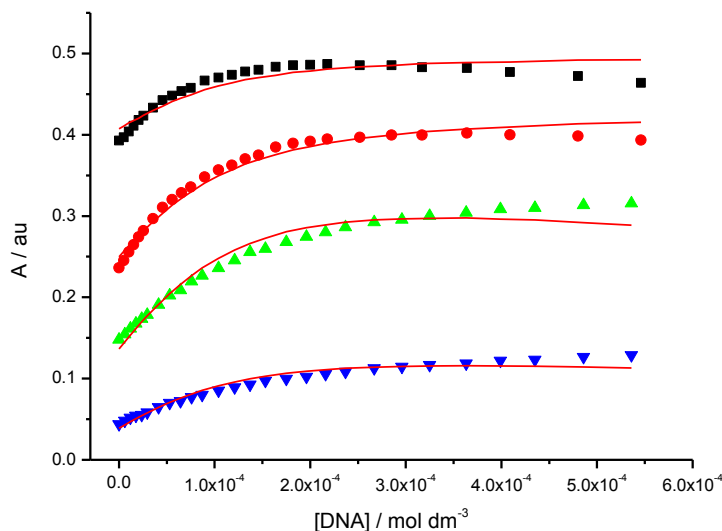
Figure 5.29 Absorbance at (■) 315 nm, (●) 325 nm, (▲) 330 nm and (▼) 345 nm plotted against DNA concentration for 3.80×10^{-2} mM and 3.44×10^{-2} mM **5.3** in 25 mM MOPS, 50 mM NaCl and 1 mM EDTA, pH 7.0, at 25 °C. Solid lines represent a global fit to a multiple independent sites model.

The data in the titration curve of Figure 5.29 was analysed globally using the multiple independent binding sites model. The binding constant (*K*) for **5.3** binding to DNA is $(5.1 \pm 2.9) \times 10^{4}$ M^{-1} and the stoichiometry (*n*) is 2.7 ± 0.7, i.e. 2.7 base pairs of DNA are needed for the ligand to bind. Again, this binding site is rather short in comparison with the length of **5.3**, suggesting that **5.3** may be binding in a side-by-side manner, or that other complexities are playing a role.

Circular dichroism

In order to study the interaction mode for **5.3** binding to calf thymus DNA we used circular dichroism spectroscopy. Induced circular dichroism spectra for **5.3** in the presence of varying concentrations of calf thymus DNA in 25 mM MOPS, 50 mM NaCl and 1 mM EDTA, pH 7 at 25 °C were recorded (Figure 5.30).
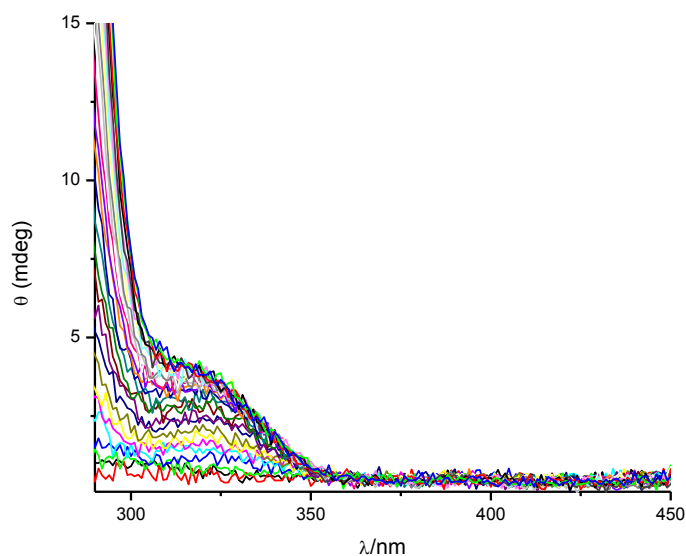
Figure 5.30 Induced circular dichroism spectra for 3.80×10^{-2} mM **5.3** upon addition of aliquots of a 3 mM calf thymus DNA solution (in 25 mM MOPS, 50 mM NaCl and 1 mM EDTA, pH 7 at 25 °C).

A positive induced signal around 322 nm is observed and this signal increases upon addition of DNA during the titration. This positive signal suggests that **5.3** is a minor groove binder.[3]

A titration curve (Figure 5.31) was extracted from the ICD titration data.
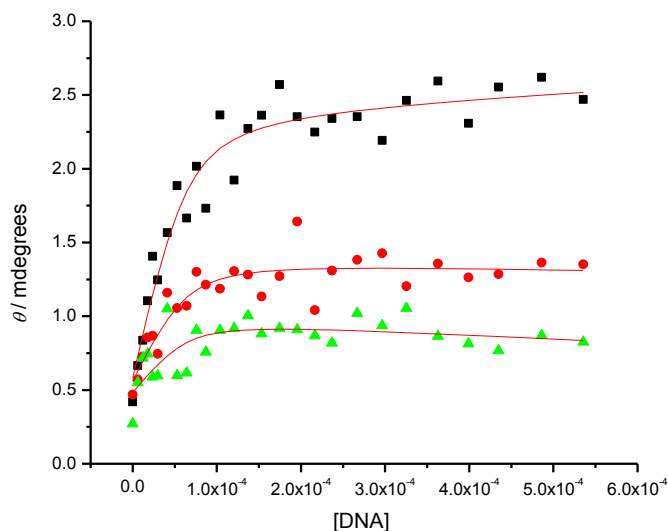
Figure 5.31 Ellipticity at (■) 335 nm, (●) 345 nm and (▲) 350 nm plotted against calf thymus DNA concentration for **5.3** (3.80×10^{-2} mM), in 25 mM MOPS, 50 mM NaCl and 1 mM EDTA, pH 7.0, at 25 °C. The solid lines represent a global fit to a multiple independent sites model.

The data in the titration curve of Figure 5.31 was analysed using the multiple independent binding sites model. The binding constant (K) for **5.3** binding to DNA is $(2.8 \pm 0.9) \times 10^5$ M^{-1} and the stoichiometry (n) is 1.7 (restricted). The stoichiometry was restricted because the fit does not give reasonable parameters with variable stoichiometry.

Viscosity

The mode of the binding for **5.3** with double-stranded DNA was further studied by viscosimetry to confirm the conclusion from circular dichroism spectroscopy that **5.3** is a groove binder.
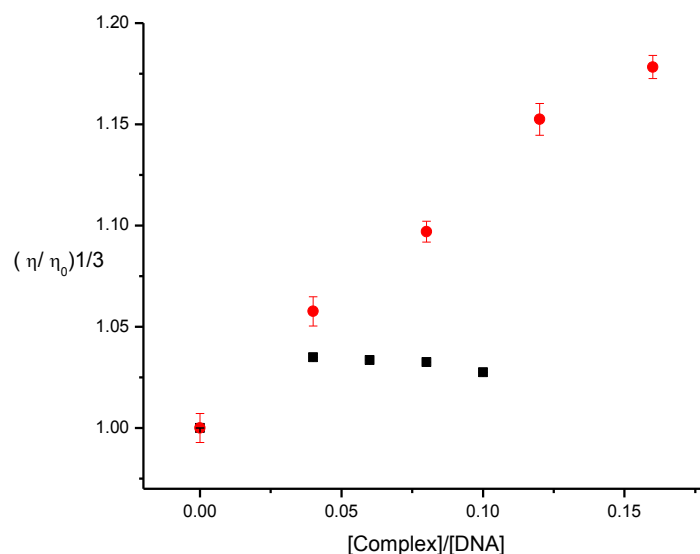
Figure 5.32 Relative viscosities of 0.5 mM CT-DNA solutions upon addition of **5.3** (■) and ethidium bromide (■) at 25 °C in 25 mM MOPS, 50 mM NaCl, 1mM EDTA, pH 7.0.

Figure 5.32 shows a small increase in viscosity upon the first addition of **5.3** followed by no further increase, suggesting a dominant minor groove binding mode, confirming the conclusion of a minor groove binding mode for **5.3** based on the circular dichroism data.

Isothermal titration calorimetry (ITC)

To investigate further the binding of dicationic oligoheteroaromatic **5.3** with DNA, we used isothermal titration calorimetry (ITC). The differential heat flow and derived integrated heat effects for titration of a 4.11 mM solution of **5.3** into a 0.5 mM calf thymus DNA solution were measured in 25 mM MOPS, 50 mM NaCl and 1 mM EDTA, pH 7.0, at 25 °C (Figure 5.33).
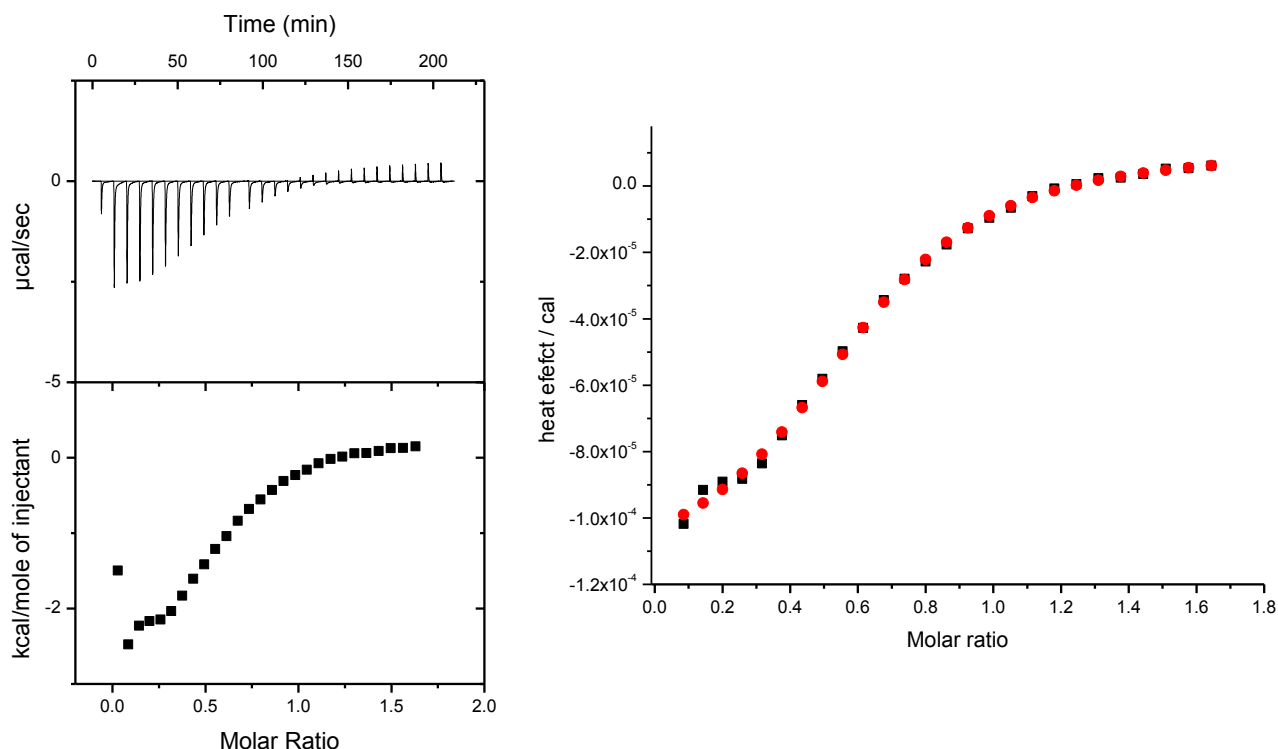
Figure 5.33 Titration of a 4.11 mM solution of **5.3** into a 0.5 mM solution of CT-DNA in 25 mM MOPS, 50 mM NaCl and 1 mM EDTA, pH 7, at 25 °C (left). Integrated heat effects for the same titration analysed in terms of one binding site size model with ligand aggregation not included (right).

The titration of **5.3** into CT-DNA suggests one single binding event. The data were analysed in terms of a one binding mode model without taking into account self aggregation of **5.3**. The reason for not taking self aggregation into account is using a low concentration of **5.3** in the titration (4.11 mM). The fit to the one-binding site model indicates that this binding model reproduces the data very well. The thermodynamics parameter for the interaction of dicationic heteroaromatic **5.3** with CT-DNA in 25 mM MOPS, 50 mM NaCl and 1 mM EDTA, pH 7, at 25 °C are summarised in Table 5.1.

Table 5.1 Thermodynamic parameters for binding of **5.3** to CT-DNA in MOPS buffer, pH 7.0, at 25 °C

		aggregation not included			
$[L]_{syringe}$ (mM)	$[DNA]_{cell}$ (mM)	K_A (10^4 M^{-1})	ΔH_{A1} (10^3 cal mol^{-1})	$-T \times \Delta S_{A1}$ (10^3 kcal mol^{-1})	$1/n_{A1}$
4.11	0.50	2.17	-3.18	-2.73	1.6

The negative values for enthalpy and entropy suggest that **5.3** binds to CT-DNA in the minor groove. The binding site size is 1.6 base pairs.

Sequence selectivity

The selectivity of **5.3** for selected specific sequences of DNA, viz. poly(dGdC)$_{40}$ and poly(dA)$_{80}$•poly(dT)$_{80}$, was studied using UV-visible and circular dichroism spectroscopy.

UV-visible spectroscopy for 5.3 interacting with poly(dGdC)$_{40}$

The binding of oligoheteroaromatic **5.3** to poly(dGdC)$_{40}$ was studied using UV-visible spectroscopy. The titration of **5.3** with poly(dGdC)$_{40}$ was carried out in buffer (25 mM MOPS, 50 mM NaCl and 1 mM EDTA) at 25 °C.
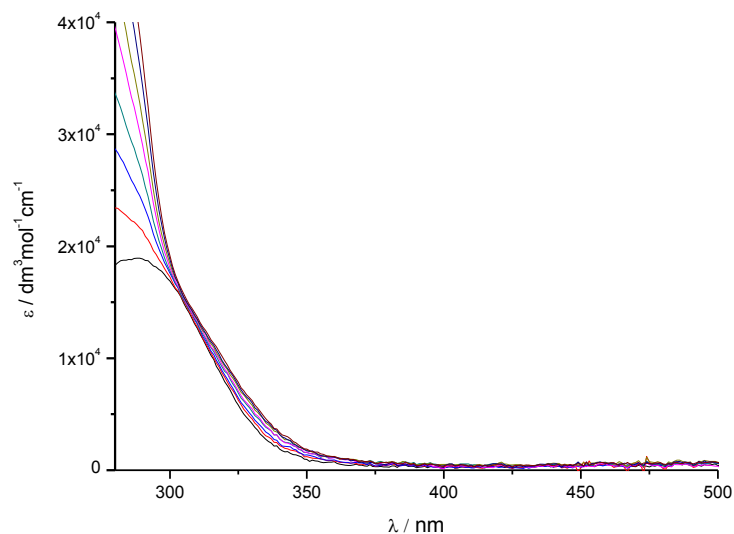
Figure 5.34 UV-visible spectra for 2.92×10^{-2} mM dicationic oligoheteroaromatic **5.3** upon addition of aliquots of a 2.85 mM solution of poly(dGdC)$_{40}$ in 25 mM MOPS, 50 mM NaCl and 1 mM EDTA, pH 7.0, at 25 °C.

Figure 5.34 shows that the absorbance of poly(dGdC)$_{40}$ overlaps the spectrum for **5.3** with only minimal changes elsewhere in the spectrum. As a result, the data cannot be analysed to quantify the binding constant (*K*) and the binding site size (*n*).

Circular dichroism for 5.3 interacting with poly(dGdC)$_{40}$

In an attempt to gather information on the binding affinity of 5.3 for poly(dGdC)$_{40}$ through another means and in order to study the binding mode, circular dichroism spectra were recorded (Figure 5.35).
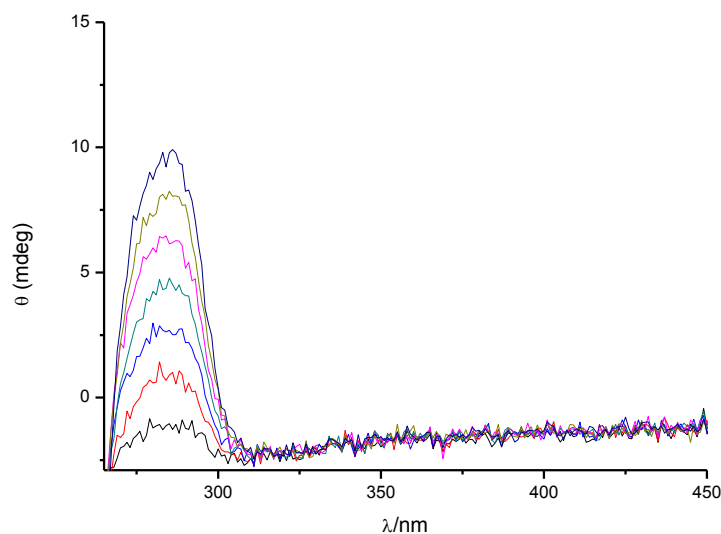
Figure 5.35 Circular dichroism spectra for 2.92×10^{-2} mM **5.3** in the presence of varying concentrations of poly(dGdC)$_{40}$ (added as aliquots of a 2.85 mM solution of poly(dGdC)$_{40}$) in buffer 25 mM MOPS, 50 mM NaCl and 1 mM EDTA, pH 7 at 25 °C.

Figure 5.35 shows the circular dichroism spectra for a solution of **5.3** in the presence of varying concentrations of poly(dGdC)$_{40}$, in 25 mM MOPS, 50 mM NaCl and 1 mM EDTA, pH 7 at 25 °C. No ICD spectrum is observed for wavelengths above 300 nm upon addition of poly(dGdC)$_{40}$ up to concentrations of poly(dGdC)$_{40}$ of 9.5×10^{-2} mM. This result suggests that **5.3** does not bind particularly intimately to poly(dGdC)$_{40}$ and most likely not through groove binding or intercalation.

UV-visible spectroscopy for 5.3 interacting with poly(dA)$_{80}$•poly(dT)$_{80}$

The binding of oligoheteroaromatic **5.3** to poly(dA)$_{80}$•poly(dT)$_{80}$ was studied using UV-visible spectroscopy. The titration of **5.3** with poly(dA)$_{80}$•poly(dT)$_{80}$ was carried out in buffer (25 mM MOPS, 50 mM NaCl and 1 mM EDTA) at 25 °C. Figure 5.36 shows the changes in absorbance with increasing poly(dA)$_{80}$•poly(dT)$_{80}$ concentration.
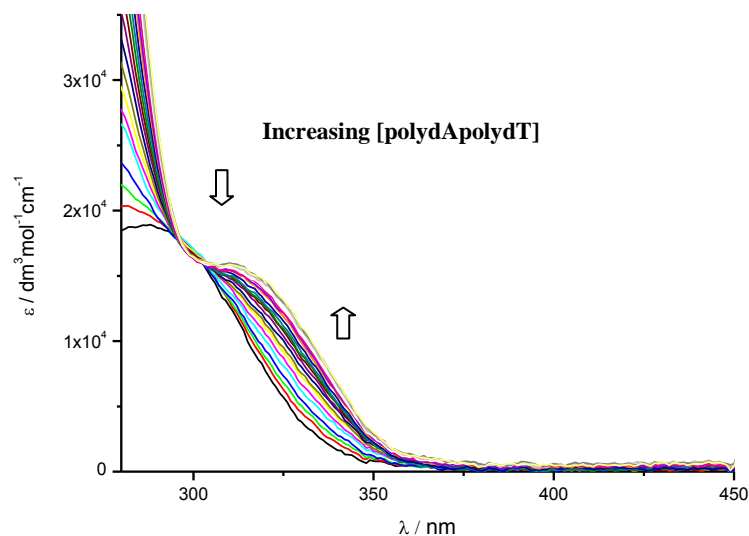
Figure 5.36 UV-visible spectra for 2.73×10^{-2} mM dicationic oligoheteroaromatic **5.3** upon addition of aliquots of a 1.83 mM solution of poly(dA)$_{80} \bullet$poly(dT)$_{80}$in 25 mM MOPS, 50 mM NaCl and 1 mM EDTA, pH 7.0, at 25 °C.

The absorption maximum of the free ligand decreases while the absorption maximum of the complex increases and DNA-binding of **5.3** is accompanied by a bathochromic shift. As before, we attribute the bathochromic shift to formation of a complex in which the bound ligand is forced to adopt a more planar conformation, increasing effective conjugation length. A binding isotherm (Figure 5.37) was extracted from the UV-visible data to quantify the binding of **5.3** to poly(dA)$_{80} \bullet$poly(dT)$_{80}$.
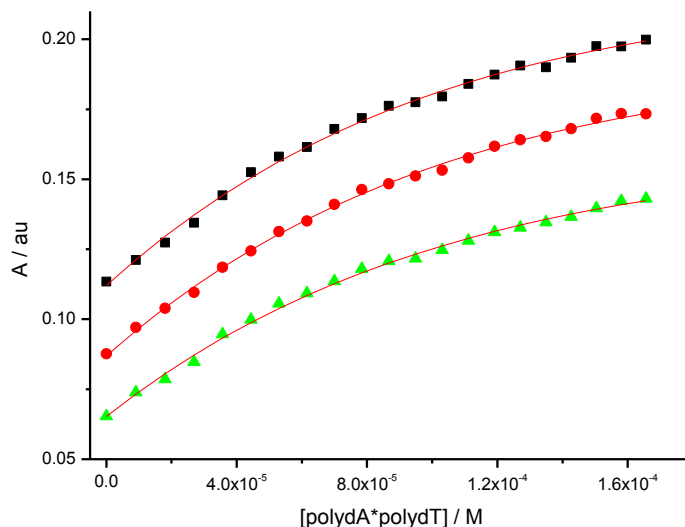
Figure 5.37   Absorbance at (■) 325 nm, (●) 330 nm and (▲) 335 nm plotted against poly(dA)$_{80}$●poly(dT)$_{80}$concentration for **5.3** (2.73×10^{-2}mM) in 25 mM MOPS, 50 mM NaCl and 1 mM EDTA, pH 7.0, at 25 °C. Solid lines represent a global fit to a multiple independent sites model.

The binding isotherm in Figure 5.37 was analysed using the same model as was used for the data in Figure 5.2. The binding constant (*K*) for **5.3** binding to poly(dA)$_{80}$●poly(dT)$_{80}$is (1.6 ± 0.001) ×10^{6} M^{-1} and the binding site size (*n*) is 2 (restricted) . The stoichiometry was restricted because the fit does not give reasonable parameters with variable stoichiometry.

The affinity of the binding for **5.3** for poly(dA)$_{80}$●poly(dT)$_{80}$is high compared with the affinity for poly(dGdC)$_{40}$. This is in agreement with the general observation that minor groove binders typically prefer A●T-rich sequences over G●C rich sequences.

Circular dichroism for 5.3 interacting with poly(dA)$_{80}$•poly(dT)$_{80}$

In order to study the binding mode for 5.3 binding to poly(dA)$_{80}$•poly(dT)$_{80}$, circular dichroism spectra were recorded for **5.3** in the presence of varying concentrations of poly(dA)$_{80}$•poly(dT)$_{80}$ (Figure 5.38).
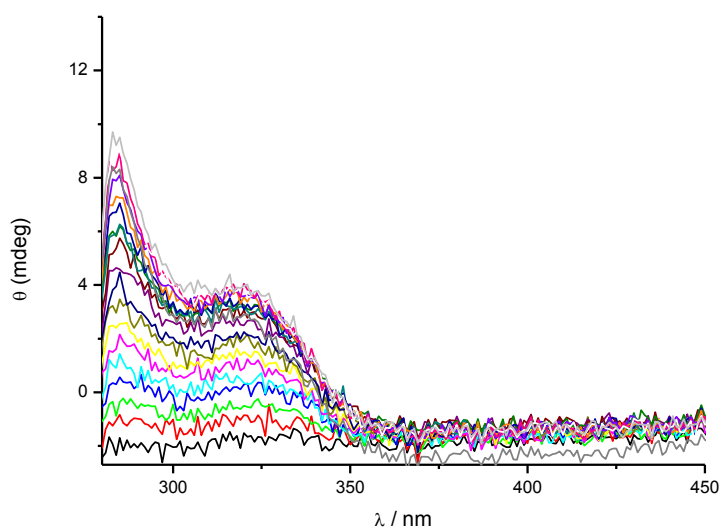
Figure 5.38 Induced circular dichroism spectra for 2.73×10^{-2} mM of **5.3** in the presence of poly(dA)$_{80}$•poly(dT)$_{80}$ (added as aliquots of a 1.83 mM solution) in buffer (25 mM MOPS, 50 mM NaCl and 1 mM EDTA, pH 7 at 25 °C).

Figure 5.38 shows positive induced circular dichroism at wavelengths above 300 nm for the interaction of **5.3** with poly(dA)$_{80}$•poly(dT)$_{80}$, in 25 mM MOPS, 50 mM NaCl and 1 mM EDTA, pH 7 at 25 °C. This result suggests a minor groove binding mode for **5.3** binding to poly(dA)$_{80}$•poly(dT)$_{80}$.

A binding isotherm (Figure 5.39) was extracted from the ICD titration data.
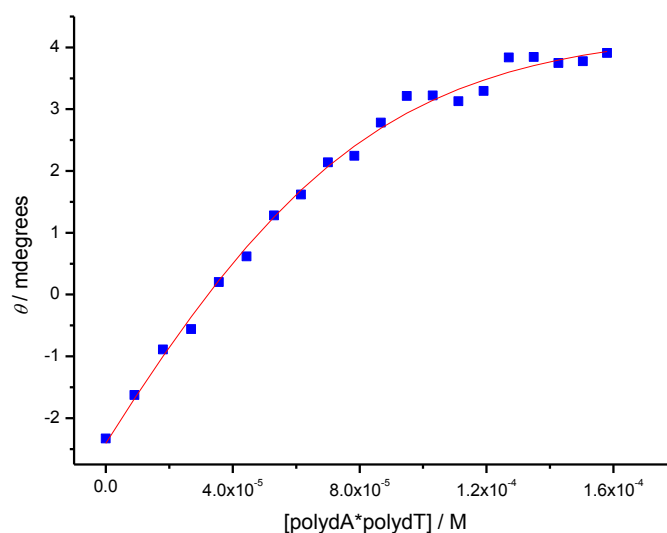
Figure 5.39 Ellipticity at (■) 350 nm nm plotted against polydA●polydT concentration, for the solution of **5.3** (2.73×10^{-2} mM) interacting with poly(dA)$_{80}$●poly(dT)$_{80}$, in 25 mM MOPS, 50 mM NaCl and 1 mM EDTA, pH 7.0, at 25 °C. Solid lines represent a global fit to a multiple independent sites model.

The data in the titration curve of Figure 5.39 were analysed using the same multiple independent binding sites model as used before. The binding constant (K) for **5.3** binding to poly(dA)$_{80}$●poly(dT)$_{80}$is (1.3 ± 0.3) $\times 10^5$ M^{-1} for a stoichiometry (n) of 3 (restricted). We restricted the stoichiometry, because the fit does not give reasonable parameters with variable stoichiometry. This result is in agreement with the UV-visible data. These results again indicate high affinity of **5.3** for poly(dA)$_{80}$●poly(dT)$_{80}$.

Summary

Dicationic oligoheteroaromatic **5.3** binds to DNA binds with a binding constant of $(5.1 \pm 2.9) \times 10^4 \, M^{-1}$ and a binding site size of 2.7 ± 0.7 base pairs. The interaction of dicationic **5.3** with CT-DNA results in a positive ICD signal. The binding site size and the induced circular dichroism together suggest "side-by-side" binding of **5.3** in the minor groove. Following an increase in the viscosity upon addition of the first aliquot of **5.3**, no further increase in the viscosity of a DNA solution was observed for dicationic oligoheteroaromatic **5.3** interacting with CT-DNA, suggesting minor groove binding. The binding mode is supported by ITC, which shows only one binding event for **5.3** interacting with DNA with thermodynamic parameters in line with groove binding. Dicationic oligoheteroaromatic **5.3** weakly bound to poly(dGdC)$_{40}$ without specific binding mode. In contrast, **5.3** strongly bound to poly(dA)$_{80}$•poly(dT)$_{80}$, with a minor groove binding mode. The driving forces for binding of **5.3** to DNA are again assumed to be as described for **5.1**.

5.3.4 Dicationic oligoheteroaromatic 5.4 binding to DNA

The binding of dicationic oligoheteroaromatic **5.4** to calf thymus DNA was studied using UV-visible spectroscopy; the changes in absorption of **5.4** upon addition of calf thymus DNA were measured in buffer (25 mM MOPS, 50 mM NaCl and 1 mM EDTA) at 25 °C (Figure 5.40).
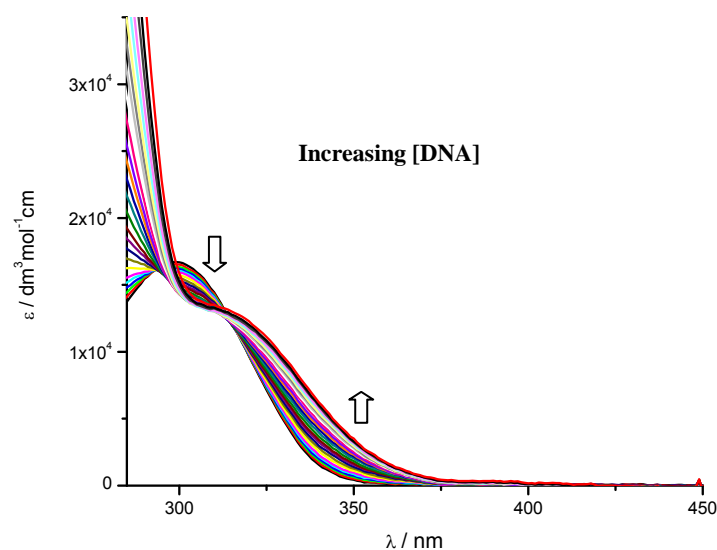
Figure 5.40 UV-visible spectra for 3.03×10^{-2} mM dicationic oligoheteroaromatic **5.4** upon addition of aliquots of a 5.2 mM calf thymus DNA solution in 25 mM MOPS, 50 mM NaCl and 1 mM EDTA, pH 7.0, at 25 °C

Figure 5.40 shows that the absorption of the free ligand decreases while a new absorption band attributed to the complex increases. DNA-binding of **5.4** is accompanied by a bathochromic shift. This bathochromic shift is attributed to an increasing effective conjugation length; upon binding to DNA the freely rotating rings in the ligand become fixed in more planar relative orientations. Titration data for selected wavelengths was extracted from the UV-visible data in Figure 5.40, and from a second titration, to generate binding isotherms for **5.4** interacting with calf thymus DNA (Figure 5.40).
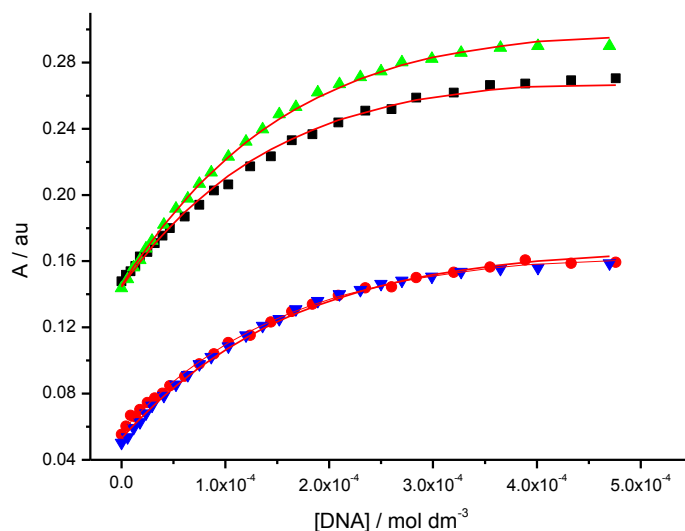
Figure 5.41 Absorbance at (■) 333 nm, (●) 346 nm, (▲) 335 nm and (▼) 348 nm plotted against calf thymus DNA concentration for **5.4** (3.53×10^{-2} mM and 2.85×10^{-2} mM), in 25 mM MOPS, 50 mM NaCl and 1 mM EDTA, pH 7.0, at 25 °C. Solid lines represent a global fit to a multiple independent binding sites model.

The data in Figure 5.41 was analysed globally using the multiple independent binding sites model. The binding constant (K) for **5.4** binding to DNA is $(1.39 \pm 0.05) \times 10^4$ M^{-1} and the stoichiometry (n) is 2.5 (restricted). Again, this binding site is rather short in comparison with the length of **5.4**, suggesting that **5.4** may be binding in a side-by-side manner, or that other complexities are playing a role.

Circular dichroism

In order to study the interaction mode of **5.4** with calf thymus DNA we used circular dichroism spectroscopy. Induced circular dichroism spectra for **5.4** in the presence of varying concentrations of calf thymus DNA in 25 mM MOPS, 50 mM NaCl and 1 mM EDTA, pH 7 at 25 °C were recorded (Figure 5.42).
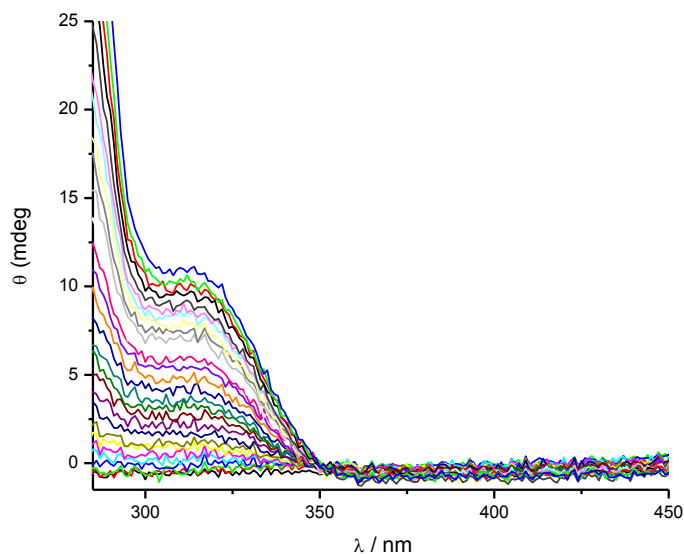
Figure 5.42 Induced circular dichroism spectra for 3.53×10^{-2} mM **5.4** upon addition of aliquots of a 3 mM calf thymus DNA solution (in 25 mM MOPS, 50 mM NaCl and 1 mM EDTA, pH 7 at 25 °C).

A positive induced signal around 314 nm is observed and this signal increases upon addition of DNA during the titration. This positive signal suggests that **5.4** is a minor groove binder as before.[3]

A titration curve (Figure 5.43) was extracted from the ICD titration data.
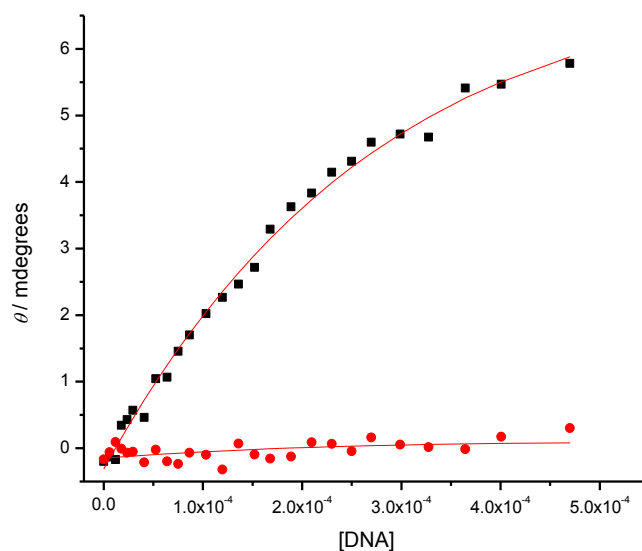
Figure 5.43 Ellipticity at (■) 332 nm, (●) 349 nm is plotted against calf thymus DNA concentration. for **5.4** (3.53×10^{-2} mM), in 25 mM MOPS, 50 mM NaCl and 1 mM EDTA, pH 7.0, at 25 °C. The solid lines represent a global fit to a multiple independent binding sites model.

The titration curve in Figure 5.43 was analysed using the multiple independent binding site model. The binding constant (*K*) for **5.4** binding to DNA is $(6.9 \pm 0.1) \times 10^3$ M^{-1} and the stoichiometry (*n*) is 3 (restricted). The stoichiometry was restricted because the fit does not give reasonable parameters with variable stoichiometry.

Viscosity

The mode of binding for **5.4** interacting with double-stranded DNA was further studied by viscosimetry to confirm the conclusion from circular dichroism spectroscopy that **5.4** is a groove binder.
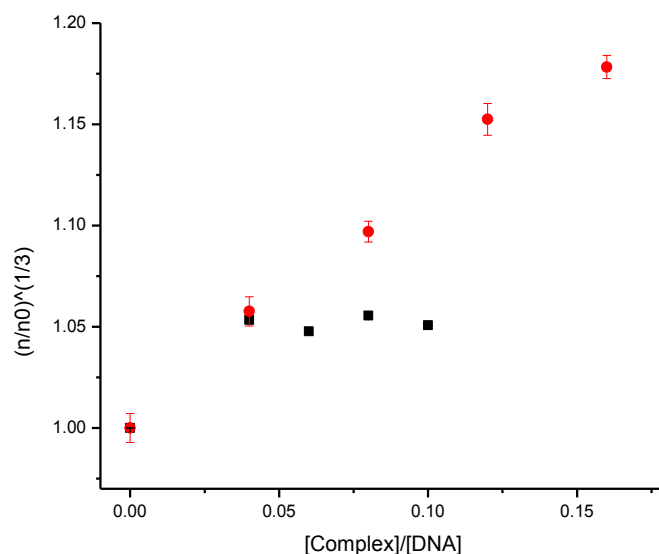
Figure 5.44 Relative viscosities of 0.5 mM CT-DNA solutions upon addition of **5.4** (■) and ethidium bromide (■) at 25 °C in 25 mM MOPS, 50 mM NaCl, 1mM EDTA, pH 7.0.

Figure 5.44 shows the usual small increase in viscosity upon the first addition of **5.4** but no further increase, suggesting a dominant minor groove binding mode, confirming the minor groove binding mode for **5.4**.

Isothermal titration calorimetry (ITC)

To investigate further the binding of dicationic oligoheteroaromatic **5.4** with DNA, we used isothermal titration calorimetry (ITC). The differential heat flow and derived integrated heat effects for titration of a 5.44 mM solution of **5.4** into a 0.45 mM calf thymus DNA solution were measured in 25 mM MOPS, 50 mM NaCl and 1 mM EDTA, pH 7.0, at 25 °C (Figure 5.45).
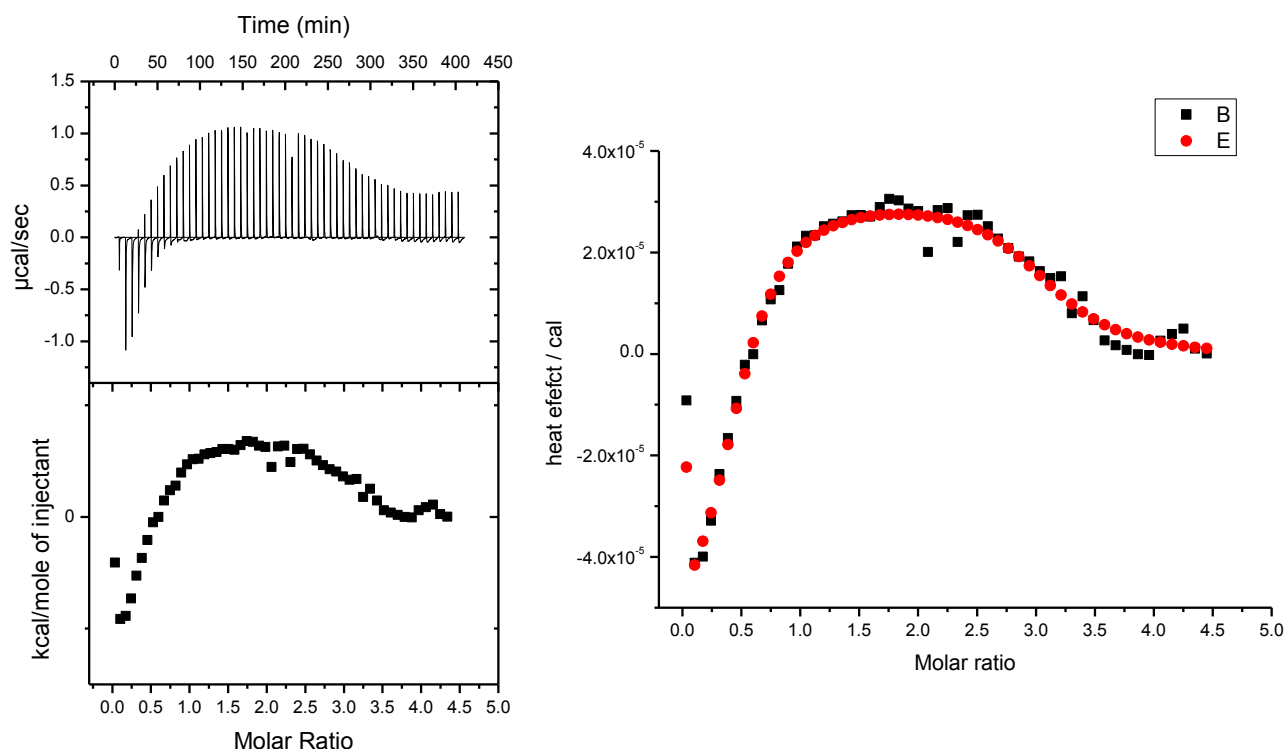
Figure 5.45 Titration of a 5.44 mM solution of **5.4** into a 0.45 mM solution of CT-DNA in 25 mM MOPS, 50 mM NaCl and 1 mM EDTA, pH 7, at 25 °C (left). Integrated heat effects for the same titration analysed in terms of a binding model involving two types of binding sites with aggregation not included.

The titration of **5.4** with CT-DNA clearly indicates two binding events. The data was analysed in terms of a model involving two types of binding sites without taking into account the self aggregation of **5.4**. As we mentioned before, the reason for ignoring self aggregation is that we use a low concentration of **5.4** in the titration (5.44 mM) andat this concentration **5.4** does not show strong self aggregation. The fit to the two independent binding sites model indicates that this binding model reproduces the data quite well. The thermodynamic parameters for the interaction of dicationic heteroaromatic **5.4** with CT-DNA in 25 mM MOPS, 50 mM NaCl and 1 mM EDTA, pH 7, at 25 °C are summarised in Table 5.2.

Table 5.2 Thermodynamic parameters for binding of **5.4** to CT-DNA in MOPS buffer, pH 7.0, at 25 °C

		aggregation not included			
$[L]_{syringe}$ (mM)	$[DNA]_{cell}$ (mM)	K_A (10^6 M^{-1})	ΔH_{A1} (10^3 cal mol^{-1})	$-T \times \Delta S_{A1}$ (10^3 kcal mol^{-1})	$1/n_{A1}$
4.5	0.45	1.34	-1.41	-6.95	2.16
$[L]_{syringe}$ (mM)	$[DNA]_{cell}$ (mM)	K_B (10^5 M^{-1})	ΔH_{B1} (10^3 cal mol^{-1})	$-T \times \Delta S_{B1}$ (10^3 kcal mol^{-1})	$1/n_{B1}$
4.5	0.45	5.69	7.32	-13.80	0.40

Table 5.2 shows that dicationic oligoheteroaromatic **5.4** binds to CT-DNA with an affinity of $\sim10^6$ M^{-1}. The binding site size is 2.16 in reasonable agreement with the binding site size obtained from the UV-visible titrations. The first binding event is characterised by negative enthalpy and entropy change. The negative values for enthalpy and entropy suggest that **5.4** binds to CT-DNA in the minor groove.

Affinity for *poly(dA)$_{80}$•poly(dT)$_{80}$*

The affinity of **5.4** for poly(dA)$_{80}$•poly(dT)$_{80}$, was studied using UV-visible and circular dichroism spectroscopy.

UV-visible spectroscopy for 5.4 interacting with poly(dA)$_{80}$•poly(dT)$_{80}$

The binding of oligoheteroaromatic **5.4** to poly(dA)$_{80}$•poly(dT)$_{80}$ was studied using UV-visible spectroscopy. The titration of **5.4** with poly(dA)$_{80}$•poly(dT)$_{80}$ was carried out in buffer (25 mM MOPS, 50 mM NaCl and 1 mM EDTA) at 25 °C. Figure 5.46 shows the changes in absorbance with increasing poly(dA)$_{80}$•poly(dT)$_{80}$ concentration.
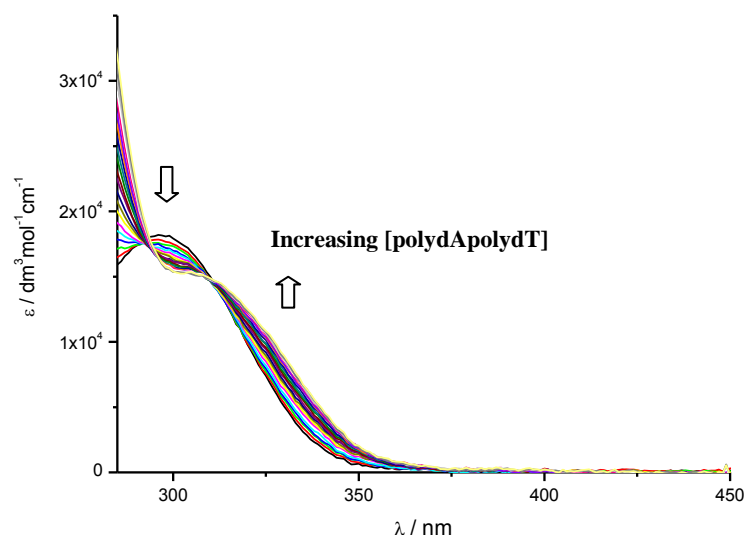
Figure 5.46 UV-visible spectra for 3.65×10^{-2} mM dicationic oligoheteroaromatic **5.4** upon addition of aliquots of a 1.83 mM solution of poly(dA)$_{80}\bullet$poly(dT)$_{80}$ in 25 mM MOPS, 50 mM NaCl and 1 mM EDTA, pH 7.0, at 25 °C.

The absorption peak for the free ligand decreases while new higher wavelength absorption attributed to the complex increases. As before, we attribute the bathochromic shift to formation of a complex in which the bound ligand is forced to adopt a more planar conformation, increasing effective conjugation length. A binding isotherm (Figure 5.47) was extracted from the UV-visible data to quantify the binding of **5.4** to poly(dA)$_{80}\bullet$poly(dT)$_{80}$.
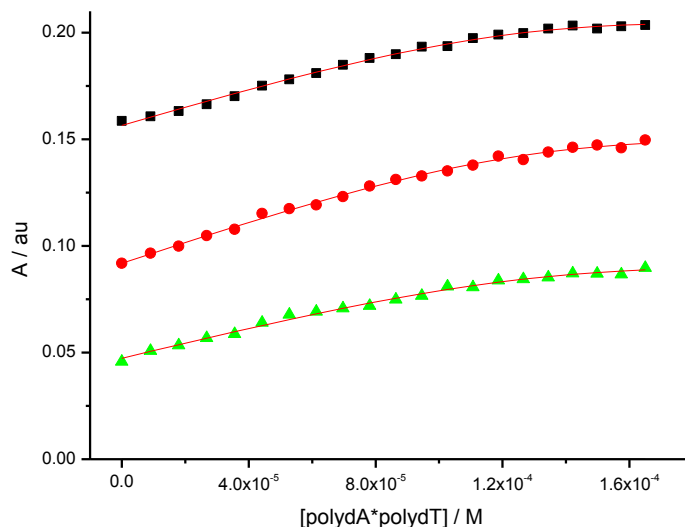
Figure 5.47 Absorbance at (■) 325 nm, (●) 333 nm and (▲) 342 nm plotted against poly(dA)$_{80}$•poly(dT)$_{80}$ concentration for **5.4** (3.65×10^{-2} mM) interacting with poly(dA)$_{80}$•poly(dT)$_{80}$, in 25 mM MOPS, 50 mM NaCl and 1 mM EDTA, pH 7.0, at 25 °C. Solid lines represent a global fit to a multiple independent sites model.

The binding isotherm in Figure 5.47 was analysed using the same model as was used for the data in Figure 5.2. The binding constant (K) for **5.4** binding to poly(dA)$_{80}$•poly(dT)$_{80}$ is $(3.2 \pm 1.2) \times10^{5}$ M^{-1} and the binding site size (n) is 3.9 ± 0.1 base pairs.

Circular dichroism for 5.4 interacting with poly(dA)$_{80}$•poly(dT)$_{80}$

In order to study the binding mode, circular dichroism spectra were recorded for **5.2** in the presence of varying concentrations of poly(dA)$_{80}$•poly(dT)$_{80}$ (Figure 5.48).
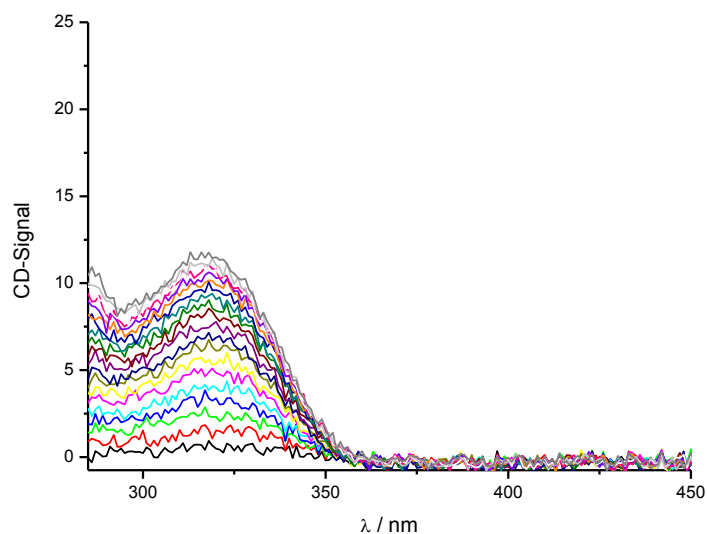
Figure 5.48 Induced circular dichroism spectra for 3.65×10^{-2} mM of **5.4** in the presence of varying concentrations of poly(dA)$_{80}$•poly(dT)$_{80}$ in buffer (25 mM MOPS, 50 mM NaCl and 1 mM EDTA, pH 7 at 25 °C).

Figure 5.48 shows positive induced circular dichroism at wavelengths above 300 nm for the interaction of **5.4** with poly(dA)$_{80}$•poly(dT)$_{80}$, in 25 mM MOPS, 50 mM NaCl and 1 mM EDTA, pH 7 at 25 °C. This result suggests a minor groove binding mode for **5.4** binding to poly(dA)$_{80}$•poly(dT)$_{80}$.

A binding isotherm (Figure 5.49) was extracted from the ICD titration data.
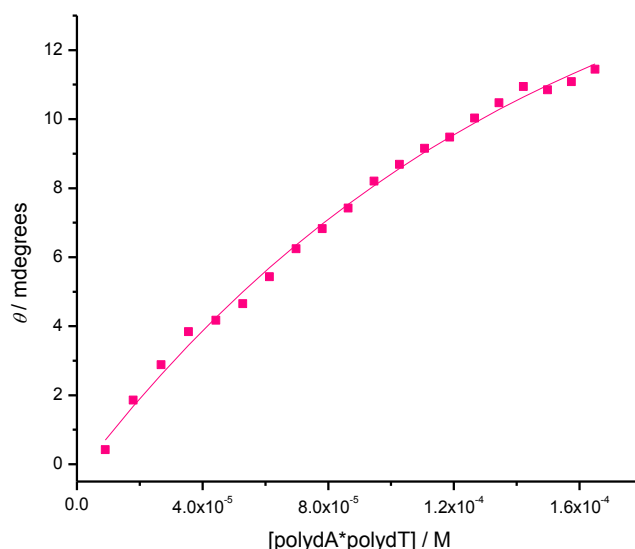
Figure 5.49   Ellipticity at (■) 317 nm plotted against poly(dA)$_{80}$•poly(dT)$_{80}$ concentration, for a solution of **5.4** (2.64×10^{-2} mM) interacting with poly(dA)$_{80}$•poly(dT)$_{80}$, in 25 mM MOPS, 50 mM NaCl and 1 mM EDTA, pH 7.0, at 25 °C. Solid lines represent a global fit to a multiple independent sites model

The data in the titration curve of Figure 5.49 were analysed using the same multiple independent binding sites model as before. The binding constant (K) for **5.4** binding to poly(dA)$_{80}$•poly(dT)$_{80}$ is $(1.39 \pm 0.05) \times10^4$ M^{-1} for a stoichiometry (n) of 2 (restricted). This result is in agreement with the UV-visible data.

Summary

Dicationic oligoheteroaromatic **5.4** binds to DNA with a binding constant of (1.1 ± 0.6) $\times10^4$ M^{-1} for a binding site size of 2.5 (restricted). The interaction of dicationic **5.4** with CT-DNA results in a positive ICD signal, suggesting binding of **5.4** in the minor groove. Following an initial increase, no further increase in the viscosity of a DNA solution was observed for dicationic oligoheteroaromatic **5.4** interacting with CT-DNA, suggesting minor groove binding as the dominant binding mode. ITC shows two binding events for

5.4 interacting with DNA. Dicationic oligoheteroaromatic **5.4** bound to

poly(dA)$_{80}$•poly(dT)$_{80}$ in the minor groove with significant affinity.

The driving forces for binding of **5.4** to DNA are presumed to be those described in **5.1**.

5.3.5 Tricationic oligoheteroaromatic 5.5 binding to DNA

The binding of tricationic oligoheteroaromatic **5.5** to calf thymus DNA was studied using

UV-visible spectroscopy; the changes in absorption of **5.5** upon addition of calf thymus

DNA were measured in buffer (25 mM MOPS, 50 mM NaCl and 1 mM EDTA) at 25 °C

(Figure 5.50).
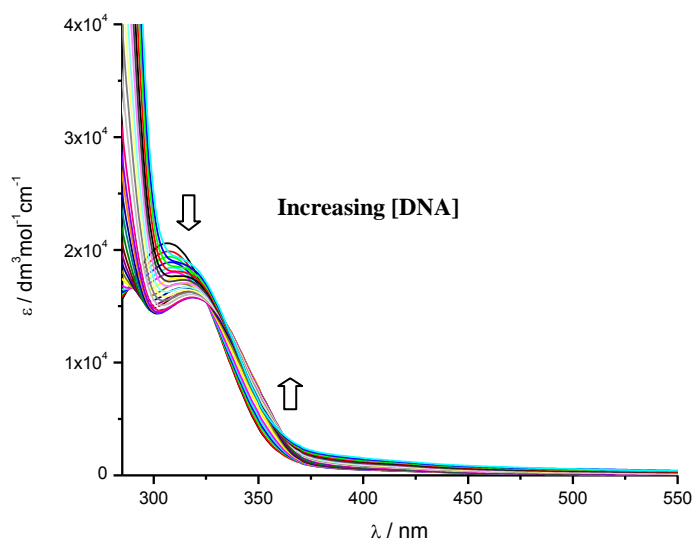
Figure 5.50 UV-visible spectra for 3.18×10^{-2} mM tricationic oligoheteroaromatic **5.5** upon addition of aliquots of a 3 mM calf thymus DNA solution in 25 mM MOPS, 50 mM NaCl and 1 mM EDTA, pH 7.0, at 25 °C.

Figure 5.50 shows that the absorption maximum associated with the free ligand decreases

while a new absorption attributed to the complex increases. DNA-binding of **5.5** is

accompanied by a bathochromic shift. This bathochromic shift is attributed to an

increasing effective conjugation length; upon binding to DNA the freely rotating rings in the ligand become fixed. Titration data for selected wavelengths was extracted from the UV-visible data in Figure 5.51 and from a second titration to generate binding isotherms for **5.5** interacting with DNA (Figure 5.51).
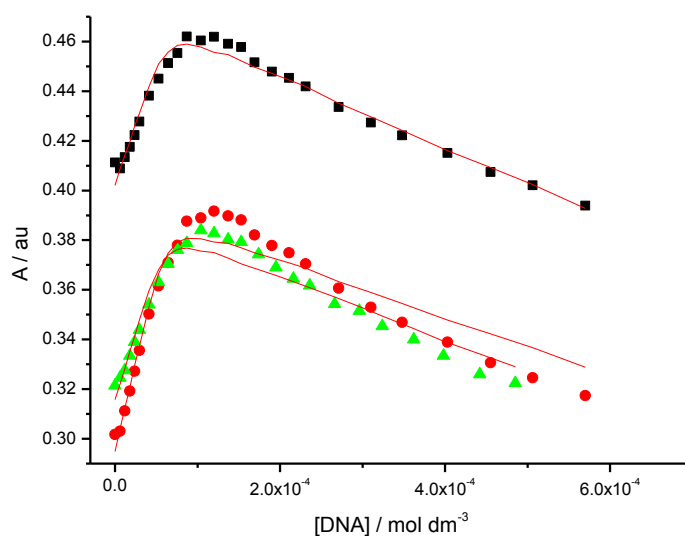
Figure 5.51 Absorbance at (■) 333 nm, (●) 340 nm and (▲) 335 nm plotted against DNA concentrationfor **5.5** (3.18×10^{-2} mM and 3.03×10^{-2} mM), in 25 mM MOPS, 50 mM NaCl and 1 mM EDTA, pH 7.0, at 25 °C. Solid lines represent a global fit to a multiple independent sites model.

The data in the titration curve were analysed globally using the multiple independent binding sites model. The binding constant (*K*) for **5.5** binding to DNA is $(1.1 \pm 0.5) \times 10^{6}$ M^{-1} a stoichiometry (*n*) restricted to 2.

Circular dichroism

In order to study the interaction mode of **5.5** with calf thymus we used circular dichroism spectroscopy. Induced circular dichroism spectra for **5.5** in the presence of varying concentrations of calf thymus DNA in 25 mM MOPS, 50 mM NaCl and 1 mM EDTA, pH 7 at 25 $^{\circ}$C were recorded (Figure 5.52).
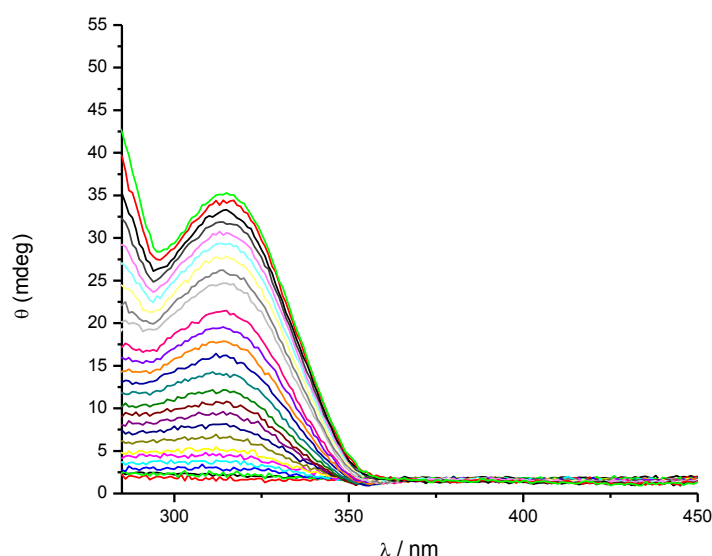
Figure 5.52 Induced circular dichroism spectra for 3.03×10^{-2} mM **5.5** upon addition of aliquots of a 3 mM calf thymus DNA solution (in 25 mM MOPS, 50 mM NaCl and 1 mM EDTA, pH 7 at 25 °C).

A positive induced signal around 315 nm is observed and this signal increases upon addition of DNA during the titration. This positive signal suggests that **5.5** is a minor groove binder.[3]

A titration curve (Figure 5.53) was extracted from the ICD titration data.
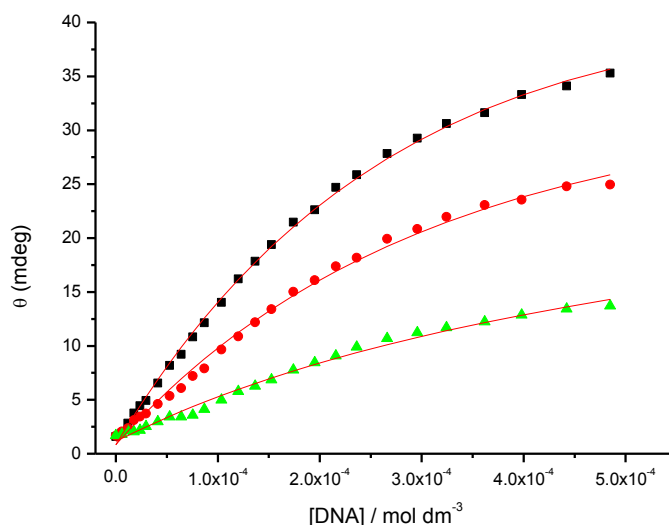
Figure 5.53 Ellipticity at (■) 315 nm, (●) 330 nm and (▲) 340 nm plotted against calf thymus DNA concentration for **5.5** (3.03×10^{-2} mM), in 25 mM MOPS, 50 mM NaCl and 1 mM EDTA, pH 7.0, at 25 °C. The solid lines represent a global fit to a multiple independent sites model.

The data in the titration curve of Figure 5.53 was analysed using the multiple independent binding site model. The binding constant (K) for **5.5** binding to DNA is $(7.3 \pm 0.4) \times 10^3$ M^{-1} for a stoichiometry (n) restricted to 3. The stoichiometry was restricted because the fit does not give reasonable parameters with variable stoichiometry.

Viscosity

The mode of the binding for **5.5** with double-stranded DNA was further studied by viscosimetry to confirm the conclusion from circular dichroism spectroscopy that **5.5** is a groove binder.

215
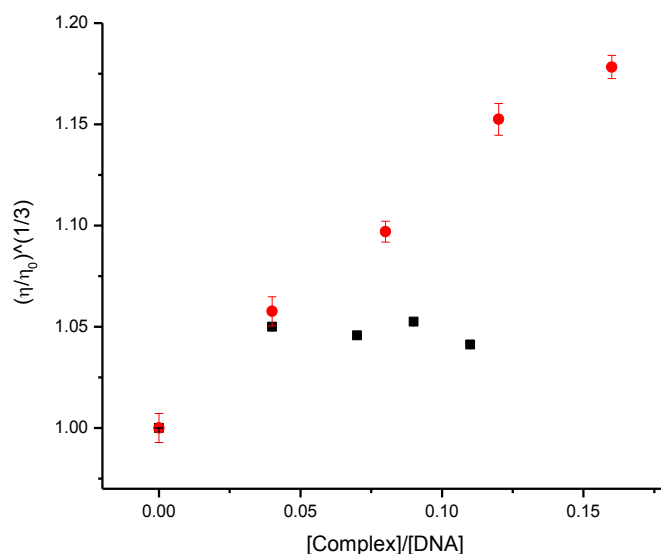
Figure 5.54 Relative viscosities of 0.5 mM CT-DNA solutions upon addition of **5.5** (■) and ethidium bromide (■) at 25 °C in 25 mM MOPS, 50 mM NaCl, 1mM EDTA, pH 7.0.

Figure 5.54 again shows a small increase in viscosity upon the first addition of **5.5** followed by no further increase, suggesting a dominant minor groove binding mode, confirming the minor groove binding mode for **5.5** deduced from the positive induced circular dichroism.

Isothermal titration calorimetry (ITC)

To probe further the binding of tricationic oligoheteroaromatic **5.5** with DNA, we used isothermal titration calorimetry (ITC). The differential heat flow and derived integrated heat effects for titration of a 4.5 mM solution of **5.5** into a 0.5 mM calf thymus DNA solution were measured in 25 mM MOPS, 50 mM NaCl and 1 mM EDTA, pH 7.0, at 25 °C (Figure 5.55).
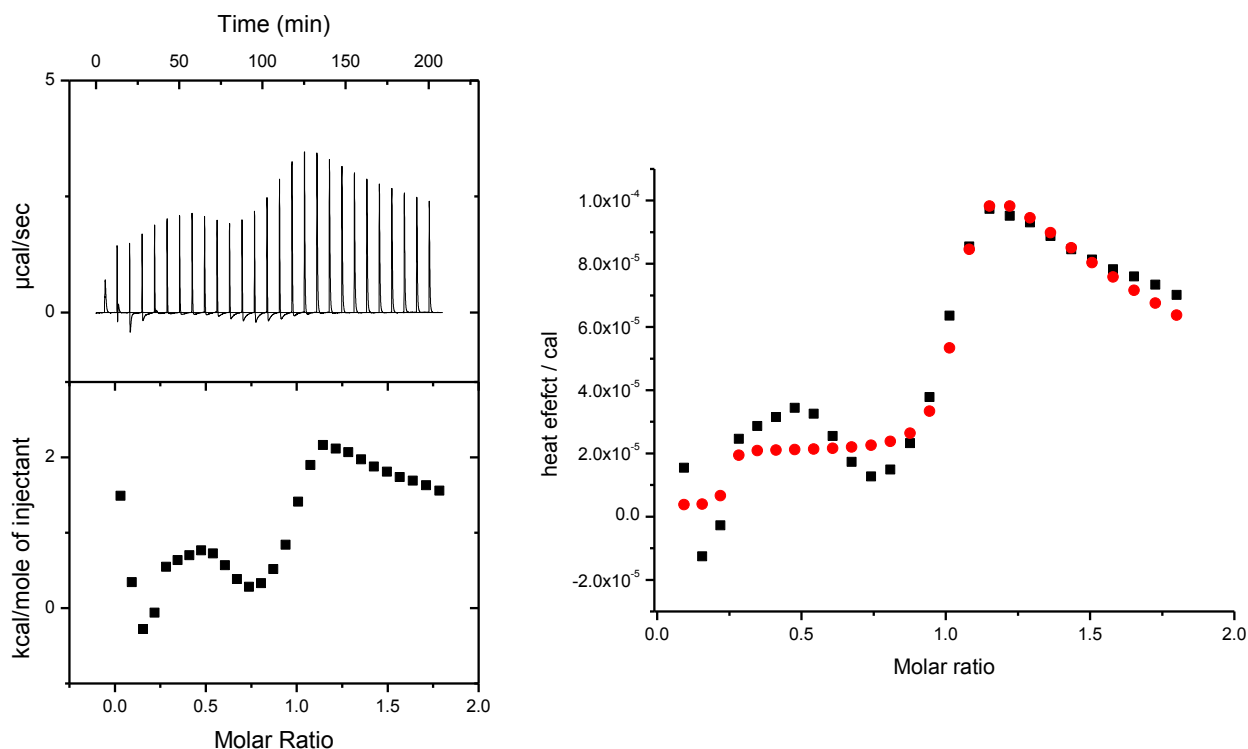
Figure 5.55 Titration of a 4.50 mM solution of **5.5** into a 0.50 mM solution of CT-DNA in 25 mM MOPS, 50 mM NaCl and 1 mM EDTA, pH 7, at 25 °C (left). Integrated heat effects for the same titration analysed in terms of a two binding sites model with aggregation included (right).

The titration of **5.5** with CT-DNA suggests (at least) two binding events followed by ligand dilution. The data was analysed in terms of two binding modes model, also taking into account the self aggregation of **5.5**, because **5.5** at 4.50 mM concentration shows self aggregation. The fit to the two-binding-modes model indicates that this binding model reproduces some aspects of the data, but does not generate an overall good fit. The thermodynamics parameter for the interaction of dicationic hetroaromatic **5.5** with CT-DNA in 25 mM MOPS, 50 mM NaCl and 1 mM EDTA, pH 7, at 25 °C are summarised in Table 5.3.

Table 5.3 Thermodynamic parameters for binding of **5.5** to CT-DNA in MOPS buffer, pH 7.0, at 25 °C

			Aggregation included		
$[L]_{syringe}$ (mM)	$[DNA]_{cell}$ (mM)	K_A $(10^9 \, M^{-1})$	ΔH_{A1} $(10^3 \, cal \, mol^{-1})$	$-T \times \Delta S_{A1}$ $(10^3 \, kcal \, mol^{-1})$	$1/n_{A1}$
4.5	0.50	1.89	-2.63	-6.88	4.6
$[L]_{syringe}$ (mM)	$[DNA]_{cell}$ (mM)	K_B $(10^5 \, M^{-1})$	ΔH_{B1} $(10^3 \, cal \, mol^{-1})$	$-T \times \Delta S_{B1}$ $(10^3 \, kcal \, mol^{-1})$	$1/n_{B1}$
4.5	0.50	9.22	-2.25	-14.30	1.25

Table 5.4 shows that dicationic oligohetroaromatic **5.5** binds to CT-DNA with an affinity of $\sim 10^9 \, M^{-1}$. The binding site size is 4.5. The binding is characterised by negative enthalpy and entropy changes. The negative values for enthalpy and entropy suggest that **5.5** binds to CT-DNA through a minor groove binding mode.

Sequence selectivity

The affinity of **5.5** for selected specific sequences of DNA, viz. poly(dGdC)$_{40}$and poly(dA)$_{80}$•poly(dT)$_{80}$, was studied using UV-visible and circular dichroism spectroscopy.

UV-visible spectroscopy for 5.5 interacting with poly(dGdC)$_{40}$

The binding of oligoheteroaromatic **5.5** to poly(dGdC)$_{40}$was studied using UV-visible spectroscopy. The titration of **5.5** with poly(dGdC)$_{40}$was carried out in buffer (25 mM MOPS, 50 mM NaCl and 1 mM EDTA) at 25 °C. Figure 5.56 shows the changes in absorbance of **5.5** with increasing poly(dGdC)$_{40}$ concentration.

Figure 5.56 UV-visible spectra for 2.64×10^{-2} mM tricationic oligoheteroaromatic **5.5** upon addition of aliquots of a 2.85 mM poly(dGdC)$_{40}$solution in 25 mM MOPS, 50 mM NaCl and 1 mM EDTA, pH 7.0, at 25 °C.

Figure 5.56 shows that the absorption maximum of the free ligand decreases while the absorption maximum of the complex increases with an isosbestic point at 326 nm suggesting the presence of only two ligand species in solution (free and bound ligand). DNA-binding of **5.5** is accompanied by a bathochromic shift, which is attributed to the ligand adopting a more planar conformation when bound to DNA, increasing the effective conjugation length.

A set of titration curves (Figure 5.57) was extracted from the UV-visible data to quantify the binding of **5.5** to poly(dGdC)$_{40}$.
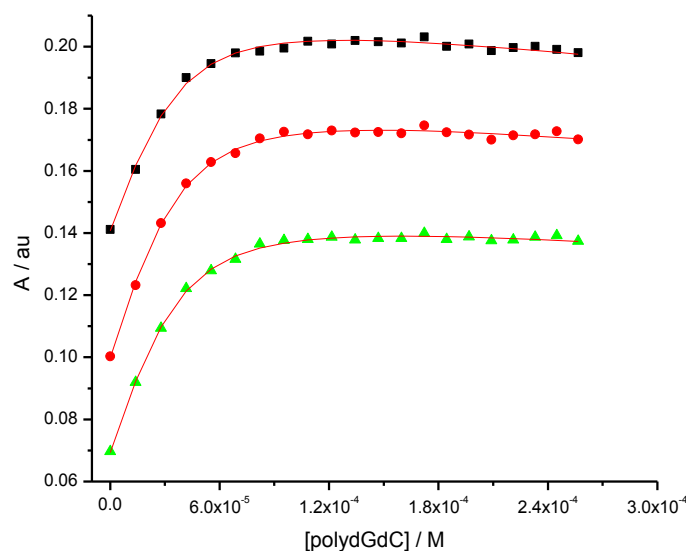
Figure 5.57 Absorbance at (■) 340 nm, (●) 347 nm and (▲) 354 nm plotted against poly(dGdC)$_{40}$concentration, for **5.5** (2.64×10^{-2} mM), in 25 mM MOPS, 50 mM NaCl and 1 mM EDTA, pH 7.0, at 25 °C. Solid lines represent a global fit to a multiple independent sites model.

The data in Figure 5.57 were analysed using the same model as used for the data in Figure

5.5. The binding constant (*K*) for **5.5** binding to poly(dGdC)$_{40}$is $(1.3 \pm 0.1) \times 10^5$ M^{-1} and

the binding site size (*n*) is 1.3 ± 0.06.

Circular dichroism for 5.5 interacting with poly(dGdC)$_{40}$

In order to study the binding mode of **5.5** with poly(dGdC)$_{40}$, circular dichroism spectra

were recorded (Figure 5.58).
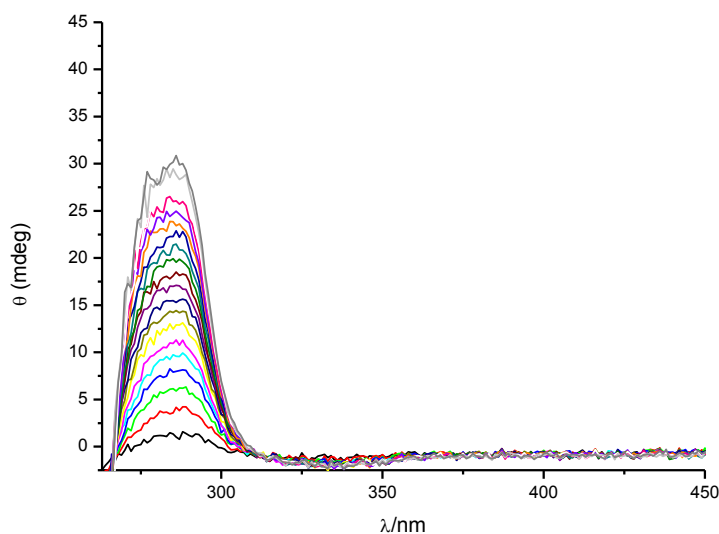
Figure 5.58 Circular dichroism spectra for 2.64×10^{-2} mM **5.5** in the presence of varying concentrations of poly(dGdC)$_{40}$ (added as aliquots of a 2.85 mM solution of poly(dGdC)$_{40}$) in buffer 25 mM MOPS, 50 mM NaCl and 1 mM EDTA, pH 7 at 25 °C.

Figure 5.58 shows the circular dichroism spectra for a solution of **5.5** in the presence of varying concentrations of poly(dGdC)$_{40}$, in 25 mM MOPS, 50 mM NaCl and 1 mM EDTA, pH 7 at 25 °C. No ICD spectra is observed for wavelengths above 300 nm upon addition of poly(dGdC)$_{40}$up to concentrations of poly(dGdC)$_{40}$of 2.2×10^{-1} mM. This result suggests that **5.5** does not bind particularly intimately to poly(dGdC)$_{40}$ and most likely not through groove binding or intercalation. In this respect, the binding affinity as reported by the UV-visible experiment (vide infra) is remarkably high.

UV-visible spectroscopy for 5.5 interacting with poly(dA)$_{80}$•poly(dT)$_{80}$

The binding of dicationic oligoheteroaromatic **5.5** to poly(dA)$_{80}$•poly(dT)$_{80}$ sequence was studied using UV-visible spectroscopy. The titration of **5.5** with poly(dA)$_{80}$•poly(dT)$_{80}$ was carried out in buffer (25 mM MOPS, 50 mM NaCl and 1 mM

EDTA) at 25 °C. Figure 5.59 shows the changes in absorbance with increasing poly(dA)$_{80}$•poly(dT)$_{80}$ concentration.
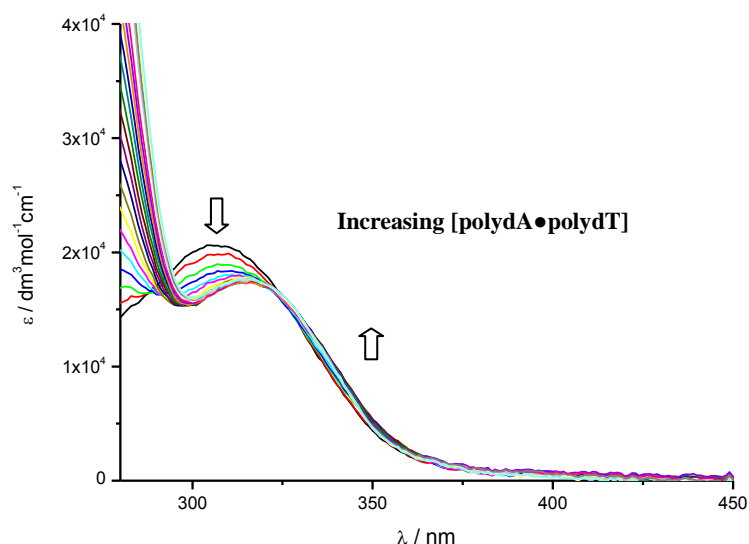
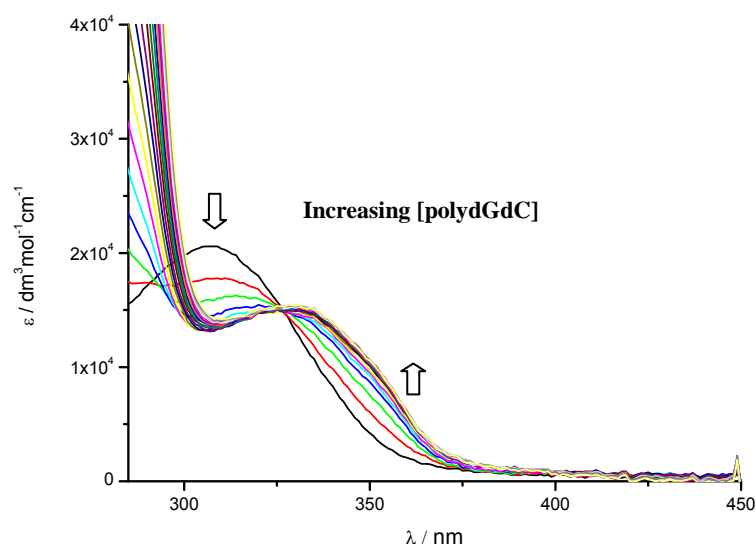**Figure 5.59** UV-visible spectra for 2.56×10^{-2} mM dicationic oligoheteroaromatic **5.5** upon addition of aliquots of a 1.83 mM solution of poly(dA)$_{80}$•poly(dT)$_{80}$ in 25 mM MOPS, 50 mM NaCl and 1 mM EDTA, pH 7.0, at 25 °C.

The absorption of the free ligand decreases while the absorption attributed to the complex increases and DNA-binding of **5.5** is accompanied by a bathochromic shift. As before, we attribute this bathochromic shift to formation of a complex in which the bound ligand is forced to adopt a more planar conformation, increasing effective conjugation length. A binding isotherm (Figure 5.60) was extracted from the UV-visible data to quantify the binding of **5.5** to poly(dA)$_{80}$•poly(dT)$_{80}$.
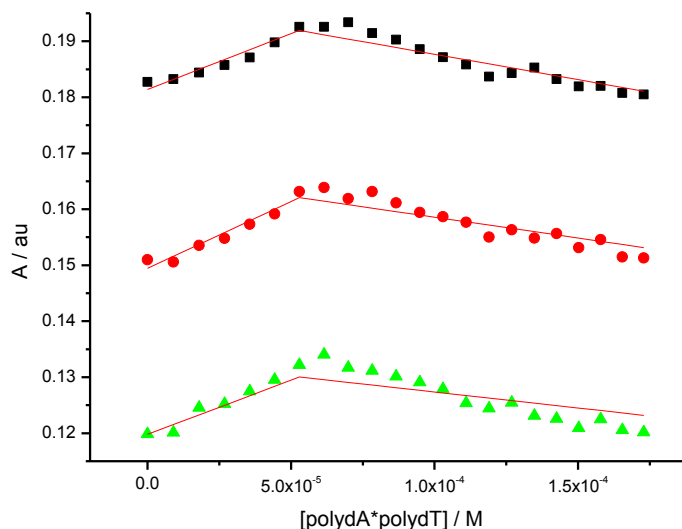
Figure 5.60 Absorbance at (■) 333 nm, (●) 338 nm and (▲) 343 nm is plotted against poly(dA)$_{80}$●poly(dT)$_{80}$ concentration, for **5.5** (2.56×10^{-2} mM) interacting with polydA●polydT, in 25 mM MOPS, 50 mM NaCl and 1 mM EDTA, pH 7.0, at 25 °C. Solid lines represent a global fit to a multiple independent sites model.

The data in the titration curve of Figure 5.60 was analysed using the same model as before, but we could not find reasonable parameters. Nevertheless, the data and the fitted lines suggest that this ligand could be a strong binder to poly(dA)$_{80}$●poly(dT)$_{80}$, but which unfortunately does not show a significant change in its absorption spectrum.

Circular dichroism for 5.5 interacting with poly(dA)$_{80}$●poly(dT)$_{80}$

In order to study the binding mode, circular dichroism spectra were recorded for **5.5** in the presence of varying concentrations of poly(dA)$_{80}$●poly(dT)$_{80}$ (Figure 5.61).
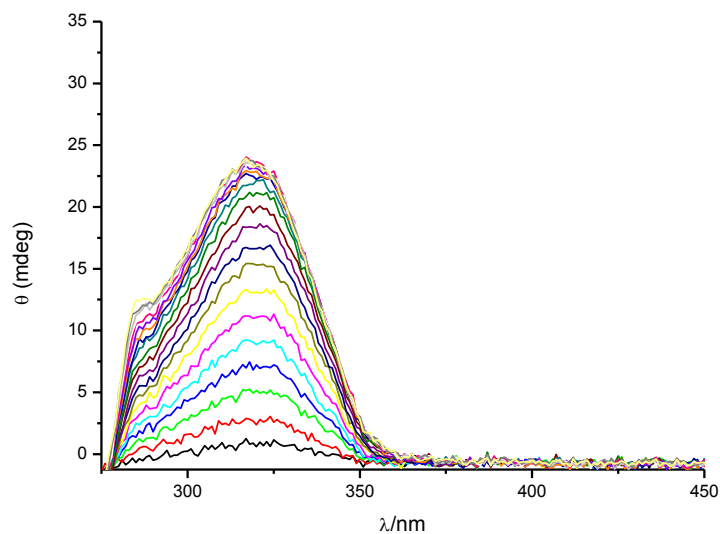
Figure 5.61 Induced circular dichroism spectra for 2.56×10^{-2} mM of **5.5** in the presence of varying concentrations of poly(dA)$_{80}$•poly(dT)$_{80}$ in buffer (25 mM MOPS, 50 mM NaCl and 1 mM EDTA, pH 7 at 25 °C).

Figure 5.61 shows induced circular dichroism at wavelengths above 300 nm for the interaction of **5.5** with poly(dA)$_{80}$•poly(dT)$_{80}$, in 25 mM MOPS, 50 mM NaCl and 1 mM EDTA, pH 7 at 25 °C. This result suggests a minor groove binding mode for **5.5** binding to poly(dA)$_{80}$•poly(dT)$_{80}$.

A binding isotherm (Figure 5.62) was extracted from the ICD titration data.
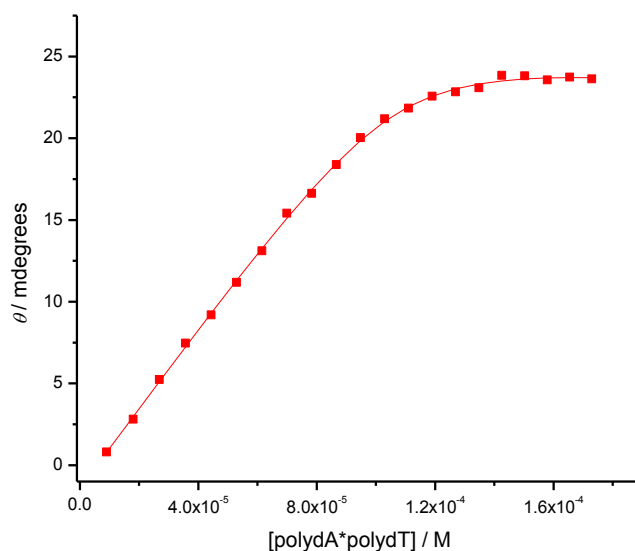
Figure 5.62 Absorbance at (■) 318 nm plotted against poly(dA)$_{80}$•poly(dT)$_{80}$ concentration, for the solution of **5.5** (2.56×10^{-2} mM) interacting with poly(dA)$_{80}$•poly(dT)$_{80}$, in 25 mM MOPS, 50 mM NaCl and 1 mM EDTA, pH 7.0, at 25 °C. Solid lines represent a global fit to a multiple independent sites model.

The data in the titration curve of Figure 5.62 were analysed using the same multiple independent binding sites model as before. The binding constant (*K*) for **5.5** binding to poly(dA)$_{80}$•poly(dT)$_{80}$ is (1.5 ± 0.3) × 10^6 M^{-1} and the stoichiometry (*n*) is 4.5 ± 0.05. These results again indicate sequence selectivity for **5.5** for poly(dA)$_{80}$•poly(dT)$_{80}$ over poly(dGdC)$_{40}$.

Summary

Tricationic oligoheteroaromatic **5.5** binds to DNA with a binding constant of (1.1 ± 0.6) ×10^4 M^{-1} and a binding site size of 1.4 ± 0.18 base pairs. The interaction of tricationic **5.5** with CT-DNA results in a positive ICD signal, suggesting binding of **5.5** in the minor groove. Following the usual increase in relative viscosity upon addition of the first aliquot of **5.5**, there is no further increase in the viscosity of a DNA solution upon addition of more tricationic oligoheteroaromatic **5.5**, suggesting a minor groove binding. A complex

binding mode is supported by ITC, which shows at least two binding events for **5.5** interacting with DNA. Tricationic oligoheteroaromatic **5.5** weakly bound to poly(dGdC)$_{40}$ without specific binding mode. On the other hand, **5.5** strongly bound to poly(dA)$_{80}$•poly(dT)$_{80}$ following the minor groove binding mode.

The driving forces for binding of **5.5** to DNA are again assumed to be as described for **5.1**.

5.3.6 Tricationic oligoheteroaromatic 5.6 binding to DNA

The binding of dicationic oligoheteroaromatic **5.6** to calf thymus DNA was studied using UV-visible spectroscopy; the changes in absorption of **5.6** upon addition of calf thymus DNA were measured in buffer (25 mM MOPS, 50 mM NaCl and 1 mM EDTA) at 25 °C (Figure 5.63).
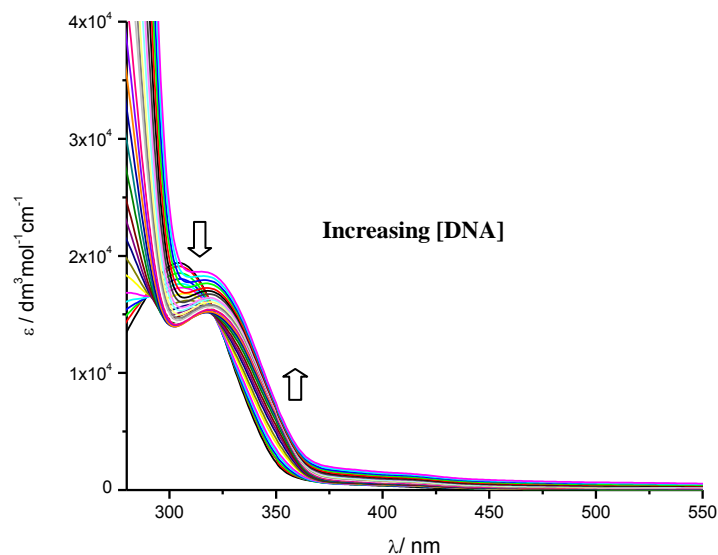
Figure 5.63 UV-visible spectra for 3.12×10^{-2} mM tricationic oligoheteroaromatic **5.6** upon addition of aliquots of a 3 mM solution of calf thymus DNA in 25 mM MOPS, 50 mM NaCl and 1 mM EDTA, pH 7.0, at 25 °C.

Figure 5.63 shows that the absorption of the free ligand decreases while the absorption attributed to the complex increases. DNA-binding of **5.6** is accompanied by a

bathochromic shift. This bathochromic shift is attributed to an increasing effective conjugation length; upon binding to DNA the freely rotating rings in the ligand become fixed. Titration data for selected wavelengths was extracted from the UV-visible data in Figure 5.62 and from a second titration to generate binding isotherms for **5.6** interacting with DNA (Figure 5.64).
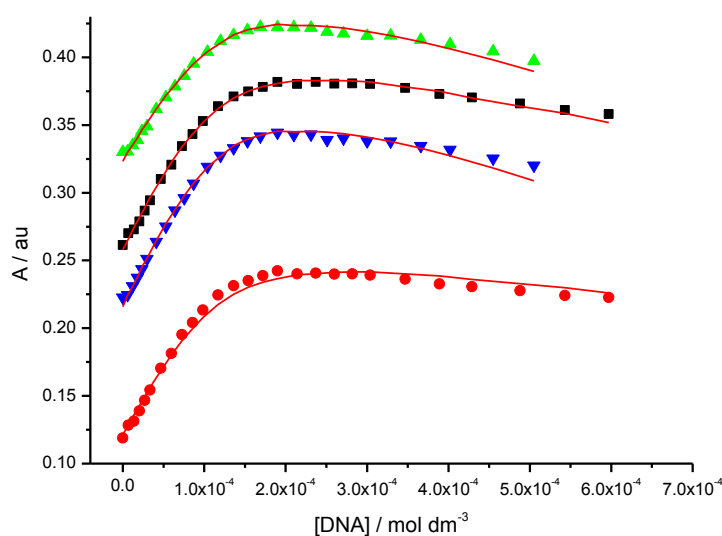
Figure 5.64 Absorbance at (■) 337 nm, (●) 349 nm, (▲) 333 nm and (▼) 340 nm plotted against DNA concentration for **5.6** (3.12×10^{-2} mM and 2.35×10^{-2} mM), in 25 mM MOPS, 50 mM NaCl and 1 mM EDTA, pH 7.0, at 25 °C. Solid lines represent a global fit to a multiple independent sites model.

The data in the titration curve of Figure 5.64 were analysed globally using the multiple independent binding sites model. The binding constant (*K*) for **5.6** binding to DNA is ($1.1 \pm 0.003) \times 10^7$ M^{-1} and the binding site size is 2.4 ± 0.2 base pairs. This binding site is rather short in comparison with the length of **5.6**, suggesting that **5.6** may be binding in a side-by-side manner, or that other complexities are playing a role.

Circular dichroism

In order to study the interaction mode for **5.6** with calf thymus we used circular dichroism spectroscopy. Induced circular dichroism spectra for **5.6** in the presence of varying concentrations of calf thymus DNA in 25 mM MOPS, 50 mM NaCl and 1 mM EDTA, pH 7 at 25 °C were recorded (Figure 5.65).
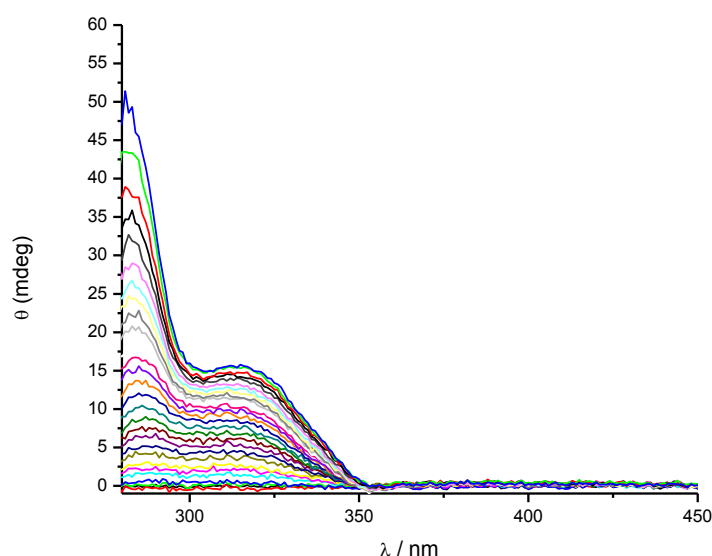
Figure 5.65 Induced circular dichroism spectra for 3.26×10^{-2} mM **5.6** upon addition of aliquots of a 2.6 mM calf thymus DNA solution (in 25 mM MOPS, 50 mM NaCl and 1 mM EDTA, pH 7 at 25 °C).

A positive induced signal around 315 nm is observed and this signal increases upon addition of DNA during the titration. This positive signal suggests that **5.6** is a minor groove binder.[3]

A titration curve (Figure 5.66) was extracted from the ICD titration data.
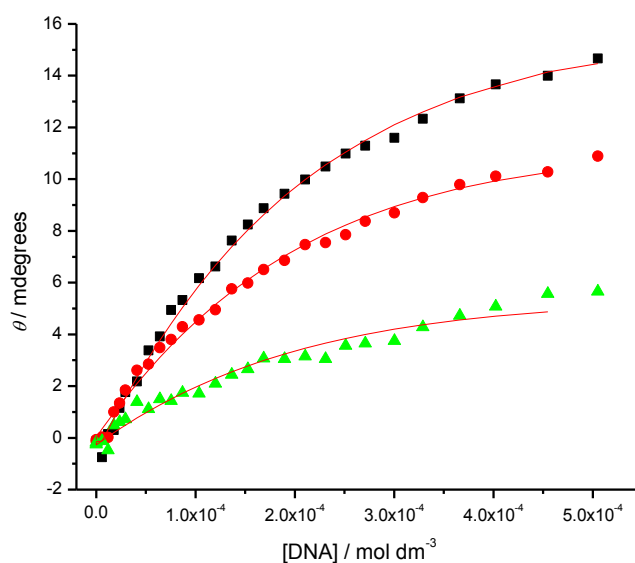
Figure 5.66 Ellipticity at (■) 320 nm, (●) 330 nm and (▲) 340 nm plotted against calf thymus DNA concentrationfor **5.6** (3.26×10^{-2} mM), in 25 mM MOPS, 50 mM NaCl and 1 mM EDTA, pH 7.0, at 25 °C. . The solid lines represent a global fit to a multiple independent sites model.

The data in the titration curve of Figure 5.66 was analysed using the multiple independent binding site model. The binding constant (*K*) for **5.6** binding to DNA is $(1.7 \pm 0.1) \times 10^{4}$ M^{-1} for a stoichiometry (*n*) restricted to 3.8. The stoichiometry was restricted because the fit does not give reasonable parameters with variable stoichiometry.

Viscosity

The mode of the binding for **5.6** with double-stranded DNA was further studied by viscosimetry to confirm the result from the circular dichroism (Figure 5.67).
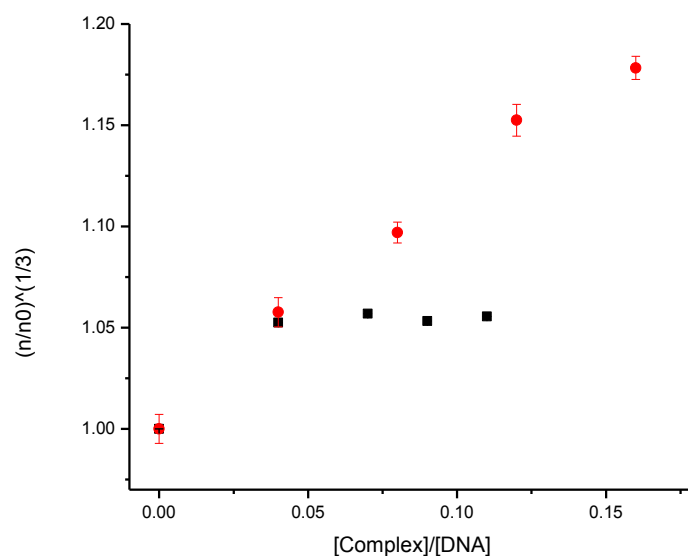
Figure 5.67 Relative viscosities of 0.5 mM CT-DNA solutions upon addition of **5.6** (■) and ethidium bromide (■) at 25 °C in 25 mM MOPS, 50 mM NaCl, 1mM EDTA, pH 7.0.

Figure 5.67 shows a small increase in viscosity upon the first addition of **5.6** followed by no further increase, suggesting a dominant minor groove binding mode, confirming the minor groove binding mode for **5.6**.

Isothermal titration calorimetry (ITC)

To explore further the binding of tricationic oligoheteroaromatic **5.6** with DNA, we used isothermal titration calorimetry (ITC). The differential heat flow and derived integrated heat effects for titration of a 4.39 mM solution of **5.6** into a 0.5 mM calf thymus DNA solution were measured in 25 mM MOPS, 50 mM NaCl and 1 mM EDTA, pH 7.0, at 25 °C (Figure 5.68).
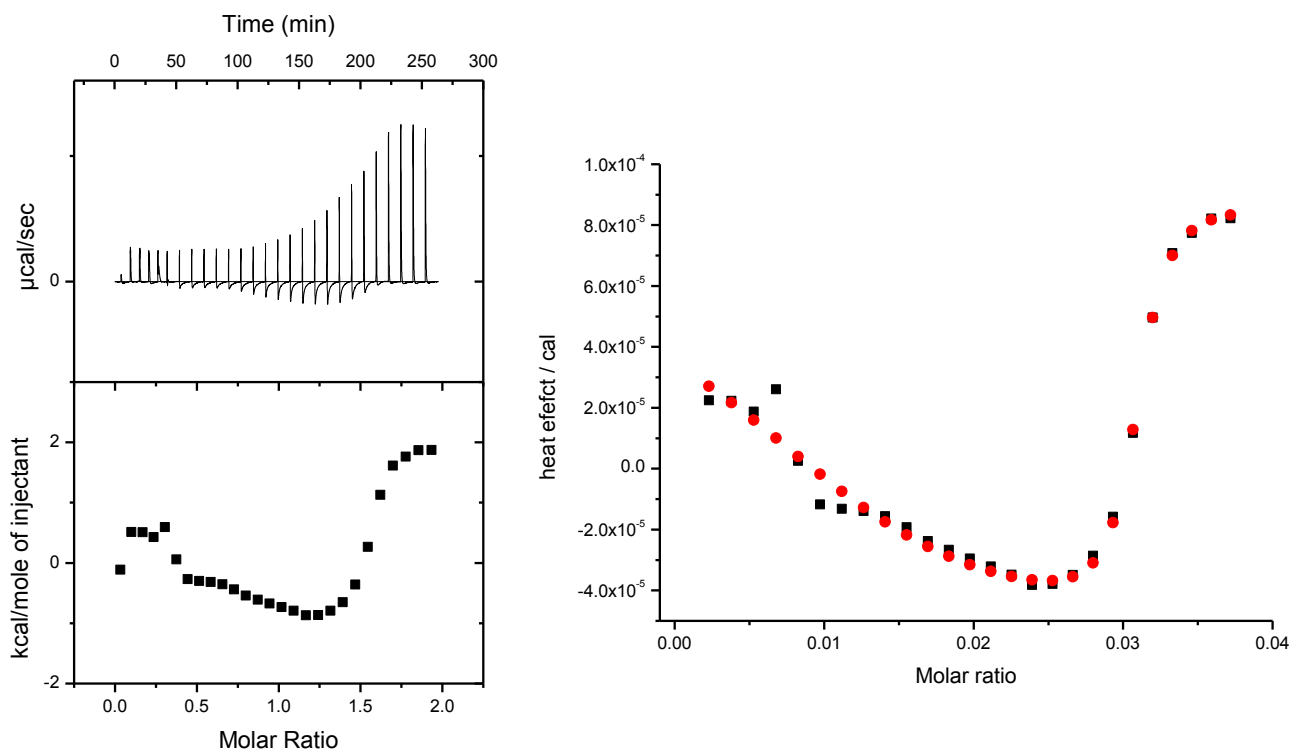
Figure 5.68 Titration of a 4.39 mM solution of **5.6** into a 0.45 mM solution of CT-DNA in 25 mM MOPS, 50 mM NaCl and 1 mM EDTA, pH 7, at 25 °C (left). Integrated heat effects for the same titration analysed in terms of one type of independent binding sites model with aggregation included (right).

The interaction of **5.6** with CT-DNA clearly indicates two binding events with rather similar binding affinities. The data was analysed in term of a model involving two binding modes, also taking into account the self aggregation of **5.6**, because **5.6** at 4.50 mM concentration shows self aggregation. The fit to the two-binding site types model indicates that this binding model fits the data well. The thermodynamic parameters for the interaction of tricationic hetroaromatic **5.6** with CT-DNA in 25 mM MOPS, 50 mM NaCl and 1 mM EDTA, pH 7, at 25 °C are summarised in Table 5.4.

Table 5.4 Thermodynamic parameters for binding of **5.6** to CT-DNA in MOPS buffer, pH 7.0, at 25 °C

Aggregation included					
$[L]_{syringe}$ (mM)	$[DNA]_{cell}$ (mM)	K_A $(10^6 M^{-1})$	ΔH_{A1} $(10^2 cal\ mol^{-1})$	$-T \times \Delta S_{A1}$ $(10^3 kcal\ mol^{-1})$	$1/n_{A1}$
4.39	0.45	2.66	-1.62	-9.88	2.4
$[L]_{syringe}$ (mM)	$[DNA]_{cell}$ (mM)	K_B $(10^5 M^{-1})$	ΔH_{B1} $(10^3 cal\ mol^{-1})$	$-T \times \Delta S_{B1}$ $(10^3 kcal\ mol^{-1})$	$1/n_{B1}$
4.39	0.45	6.42	-3.75	-5.33	0.90

Table 5.4 indicates that tricationic oligoheteroaromatic **5.6** binds to CT-DNA with an affinity of ~$10^6 M^{-1}$. The binding site size of 2.4 is in agreement with the binding site size from UV-visible titration. The binding is characterised by negative enthalpy and entropy change. These negative values for enthalpy and entropy suggest that **5.6** binds to CT-DNA in the minor groove.

Sequence selectivity

The selectivity of **5.6** for selected specific sequences of DNA, viz. poly(dGdC)$_{40}$ and poly(dA)$_{80}$•poly(dT)$_{80}$, was studied using UV-visible and circular dichroism spectroscopy.

UV-visible spectroscopy for 5.6 interacting with poly(dGdC)$_{40}$

The binding of oligoheteroaromatic **5.6** to poly(dGdC)$_{40}$ was studied using UV-visible spectroscopy. The titration of **5.6** with poly(dGdC)$_{40}$ was carried out in buffer (25 mM MOPS, 50 mM NaCl and 1 mM EDTA) at 25 °C.

Figure 5.69 shows the changes in absorbance of **5.6** with increasing poly(dGdC)$_{40}$ concentration.

Figure 5.69 UV-visible spectra for 3.23×10^{-2} mM tricationic oligoheteroaromatic **5.6** upon addition of aliquots of a 2.85 mM poly(dGdC)$_{40}$ solution in 25 mM MOPS, 50 mM NaCl and 1 mM EDTA, pH 7.0, at 25 °C.

Figure 5.69 shows that the absorption maximum of the free ligand decreases while the absorption maximum of the complex increases, with an isosbestic point at 324 nm suggesting the presence of only two ligand species in solution (free and bound ligand). DNA-binding of **5.6** is accompanied by a bathochromic shift, which is attributed to the ligand adopting a more planar conformation when bound to DNA, increasing the effective conjugation length.

The titration in Figure 5.70 was extracted from the UV-visible data to quantify the binding of **5.6** to poly(dGdC)$_{40}$.
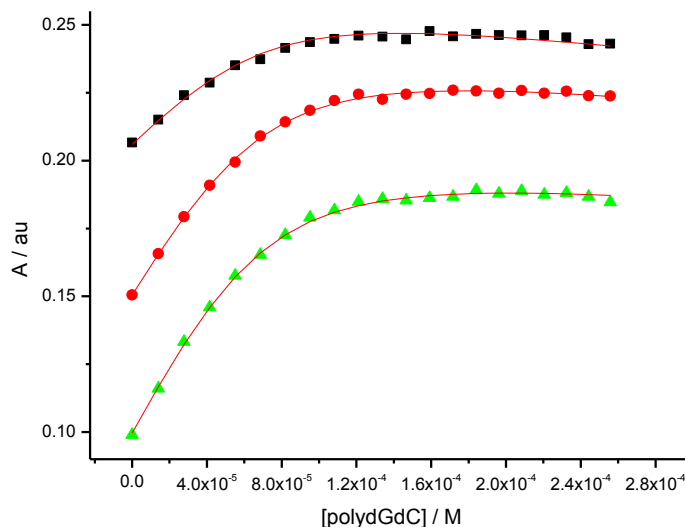
Figure 5.70 Absorbance at (■) 330 nm, (●) 337 nm and (▲) 344 nm plotted against poly(dGdC)$_{40}$ concentration, for **5.6** (3.23×10^{-2} mM), in 25 mM MOPS, 50 mM NaCl and 1 mM EDTA, pH 7.0, at 25 °C. Solid lines represent a global fit to a multiple independent sites model.

The data in Figure 5.69 were again analysed using the multiple independent binding sites model. The binding constant (*K*) for **5.6** binding to poly(dGdC)$_{40}$ is (1.5 ± 0.2)×10^{5} M^{-1} and the binding site size (*n*) is 2.2 ± 0.08 base pairs.

Circular dichroism for 5.6 interacting with poly(dGdC)$_{40}$

In order to study the binding mode of **5.6** and poly(dGdC)$_{40}$, circular dichroism spectra were recorded (Figure 5.71).
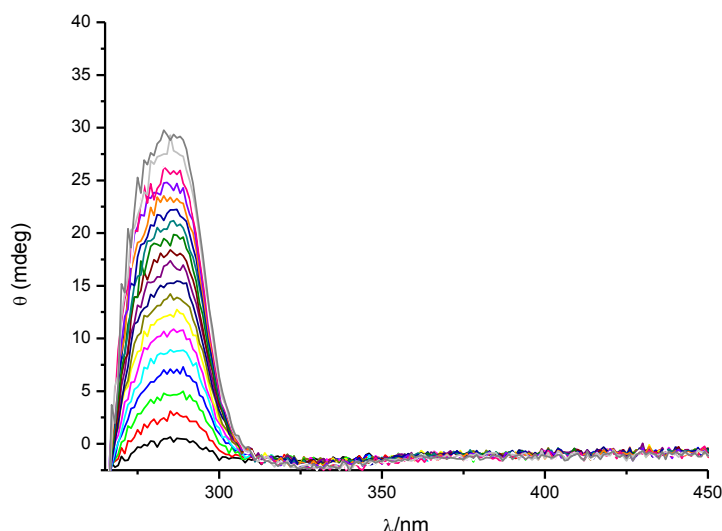
Figure 5.71 Circular dichroism spectra for 3.23×10^{-2} mM **5.6** in the presence of varying concentrations of poly(dGdC)$_{40}$ (added as aliquots of a 2.85 mM solution of poly(dGdC)$_{40}$) in buffer 25 mM MOPS, 50 mM NaCl and 1 mM EDTA, pH 7 at 25 °C.

Figure 5.71 illustrates the circular dichroism spectra for a solution of **5.6** in the presence of varying concentrations of poly(dGdC)$_{40}$, in 25 mM MOPS, 50 mM NaCl and 1 mM EDTA, pH 7 at 25 °C. No ICD is observed for wavelengths above 300 nm upon addition of poly(dGdC)$_{40}$ up to concentrations of poly(dGdC)$_{40}$ of 2.5×10^{-1} mM. This result suggests that **5.6** does not bind particularly intimately to poly(dGdC)$_{40}$ and most likely not through groove binding or intercalation.

UV-visible spectroscopy for 5.6 interacting with poly(dA)$_{80}$•poly(dT)$_{80}$

The binding of oligoheteroaromatic **5.6** to poly(dA)$_{80}$•poly(dT)$_{80}$ was studied using UV-visible spectroscopy. The titration of **5.6** with poly(dA)$_{80}$•poly(dT)$_{80}$ was carried out in buffer (25 mM MOPS, 50 mM NaCl and 1 mM EDTA) at 25 °C. Figure 5.72 shows the changes in absorbance with increasing poly(dA)$_{80}$•poly(dT)$_{80}$ concentration.
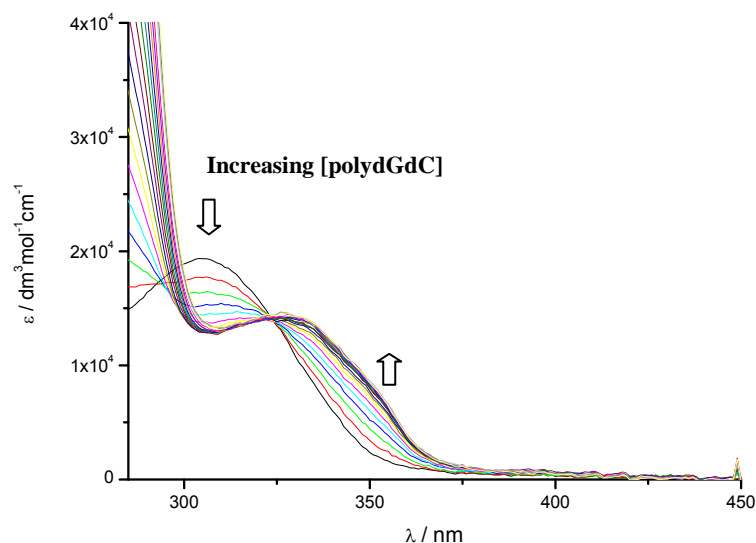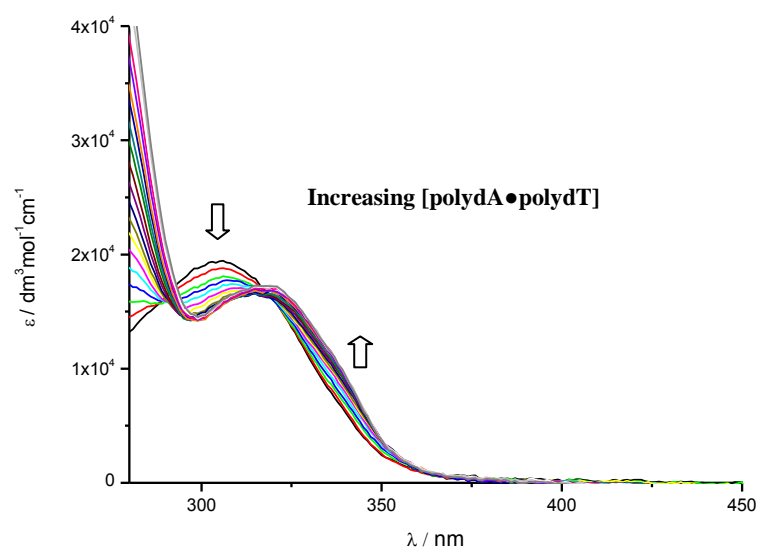
Figure 5.72 UV-visible spectra for 3.13×10^{-2} mM tricationic oligoheteroaromatic **5.6** upon addition of aliquots of a 1.83 mM solution of poly(dA)$_{80}$•poly(dT)$_{80}$ in 25 mM MOPS, 50 mM NaCl and 1 mM EDTA, pH 7.0, at 25 °C.

The absorption maximum of the free ligand decreases while the absorption maximum of the complex increases and DNA-binding of **5.6** is accompanied by a bathochromic shift. As before, we attribute this to formation of a complex in which the bound ligand is forced to adopt a more planar conformation, increasing effective conjugation length. A binding isotherm (Figure 5.73) was extracted from the UV-visible data to quantify the binding of **5.6** to poly(dA)$_{80}$•poly(dT)$_{80}$.   .
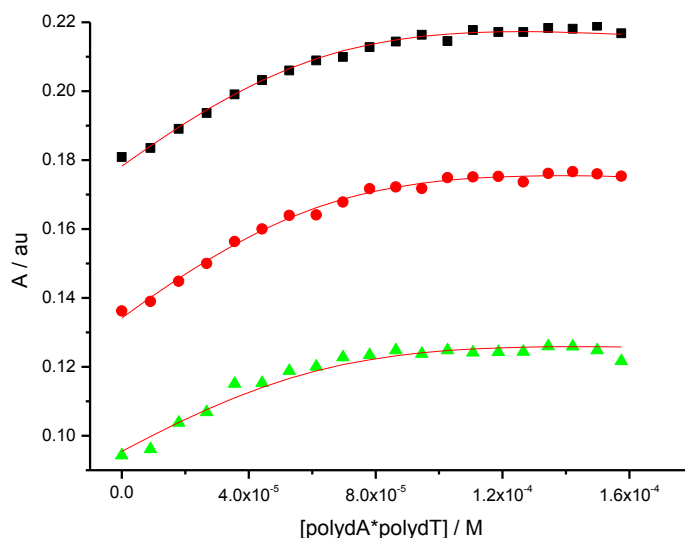
Figure 5.73 Absorbance at (■) 333 nm, (●) 339 nm and (▲) 345 nm plotted against poly(dA)$_{80}$•poly(dT)$_{80}$ concentration, for **5.6** (3.13×10^{-2} mM) interacting with poly(dA)$_{80}$•poly(dT)$_{80}$, in 25 mM MOPS, 50 mM NaCl and 1 mM EDTA, pH 7.0, at 25 °C. Solid lines represent a global fit to a multiple independent sites model.

The binding isotherm in Figure 5.73 was analysed using the same model as was used for the data in Figure 5.2. The binding constant (K) for **5.6** binding to poly(dA)$_{80}$•poly(dT)$_{80}$ is $(1.5 \pm 0.6) \times10^{5}\,M^{-1}$ and the binding site size (n) is 2.3 ± 0.2 base pairs.

Circular dichroism for 5.6 interacting with poly(dA)$_{80}$•poly(dT)$_{80}$

In order to study the binding mode, circular dichroism spectra were recorded for **5.6** in the presence of varying concentrations of poly(dA)$_{80}$•poly(dT)$_{80}$ (Figure 5.74).
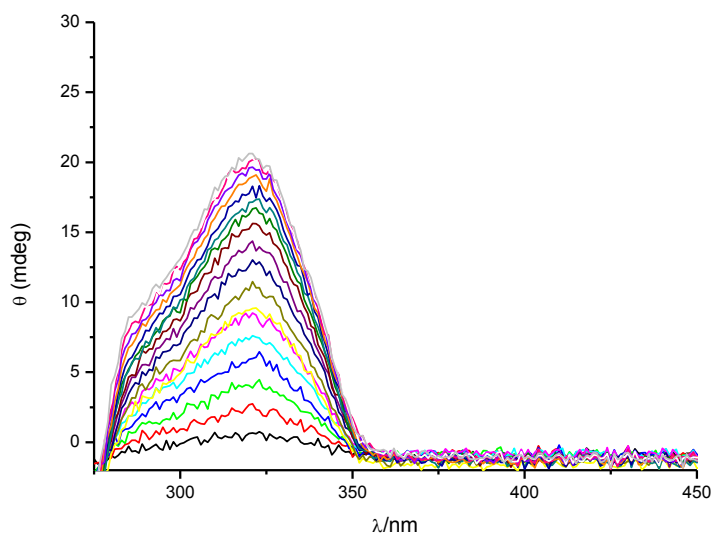
Figure 5.74 Induced circular dichroism spectra for 3.13×10^{-2} mM of **5.6** in the presence of varying concentrations of poly(dA)$_{80}$•poly(dT)$_{80}$ in buffer (25 mM MOPS, 50 mM NaCl and 1 mM EDTA, pH 7 at 25 °C).

Figure 5.74 shows induced circular dichroism at wavelengths above 300 nm for the interaction of **5.6** with poly(dA)$_{80}$•poly(dT)$_{80}$, in 25 mM MOPS, 50 mM NaCl and 1 mM EDTA, pH 7 at 25 °C. This result suggests a minor groove binding mode for **5.6** binding to poly(dA)$_{80}$•poly(dT)$_{80}$.

A binding isotherm (Figure 5.75) was extracted from the ICD titration data.
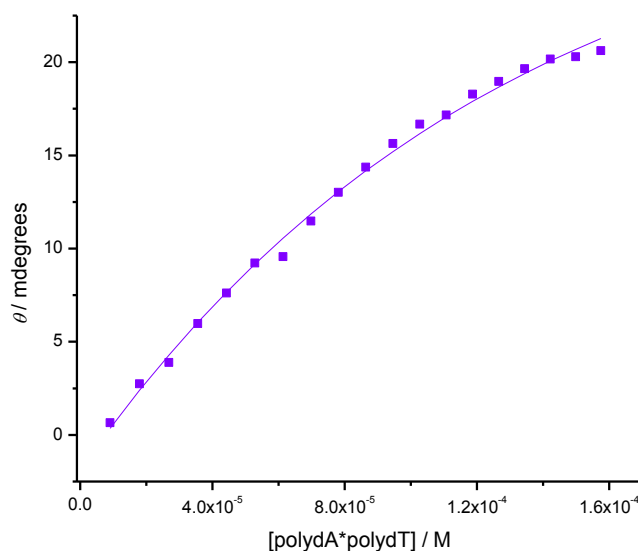
Figure 5.75 Ellipticity at ($\blacksquare$) 318 nm plotted against poly(dA)$_{80}$•poly(dT)$_{80}$ concentration, for **5.6** (3.13×10^{-2} mM) interacting with poly(dA)$_{80}$•poly(dT)$_{80}$, in 25 mM MOPS, 50 mM NaCl and 1 mM EDTA, pH 7.0, at 25 °C. Solid lines represent a global fit to a multiple independent sites model for the solution.

The data in the titration curve of Figure 5.75 were analysed using the same multiple independent binding sites model as used before. The binding constant (*K*) for **5.6** binding to poly(dA)$_{80}$•poly(dT)$_{80}$ is $(1.3 \pm 0.2) \times 10^4$ M^{-1} for a stoichiometry (*n*) restricted to 2 base pairs. The stoichiometry was restricted because the fit does not give reasonable parameters with variable stoichiometry.

Summary

Dicationic oligoheteroaromatic **5.6** binds to DNA binds with a binding constant of $(1.1 \pm 0.003) \times 10^7$ M^{-1} and a binding site size of 2.4 ± 0.2 base pairs. The interaction of tricationic **5.6** with CT DNA results in a positive ICD signal, suggesting binding of **5.6** in the minor groove. There is no further increase in the viscosity of a DNA solution upon addition of **5.6** following the customary initial increase, suggesting a minor groove

binding. The binding mode is supported by ITC, which shows two binding events for **5.6** interacting with DNA. Tricationic oligoheteroaromatic **5.6** bound to poly(dGdC)$_{40}$ without specific binding mode. On the other hand, **5.6** bound to poly(dA)$_{80}$•poly(dT)$_{80}$ with a minor groove binding mode. The driving forces for binding of **5.6** to DNA are again presumed to be as described for **5.1**.

5.4 Summary

UV-visible spectroscopy

The UV-visible titrations show that all synthesised cationic oligoheteroaromatic compounds **5.1**-**5.6** bind to duplex CT-DNA. The affinities of these compounds for CT-DNA are summarised in Table 5.5.

Table 5.5 Binding affinities and binding site sizes for binding of 5.1-5.6 to CT-DNA, in MOPS buffer, pH 7.0, at 25 °C.

Ligand	Binding constant K / M^{-1}	Binding site size n / bp
5.1	$(7.7 \pm 1.4) \times 10^4$	2.8 ± 0.2
5.2	$(1.1 \pm 0.5) \times 10^4$	1.4 ± 0.2
5.3	$(5.1 \pm 2.9) \times 10^4$	2.6 ± 0.7
5.4	$(1.4 \pm 0.1) \times 10^4$	2.5 ± 0
5.5	$(1.1 \pm 0.4) \times 10^6$	2 ± 0
5.6	$(1.1 \pm 0.002) \times 10^7$	2.3 ± 0.3

All oligoheteroaromatic compounds bind to CT-DNA with different affinity. The strongest binders are tricationic oligoheteroaromatics **5.5** and **5.6** with binding constants of ~10^6 and 10^7 M^{-1}. In contrast, dicationic oligoheteroaromatic compounds **5.1-5.4** have a moderate affinity ~10^4. The binding site sizes (in terms of basepairs) for all oligoheteroaromatic

compounds **5.1-5.6** equals almost half of the aromatic rings of the ligands. Because each ring covers approximately one base pair, this suggeststhat these ligands could bind to CT-DNA in the minor groove in "side-by-side" fashion.

Circular dichroism

In order to study the binding modes for the interaction of dicationic oligohetroaromatic compounds **5.1-5.4** and tricationic oligoheteroaromatics **5.5** and **5.6** with CT-DNA, we used circular dichroism spectroscopy. The results are summarised in Table 5.6.

Table 5.6 ICD data for binding of 5.1-5.6 to CT-DNA in MOPS buffer, pH 7.0, at 25 °C.

Ligand	ICD-Signal	Binding constant K/M^{-1}	Binding site size n / bp
5.1	Positive	$(3.4 \times \pm 0.2) \times 10^4$	1.5 ± 0
5.2	Positive	$(2.7 \times \pm 0.9) \times 10^5$	1.7 ± 0
5.3	Positive	$(1.7 \times \pm 0.6) \times 10^5$	1.7 ± 0
5.4	Positive	$(6.9 \times \pm 0.9) \times 10^3$	3 ± 0
5.5	Positive	$(7.3 \times \pm 0.4) \times 10^3$	3 ± 0
5.6	Positive	$(1.7 \times \pm 0.01) \times 10^4$	3.8 ± 0

An induced circular dichroism spectrum was recorded. For all the ligands a positive induced signal was observed and this signal increased with the addition of DNA during the titrations, suggesting that all these ligands are minor groove binders. The binding affinities of **5.1-5.6** from the CD titrations in the range between 10^3 to 10^5 are in reasonable agreement with the results from the UV-visible titrations. The binding site size for all ligands is restricted to a good fit for the titration curve.

Viscosity

The mode of the binding for di- and tricationic oligoheteroaromatic **5.1-5.6** with double-stranded CT-DNA was further studied by viscosimetry to confirm the conclusion from circular dichroism spectroscopy that these binders are all minor groove binder. Following an initial increase, further increases in the relative viscosity of CT-DNA solutions upon addition of ligands **5.1-5.6** were found to be negligible compared with a significant increase for ethidium bromide, confirming a predominant minor groove binding mode for all ligands.

Isothermal titration calorimetry (ITC)

The interactions of di- and tricationic oligoheteroaromatic **5.1-5.6** were further investigated by isothermal titration calorimetry. The results for all ligands are summarised in Table 5.7

Table 5.7 ITC parameters for binding of 5.1-5.6 to CT-DNA in MOPS buffer, pH 7.0, at 25 °C.

Ligand	binding events	$K_{A1,B1}$ (M^{-1})	$\Delta H_{A1,B1}$ $(cal\ mol^{-1})$	$-T \times \Delta S_{A1,B1}$ $(kcal\ mol^{-1})$	$1/n_{A1,B1}$ (base pairs)
5.1	3	multiple binding events			
5.2	3	multiple binding events			
5.3	1	217×10^4	-3.18×10^3	-2.73×10^3	1.6
5.4	2	1.34×10^6	-1.41×10^3	-6.95×10^3	2.1
		5.69×10^5	7.32×10^3	-13.80×10^3	0.40
5.5	2	1.89×10^9	-2.63×10^3	-6.88×10^3	4.6
		9.22×10^5	-2.25×10^3	-14.30×10^3	1.2
5.6	2	2.66×10^6	-1.62×10^2	-9.88×10^3	2.4
		6.42×10^5	-3.75×10^3	-5.33×10^3	0.90

The enthalpograms for dicationic oligoheteroaromatic **5.1** and **5.2** interacting with DNA indicate three binding events, therefore the data is too complex to be analysed. Dicationic oligoheteroaromatic **5.3** binds to CT-DNA with an affinity of ~10^4 M^{-1}. The binding site size is 1.6 with only one type of binding event. The binding is characterised by negative enthalpy and entropy change. On the other hand, **5.4**, **5.5** and **5.6** bind to CT- DNA with high affinities of between 10^5 M^{-1} to 10^9 M^{-1}. The binding site sizes as shown in the table. The binding is characterised by negative enthalpy and entropy change. These ITC results are also in agreement with a minor groove binding mode for the ligands **5.3, 5.4, 5.5** and **5.6**.

Sequence selectivity

An important goal in our project is to explore sequence selectivity of the synthesised cationic oligoheetroaromatic compounds **5.1**-**5.6** with different DNA sequences, such as poly(dGdC)$_{40}$ and poly(dA)$_{80}$•poly(dT)$_{80}$. The affinities for these sequences were studied using UV-visible and circular dichroism spectroscopy. The results are summarised in Tables 5.8 and 5.9.

Table 5.8 Binding parameters from UV-visible spectroscopic titrationsfor 5.1-5.6 binding to poly(dGdC)$_{40}$ and poly(dA)$_{80}$•poly(dT)$_{80}$, in MOPS buffer, pH 7.0, at 25 °C.

Ligand	poly(dGdC)$_{40}$		poly(dA)$_{80}$•poly(dT)$_{80}$	
	Binding constant K/M^{1}	*Binding site size n / bp*	*Bindingconstant K/M^{1}*	*Binding site size n / bp*
5.1	$(4.1 \pm 0.8) \times 10^4$	2 ± 0	$(1.2 \pm 0.3) \times 10^6$	4.0 ± 0.1
5.2	$(2.2 \pm 0.9) \times 10^4$	1 ± 0.26	$(3.4 \pm 1.18) \times 10^6$	2.5 ± 0.03
5.3	$(1.6 \pm 0.001) \times 10^6$	2 ± 0	$(1.6 \pm 0.001) \times 10^3$	2 ± 0
5.4	n.d.[a]	n.d.[a]	$(3.2 \pm 1.25) \times 10^5$	3.9 ± 0.1
5.5	$(1.3 \pm 0.1) \times 10^5$	1.3 ± 0.06	n.d.[a]	n.d.[a]
5.6	$(1.5 \pm 0.1) \times 10^5$	2.2 ± 0.07	$(1.5 \pm 0.6) \times 10^4$	2.2 ± 0.2
a) not determined				

All ligands **5.1-5.3, 5.5** and **5.6** bind to poly(dGdC)$_{40}$ (no titration was carried out for **5.4**). The binding affinities are between 10^4 and 10^6 M^{-1} which is a good affinity. The binding site size for ligands **5.1-5.6** is between 1 to 2 base pairs. The binding site sizes are surprisingly small.

Also, all the ligands **5.1-5.6** strongly bound to poly(dA)$_{80}$•poly(dT)$_{80}$ with binding affinities between 10^5 to 10^6 M^{-1}. The binding site sizes for the ligands **5.1-5.6** is between 2 to 4 base pairs. The binding affinity and the binding site size for the ligands bound to poly(dA)$_{80}$•poly(dT)$_{80}$ is higher than the affinities for poly(dGdC)$_{40}$.

The mode of the interaction of the ligands to the different sequences was investigated by circular dichroism.

Table 5.9 Binding parameters from circular dichroism spectroscopy for 5.1-5.6 binding to poly(dGdC)40 and poly(dA)$_{80}$•poly(dT)$_{80}$, in MOPS buffer, pH 7.0, at 25 °C.

Ligand	poly(dGdC)$_{40}$		Poly(dA)$_{80}$•poly(dT)$_{80}$	
	ICD-Signal	*ICD-Signal*	*Binding constant K / M^{-1}*	*Binding site size n / bp*
5.1	*No signal*	*Positive*	$(1.4 \pm 0.9) \times 10^6$	4.5 ± 0.2
5.2	*No signal*	*Positive*	$(2.9 \pm 0.9) \times 10^5$	2 ± 0
5.3	*No signal*	*Positive*	$(3.4 \pm 0.3) \times 10^5$	3 ± 0
5.4	*No signal*	*Positive*	$(1.1 \pm 0.1) \times 10^4$	2 ± 0
5.5	*No signal*	*Positive*	$(1.5 \pm 0.2) \times 10^6$	4.4 ± 0
5.6	*No signal*	*Positive*	$(1.3 \pm 0.2) \times 10^4$	2 ± 0

The results in Table 5.9 indicate that none of the ligands **5.1-5.6** show induced circular dichroism when interacting with poly(dGdC)$_{40}$. This suggests there are no particularly intimate interactions between the ligands and poly(dGdC)$_{40}$. In contrast, the ligands **5.1-5.6** show positive ICD together with with high affinities of around 10^6 M^{-1} when interacting with poly(dA)$_{80}$•poly(dT)$_{80}$, suggesting selectivity for binding in the minor groove of poly(dA)$_{80}$•poly(dT)$_{80}$.

5.5 Conclusions

All cationic oligoheteroaromatics **5.1-5.6** bind to DNA. The binding is accompanied by bathochromic (red shift) in the UV-visible absorption. This bathochromic shift can be explained through increased effective conjugation length upon interaction with DNA. The binding constants for **5.1-5.6** are in the range of between 10^4 to 10^7 M^{-1}. The binding affinities for dicationic oligoheteroaromatic **5.1-5.4** are $\sim 10^4$ M^{-1}. On the other hand, tricationic oligoheteroaromatic **5.5-5.6** interact more strongly with DNA with binding constants $\sim 10^7 \, M^{-1}$, showing the importance of increasing the hydrophobic surface and the cationic charge. The binding site sizes for **5.1-5.6** are between 2-2.8 base pairs. These binding sites appear quite small, equalling approximately half the number of aromatic rings in the ligands in number, suggesting that the binders may bind to DNA according to a "side by side" mode, although the difference with the binding site sizes found for poly(dGdC)$_{40}$ and poly(dA)$_{80}$•poly(dT)$_{80}$ suggests that further complexities may play a role as well.

Circular dichroism spectroscopy showed that all cationic oligoheteroaromatics **5.1-5.6** show a positive ICD signal and high affinities, which was explained by a minor groove binding mode. The binding mode was further investigated using viscosimetry. All ligands **5.1-5.6** cause an initial relatively small increase in viscosity, followed by negligible further increases in relative viscosity compared with the known intercalator ethidium bromide which causes a significant increase in viscosity. These results confirm the minor groove binding modes for these ligands. Isothermal titration calorimetry indicates three binding events for **5.1** and **5.2** binding to CT-DNA. Precipitation was observed at the end of these titrations, which was attributed to DNA-ligand complexes sticking together in the solution; this aggregation is the result of the negative charges on the DNA being

neutralised by the positive charges on the ligands. Compound **5.3** shows one DNA binding event with thermodynamic parameters suggesting a minor groove binding mode. In contrast, **5.4-5.6** show two distinct binding types with the highest affinity binding event accompanied by negative enthalpy and entropy, in agreement with minor groove binding.

The driving forces for **5.1-5.6** binding to DNA could be provided by hydrophobic interactions between the conjugated aromatic framework and hydrophobic walls of the minor groove, in combination with electrostatic interaction between the cationic charge on the ammonium group and the negative charges on DNA. Also, there is a possibility of forming a hydrogen bond between nitrogen atoms on the triazole ring and hydrogen bond donors on the DNA base pairs.

5.6 Materials and Methods

DNA preparation

The synthesis of all di- and tricationic oligoheteroaromatic compounds and full characterisation are described in Chapter 4. The buffer components were purchased from Acros and Sigma-Aldrich. All experiments were carried out in buffer (25 mM MOPS, 50mM NaCl and 1 mM EDTA). Buffer was titrated by an aqueous solution of sodium hydroxide NaOH to pH 7.0. The pH of the buffer was determined using a Hanna Instruments pH 210 pH meter equipped with a VWR 662-1759 glass electrode. Calf thymus DNA was purchased from Sigma-Aldrich. A stock solution of calf thymus DNA was prepared by sonicating a solution of CT-DNA in buffer for 30 minutes. The DNA solution was dialysed against 2 litres of buffer using 3.5 kDa MWCO dialysis membrane for 2 days. The dialysis buffer was changed after 1 day. The concentration of calf thymus

DNA was determined by UV-visible spectroscopy using an extension coefficient of 12824 $M^{-1}cm^{-1}$ at 260 nm^{14}.

Spectroscopic studies

UV-visible spectra were recorded using a Jasco V-630Bio UV-visible spectrophotometer with a Peltier temperature controller at 25 °C. Circular dichroism spectra were recorded on a Chirascan CD spectrophotometer. Stock solutions **5.1-5.6** were prepared in buffer and used as fresh solutions. Concentrations were determined using the extinction coefficients of **5.1-5.6** of $(29.47 \pm 1.1) \times 10^3$, $(17.15 \pm 1.2) \times 10^3$, $(18.92 \pm 0.5) \times 10^3$, $(18.20 \pm 0.33) \times 10^3$, $(20.48 \pm 0.3) \times 10^3$ and $(19.35 \pm 0.18) \times 10^3$ dm^3 mol^{-1} cm^{-1} respectively. (see Appendix). All UV-visible titrations were carried out in a 1 cm path length cuvette by adding aliquots of the DNA stock solution to the ligand solution in the cuvette, measuring the absorption after every addition in the range of 200-600 nm. The multiple independent binding sites model was used to analyse the UV-visible spectra by Origin 7.5, plotting absorptions at selected wavelengths against DNA concentration, but also taking binder concentrations into account. The same steps were followed for CD titrations, using ICD signals instead of absorptions in UV-visible titrations.

Viscometry

All viscosimetry experiments were carried out in buffer (25 mM MOPS, 50mM NaCl and 1 mM EDTA). A Cannon-Fenske routine viscometer was used and the flow time of the solutions was measured with the viscometer immersed in a temperature-controlled circulated water bath at 25 °C. All the solutions were prepared and mixed in small glass vials. Each time, the viscometer was filled with a fixed volume of solution of 6 ml, changing the ligand concentration but keeping the DNA concentration constant in each experiment. The flow time was measured three times for each sample and the results were

averaged. The relative viscosity was calculated and plotted against the ratio of [complex] / [DNA].

Isothermal titration calorimetry

All ITC experiments were carried out using a Microcal VP ITC microcalorimeter. The ligand solutions were prepared in buffer (25 mM MOPS, 50 mM NaCl and 1 mM EDTA). All the concentrations were determined by UV-visible spectroscopy based on the extinction coefficients (*vide supra*). The sample cell and the syringe were cleaned with distilled water before starting any experiment. The sample cell was filled with a CT DNA solution (approximately 1.86 ml). The syringe was filled with ligand solution with a concentration significantly higher than the DNA solution (exact ratios depend on the individual experiments). The ligand solution was then added in 27 injections of 10 μl each to the sample cell, automatically, injecting every 400 seconds at 25 $^\text{O}$C. The heat effects per injection (dh) were calculated using Origin (Microcal, Inc). The in-house developed program IC ITC was used to analyse these heat effects.

References

1. John W. Moore, R. G. P. a. A. A. F., *Kinetics and Mechanism;*. John Wiley and Sons: 1981.

2. Donald L. Pavia, G. M. L. a. G. S. K., *Introduction to spectroscopy*. Washington, 2001.

3. Garbett, N. C.; Ragazzon, P. A.; Chaires, J. B., *Nature Protocols* **2007,** *2* (12), 3166-3172.

4. Eriksson, M. N., B, *Drug-Nucleic Acid Interactions* **2001,** *340*, 68-98.

5. Satyanarayana, S.; Dabrowiak, J. C.; Chaires, J. B., *Biochemistry* **1993,** *32* (10), 2573-2584.

6. Suh, D.; Chaires, J. B., *Bioorg. Med. Chem.* **1995,** *3* (6), 723-728.

7. Cohen, G.; Eisenber.H, *Biopolymers* **1969,** *8* (1), 45-&.

8. Bjelic, S.; Jelesarov, I., *Journal of Molecular Recognition* **2008,** *21* (5), 289-311.

9. Jelesarov, I.; Bosshard, H. R., *Journal of Molecular Recognition* **1999,** *12* (1), 3-18.

10. Buurma, N. J.; Haq, I., *Methods* **2007,** *42* (2), 162-172.

11. Buurma, N. J.; Haq, I., *Journal of Molecular Biology* **2008,** *381* (3), 607-621.

12. Press, W. H. F., B. P.; Teukolsky, S. A.; Vetterling, W. T.,, *Teukolsky, S. A.; Vetterling, W. T., Numerical Recipes in Pascal*. 2004.

13. Chaires, J. B., *Archives of Biochemistry and Biophysics* **2006,** *453* (1), 26-31.

14. Ren, J. S.; Chaires, J. B., *Biochemistry* **1999,** *38* (49), 16067-16075.

EPILOGUE

Abstract

This chapter describes the synthesis of selected extended cationic oligoheteroaromatic compounds and their subsequent investigation as DNA binders using UV-visible and circular dichroism spectroscopy. The Chapter finishes with general conclusions arising from this study and the outlook for future work.

6.1. Introduction

In addition to the work detailed in previous chapters, this study has also conducted the synthesis and investigation of certain specific cationic oligoheteroaromatic compounds as DNA binders. This chapter also includes general conclusions from the work and a commentary on possible future work.

6.2 Synthetic studies

6.2.1. Synthesis of di-cationic oligoheteroaromatic 6.3

Dicationic **6.3** was synthesised according to Scheme 6.1. The first step involves the reaction of 1 equivalent of 1,4-diethynylbenzene **2.23** with 2 equivalents of 2-(2-(4-azidophenyl)thiophen-3-yl)ethanol **3.6** in the presence of copper iodide as catalyst. Triethylamine was used as a base in the reaction and the solvent used was EtOH: H_2O (1:1) at 60 ^{O}C. Compound **6.1** was obtained in 67% yield. Subsequent to the click reaction, conjugated oligoheteroaromatic **6.2** was prepared using an Appel reaction for the conversion of the hydroxyl groups into the bromides. The compound was reacted with an excess of carbon tetrabromide and triphenylphosphine at 0 ^{O}C under a nitrogen atmosphere in extra dry DCM, which resulted in **6.2** being obtained in 48% yield. Compound **6.2** was then synthesised through the conversion of **6.2** into the corresponding quaternary ammonium salt by adding trimethylamine in ethanol to **6.2** and allowing to react at room temperature for 5 days, producing **6.3** in poor yield (Scheme 6.1).
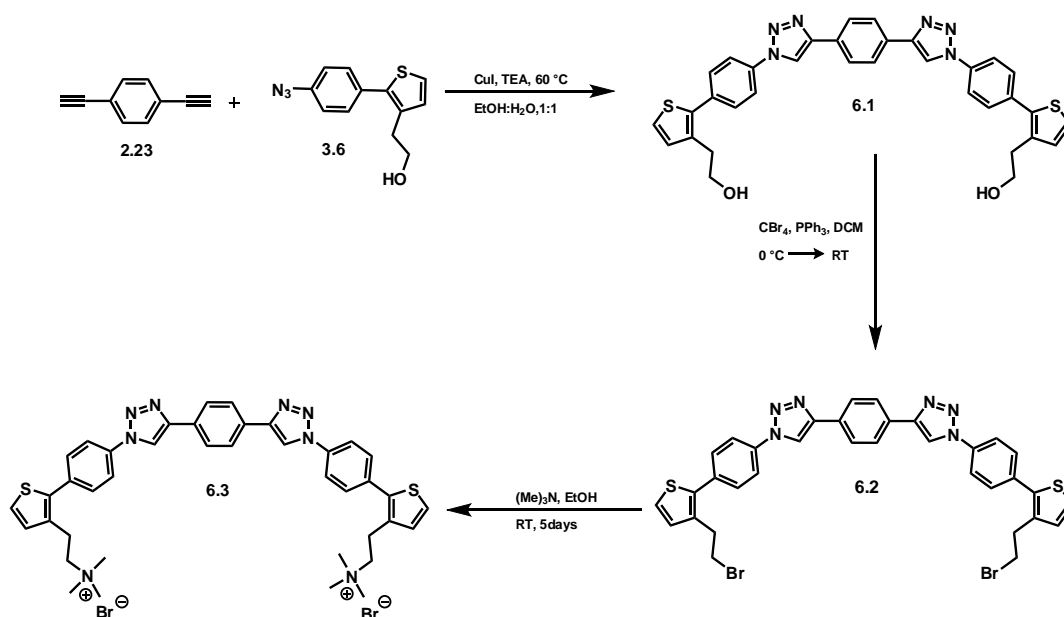
Scheme 6.1

6.2.2. Synthesis of mono-cationic oligoheteroaromatic compound 6.6

The preparation of **6.6** involved the same synthetic strategy utilised in **6.3**, (Scheme 6.2).
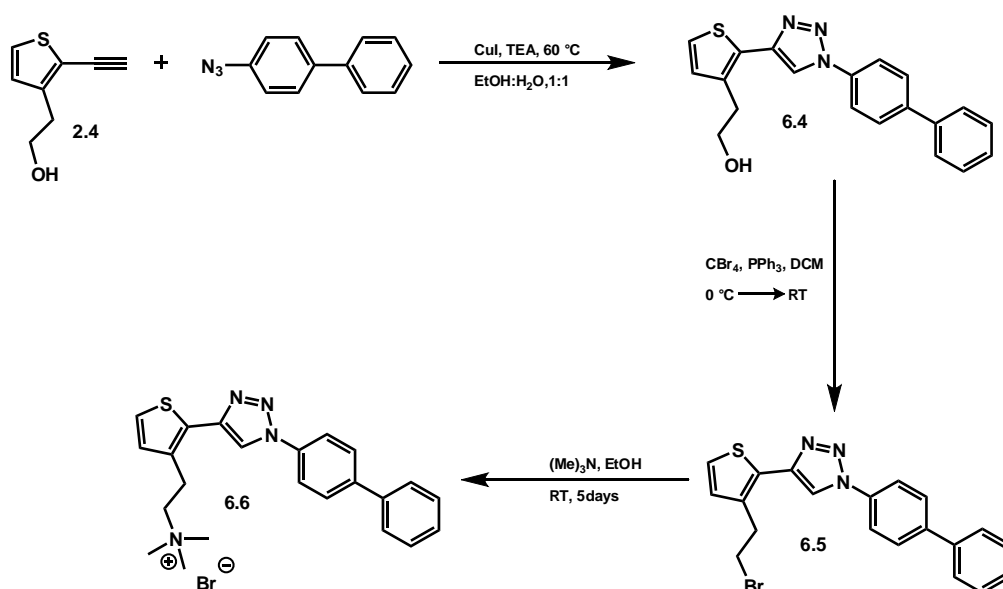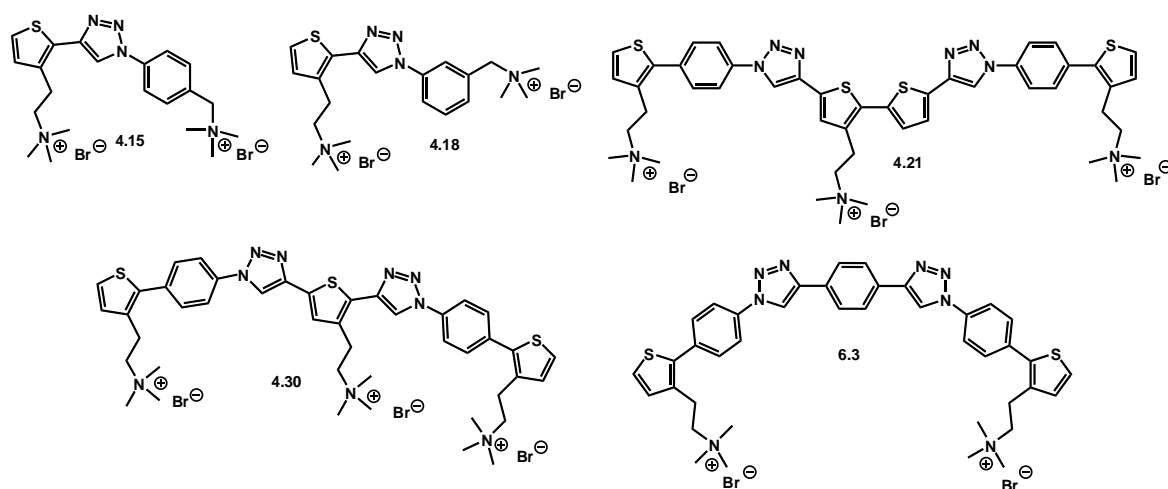

Scheme 6.2

Firstly, reacting 1 equivalent of 2-(2-ethynylthiophen-3-yl)ethanol **2.4** with 1 equivalent of 4-azidobiphenyl afforded desired **6.4** in 61% yield. Subsequent use of the Appel reaction allowed the conversion of the hydroxyl group into the bromide, returning **6.5** in 49% yield. The final step involved the conversion of bromide **6.5** into the corresponding quaternary ammonium salt by means of a substitution reaction involving the addition of trimethylamine in ethanol to **6.5** at room temperature, allowing to react for 5 days resulting in **6.6** in 67% yield.

6.3. Binding studies of cationic oligoheteroaromatics

The DNA binding of several cationic heteroaromatics (Scheme 6.3) was studied.

Scheme 6.3

6.3.1. Dicationic oligoheteroaromatic 4.15 binding to DNA

UV-visible spectroscopy

The binding of oligoheteroaromatic **4.15** to calf thymus was studied with the use of UV-visible spectroscopy. The changes in absorption of **4.15** upon the addition of calf thymus DNA were measured in a buffer (25 mM MOPS, 50 mM NaCl and 1 mM EDTA) at 25 °C (Figure 6.1).
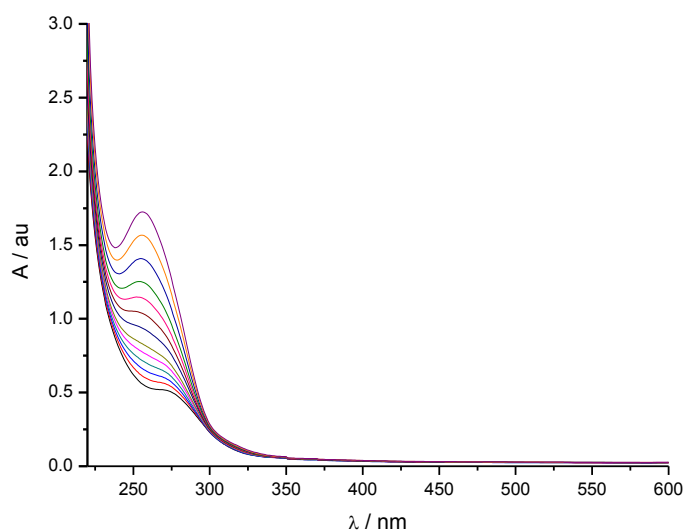
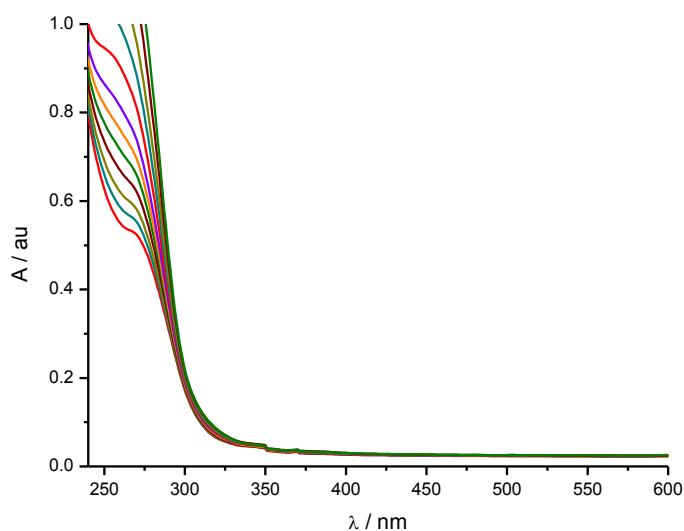**Figure 6.1** UV-Visible spectrum for of **4.15** in the presence of 3 mM calf thymus DNA in buffer 25 mM MOPS, 50 mM NaCl and 1 mM EDTA, pH 7 at 25 °C.

Figure 6.1 demonstrates that the absorbance of **4.15** overlaps the absorbance of DNA and no new peaks appear at wavelengths higher than 300 nm. Therefore, no change in the absorbance can be analysed to quantify the binding constant and the binding site size.

Circular dichroism

An attempt to explore the binding mode for the interaction of **4.15** with calf thymus DNA was carried out using circular dichroism spectroscopy (Figure 6.2).
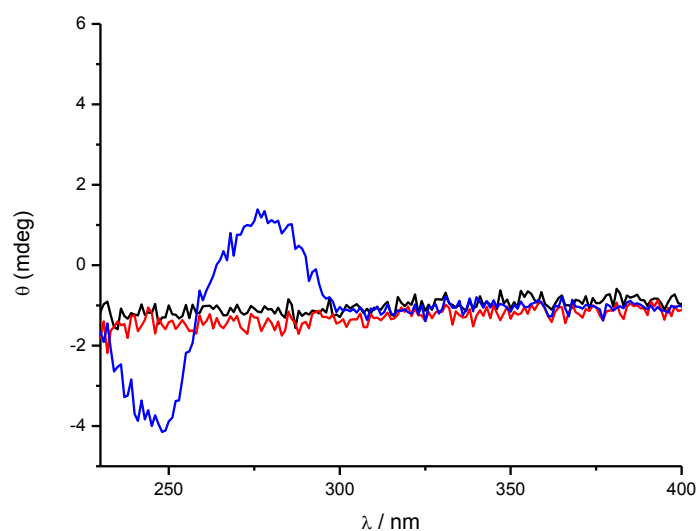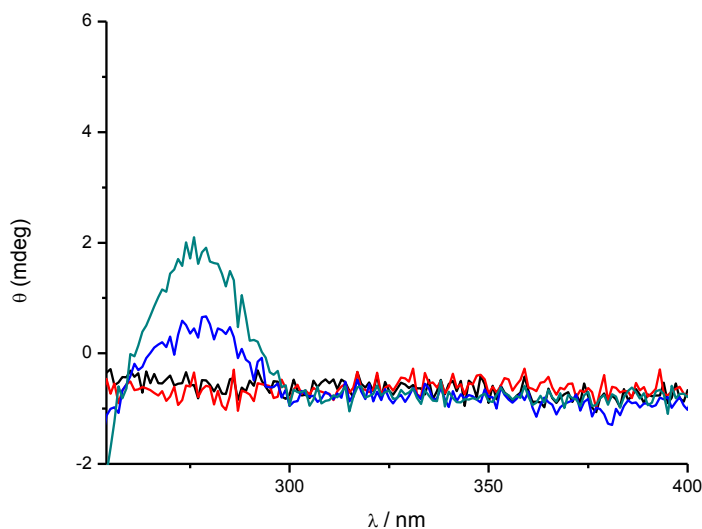

Figure 6.2 Circular dichroism spectra for 3.6×10^{-2} mM **4.15** in the presence of a 3 mM calf thymus DNA in buffer (25 mM MOPS, 50 mM NaCl and 1 mM EDTA, pH 7) at 25 ^{O}C.

Figure 6.2 illustrates the circular dichroism spectra for the interaction of **4.15** with calf thymus DNA, which was conducted in 25 mM MOPS, 50 mM NaCl and 1 mM EDTA, pH 7 at 25 ^{O}C. No induced circular dichroism spectrum is observed (the blue line represents the circular dichroism spectrum of calf thymus DNA.[1]

6.3.2. Dicationic oligoheteroaromatic 4.18 binding to DNA

UV-visible spectroscopy

The binding of oligoheteroaromatic **4.18** to calf thymus was studied using UV-visible spectroscopy. The absorption spectra of a solution of 5.4×10^{-2} mM **4.18** upon addition of calf thymus DNA were measured in buffer which consist of 25 mM MOPS, 50 mM NaCl and 1 mM EDTA at 25 °C (Figure 6.3).

Figure 6.3 UV-Visible spectra for 5.4×10^{-2} mM **4.18** in the presence of a 3 mM calf thymus DNA in buffer 25 mM MOPS, 50 mM NaCl and 1 mM EDTA, pH 7 at 25 °C.

Figure 6.3 shows that the absorbance of the ligand **4.18** overlaps with the spectrum of DNA. Therefore, there is no change in the absorbance that can be analysed in order to quantify the binding constant and the binding site size.

Circular dichroism

In an attempt to study the binding mode for the interaction of **4.18** with calf thymus DNA, circular dichroism spectroscopy was utilised. The induced circular dichroism spectrum was recorded, as illustrated in Figure 6.4.

Figure 6.4 Circular dichroism spectra for a solution of 3.2×10^{-2} **4.18** in the presence of a 3 mM calf thymus DNA in buffer 25 mM MOPS, 50 mM NaCl and 1 mM EDTA, pH 7 at 25 ^{O}C.

Figure 6.4 shows no induced circular dichroism for the interaction of **4.18** with calf thymus DNA, in 25 mM MOPS, 50 mM NaCl and 1 mM EDTA, pH 7 at 25 ^{O}C. As before, only the circular dichroism spectrum intrinsic to DNA is observed.

6.3.3. Tricationic oligoheteroaromatic 4.21 binding to DNA

UV-visible spectroscopy

The binding of oligoheteroaromatic **4.21** to calf thymus was studied using UV-visible spectroscopy. The changes in absorption of **4.21** upon the addition of calf thymus DNA

259

were measured in a buffer that consisted of 25 mM MOPS, 50 mM NaCl and 1 mM EDTA at 25 °C (Figure 6.6). A precipitate was formed upon the additions of DNA solution during the titration. Although this suggests that **4.21** strongly binds to DNA, there is no possibility to analyse the titration curve in order to quantify the binding constant and the binding site size.
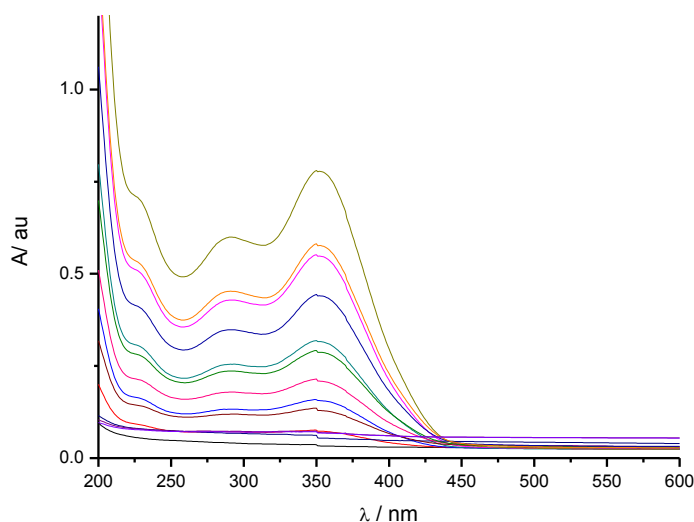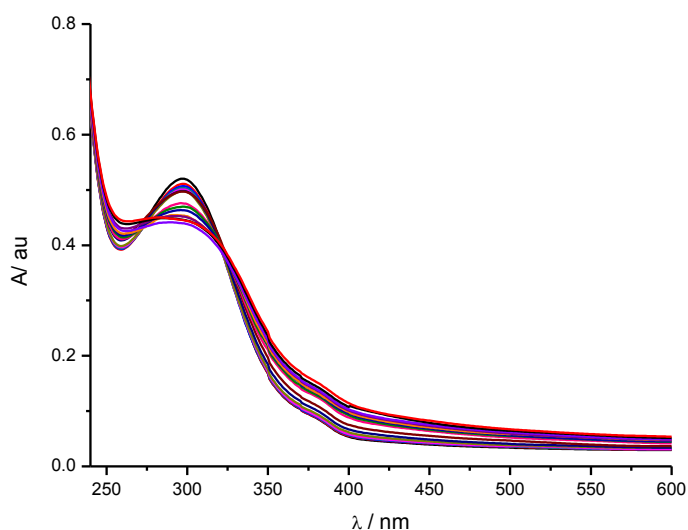

Figure 6.5 UV-Visible spectra for a 3.2×10^{-2} mM solution of **4.21** in the presence of a 5.2 mM calf thymus DNA in buffer 25 mM MOPS, 50 mM NaCl and 1 mM EDTA, pH 7 at 25 °C.

6.3.4. Dicationic oligoheteroaromatic 6.3 binding to DNA

UV-visible spectroscopy

The binding of oligoheteroaromatic **6.3** to calf thymus was studied with the use of UV-visible spectroscopy. The changes in absorption of **6.3** that occurred upon the addition of calf thymus DNA were measured in a buffered solution (25 mM MOPS, 50 mM NaCl and 1 mM EDTA) at 25 °C (Figure 6.6).
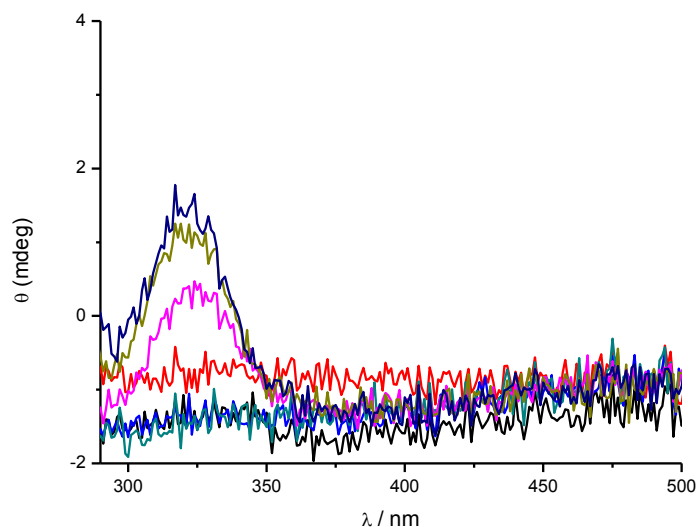
Figure 6.6 UV-Visible spectrum for **6.3** in the presence of of calf thymus DNA in buffer 25 mM MOPS, 50 mM NaCl and 1 mM EDTA, pH 7 at 25 °C.

Figure 6.6 illustrates that the base line in the UV-visible spectra increases even at high wavelengths. We attribute this to the formation of a fine precipitate that formed upon the addition of DNA solution during the titration. This suggests that compound **6.3** strongly binds to DNA, although it is impossible to analyse the titration curve in order to quantify the binding constant and the binding site size.

Circular dichroism

In order to study the binding mode for the interaction of **6.3** with calf thymus DNA, circular dichroism spectroscopy was used (Figure 6.7).

Figure 6.7 Circular dichroism spectra for of **6.3** in the presence of calf thymus DNA in buffer 25 mM MOPS, 50 mM NaCl and 1 mM EDTA, pH 7 at 25 ^{O}C.

Figure 6.7 again shows no signs of induced circular dichroism.

6.3.5. Ticationic oligoheteroaromatic 4.30 binding to DNA

UV-visible spectroscopy

The binding of oligoheteroaromatic **4.30** to calf thymus was studied using UV-visible spectroscopy. The changes in absorption of **4.30** that occurred upon the addition of calf thymus DNA were measured in a buffer that consisted of 25 mM MOPS, 50 mM NaCl and 1 mM EDTA at 25 °C. Figure 6.9 shows the absorbance spectra with increasing DNA concentration.
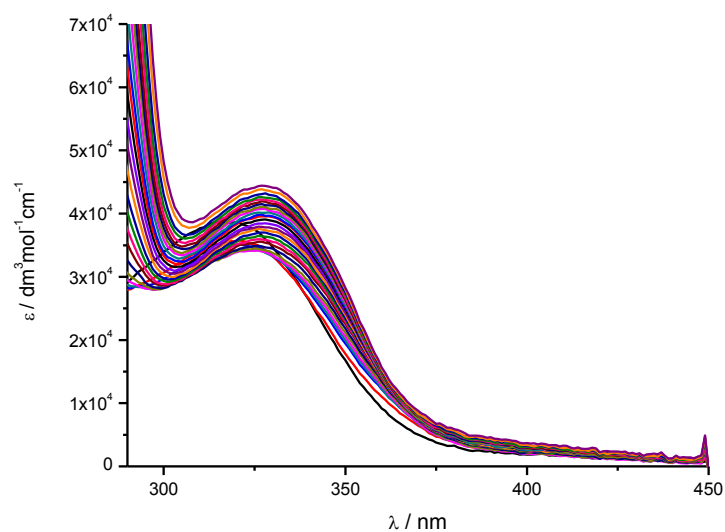
Figure 6.8 UV-visible spectra for 1.13×10^{-2} mM dicationic oligoheteroaromatic **4.30** upon addition of a 3.5 mM calf thymus DNA in 25 mM MOPS, 50 mM NaCl and 1 mM EDTA, pH 7.0, at 25 °C.

As can be seen from Figure 6.8, the maximum absorption of the free ligand decreases, while the maximum absorption of the complex increases. DNA-binding of **4.30** is accompanied by a bathochromic shift. The binding isotherm in Figure 6.9 was extracted from the UV-visible data to show the binding of **4.30** to DNA.
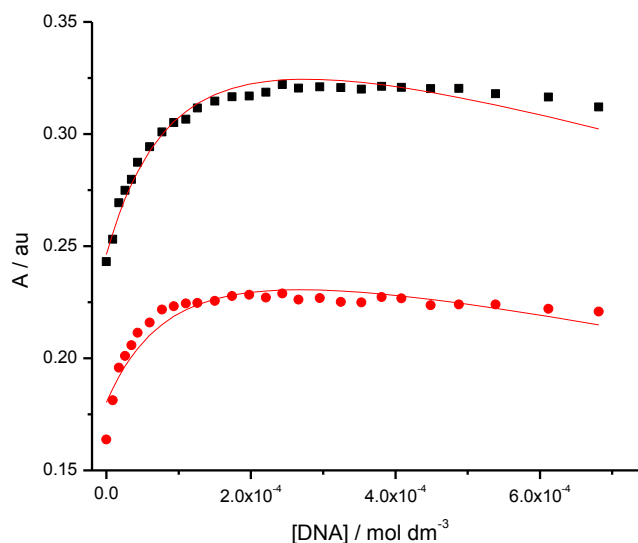
Figure 6.9 Absorbance at (■) 347 nm and (●) 355 plotted against DNA concentration, solid lines represent a global fit to a multiple independent sites model, for a solution of **4.30** (1.13×10^{-2} mM), in 25 mM MOPS, 50 mM NaCl and 1 mM EDTA, pH 7.0, at 25 °C.

The binding constant (K) for **4.30** binding to DNA is $(2.9 \pm 0.4) \times 10^{4}$ M^{-1} for a stoichiometry (n) restricted to 2.5. This result suggests that **4.30** binds to DNA with an affinity that is close to the affinity of all ligands described in chapter 5.

Circular dichroism

The binding mode for the interaction of **4.30** with calf thymus DNA was studied by means of circular dichroism spectroscopy (Figure 6.10).
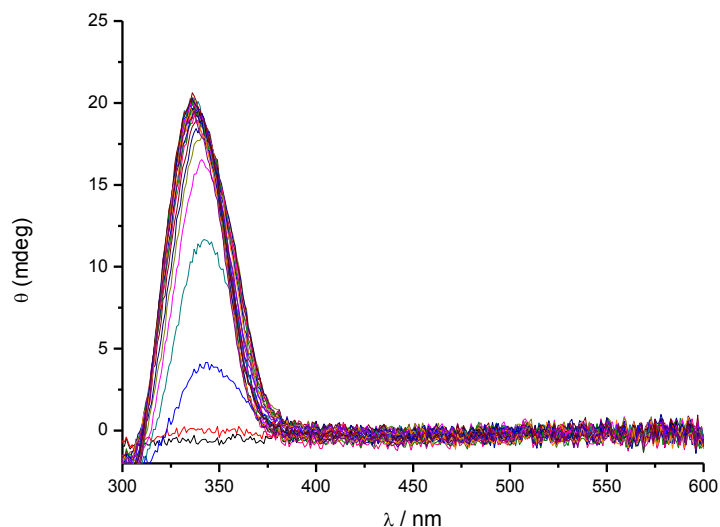
Figure 6.10 Induced circular dichroism spectra for 1.2×10^{-2} mM **4.30** in the presence of 3.5 mM of calf thymus DNA in buffer 25 mM MOPS, 50 mM NaCl and 1 mM EDTA, pH 7 at 25 ^{O}C.

Figure 6.10 illustrates the induced circular dichroism for the interaction of **4.30** with calf thymus DNA, in 25 mM MOPS, 50 mM NaCl and 1 mM EDTA, pH 7 at 25 ^{O}C. A positive signal at 342 nm is observed, which increased upon the addition of DNA during the titration. This positive signal suggests that **4.30** is a minor groove binder.

Conclusion epilogue

The triazole ring is not a good element for extending conjugated systems; short systems do not show absorbances above 300 nm, making binding studies difficult. Highly cationic systems appear to bind very strongly but also cause precipitation.

6.4. Conclusions

The main aim of this work was to identify how to design and synthesise large numbers of new molecules that hopefully combine some of the suitable properties of Dervan's polyamides and conjugated polymers. This thesis describes our approach to the indentification of novel binders through the synthesis of cationic oligoheteroaromatic compounds using click chemistry. The synthesic aspects of the work were presented in Chapters 2, 3 and 4. Click chemistry was found to be an excellent methodology to make various structures that can be tested for binding to DNA. Of particular interest is the triazole ring, a product of click reaction,[2] and was an interesting link in our strategy for the binding affinity to DNA.

The second part of this thesis describes the binding of these molecules as studied by different techniques. We determined both the affinities and the modes of binding to ds-DNA. Based on our results for cationic oligoheteroaromatics interacting with ds-DNA, increasing the conjugation long and the cationic charge of the oligoheteroaromatic chain results in stronger binders to ds-DNA. The inclusion of one or more triazole rings in the oligoheteroaromatic could also lead to the formation of more hydrogen bonds between the ligand and the DNA base pairs; however, we have no clear-cut evidence for this.

In respect of selectivity, all our binders were found to bind in the minor groove of DNA, which was the main target of this work. The sequence selectivity studies indicated that cationic oligoheteroaromatic molecules **5.1-5.6** prefer A•T-rich DNA – in fact, our ligands bind to poly$(dA)_{80}$•poly$(dT)_{80}$ with very high affinity. In contrast, there is very limited to no affinity for G•C-rich DNA which could be due to the hindrance effect of NH_2. This suggests a potentially significant challenge for the future development of our binders to bind selectively to G•C, in line with findings by others (See Chapter 1).

In summary, Chapter 6 has described the synthesis of more cationic oligoheteroaromatic compounds. Additionally, this Chapter has demonstrated and discussed some binding studies for several ligands. As explained, it was not possible to interpret the binding of these ligands with DNA for different reasons; precipitation for the long compounds **4.21-6.3** and spectral overlap for ligands **4.15 - 4.18** with DNA.

6.5. Suggestions for future work

In the short term, further physical studies should be conducted on our oligoheteroaromatic compounds, which could potentially open routes to discover new applications. First and foremost, self aggregation should be studied by diffusion NMR (PGSE NMR). Such diffusion NMR studies would ideally be complemented by small-angle neutron scattering to confirm the mode of self aggregation and the shape of the aggregates in aqueous solutions for all cationic oligoheteroaromatic compounds that were synthesised.

In the longer term, the synthesis of potential DNA binders should be continued based on our experience in this study, in order to develop and design new ligands. The ultimate goal of this investigative process will be the preparation of sequence-selective oligoheteroaromatics that bind to DNA, in the hope that this could lead to application of this type of compound as drugs and biosensors. Other important future goals include the synthesis of various molecules that possess biological and pharmacological activities, exploring their potential application and use in the medical field.

Based on our studies we found click chemistry is an effective method to synthesis various types of oligoheteroarmatic compounds, but triazole ring is not a good element for extending conjugated systems to study the binding to DNA, therefore our next goal for the synthesis is to use different aromatic rings such as Pyrroles, Imidazoles and oxazoles. Also for the number of aromatic rings we will try to make short aromatic system between 4-6
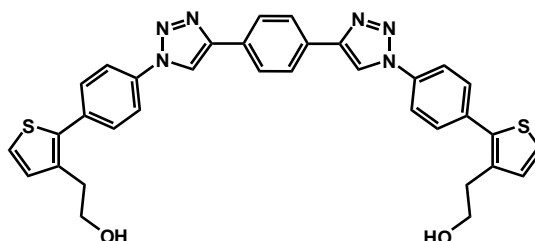
rings as well as less cationic charge to avoid any difficulties for the solubility and the precipitation.

As we noticed that binding site size is not compatible with the length of oligoheteroarmatic compounds, so we plan to prepare dimeric molecules in attempt to force the molecules to bind in side-by-side manner.
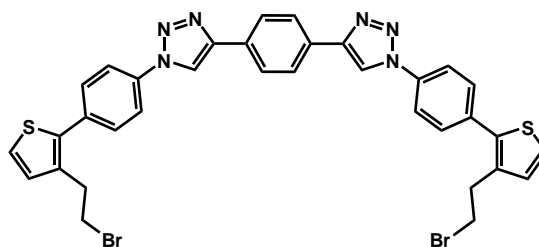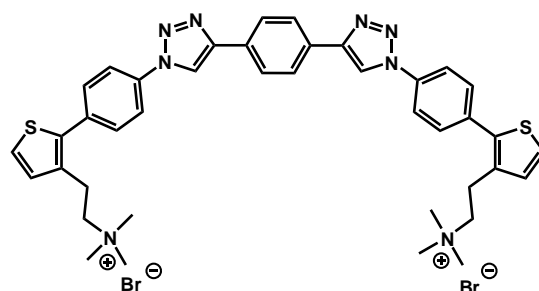
6.6 Experimental

6.6.1 Synthesis

Synthesis of **6.1**

The experimental procedures selected for the synthesis of **6.1** were as described for the synthesis of **4.1**. 1,4-Diethynylbenzene **2.23** (0.05g, 0.39 mmol) was reacted with 0.19 g (0.79 mmol) of 2-(2-(4-azidophenyl)thiophen-3-yl)ethanol **3.6**. 0.16 g of compound **6.1** was obtained after filtration without further purification as a brown powder (67% yield).

^{1}H-NMR (DMSO, 400 MHz, ppm): 9.43 (s, 2H), 8.1 (s, 4H), 8.0 (d, *J*=8.1, 4H), 7.76 (d, *J*=8.1, 4H), 7.56 (d, *J*=4.9, 2H), 7.14 (d, *J*=4.9, 2H), 4.79 (s, 2H), 3.6 (q, *J*=5.9, 4H), 2.82 (t, *J*=6.2, 4H). **^{13}C-NMR (d6-DMSO, 126 MHz, ppm)**: 160.64, 133.15, 129.11, 128.05, 126.19, 125.89, 124.87, 124.16, 121.00, 47.59, 12.08. **HRMS (EI)** calcd for [$C_{34}H_{29}N_6O_2S_2$] (M$^+$+H) 617.1793 found 617.1771.

Synthesis of **6.2**

The experimental procedure used for this reaction was as described for **4.2**. 0.25 g (0.40 mmol) **4.13** of was reacted with 0.53 g (1.6 mmol) of carbon tetrabromide and 0.42 g (1.6 mmol) of triphenylphosphine. The resulting product was then purified by column chromatography using first hexane, then DCM:diethyl ether (9:1) as eluent. 0.14 g of compound **6.2** was obtained as a white solid (48% yield). **^{1}H-NMR (d6-DMSO, 101 MHz, ppm)**: 9.43 (s, 2H), 8.12 (t, *J*=8. 5, 8H), 8.06 (d, *J*=8.5 4H), 7.60 (d, *J*=5.2, 2H), 7.26 (d, *J*=5.1, 2H), 3.81 (t, *J*=7.3, 4H), 3.24 (t, *J*=7.3, 4H). **HRMS (EI)** calcd for [$C_{34}H_{27}N_6S_2Br_2$] (M^++H) 741.0105 found 741.0118.

Synthesis of **6.3**

The experimental procedure used was as described for **4.3**. 0.15 g (0.294 mmol) of **4.5** was reacted with trimethylamine in ethanol. The product was obtained as a white powder with very poor yield. **^{1}H-NMR (ds-DMSO, 400 MHz, ppm)**: 9.40 (s, 2H), 8.09 (d, *J*=8.6, 4H), 7.80 (d, *J*=8.6, 4H), 7.71 (d, *J*=6.1, 2H), 7.60(d, *J*=5.1, 2H), 7.60 (d, *J*=4.6, 2H), 7.20 (d, *J*=5.1, 2H) 3.80 (t, *J*=7.3, 4H), 3.27 (t, *J*=7.3, 4H), 3.16 (s, 18H).
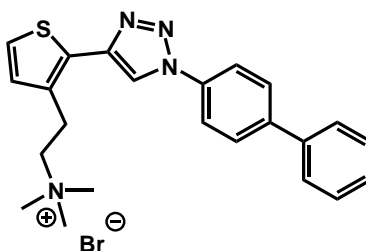
Synthesis of **6.4**
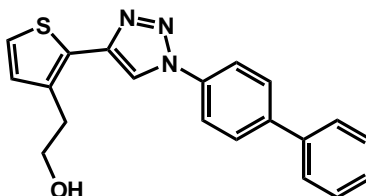
The experimental procedure used for this reaction was as described for **4.1**. **^{1}H-NMR (CDCl$_3$, 400 MHz, ppm)**: 8.14 (s, 1H), 7.79 (d, *J*=8.6, 2H), 7.70 (d, *J*=8.2, 2H), 7.55 (d, *J*= 7.6, 2H), 7.42 (t, *J*=7.1, 2H), 7.34 (t, *J*=7.1, 1H), 7.25 (d, *J*=5.7, 1H), 6.96 (d, *J*=4.8, 1H), 3.93 (t, *J*=5.9, 2H), 3.07 (t, *J*=5.9, 2H), 2.46 (s, 1H). **^{13}C-NMR (CDCl$_3$, 101 MHz, ppm)**: 143.14, 142.26, 139.89, 137.73, 136.16, 130.62, 129.43, 128.75, 128.44, 127.79, 127.49, 125.52, 121.16, 119.11, 63.31, 32.86. **HRMS (EI)**: calcd [C$_{20}$H$_{18}$N$_3$OS] 348.1171 found 348.1167

Synthesis of **6.5**
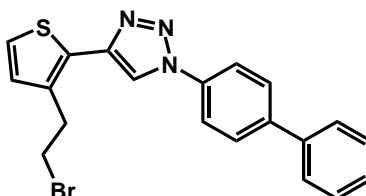
The experimental procedures mirrored those described for **4.2**. **^{1}H-NMR (CDCl$_3$, 400 MHz, ppm)**: 8.09 (s, 1H), 7.96 (t, *J*=2.1, 1H), 7.69 (d, *J* = 8.2, 1H), 7.60-7.64 (m, 4H), 7.43 (t, *J*=7.2, 2H), 7.35 (t, *J* =7.3, 1H), 7.24 (d, *J* = 5.2, 1H), 6.99 (d, *J*=5.2, 1H), 3.65 (t, *J* =7.3, 2H), 3.44 (t, *J*=7.2, 2H). **^{13}C-NMR (CDCl$_3$, 126 MHz, DEPT 45/90/135, ppm)**: 143.31, 142.67, 137.04, 130.22, 130.01, 129.04, 128.20, 127.78, 127.63, 127.23, 124.79, 119.32, 119.18, 118.45, 32.91, 32.18. **HRMS (EI)**: calcd [C$_{20}$H$_{16}$N$_3$S] 330.1065 found 330.1062.

Synthesis of **6.6**

Compound **6.6** was synthesised analogously to compound **4.3**. **^{1}H-NMR (ds-DMSO, 400 MHz, ppm)**: 8.73 (s, 1H), 7.91 (s, 1H), 7.50-7.54 (m, 4H), 7.30-7.33 (m, 4H), 7.24 (s, 2H), 6.94 (s, 1H), 3.35 (s, 2H), 3.18 (s, 2H), 2.90 (s, 9H). **^{13}C-NMR (d6_DMSO, 101 MHz, ppm)**: 128.88, 128.06, 127.44, 126.65, 125.91, 124.69, 118.97, 117.62, 116.76, 36.34. **HRMS (EI)**: calcd [$C_{23}H_{25}N_4S$] 389.1800 found 389.1781.

6.6.2 Binding studies

Binding studies were performed following the protocols described in Chapter 5.

References

1. Garbett, N. C.; Ragazzon, P. A.; Chaires, J. B., *Nature Protocols* **2007,** *2* (12), 3166-3172.

2. Kolb, H. C.; Finn, M. G.; Sharpless, K. B., *Angewandte Chemie-International Edition* **2001,** *40* (11), 2004.

A1 Dicationic oligoheteroaromatic 5.1

1.1 Extinction coefficient

Stock solution of **5.1** (13.9 mM) in water was prepared. A total volume of 9 μl of this solution was added to 2500 μl of water in a 1.00 cm pathlength cuvette. A further 12 μl of the same stock solution (6.95 mM) was added in to 2500 μl buffer in a 1.00cm cuvette .Ligand absorbance at λ_{max} 302 nm was plotted against ligand concentration and a linear fit (red line) was applied to obtain the extinction coefficient of $(29.47 \pm 1.1) \times 10^3$ dm^3 mol^{-1} cm^{-1} (Figure A1).
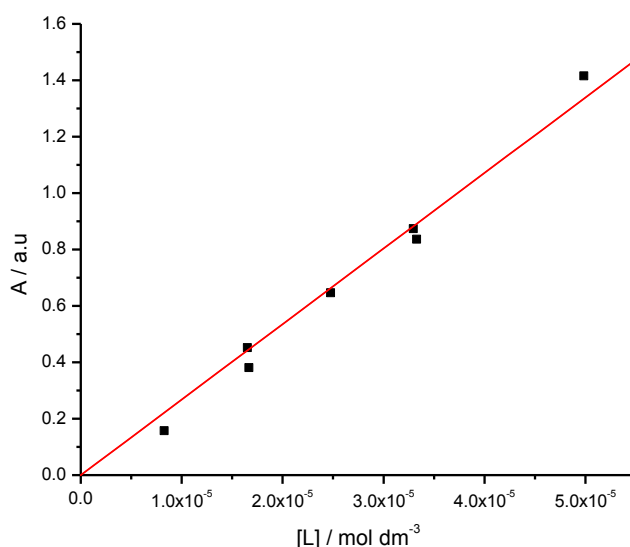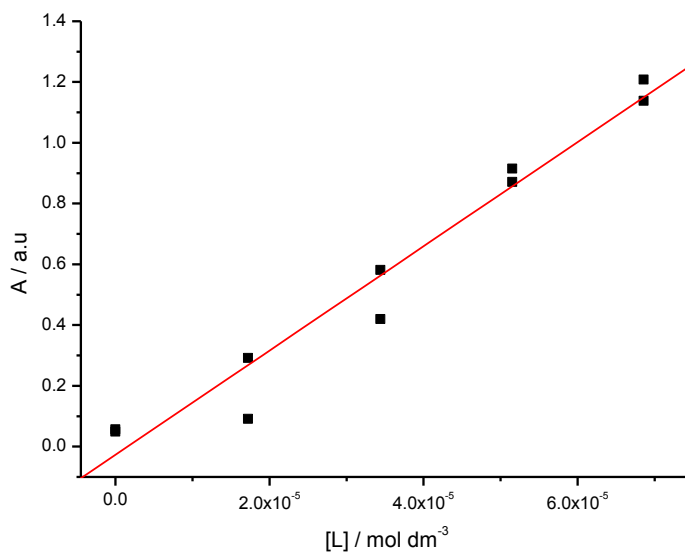

Figure A1 Absorbance for **5.1** as a function of concentration

A2 Dicationic oligoheteroaromatic 5.2

2.1 Extinction coefficient

Stock solution of **5.2** (11.5 mM) in water was prepared. A total volume of 12 μl of this solution was added to 2000 μl of water in a 1.00 cm pathlength cuvette. A further 12 μl of the same stock solution (11.5 mM) was added in to 2000 μl buffer in a 1.00cm cuvette. Ligand absorbance at λ_{max} 315 nm was plotted against ligand concentration and a linear fit (red line) was applied to obtain the extinction coefficient of $(17.15 \pm 1.2) \times 10^3$ dm^3 mol^{-1} cm^{-1} (Figure A2).
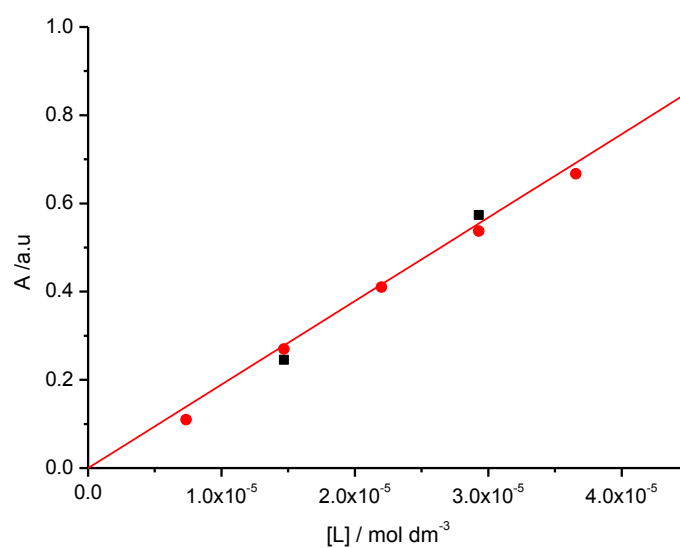
Figure A2 Absorbance for **5.2** as a function of concentration

A3 Dicationic oligoheteroaromatic 5.3

3.1 Extinction coefficient

Stock solution of **5.3** (5.4 mM) in water was prepared. A total volume of 12 μl of this solution was added to 2200 μl of water in a 1.00 cm pathlength cuvette. A further 9 μl of the same stock solution (11.5 mM) was added in to 11000 μl buffer in a 0.5 cm cuvette. Ligand absorbance at λ_{max} 287 nm was plotted against ligand concentration and a linear fit (red line) was applied to obtain the extinction coefficient of $(18.92 \pm 0.5) \times 10^3$ dm^3 mol^{-1} cm^{-1} (Figure A3).
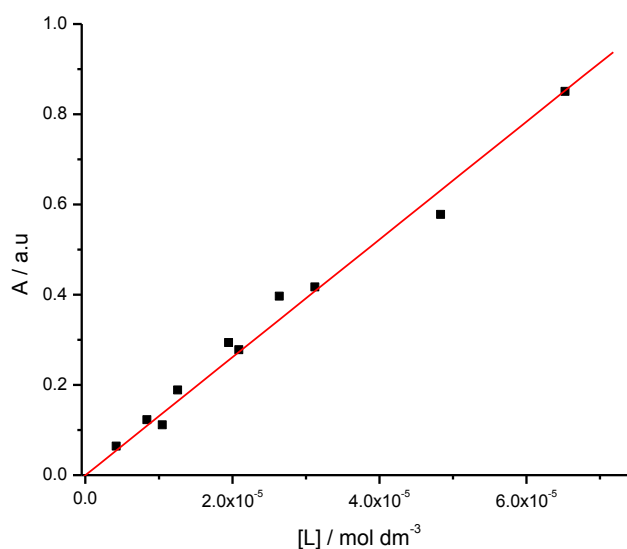
Figure A3 Absorbance for **5.3** as a function of concentration

3.2. **Error margins for Isothermal titration calorimetry**.

Titration of 4.11 mM solution of **5.3** into 0.5 mM solution of CT DNA, at 25°C.
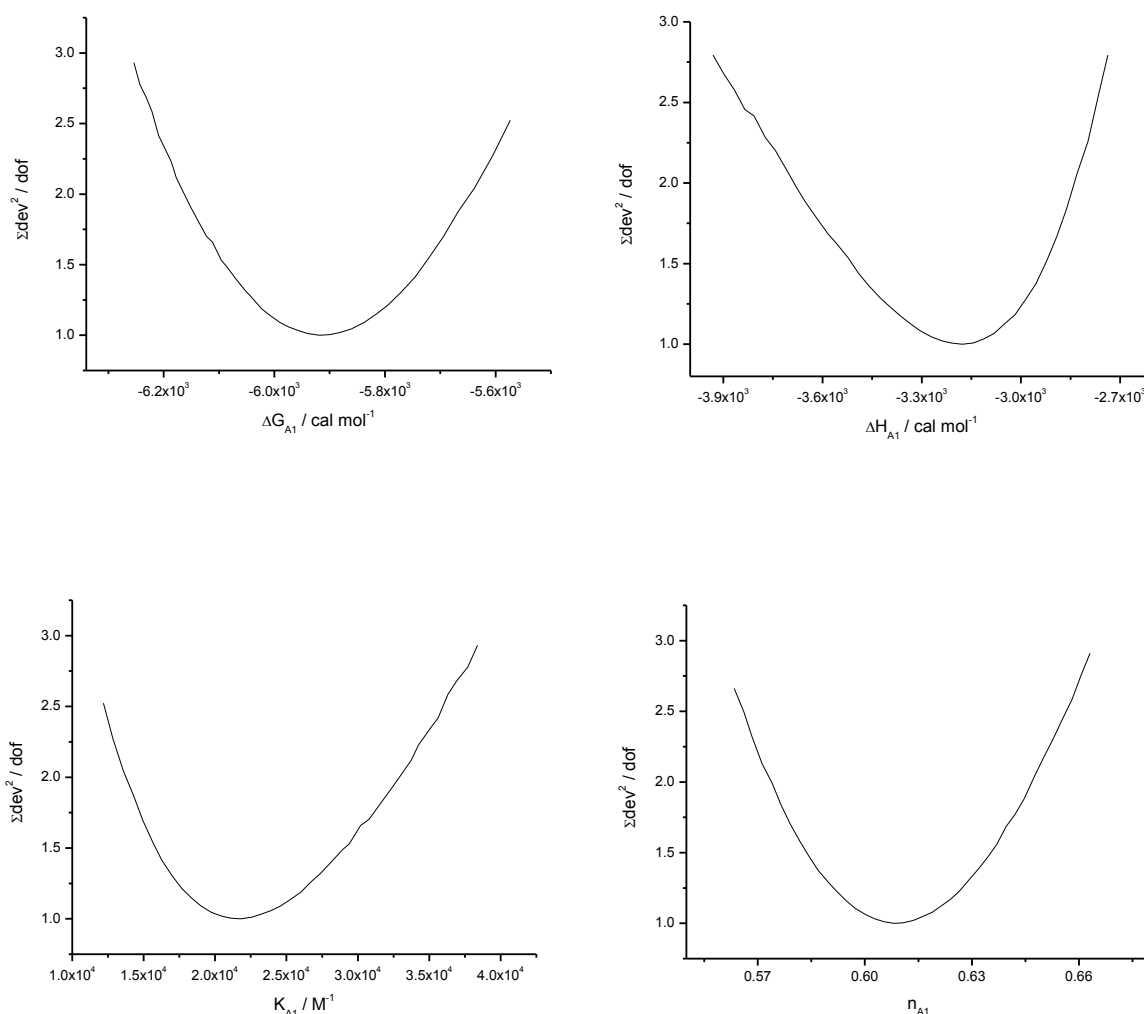
Figure A4 Normalised $\Sigma dev^2/dof$ for binding parameters. Error margins calculated from the fitting to one binding site model.

A4 Dicationic oligoheteroaromatic 5.4

4.1 Extinction coefficient

Stock solution of **5.4** (4.4 mM) in water was prepared. A total volume of 16 μl of this solution was added to 2500 μl of water in a 1.00 cm pathlength cuvette. Ligand absorbance at λ_{max} 301 nm was plotted against ligand concentration and a linear fit (red line) was applied to obtain the extinction coefficient of $(18.20 \pm 0.33) \times 10^3$ dm^3 mol^{-1} cm^{-1} (Figure A5).

Figure A5 Absorbance for **5.4** as a function of concentration

4.2 Error margins for Isothermal titration calorimetry of 5.4.

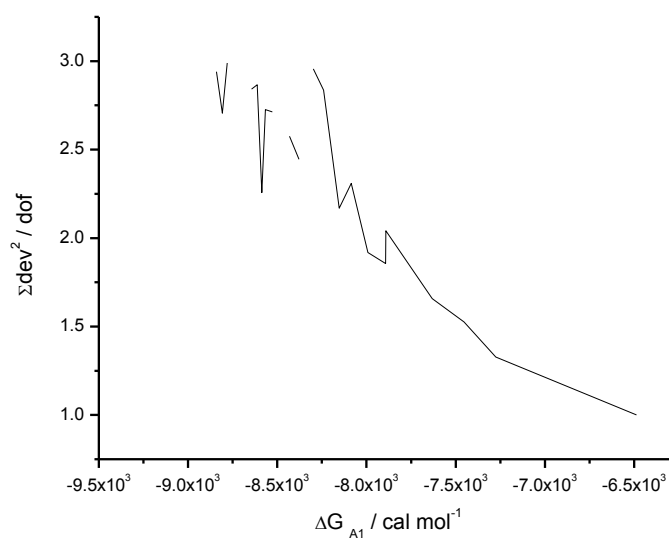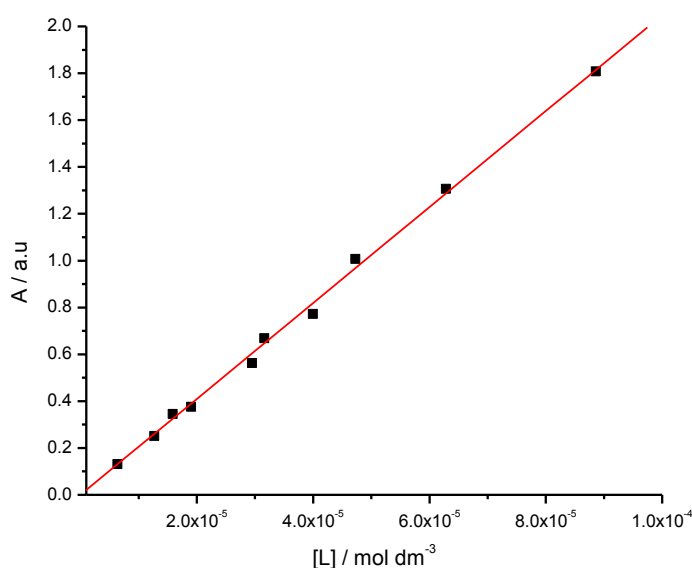Titration of 4.5 mM solution of **5.4** into 0.45 mM solution of CT DNA, at 25°C.

Figure A6 Normalised $\Sigma\mathrm{dev}^2/dof$ for binding parameters. Errors margins are calculated from the fitting to tow binding site model.

A5 tricationic oligoheteroaromatic 5.5

5.1 Extinction coefficient

Stock solution of **5.4** (5.3 mM) in water was prepared. A total volume of 19 µl of this solution was added to 2500 µl of water in a 1.00 cm pathlength cuvette. A further 19 µl of the same stock solution (5.3 mM) was added in to 1000 µl water in a 0.5 cm cuvette. Ligand absorbance at λ_{max} 306 nm was plotted against ligand concentration and a linear fit (red line) was applied to obtain the extinction coefficient of $(20.48\pm 0.3) \times 10^3$ dm^3 mol^{-1} cm^{-1} (Figure A7).

Figure A7 Absorbance for **5.5** as a function of concentration

5.2 Error margins for Isothermal titration calorimetry of 5.5.

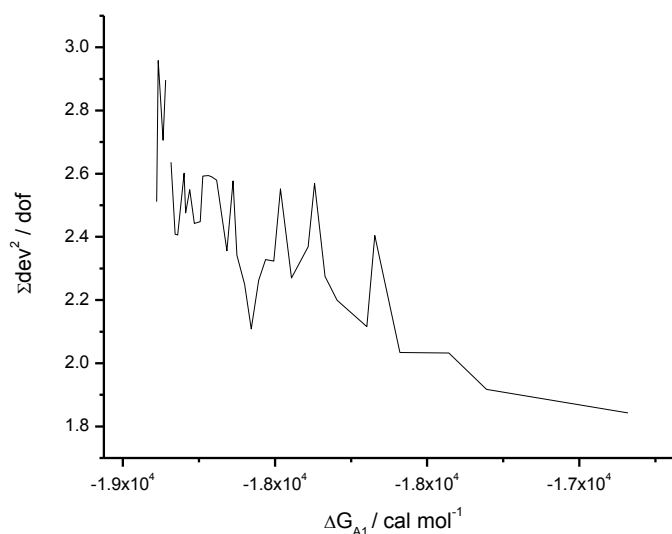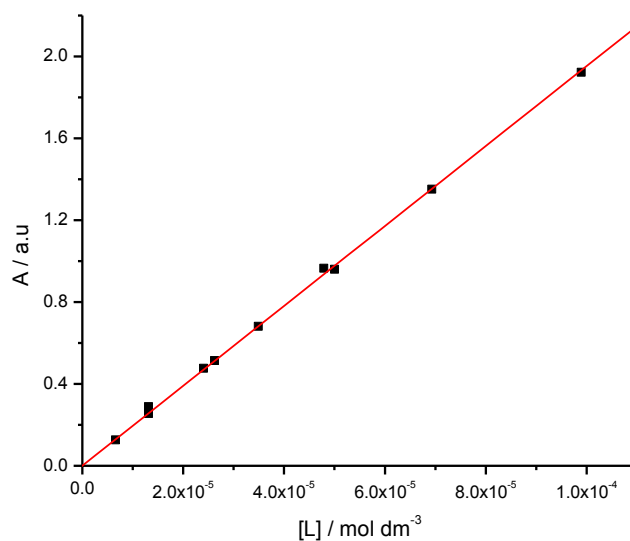Titration of 4.5 mM solution of **5.5** into 0.5 mM solution of CT DNA, at 25°C.

Figure A8 Normalised $\Sigma dev^2/dof$ for binding parameters. Errors margins are calculated from the fitting to tow binding site model.

A6 tricationic oligoheteroaromatic 5.6

6.1 Extinction coefficient

Stock solution of **5.6** (4.4 mM) in water was prepared. A total volume of 23 μl of this solution was added to 2000 μl of water in a 1.00 cm pathlength cuvette. A further 23 μl of the same stock solution (4.4 mM) was added in to 1000 μl water in a 0.5 cm cuvette. Ligand absorbance at λ_{max} 301 nm was plotted against ligand concentration and a linear fit (red line) was applied to obtain the extinction coefficient of $(19.35 \pm 0.18) \times 10^3$ dm^3 mol^{-1} cm^{-1} (Figure A9).

Figure A9 Absorbance for **5.6** as a function of concentration

6.2 Error margins for Isothermal titration calorimetry of 5.5.

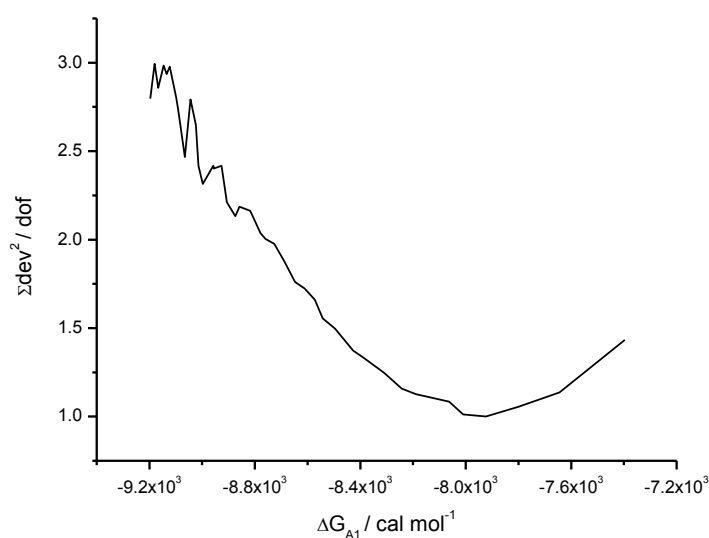Titration of 4.39 mM solution of **6.5** into 0.45 mM solution of CT DNA, at 25°

Figure A10 Normalised Σdev^2/*dof* for binding parameters. Errors margins are calculated from the fitting to tow binding site model.

A7 Dicationic oligoheteroaromatic 4.30

7.1 Extinction coefficient

Stock solution of **4.30** (4.5 mM) in water was prepared. A total volume of 23 μl of this solution was added to 2500 μl of water in a 1.00 cm pathlength cuvette. Ligand absorbance at λ_{max} 301 nm was plotted against ligand concentration and a linear fit (red line) was applied to obtain the extinction coefficient of $(38.18 \pm 0.4) \times 10^3$ dm^3 mol^{-1} cm^{-1} (Figure A11).
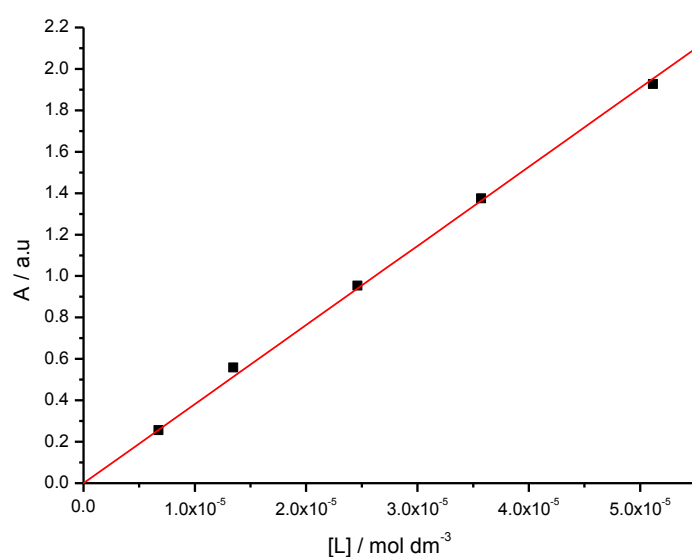

Figure A11 Absorbance for **5.6** as a function of concentration

A8 Dicationic oligoheteroaromatic 4.15

8.1 Extinction coefficient

Stock solution of **4.15** (9.05 mM) in water was prepared. A total volume of 19 μl of this solution was added to 2000 μl of water in a 1.00 cm pathlength cuvette. Ligand absorbance at λ_{max} 246 nm was plotted against ligand concentration and a linear fit (red line) was applied to obtain the extinction coefficient of $(11.60 \pm 0.07) \times 10^3$ dm^3 mol^{-1} cm^{-1} (Figure A12).
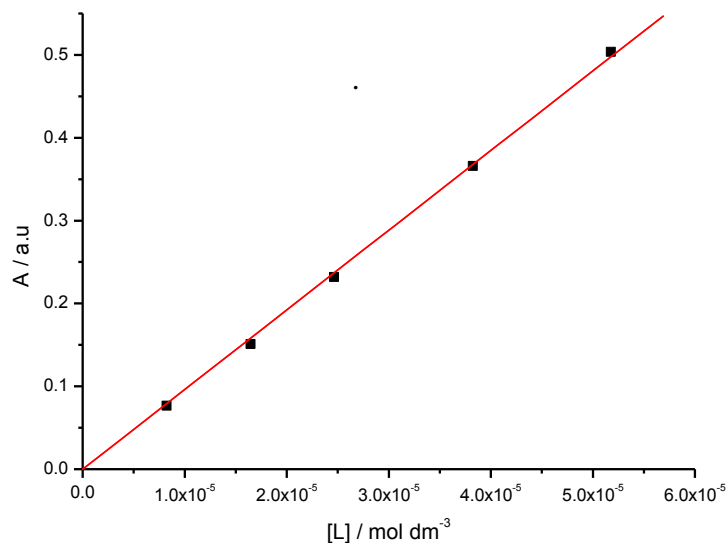
Figure A12 Absorbance for **4.15** as a function of concentration

A9 Dicationic oligoheteroaromatic 4.18

9.1 Extinction coefficient

Stock solution of **4.18** (5.55 mM) in water was prepared. A total volume of 19 μl of this solution was added to 2000 μl of water in a 1.00 cm pathlength cuvette. Ligand absorbance at λ_{max} 247 nm was plotted against ligand concentration and a linear fit (red line) was applied to obtain the extinction coefficient of $(9.84 \pm 0.1) \times 10^3$ dm^3 mol^{-1} cm^{-1} (Figure A13).
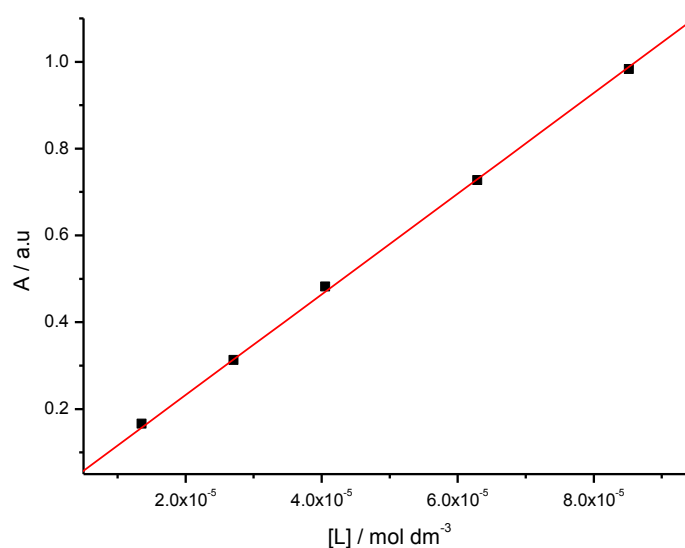

Figure A13 Absorbance for **4.18** as a function of concentration

A10 Dicationic oligoheteroaromatic 4.21

10.1 Extinction coefficient

Stock solution of **4.21** (1.14 mM) in water was prepared. A total volume of 35 μl of this solution was added to 2000 μl of water in a 1.00 cm pathlength cuvette. Ligand absorbance at λ_{max} 349 nm was plotted against ligand concentration and a linear fit (red line) was applied to obtain the extinction coefficient of $(26.19 \pm 0.23) \times 10^3$ dm^3 mol^{-1} cm^{-1} (Figure A14).
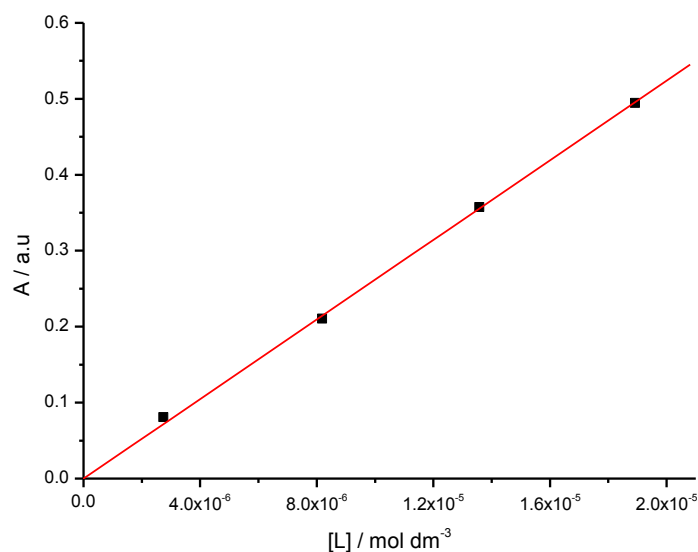

Figure A14 Absorbance for **4.21** as a function of concentration